Ontogeny, phylogeny and functional morphology of the hominoid shoulder girdle

Thesis submitted in fulfilment of the degree of Doctor of Philosophy in Biological Anthropology

Department of Anthropology
University College London

Anna Barros
2013

I, Anna Barros confirm that the work presented in this thesis is my own. Where information has been derived from other sources, I confirm that this has been indicated in the thesis.

To mom and dad.

Acknowledgements

I would like to thank my supervisors Dr. Christophe Soligo (UCL) and Prof. Christopher Dean (UCL) for their guidance and support over the past 4 years. I would also like to thank Dr. Wendy Dirks (Newcastle University) and Dr. Julia Boughner (University of Saskatchewan) for generously sharing their X-rays of gibbon, bonobo, chimpanzee dentition. Additionally, I would like to thank the following people for kindly granting access to human and non-human primate osteological collections: Dr. Marcia Ponce de León (Universität Zürich Anthropological Institute and Museum), Michael Hiermeier (Zoologische Staatssammlung München), Dr. Robert Kruszynski and Dr. Roberto Portela Miguez (Natural History Museum, London), Angela Gill (Powell-Cotton Museum, Birchington-on-Sea), Dr. Emmanuel Gilissen (Koninklijk Museum voor Midden-Afrika, Tervuren), Dr. Hugo Cardoso (Anthropological and Zoological Collections of the Bocage Museum, Lisbon). I also thank my funding body, the Fundação para a Ciência e a Tecnologia (grant SFRH/BD/60349/2009), for allowing me to pursue this degree and research project. I would also like to thank the my reviewers, Dr Susannah Thorpe and Dr Kevin Kuykendall for the insightful comments and feedback that made the final version of this thesis possible. Finally I would like to thank Dr. Jeroen Smaers for his help and collaboration – in particular for the use of his method, including unpublished statistical procedures –, as well as my lovely colleagues and friends in the Aiello Lab at UCL for their friendship and support.

Above all, I would like to thank my parents for their unconditional support, both emotional and financial over the years, without which this project would not have been carried out. I will forever be in debt to you.

Abstract

The shoulder is of particular relevance for resolving issues of locomotor ancestry since, as a group, living hominoids can be defined by the set of functional similarities that they share at this anatomical area (such as a scapula located on the back of the ribcage, and a shoulder joint adapted to allow extensive abduction). However, there is ongoing debate over which selective pressures are responsible for these shared morphologies. The current study addresses the question of whether the similarities in this anatomical structure in hominoids are a product of common ancestry (homology) or rather the product of parallelism (homoplasy) from an ontogenetic and phylogenetic perspectives. To this end, 30 measurements were collected on the clavicle, scapula and humerus of six hominoid species (*Homo sapiens, Pan troglodytes, Pan paniscus, Gorilla gorilla, Pongo pygmaeus and Hylobates lar*) and one macaque species (*Macaca fascicularis*); information on the dental development of each individual specimen was collected for the purpose of creating an ontogenetic sample for each species; all measurements were collected on surface scans of individual bones and analysed in a 3D environment (Geomagic Suite 12.1 and Amira 3.1), and all statistical analyses (ontogenetic, phylogenetic as well as within- and between-species differences) were conducted using R version 2.12.2 (R Core Team 2011). Overall my results provide a more detailed understanding of ontogenetic change in shoulder morphology across hominoid species, and demonstrate (1) a relative lack of phenotypic plasticity in other key traits (such as the proximal curvature of the clavicle and glenoid-axillary angle of the scapula), and (2) high levels of plasticity in key diagnostic traits of hominoid shoulder morphology in humeral torsion, the distal curvature of the clavicle, and the orientation of the scapular spine and glenoid fossa (all correlated with each other). However these seem to operate within phylogenetic constraints and to be modulated by the underlying anatomy of the thorax and shoulder girdle. Overall my results support the notion of an arboreal origin to the ape lineages and parallel evolution of quadrupedalism in the great apes.

Table of Contents

List of Tables

List of Figures

– Chapter 1 –

Introduction and literature review

1. Introduction

It is generally agreed that living apes are best defined by similarities in upper limb and trunk morphology (e.g., Larson 1998; Ward 2007; Crompton et al. 2008). Observations of extant hominoid upper limb morphologies have therefore led to divided opinions regarding (1) the mode of locomotion of the Last Common Ancestor (LCA) of living crown hominoids (Avis 1962; Lewis 1969, 1985; Fleagle 1976; Stern 1971; Cartmill and Milton 1977; Fleagle et al. 1981), and (2) the mode of locomotion of the LCA of panines and hominines (i.e., the mode of locomotion from which bipedalism arose) (e.g., Young 2003; Thorpe et al. 2007; Ward 2007; Crompton et al. 2008; Lovejoy et al. 2009; White et al. 2009; Crompton et al. 2010; Green and Alemseged 2012; Churchill et al. 2013).

The shoulder is of particular relevance for resolving issues of locomotor ancestry since, as a group, living hominoids can be defined by the set of functional similarities that they share at this anatomical area (such as a scapula located on the back of the ribcage, and a shoulder joint adapted to allow extensive abduction) (Rose 1993, 1997; Larson 1998; Crompton et al. 2008). However, there is ongoing debate over which selective pressures are responsible for these shared morphologies of all hominoids: quadrumanous climbing (e.g., Fleagle 1976), cautious quadrupedalism and/or brachiation (e.g., Cartmill and Milton 1977), orthogrady (e.g., Thorpe and Crompton 2006; Thorpe et al. 2007; Crompton 2008). With regards to the panine-hominine split, on the other hand, the focus is on the origins of bipedalism with the discussion being mainly divided between those who envision the pre-human ancestor as a terrestrial knuckle-walker, a behaviour frequently used by the African apes (e.g., Washburn

1967; Begun 1992c; Hunt 1991a, 1994; Gebo 1996; Richmond and Strait 2000; Richmond et al. 2001; Begun 2004), and those who defend that bipedalism evolved from a more generalized arboreal, climbing-oriented ancestor, a locomotor repertoire used by all living apes (e.g., Stern 1971; Rose 1997; Schmitt 2003; Thorpe et al. 2007; Hanna and Schmitt 2011).

The difficulty in settling both these arguments comes from the fact that both the Miocene and the more recent Plio-Pleistocene fossil records show a pattern of mosaic adaptations that are at odds with what we would expect had the shoulder morphologies in extant apes been inherited from a common ancestor. In light of this apparent paradox, recent studies have suggested that homoplasy has played a central role in shaping shoulder morphologies both in stem hominoids and in each of the various crown hominoids (e.g., Larson 1996, 1998 2007b, 2009, 2013; Ward 2007). However, if current similarities in the hominoid shoulder girdle are the result of functional parallelism rather than common ancestry, then it is somewhat curious that these species have evolved to be so similar given their divergent locomotor behaviours – ranging from predominantly terrestrial and pronograde knuckle-walking (mountain gorillas) to bipedalism (humans), to virtually exclusive arboreality and generalised orthograde suspension and clambering (orangutans) (e.g., Hunt 1991a, 2004 Thorpe and Crompton 2006). The study of ontogeny – structural change during growth and development – is held to be of particular relevance for identifying homologies and homoplasies in extant organisms (e.g., Nelson 1978; Riedl and Jefferies 1978; Patterson 1982; Lieberman et al. 1996; Roth 1988; Wagner 1989; Lieberman 1999; Lovejoy et al. 1999; Wood 2007). It is generally thought that characters that are homologous arise through similar developmental processes, while characters that are homoplastic arise through different developmental processes (e.g., Collard and O'Higgins 2001); if this is indeed the case, then a detailed comparative analysis of anatomical regions in related organisms from an ontogenetic perspective will unveil homoplasies. Lending support to this idea are studies such as Macho and Dainton's (1999) and Kivell and Schmitt's (2009) analysis of the ontogeny of wrist morphology in *Pan* and *Gorilla*. In both instances the authors conclude that knuckle-

walking evolved in parallel in both species because wrist ontogenies differ in their trajectories (which implies that wrist morphology is homoplastic) in both species (but see Williams 2010). More recently, a study conducted by Green and Alemseged (2012) on the ontogeny of the hominoid scapula indicates the presence or arboreal/ suspensory behaviours from infancy in apes, and since the authors also find a lack of significant differences between the juvenile and adult *A. afarensis* scapulae, they conclude this species was actively engaging in arboreal/climbing behaviours from infancy too. Similarly, the current project aims at studying the ontogeny of the shoulder morphology (scapula, clavicle, humerus) in extant hominoids in order to identify possible homoplasies in this structure, with the intent of contributing towards an understanding of the anatomy and locomotor repertoire of LCAs of (1) living crown hominoids and (2) panines and hominines.

With this broad evolutionary framework in mind, the central focus of the present project is to answer the following questions: how does the shoulder girdle (scapula, humerus, clavicle) in hominoid primates (*Hylobates, Pongo, Pan, Gorilla, Homo sapiens*) develop through ontogeny into its adult form? Are the morphological similarities between the shoulder girdle of the great ape and human clade a result of parallelism or rather of shared ancestry? What can this tell us about the selective pressures shaping the shoulder structure throughout evolution? And what, if anything, can this say about the shoulder morphology and, ultimately, the mode of locomotion of stem apes and stem hominines?

2. The hominoid shoulder: function & anatomy

2.1. Functional relevance: the shoulder & locomotion

The shoulder girdle is an area of particular interest in primate evolution in that it is adapted to a variety of locomotor strategies (e.g., Ashton and Oxnard 1964). Compared to most other vertebrate groups, primates exhibit an exceptional amount of locomotor diversity with at least three forms of locomotion not seen among any other

extant mammals – vertical clinging and leaping, brachiation, and habitual striding bipedalism (Schmitt 2010). Adaptations to these divergent locomotor strategies in primates promote an increased reliance on the hindlimbs to power locomotion, such that we may describe primates as 'hindlimb dominated'; this decoupling of the hindlimb and forelimb functions reflects a forelimb used less in weight support and more in movements of guidance, grasping and manipulation (Schmitt 2010). Because the adoption of habitual bipedalism represents a fundamental adaptive shift away from the apes (Ward 2002), some of the most long-standing questions in paleoanthropology concern how and why human bipedalism evolved. It is therefore not surprising that these shared derived characteristics of the human and great ape shoulder can be used to make interpretations about the mode of locomotion of the LCA of apes and humans – and the one from which bipedalism arose (e.g., Richmond et al 2001; Begun 2004). Because of its functional relevance, the shoulder has therefore been one of the most extensively studied regions in comparative primate and human anatomy (Larson 2007b).

Because of its anatomical position as the connection point between the forelimb and the trunk, the shoulder is a highly relevant structure, serving an important role in both stabilizing the forelimb against dislocation, as well as in providing it with sufficient mobility (Inman and Abbot 1944; Ashton and Oxnard 1964; Oxnard 1967, 1969; Larson 1993; Chan 2006; Veeger and Van Der Helm 2007). This is made possible by the reduction (or absence, in humans) of bony constraints allowing a wide range of motion at the expense of stability, which is provided instead by the various ligaments and muscles (Nordin and Frakel, 2001). The shape and size of its different anatomical parts (clavicle, scapula, humerus) reflects, therefore, the extent to which different species are adapted to orthograde suspensory behaviours (i.e. use their forelimbs in overhead movements) or to pronograde terrestrial behaviours (i.e. use their forelimbs for weight bearing) (e.g., Oxnard 1969; Ashton et al. 1971; Young 2006; Voisin 2006). For example, long narrow scapulae, dorsally placed scapulae, and cranially oriented glenoid fossae are thought to be functionally adapted to arm-hanging and are hypothesised to have evolved to reduce muscular activity and ligamentous and

skeletal strain during unimanual suspension (e.g., Hunt 1991b). On the other hand, increased levels of humeral torsion are thought to result from the parasagittal use of the forelimbs during knuckle-walking (e.g., Larson, 1988). In our own lineage, increased reliance on bipedalism has relaxed the selective pressures acting upon the shoulder complex, freeing it almost completely from its responsibility as a locomotor structure (Larson 2007b). This has resulted in greater anatomical changes in the lower limbs than in the upper limbs between apes and humans, who retain many similarities in their shoulder structures (such as a dorsally located shoulder joints and great range of upper limb mobility) (Aiello and Dean 1990). Great apes are a particularly interesting group in this respect because they exhibit remarkable similarities in their shoulder structure despite their current divergent locomotor specializations. Indeed, because of these similarities, researchers have debated over the last half-century about which postural and locomotor adaptation characterises all hominoids, and the mode of locomotion characterising their last common ancestor: brachiation (Keith 1923), quadrumanous climbing (Fleagle 1976), arm-hanging and vertical climbing (Hunt 1991a), forelimb suspension (Gebo 1996), knuckle-walking (Richmond and Strait 2000) and generalised orthogrady (Thorpe et al 2007; see Richmond et al 2001 for a comprehensive review of the major hypotheses). Most recently it has been suggested that generalised orthograde clambering, where the trunk is upright and both fore- and hindlimbs are used in varying degrees to support body mass in suspensory or compressive loading regimes (e.g. Hunt, 1991a, Hunt et al 1996; Fleagle, 1999) is the locomotor behaviour that characterises the positional behaviour of all hominoids (e.g., Hunt 1991a; Thorpe and Crompton 2006; but see Begun et al 2007).

Part of the difficulty in identifying a shared evolved locomotor/postural behaviour in apes is the fact there is a disconnect between the behaviours that are exhibited frequently and those that place high stresses on the bone. For example, African apes spend 50-99% of their locomotor time on the ground (Tuttle and Watts 1985; Hunt, 1991a,b, 1992; Doran, 1993, 1996; Begun and Kivell 2011), but chimpanzees exhibit very clear adaptations for orthograde suspension, such as long narrow scapulae, cone-shaped rib cages, robust clavicular anchors, anteroposteriorly flattened, mobile

abductible humeri, wide manubria, and cranially oriented glenoid fossae, despite it being the less frequent activity (Hunt 1991b). Because suspensory postures are more stress-inducing or energetically expensive than terrestrial pronograde postures (due to the effects of gravity and the discontinuous 3D environments), it is therefore likely that adaptations to the former will be more evident in the ape skeleton (Thorpe and Crompton 2006). Indeed, Thorpe and Crompton (2006) argue that "positional behaviours for which an animal is well-adapted to are expected to require less muscle activity, and induce less stress in the skeleton and ligaments, than behaviours for which the animal is poorly adapted" (2006:394). This may also help make sense of the postcranial anatomy of fossil hominids, and *Australopithecus* in particular; it is possible that australopithecins were more frequently bipedal but that being efficient in the trees was selectively more important. In fact, studies have suggested that ape anatomical adaptations are directed towards avoidance of falls (Pontzer and Wrangham 2004; Thorpe and Crompton 2006) since large animals are less likely to survive if they fall from any great height (Cartmill and Milton 1977).

The notion that natural selection shapes anatomy to reduce muscular activity and structural stress in relation to the frequency of the behaviour (Basmajian, 1965; Cartmill et al., 1987; Hunt, 1991b, 1992) is problematic when trying to infer locomotor behaviours based on skeletal morphology, particularly in the fossil record, because it obscures 1) the diversity of locomotor strategies used and 2) the frequency of use of postural/locomotor behaviours employed by individual species. In this sense, interpretations of behaviour based on skeletal morphology will inevitably be biased towards those adaptations for behaviours that are the most costly rather than those that are the most frequent. Given that being efficient in the trees is selectively more important than being efficient on the ground, this may explain why all apes share specializations for arboreal locomotion despite their divergent locomotor specializations. In this context, differences in shoulder anatomy between apes are likely to result from the compromise between the need to be efficient in the trees and the need to move around terrestrially: for example, the more terrestrial gorilla has higher degrees of humeral torsion, wider scapulae with less cranially directed glenoid

fossae, while the exclusively arboreal gibbon has very low humeral torsion with obliquely oriented scapulae and cranially directed glenoid fossae. In addition, the lack of significant differences in shoulder and forelimb muscle architecture between apes may act to compensate for skeletal adaptations and facilitate behaviours for which the animal does not appear skeletally adapted to. Indeed, some studies suggest that apes are 'generalists' in terms of their shoulder and forelimb soft-tissue anatomy and are therefore adapted to their entire locomotor repertoire (e.g., Myatt et al 2012). A recent study has, for example, shown that time spent performing a particular behaviour does not seem to significantly influence shoulder and forelimb soft-tissue anatomy in apes (Myatt et al 2012).

2.2. Anatomy of the hominoid shoulder girdle

The primate shoulder (figure 1) is composed of three bones (the scapula, the humerus, and the clavicle), more than 20 muscles (the exact number depending on the particular species), and four joints (Aiello and Dean 1990).

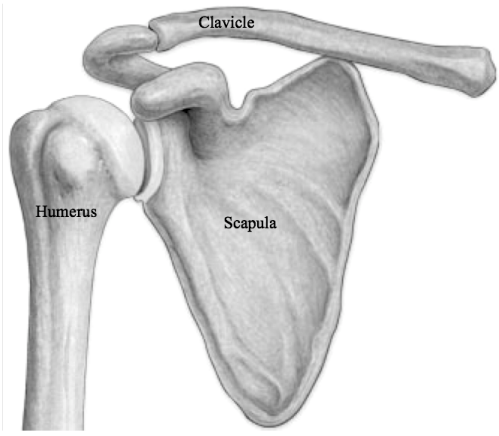

Figure 1 – The human shoulder in ventral view.

As mentioned, apes and humans are rather homogenous in their shoulder morphology and can be easily distinguished from other primates through the set of functional characteristics that they share at this anatomical area: a wide thorax, an elongated clavicle, a dorsal position of the scapula that is elongated cranio-caudally, large

scapular fossae, a cranial orientation of the glenoid fossa, a wide, round and flat glenoid fossa, medial torsion of the humeral head, lack of a supraglenoid tubercle, greater and lesser tubercles positioned below the humeral head, a laterally positioned acromion process that enhance lever advantage of the deltoid muscle, and high ratio between the length of the scapula and the insertion of the trapezius and serratus anterior which enhances the action of these two upward rotators (Miller 1932; Ashton and Oxnard 1963, 1964; Ashton et al. 1971, 1976; Oxnard, 1963, 1967; Corruccini and Ciochon 1976; Aiello and Dean 1990). This anatomical pattern affects the movement of the glenohumeral joint, which allows the entire upper limb of humans and apes to be capable of a greater range of movement at this joint than any other primate group (with the exception of some New World monkeys) (Schultz 1961; Aiello and Dean 1990; Potau et al. 2009). Osteological differences between the human and ape pectoral girdle and shoulder joint are found primarily in the scapula and clavicle which suggest that the human arm is adapted for use in lowered positions and is less powerful in raised positions than the ape arm (Aiello and Dean 1990). Furthermore, differences between the three large apes reflect the more arboreal locomotion of the orangutans on the one hand and the more terrestrial locomotion of chimpanzees and gorillas on the other (Aiello and Dean 1990).

Apart from a few exceptions, the arm and shoulder muscles of apes are identical to those of humans (Miller 1932), and in all hominoid species, the great range of movements allowed at this joint is achieved through a total of four articulations occurring at this structure: the sternoclavicular articulation, the acromioclavicular articulation, the glenohumeral articulation, and the scapulothoracic articulation (Aiello and Dean 1990). These act together in a way that produces mobility greater than that afforded by any one individual articulation, allowing the arm to be moved in all directions: flexion, extension, abduction, adduction, elevation and circumduction (Nordin and Frankel 2001).

2.2.1. The scapula

The primate scapula is a large triangular blade-like bone that rests on the thoracic cage, gliding over the back of the ribs, and articulating with the upper arm at the glenohumeral joint (figure 2) (Aiello and Dean 1990). Given its central role in forelimb use, scapular morphology is highly variable between species and its shape is largely associated with functional demands of the forelimb (Young 2006). In primates, morphological differences between species can be discriminated along a continuum from committed terrestrial quadrupedalism (i.e., baboons) to highly arboreal and suspensory non-quadrupedalism (i.e., gibbons) (Young 2006).

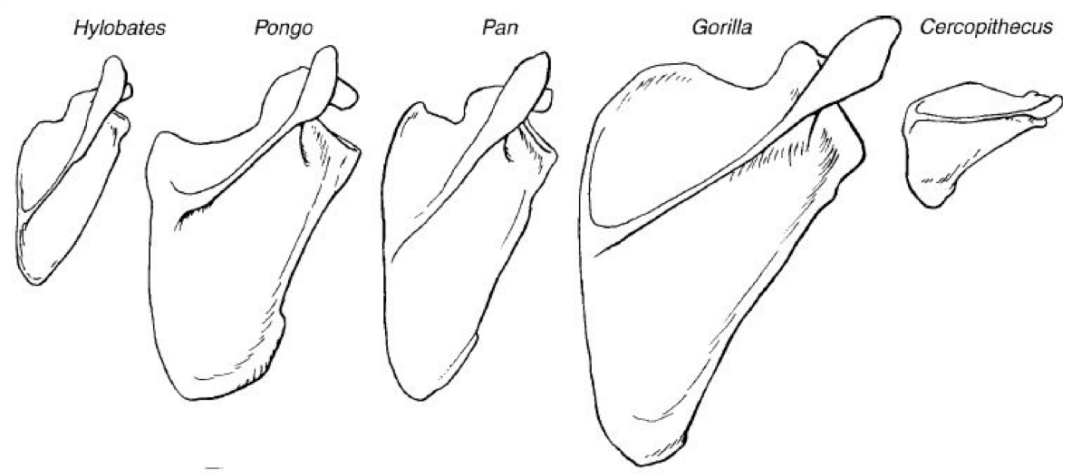

Figure 2 – The hominoid scapula (human shoulder). Taken from Larson (1998).

This bone consists of a flat or slightly concavo-convex blade, which is divided on its dorsal surface by the scapular spine into two fossae (the infra- and supraspinous fossae), with a subscapular fossa located on the ventral surface (Aiello and Dean 1990). The scapular spine is a flat plate of bone extending in a plane roughly perpendicular to that of the blade that widens into the acromion, which articulates distally with the clavicle (Aiello and Dean 1990). The head of the scapula articulates with the proximal humerus at the glenoid fossa; the coracoid process arises superior to the glenoid and does not articulate with other skeletal elements (Young 2004). Additionally, the scapula is suspended by muscle alone and is able to perform the

following movements: abduction, adduction, extension, and flexion (Rockwood 2009).

It is widely held that many differences among primate species in scapular morphology can be functionally related to differing demands on the shoulder associated with particular locomotor habits (Oxnard, 1963, 1967; Ashton and Oxnard, 1964; Ashton et al., 1965a, b, 1971; 1976; Roberts, 1974). Namely, the ratio of supraspinous fossa/infraspinous fossa size in apes is commonly viewed as an indicator of the importance of overhead use of the forelimb, with high supraspinous fossa/ infraspinous fossa ratios present in the more suspensory species (Roberts 1974). However, many smaller scale studies do not support these observations. For example, Taylor's (1997) comparison of scapular morphology between the more arboreal lowland gorillas and the more terrestrial mountain gorillas fails to observe these differences. Additionally, the African apes (the most terrestrial of the great apes), have higher scapular fossa ratios than the more suspensory orangutan (Larson and Stern, 2013). In fact orangutans, which are the most suspensory of the great apes, are characterized by having a very large infraspinous rather than a large supraspinous fossa, a feature likening them to humans (Roberts 1974; Larson and Stern 2013).

The recent discovery Dikika child DIK-1-1 scapula, and its morphological affinities to scapulae of orangutans and gorillas rather than chimpanzees has led to renewed interest in the comparative analysis of human and extant ape scapular form (Alemseged et al. 2006; Green and Alemseged 2012; Larson and Stern 2013).

2.2.2. The humerus

The humerus is a long bone that makes up the upper arm and articulates with the scapula at the glenohumeral joint (Aiello and Dean 1990). It consists of three sections: the upper extremity, which is made up of a rounded head, a narrow neck with two short tuberosities, a body that is cylindrical in its upper portion and more prismatic below, and the lower extremity which is made up of two epicondyles

(trochlea and capitulum), and three fossae (radial fossa, coronoid fossa, and olecranon fossa) (Aiello and Dean 1990). A few important muscles attaching at the humerus are the deltoid, which inserts on the deltoid tuberosity of the humerus (located mid-shaft) and has several actions including abduction, extension, and rotation of the shoulder; the supraspinatus, which inserts on the greater tubercle of the humerus, and assists in abduction of the shoulder; and the infraspinatus and teres minor, which insert on the greater tubercle, and work to laterally/externally rotate the humerus (Aiello and Dean 1990). The four muscles (supraspinatus, infraspinatus, teres minor and subscapularis) form a musculo-ligamentous girdle called the rotator cuff that stabilizes the very mobile but unstable glenohumeral joint, while the other muscles are used as counterbalances for the actions of lifting/pulling and pressing/pushing (Aiello and Dean 1990). At the shoulder, the head of the humerus articulates with the glenoid fossa of the scapula, and more distally, at the elbow, the capitulum articulates with the head of the radius, and the trochlea articulates with the olecranon process of the ulna (Aiello and Dean 1990).

Humeral torsion, because it is a shared characteristic among hominoids, is one of the most functionally relevant aspects of humeral morphology, and is often referred to in the context of ape locomotor adaptations (e.g., Evans and Krahl 1945; Krahl and Evans 1945; Krahl 1947, 1976; Edelson 1999, 2000; Larson 1996, 1998, 2007a; Cowgil 2007). Gibbons have a larger torsion angle than most monkeys, but have considerably less humeral head torsion than all other living hominoids (Larson, 1988). Larson (1988) suggests that this low degree of humeral torsion reflects a compromise between the need to maintain a transverse axis at the elbow joint and the demand for extreme positioning of the elbow during arm-swinging due to their specialized mode of locomotion (brachiation). In African apes, on the other hand, the higher degrees of humeral torsion may be linked to the need for maintaining the elbow joint moving in a parasagittal plane for knuckle-walking (Larson 2007b). The fact that among the living apes gorillas are the most terrestrial and have the most marked humeral torsion supports this association between torsion and quadrupedalism (Larson 1988). Some researchers consider this supposed shared trait (shared between African apes and

humans) to constitute evidence for knuckle-walking ancestry (e.g., Richmond et al. 2001; Begun 2004).

2.2.3. The clavicle

The clavicle is a small curved bone that sits anteriorly on the thorax and acts as a strut between the shoulder and the pectoral girdle, and is the only part of the pectoral girdle that articulates directly with the trunk, holding the arm at the side and transmitting forces from the arm to the sternum (figure 3) (Aiello and Dean 1990). The clavicle articulates with the scapula above the shoulder at the acromioclavicular joint and with the sternum at the sternoclavicular joint; the two muscles inserting on the clavicle are the trapezius (posterior superior surface of distal end) and the subclavius muscle (inferior surface of middle third of the clavicle), and the four muscles originating at the clavicle are the deltoid, the pectoralis major, the sternocleidomastoid, and the sternohyoid (Rockwood 2009).

From a comparative point of view, the clavicle is one of the most poorly studied bones in the body. Schultz (1930) reported a considerable variation in the nature and degree of clavicular curvature in humans and in the different species of ape: gibbon clavicles have a single anteriorly convex curve while orangutan clavicles are generally straight; chimpanzee and human clavicles have S-shaped curves and gorilla clavicles are generally straight except for the lateral, acromial end which is bent to various degrees. Additionally, Schultz (1930) observed that the clavicles of orangutans are not directed horizontally as in humans, but are oriented at a steep angle consistent with the very high position of the orangutan shoulder above the rib cage. Lending support to Schultz' observations, Voisin's (2006) study of living ape and human clavicles, found that in the dorsal plane, clavicle morphology allows to predict the position of the scapula in regards to the thorax (figure 3). A clavicle with two

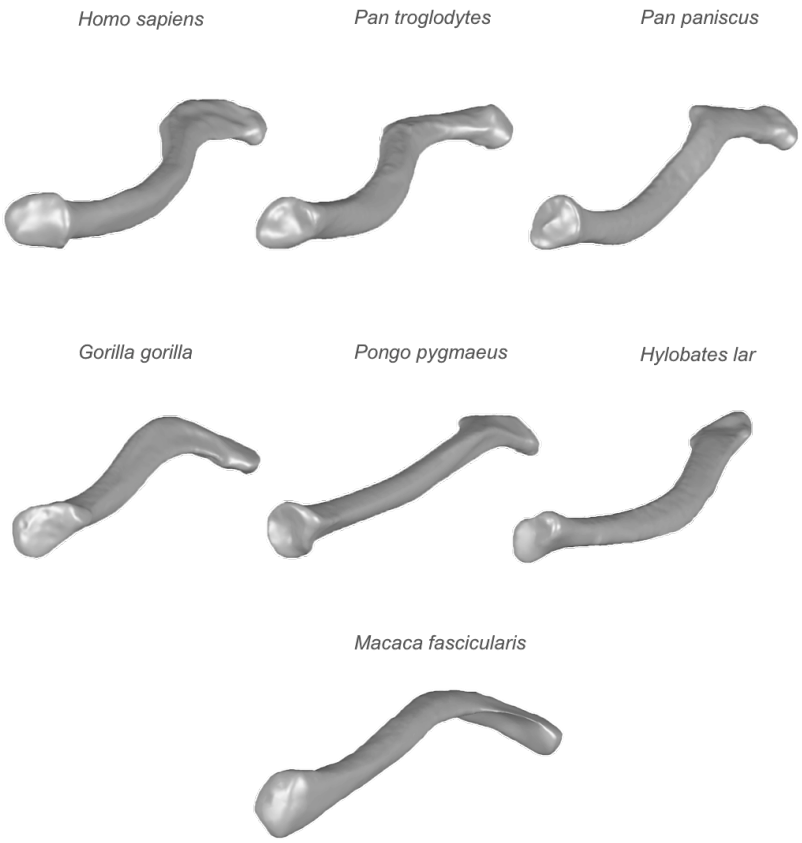

Figure 3 – Adult left clavicle of hominoids and *Macaca fascicularis* (sternal view).

curvatures like that of the chimpanzee is therefore associated with a dorsal and high scapula in regards to the thorax; a clavicle with only a superior curvature, like that of the gibbon, is associated with a dorsal and high scapula that needs an acromioclavicular joint for added rigidity; and finally, a clavicle with a unique, slightly pronounced inferior curvature, as in humans, is associated with a low and dorsal scapula (Voisin 2006).

3. Evolution of the hominoid shoulder girdle

3.1. The hominoid shoulder: homology or homoplasy?

It is not immediately clear whether it is homology or homoplasy that best explains shared ape postcranial characteristics (e.g., Young 2003), and the growing body of

evidence from the fossil record has not yet yielded any conclusive answers. In fact, as it stands, the current picture of hominoid postcranial evolution seems to be one of recurring homoplasy – as illustrated by the '*Sivapithecus* dilemma' (Pilbeam et al. 2001; Young 2003). Indeed, *Sivapithecus,* an extinct Miocene ape from Pakistan (12.5-8.5Mya) poses a dilemma precisely because its postcrania, namely its upper-arm morphology, is more similar to that of African apes, while its cranial morphology is rather *Pongo*-like. The 'dilemma' lies in whether it is the *Pongo/Sivapithecus* facial similarities that are homologous or whether it is the postcranial similarities of living apes that are homologous (Young 2003). Although today it is generally accepted that *Sivapithecus* should be placed on the *Pongo* clade, and that postcranial features tend to be more prone to homoplasy, this was not always the case (Begun 2004). Previous to the 1990's, analyses of hominoid postcranial morphology emphasized the marked postcranial differences between the hominoids compared to other primates (Oxnard 1967, 1977; Ashton et al. 1976; Corruccini 1978; Corruccini and Ciochon 1976), and therefore, homology was the standard explanation for the postcranial similarities between hominoids. Larson (1998), however, challenged this view of hominoids as a morphologically cohesive group by studying a number of ape trunk and upper limb characters. Larson has since published a number of papers (Larson 1996, 1998, 2007b, 2009, 2013; Larson et al. 2007) suggesting a scenario in which suspensory features are acquired independently in each hominoid lineage – i.e. are homoplastic. If this is correct, than this would explain why it has been difficult to find a fossil ape which exhibits all the features of the hypothetical suspensory ancestral hominoid morphotype and why fossil apes exhibit such a varying mosaic of suspensory and non-suspensory features (Young 2003). Indeed, the picture that currently emerges from the fossil record is one of morphological diversity, in which climbing and suspensory adaptations develop in mosaic fashion over evolutionary time, and that occur in different ways and even multiple times in separate hominoid lineages (Ward 2007; Begun 2007). Indeed the Miocene hominoid fossil record shows evidence of multiple instances of independent evolution of specialized suspensory adaptations (e.g., *Morotopithecus, Oreopithecus, Dryopithecus*, or *Pongo*) (Begun 2007), and the presence of knuckle-walking features in the hind limb, humerus, and wrist bones of

Sivapithecus (Begun and Kivell 2011), also supports the case of independent evolution of knuckle-walking. In particular, it has been suggested that the adaptations seen in extant apes may not have occurred as a block, as indicated by the morphologies of *Nacholapithecus* (long forelimbs but narrow torso and pronograde quadruped posture) and *Pierolapithecus* (hylobatid-like torso but short digits) (Rose 1997; Senut 2003; Ishida et al. 2004; Moya-Sola et al. 2004; Ward 2007), or the more recently discovered *Australopithecus sediba* (ape-like upper thoracic shape but *Homo*-like aspects of hand morphology) (Kivell et al. 2011; Schmid et al. 2013).

The picture is equally complicated with regards to the hominins. Larson (2007b, 2009, 2013) describes how the modern human shoulder configuration consists of a highly rotated humerus, a lateral-facing glenoid fossa of the scapula and a long clavicle – a morphology that maintains the arms in a forward-facing position for manipulation, and that reflects a shoulder well adapted for throwing activities. In great apes, on the other hand, the shoulder configuration consists of a highly rotated humerus but with a cranially directed glenoid fossa and a short clavicle – a morphology that allows for overhead suspensory movements while maintaining the forward-facing arms needed for quadrupedalism. Because of relaxations in selective pressures related to arboreality, and in light of the extant anatomical configurations, we would expect extinct hominins to possess shared features such as high degree of humeral torsion in combination with increasingly longer clavicles and more laterally positioned glenoid fossae (Larson 2007b). However, contrary to these expectations, the hominin fossil record yields a mix of morphologies that challenge these views – namely, low degrees of humeral torsion in *Homo floresiensis*, and a gorilla-like scapular morphology in *Australopithecus afarensis* (Alemseged et al. 2006; Larson 2007b). In light of this, Larson (2007b, 2009, 2013) proposes that rather than undergoing a direct change from the primitive hominid condition to that of modern humans, the hominin shoulder passed through unexpected intermediate stages, and that the highly derived modern shoulder configuration is actually relatively recent.

Morphological evidence of other anatomical parts in apes, such as the foot bones (Harcourt-Smith and Aiello 2004) and the wrist (Dainton and Macho 1999; Dainton 2001; Kivell and Schmitt 2009) further lend support to the idea that throughout evolution, different ape taxa evolved a variety of anatomical configurations in order to deal with similar locomotor challenges. However unparsimonious it may be, it seems that even such specialized locomotor adaptations as knuckle-walking and bipedalism may have evolved either in parallel or multiple times throughout hominoid evolution (Dainton 2001; Harcourt-Smith and Aiello 2004; Ward 2007; Kivell and Schmitt 2009). This accumulation of evidence suggests that the apparent shared derived characters of the shoulder girdle in hominoid apes may have in fact evolved as a result of parallelism. In order to test this assumption, one of two things must happen: either we find more fossils, or we use extant hominoid shoulder morphologies to identify homoplasies (which is the focus of the current project). However, the complex nature of shoulder morphology has made comparative analyses using traditional morphometric techniques difficult (e.g., Young 2003), and for this reason, questions surrounding the evolutionary course of shoulder morphology in the hominoid stock remain largely unanswered. The solution, as observed by Young (2003), may then lie in a more detailed account of the ontogeny of similarities within shoulder morphologies, which may reveal whether the anatomical features of the shoulder structure are a product of homology or homoplasy. If this assumption is correct, and the shared similarities in shoulder morphology between apes and humans are actually homoplasies, then they must arise in the different taxa via differing developmental mechanisms; on the contrary, if similarities in the shoulder morphology of apes and humans are due to shared ancestry (are homologous), then we expect them to arise via comparable developmental trajectories (Begun 1994; Lieberman 1999).

Of the three shoulder elements, the scapula and the humerus has received the most attention from an ontogenetic point of view. With regards to humeral torsion, Krahl (1945) and Edelson (1999) describe how torsion in humans develops throughout ontogeny and how environmental factors such as activity pattern influence the degree to which it is expressed. In contrast, Young (2006, 2008) describes how scapular

shape in great apes is conserved throughout ontogeny from birth to adulthood and therefore strongly driven by phylogenetic/genetic factors rather than functional ones. The clavicle, on the other hand, has been largely neglected in the literature (but see Voisin 2006).

3.2. Ontogeny of the hominoid shoulder girdle: a means to identifying homoplasies?

Analysing the development of morphological features throughout ontogeny is important for understanding the functional significance of morphological variation between apes. Bony morphology is thought to reflect, at least to some extent, function during development (Pearson and Lieberman 2004). The reason being that bone remodels itself according to the loads it is placed under – a concept known as "Wolff's law" (Wolf 1892) – and that bone's response to mechanical stimuli is very marked during the years preceding adulthood (Ruff et al. 2006). For example, the degree of phalangeal curvature has been shown to be positively correlated with increased arboreality in African apes during ontogeny (Paciulli 1995) and the absence of some knuckle-walking features in hominins has been attributed to lack of function during development (Richmond et al. 2001). The study of ontogeny is thus of particular interest because it provides a chance to understand how adult morphologies emerge.

However, biomechanical loadings are not the only factor guiding bone shape; genetic and environmental constraints play an equally important role in shaping these morphologies (Lockwood and Fleagle 1999), and for this reason, several authors have suggested that developmental data can be uniquely informative in perceiving homology and homoplasy in a paleoanthropological context (Lieberman 1995, 1999, 2000; Lovejoy et al. 1999; Leigh 2007). However, gaining an understanding of the relations between development and homology/homoplasy requires that we study ontogeny in organisms for which phylogenetic relationships are known, a criterion that is fortunately met by the hominoid clade (Lieberman 1999; Leigh 2007; Cartmill 1994). In studies where this condition is met, shared ontogenetic allometries can be

accepted as evidence for homology and divergent ontogenetic allometries can be in turn accepted as evidence for homoplasy (Leigh 2007). In other words: “things that resemble each other (morphological homology) because they result from common ancestry (phylogenetic homology) are likely to be similar because they grew through the same inherited processes (developmental homology).” (Lieberman 1999:146).

Comparing ontogenies between closely related taxa thus provides insight into the function of anatomical features that cannot be gained from adult morphology alone, and permits to make inferences about the morphology of the LCA (Kivell and Schmitt 2009; Zolikofer and Ponce de Leon 2010). Developmental studies have shown, for example, that cranial base flexion in humans and non-human primates may be analogous rather than homologous because they develop through a different set of processes (Lieberman et al. 2001); this may help to evaluate the phylogenetic significance of variation in cranial base angulation in hominids such as between *Australopithecus boisei*, which is highly flexed, and *A. aethiopicus*, which appears to be much more extended (Lieberman 2000). Other studies have also shown that the same is true of *Pan* and *Pongo*’s long premaxillae, which develop through differing developmental mechanisms (Begun 1994; Begun and Güleç 1998). However, because homoplasy is often the result of compromises between intrinsic factors, such as genetic constraints, and extrinsic factors, imposed by the environment (Lockwood and Fleagle 1999), it is perhaps not surprising that closely related taxa find similar morphological solutions to similar ecological challenges. Indeed, Cartmill (1994) argues that ontogeny can only be used to assess homology within the context of prior phylogenetic information because similar structures are likely to arise from homologous precursors since natural selection can operate only on available variation. This is particularly relevant when considering parallelisms (as opposed to convergences), which is the case with hominoid morphologies. If, on the one hand, the phylogenetic proximity among apes allows a comparison of their ontogeny, on the other, it is precisely this phylogenetic proximity that makes it difficult for conclusively distinguishing between a homology and a homoplasy. For this reason, there exists (1) controversy about the relevance of such developmental data for

recognizing homologies and homoplasies in the context of parallelism (Roth 1988; Cartmill 1994; Hall 2003), and (2) controversy about what these departures in ontogenetic trajectories in closely related species actually mean in terms of the evolution of locomotor behaviours (Jungers and Cole 1992; Williams 2010).

3.3. Homoplasies in the context of parallelism

For the purposes of this study, it is important to distinguish, as pointed out by Lockwood and Fleagle (1999), between convergence and parallelism: convergence being the acquisition of the same/similar biological trait in unrelated lineages (e.g., the wings of birds, bats, and insects), and parallelism being the development of a similar trait in related species descending from the same ancestor (e.g., the prehensile tails of capuchin monkeys and spider monkeys). However, convergent structures may be formed by non-homologous elements, prehensile tails of capuchins and atelines for example, are formed of homologous bones and muscles, both in the structural and developmental sense (Lockwood and Fleagle 1999), therefore, Lieberman (1999:147) describes parallelism as "a particularly pernicious form of homoplasy because the similarities are, by definition, developmentally homologous," and Gould (2002) refers to parallelisms as the "gray zone" between homologies and convergence. Understanding this distinction is particularly relevant when studying the evolution of the hominoid shoulder because this structure poses the same difficulties as the ateline/ capuchin tail since the hominoid shoulder structure is made up of homologous elements. In fact, comparing any shared morphological features in the ape clade will pose a problem because of the phylogenetic proximity between its species, and the choice of outgroup will likely bear much influence on the results produced. In this context, development alone may not be sufficient to differentiate between homology and homoplasy in the shoulder girdle, or we risk erroneously taking interspecific variations in development as absolute evidence for independent evolution (Williams 2010).

3.4. Homoplasies: evidence for independent evolution?

Some studies have demonstrated that "homologous structures may arise from developmental processes that are equivalent or non-equivalent" (Hall, 1992:21), and that in fact homology and development can often be discordant (Hall 2003; Raff 1996; Leigh 2007). Indeed Hall (2003; 2007; 2012) points out that structural homology, developmental homology and behavioural homology do not always go hand in hand. For example, homologous developmental processes can be used to generate homoplastic characters and vice versa, and even when the phenotypic character is lost, the genes and developmental mechanisms coding for the character can be retained (Hall 2007). Effectively, the genotype and phenotype can disassociate during the evolution of homologues and homoplastic characters, a process that has been called 'phenogenetic drift ' or 'developmental system drift ' (Budd, 1999; Weiss & Fullerton, 2000; True & Haag, 2001; Weiss, 2002). Given this, homology cannot be assigned solely on the basis of shared development, and homoplasy cannot be assigned solely on the basis of lack of shared development. Jungers and Cole (1992), for example, have demonstrated that the locomotor skeletons of lar gibbons (*Hylobates lar*) and siamang gibbons (*Hylobates syndactylus*) are not ontogenetically scaled, yet these authors do not propose that brachiation evolved in parallel in these species; instead they suggest that these departures from ontogenetic scaling are due to differences in the mechanics of brachiation and other suspensory behaviours (see Williams, 2010). Inouye (1992, 1994) also documents differences in metacarpal and phalangeal growth trajectories within and between *Gorilla* and *Pan*, and concludes that these are due to differences in positional behaviour, kinematics or efficiency of knuckle-walking in these taxa. Similarly, Williams (2010) proposes that the differences in *Gorilla* and *Pan* wrist ontogenies do not necessarily suggest that each species evolved knuckle-walking independently, as proposed by Dainton and Macho (1999) and more recently by Kivell and Schmitt (2009); rather the author suggests that it is possible that differences in ontogeny are due instead to differences in locomotor and positional behaviour, ecology and the biomechanics of weight-bearing (Williams 2010).

Moreover, there is a fair amount of plasticity in the postcranial skeleton since bones change in size and shape throughout life in response to a variety of stimuli (multiple genes with multiple effects [pleiotropism], and a large number of non-genetic influences [Cheverud 1982; Atchley and Hall 1991; Herring 1993; Lieberman 1992]) in order to perform numerous functions, which means that the ontogeny of morphological features can be highly mosaic and dissociated from phylogeny (Lieberman 1999). This may explain why reconstructing phylogenies from skeletal elements may be problematic (Zelditch et al. 1995; Monteiro 2000; Brehm et al. 2001; Naylor and Adams 2001; MacLeod and Forey 2002; Rohlf 2002; Hoekstra et al. 2004; Lockwood et al. 2004; Lycett and Collard 2005; Michaux et al. 2007; Cardini and Elton 2008; González-José et al. 2008; Polly 2001), especially in the case of the postcranial skeleton (e.g., Young 2003).

Perhaps a more productive way to think about 'homology versus homoplasy' in the context of developmental similarities/departures is to think of these processes as part of a continuum rather than a dichotomy, as suggested by Hall (2007; 2012):

> *"[…] When we attempt to separate homology from homoplasy mechanistically, we are not dealing with a dichotomy between homoplasy as parallelism/convergence and homology as common descent. Nor are we dealing with a dichotomy of homoplasy as the interrupted presence of the character in a lineage and homology as the continuous presence of the character. Rather we are dealing with common descent with modification, and, more specifically, with common descent with varying degrees of modification." (Hall 2007: 476)*

In other words, the more phylogenetically or temporally distant the last common ancestor the more opportunity for modification/loss and for parallelism/convergence (i.e., for homoplasy), and the more phylogenetically recent the last common ancestor, the greater the likelihood of phenotypic similarity (i.e., for homology). Consequently,

any discussion of homology and/or homoplasy in relation to developmental mechanisms must be posed within the context of a sound phylogenetic analysis. Cartmill (1994) in fact, has argued that ontogeny can only be used to assess homology within the context of prior phylogenetic information since similar structures are likely to arise from homologous precursors by virtue of the fact that natural selection can operate only on available variations. If this condition is satisfied then it is possible to work within the general premise that *(a) homologies reflect evolutionary changes arising from similar developmental processes, (b) parallelisms reflect developmental processes that may have diverged, and (c) convergences reflect divergent developmental processes* (Hall 2003). It thus follows that morphological similarities between two bones are most likely, at least partially, homologous in a developmental sense if these growth processes are the same (Lieberman 1999).

In the case of the hominoid clade, discordances between structure (phenotype) and development (ontogeny) are less likely to be an issue because of the taxonomic proximity between species. This means that homoplasies (in the strictest sense) in structure and development are unlikely to be present or difficult (see impossible) to detect since we are dealing with parallelisms and not convergences. Indeed, developmental similarities are expected to arise from similar processes, and thus may evolve independently in more than one lineage through parallelism (Lieberman 1999). In this case, rather than focusing solely on ontogenetic development – which is merely a description of the *sequence* rather than the actual processes by which morphologies grow – this project will focus more on understanding whether similarity in structures arises via similar development *mechanisms*, which is generally considered a more satisfying approach (Alberch 1985; Liberman 1999).

3.5. Ontogeny of the hominoid shoulder: a valid approach?

It is true that divergences in ontogeny do not necessarily equate independent evolution, and that homologous structures do not necessarily develop through ontogenetically homologous routes. In the case of the hominoids, where we are

dealing with a set of closely related species, some of which even share similar body weights, locomotor strategies and ecological niches, conclusions must be drawn with especial caution so as to avoid the pitfalls of overly simplistic explanations. Nonetheless, provided the subject is approached conservatively, under the guide of a strong theoretical background that allows for alternative explanations (such as biomechanics and ecology) and with the understanding that the relationships between ontogenies and evolutionary pathways are not always clear-cut, comparisons of hominoid ontogenetic development remain a promising tool for distinguishing between homologies and homoplasies in the context of parallelism.

Indeed, despite being one of the most extensively studied anatomical areas in paleoanthropology, the hominoid shoulder girdle still poses an interesting evolutionary problem: how to reconcile the morphologically cohesive extant hominoids, with a morphologically diverse Miocene and Plio-Pleistocene fossil record? – A dilemma, which has been elegantly demonstrated by Young (2003). Indeed, Young's (2003) cladistic analysis of primate postcranial morphometrics showed that (1) the great apes cluster closely together, (2) gibbons and spider monkeys cluster together, and most interestingly, (3) the factors driving this cladistic configuration are characters of the shoulder area, particularly the humeral head and the scapula. Given this evidence, even if we accept Larson's (2007b, 2009, 2013) proposition that the hominoid shoulder girdle is in fact a homoplastic structure in the extant apes, the postcranial parallelism model must still explain how these species could look so similar in the face of their locomotor diversity (Young 2003).

It is in light of this apparent paradox, and with the intention of contributing to our understanding of the selective pressures driving the evolutionary transformations of the hominoid shoulder girdle, that the present project has been designed.

4. Aims

The current project will study the growth and development (ontogeny) of the shoulder structure (scapula, humerus and clavicle) in extant hominoids (*Pan troglodytes, Pan paniscus, Pongo pygmaeus, Gorilla gorilla, Hylobates lar, Homo sapiens*), plus an outgroup of arboreal quadruped macaques: *Macaca fascicularis*. It will aim at

understanding whether the similarities in this anatomical structure in hominoids are a product of common ancestry (homology) or rather the product of parallelism (homoplasy). In order to accomplish this, 3D (surface areas, angles, torsion, curvatures) and 2D (lengths, heights, widths) measurements of the shoulder elements will be compared against variables such as differences in the timing of events in the different taxa, as well as differences in developmental trajectories between taxa.

The project is novel in that (1) it will study the shoulder structure from an ontogenetic perspective in both apes and humans, (2) it will explore some of the relationships between the three skeletal elements of the shoulder in relations to each other, and (3) it will use 3D methods of surface imaging rather than relying on landmark data alone. The results will be used to make inferences about the possible selective pressures acting upon the shoulder girdle during both the evolutionary course of hominoid apes as well as our own hominin lineage. The findings will mainly build on previous research conducted by Young (2003, 2008) and Larson (1988, 1996, 1998, 2007b) regarding similarities in the hominoid postcrania and the evolution of the hominin shoulder, respectively.

The current project rests on the following assumption, bearing in mind the caveats discussed above: characters that are homologous will arise through similar developmental processes, while characters that are homoplastic will arise through different developmental processes. In addition, this study also incorporates the use of phylogenetic comparative methods in order to complement the ontogenetic analyses and resultant observations (see Materials and Methods section for details). Due to the importance of humeral torsion as a phylogenetically and functionally diagnostic trait in hominoids, I also dedicate one chapter to the bilateral asymmetry of torsion in African apes and humans, which puts this trait into a behavioural context. Both these topics (bilateral asymmetry and phylogenetic comparisons) address the issue of plasticity and behaviour, which are central to the study of ontogeny, and the issue of ‘homology versus homoplasy’.

– Chapter 2 –

Materials and Methods

1. Introduction

In order to conduct the present research, 30 measurements were collected on the clavicle, scapula and humerus of six hominoid species (*Homo sapiens, Pan troglodytes, Pan paniscus, Gorilla gorilla, Pongo pygmaeus and Hylobates lar*) and one macaque species (*Macaca fascicularis*). Information on the dental development of each individual specimen was collected for the purpose of creating an ontogenetic sample for each species. All measurements were collected on surface scans of individual bones and analysed in a 3D environment (Geomagic Suite 12.1 and Amira 3.1), and all statistical analyses (ontogenetic, phylogenetic as well as within- and between-species differences) were conducted using R version 2.12.2 (R Core Team 2011).

2. Sample

Measurements were collected on left shoulder elements (or right elements when the left was not present or damaged) – clavicles, scapulae and humeri – of *Macaca fascicularis* (n=21), *Hylobates lar* (n=24), *Pongo pygmaeus* (n=25), *Pan paniscus* (n=23), *Pan troglodytes* (n=45), *Gorilla gorilla* (n=42) and *Homo sapiens* (n=97) of all ages (0 to 70 years in humans; 0 to 13+ years in great apes; 0 to 7+ years in *Macaca* and *Hylobates*). The *Macaca* sample was included as an outgroup because of the arboreal adaptation in this species, and its distant phylogenetic relationship to hominoids (see Appendix 1 for a comprehensive list of the sample used in this study). The macaque and gibbon samples were collected from the Universität Zürich Anthropological Institute and Museum; the orangutans from the Zoologische

Staatssammlung München and Natural History Museum, London; the chimpanzee and gorilla samples were obtained from the Natural History Museum, London, and the Powell-Cotton Museum, Birchington-on-Sea, with a few chimpanzees also derived from the Koninklijk Museum voor Midden-Afrika, Tervuren; the bonobo sample was collected from the Koninklijk Museum voor Midden-Afrika, Tervuren, and finally, the human sample was collected from the Spitalfields Collection housed at the Natural History Museum, London, and the Anthropological and Zoological Collections of the Bocage Museum, Lisbon.

3. Measurements

3.1. Scans

3D surface scans of the shoulder elements of all specimens were produced using a Handyscan 3D EXAscan from Creaform. The scans were processed and stitched together using Geomagic Suite 12.1. Measurements were taken using Geomagic Suite 12.1 and Amira 3.1 (for 3D measurements) and tpsDigs (for 2D measurements).

3.2. Measurement definitions

Ten clavicle measurements, two humerus measurements and 18 scapula measurements were taken (figures 4-7), which include lengths, widths, angles, torsion, curvatures and surface areas. Lengths, and widths were measured in Amira 3.1; torsion was measured using a combination of Amira 3.1 and tpsDigs; angles and curvatures were measured using a combination of Geomagic Suite 12.1 and tpsDigs; surface areas were measured in Geomagic Suite 12.1.

Definitions of each measurement are provided in the following section and in table 1. In particular, the protocol for measuring curvatures is novel, and I have therefore

dedicated an entire Chapter (Chapter 6) to this measurement and its application for analysing clavicular curvatures.

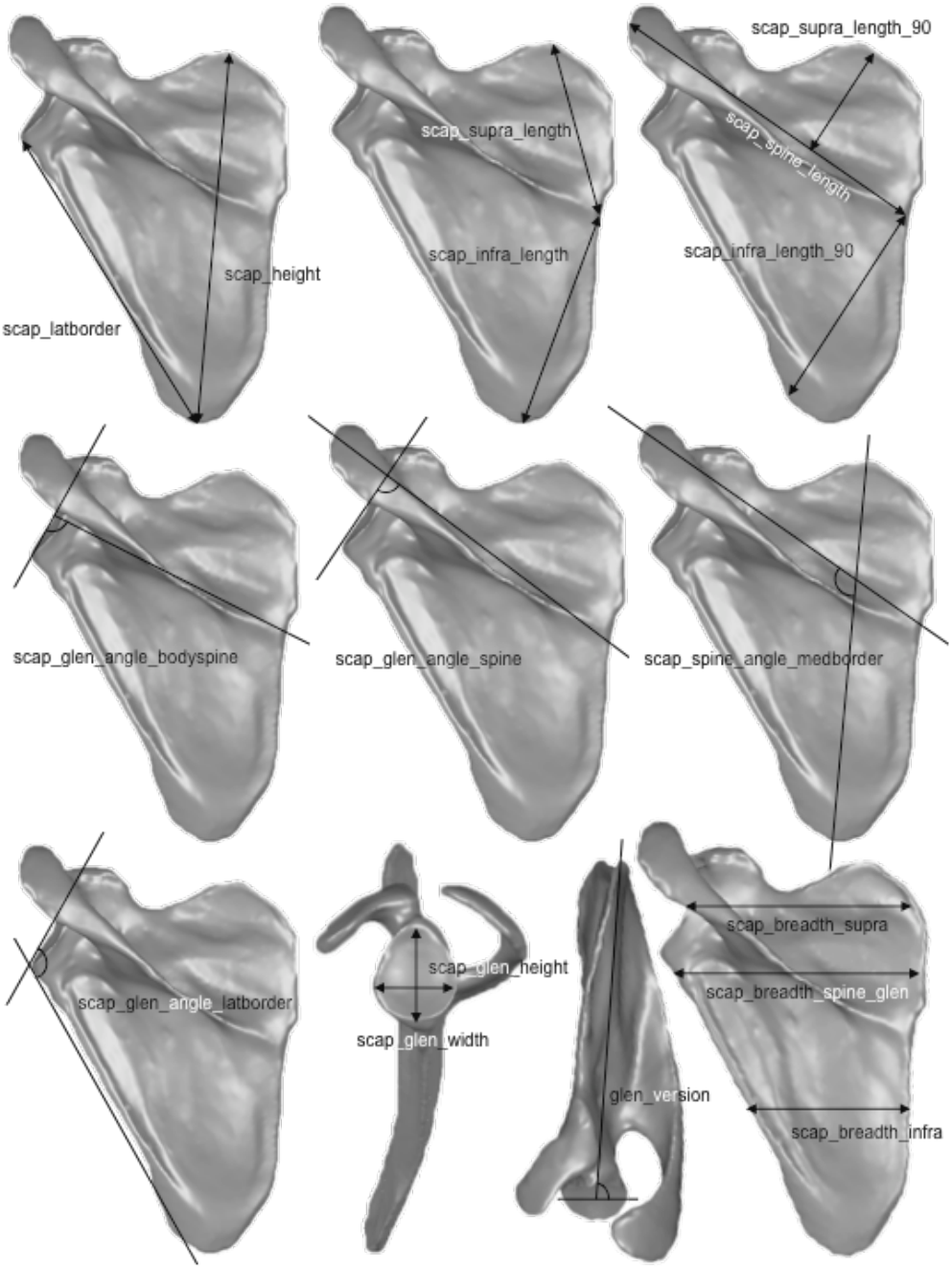

Figure 4 – Left human scapula showing the measurements collected on the scapula. (See also figure 5).

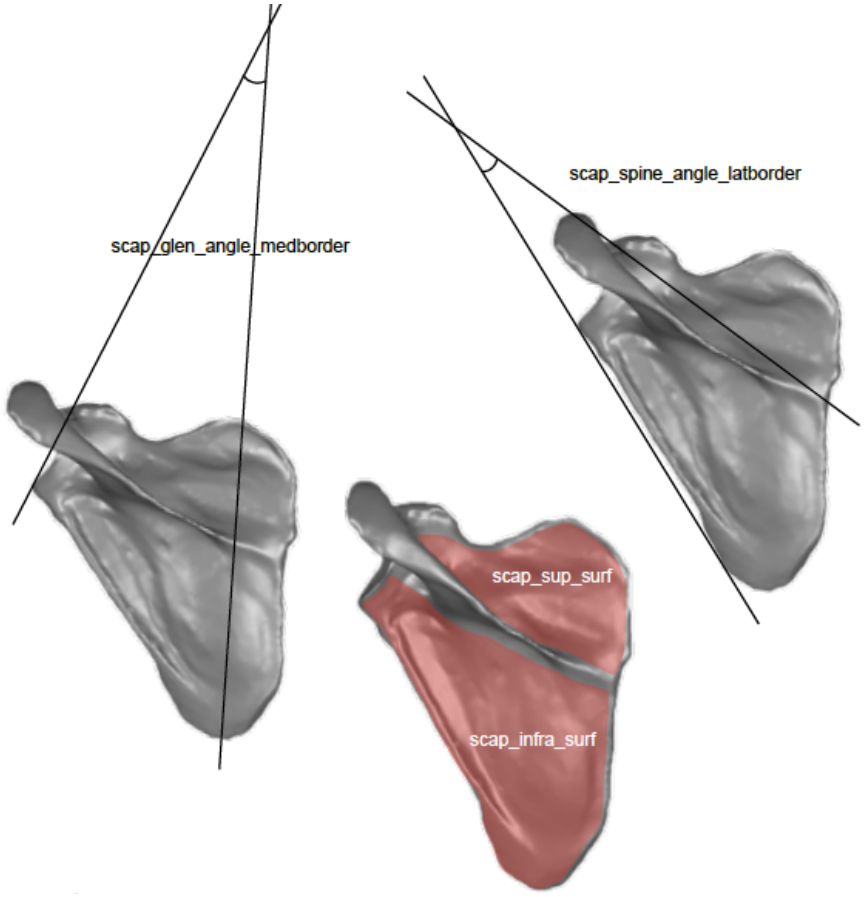

Figure 5 – Left human scapula showing the measurements collected. (See also figure 4).

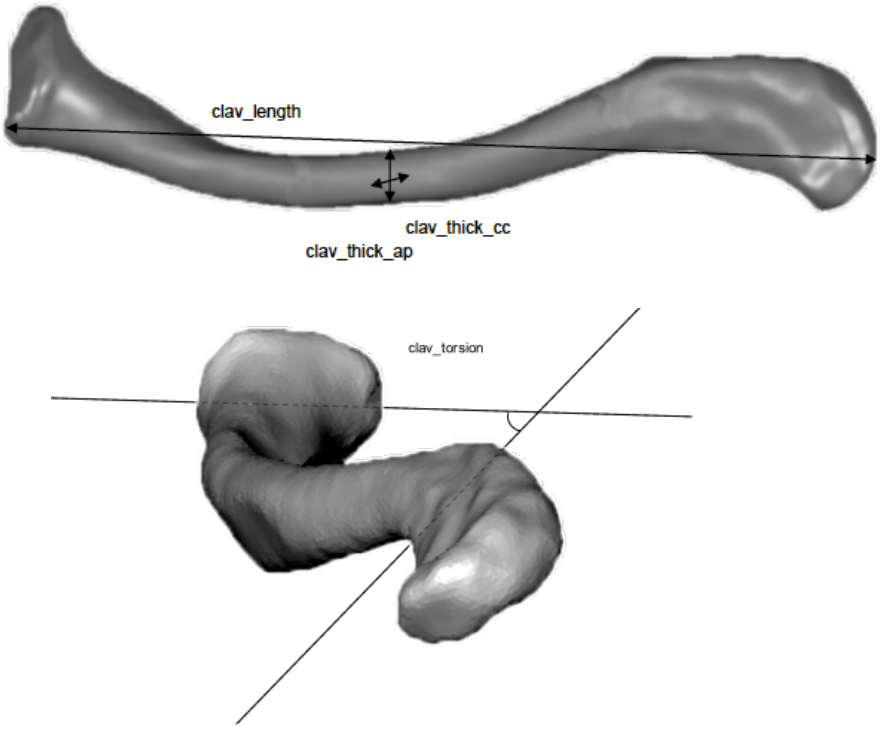

Figure 6 – Left human clavicle showing the measurements collected on the clavicle. Top: clavicle in distal (acromial view); bottom: clavicle in superior (cranial) view.

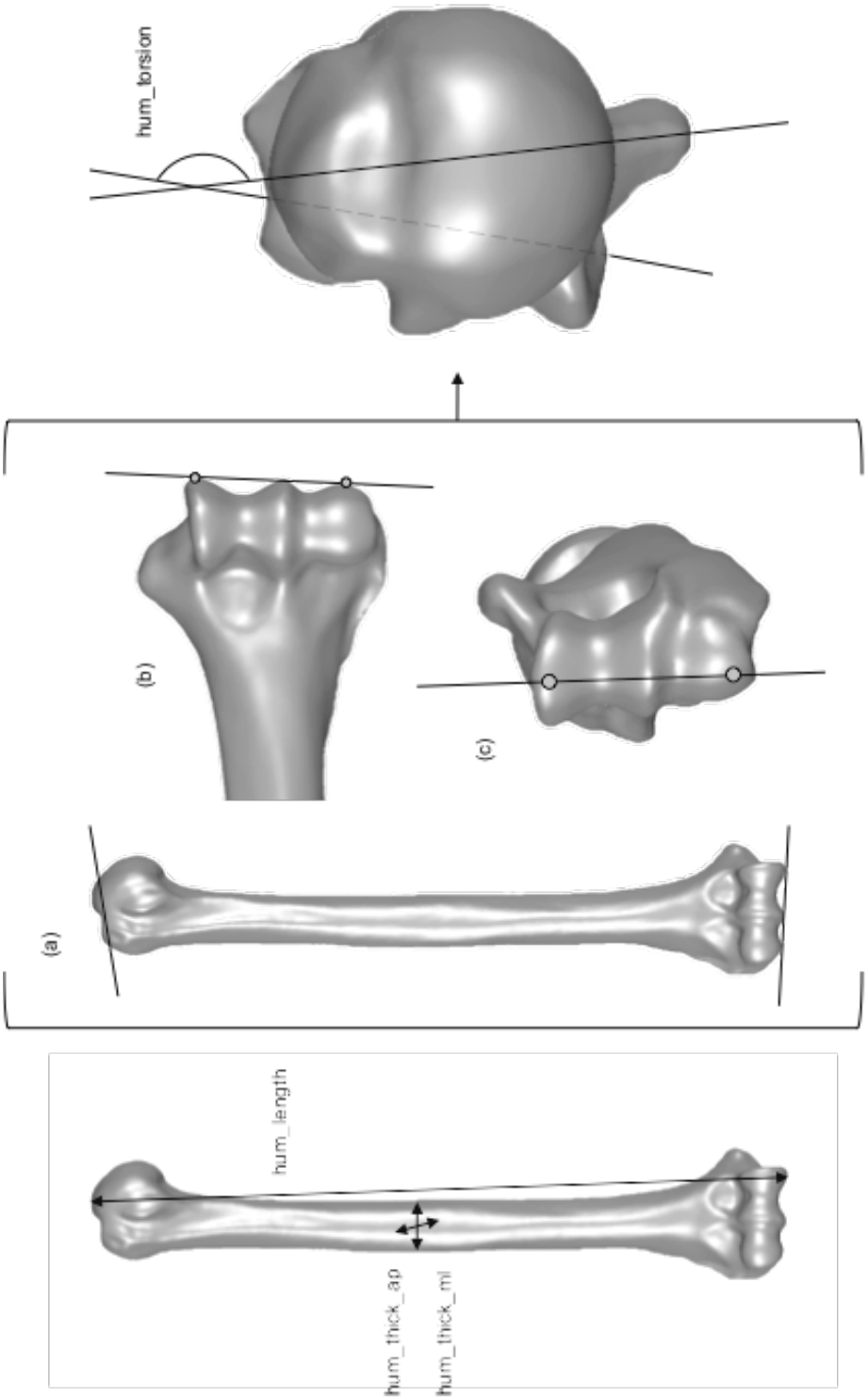

Figure 7 – Right human humerus, showing the measurements collected on the humerus. (a): humerus in anterior view; (b) distal end of the humerus in anterior view; (c) distal end of the humerus in distal view.

Table 1 – Table with the 30 shoulder measurements used in this research

Element	Measurement name	Measurement description
Clavicle	clav_length	Maximum length of the clavicle
	clav_thick_ap	Maximum thickness of the clavicle at midshaft (antero-posterior)
	clav_thick_cc	Maximum thickness of the clavicle at midshaft (cranio-caudal)
	clav_torsion	Clavicle torsion
	clav_angle_dist_ant	Distal angle of the clavicle (anterior view)
	clav_angle_dist_sup	Distal angle of the clavicle (superior/cranial view)
	clav_angle_prox_ant	Proximal angle of the clavicle (anterior view)
	clav_angle_prox_sup	Proximal angle of the clavicle (superior/cranial view)
	clav_freecurv_dist	Distal angle of the clavicle using 'freecurve' method
	clav_freecurv_prox	Proximal angle of the clavicle using 'freecurve' method
Humerus	hum_length	Maximum length of the humerus
	hum_torsion	Medial rotation of the humeral head over the humeral shaft
Scapula	scap_height	Maximum height of scapular body
	scap_breadth_spine_glen	Maximum breadth of the scapula from the glenoid fossa to where the long axis of the scapular spine and the vertebral border meet
	glen_angle_latborder	Angle of the glenoid fossa to the lateral border of the scapula
	glen_angle_medborder	Angle of the glenoid fossa to the medial border of the scapula
	glen_angle_spine	Angle of the glenoid fossa to the spine of the scapula
	glenoid_angle_bodyspine	Angle of the glenoid fossa to the scapular body below the spine
	glen_version	Version of the glenoid fossa relative to the body of the scapula
	latborder_spine_angle	Angle of the scapular spine to the lateral border of the scapula
	spine_angle_medborder	Angle of the scapular spine to the medial border of the scapula
	scap_spine_length	Maximum length of the scapular spine from the medial border to the tip of the acromion
	scap_infra_length	Maximum length of the infraspinous fossa
	scap_infra_length_90	Maximum length of the infraspinous fosssa (at 90 degree angle from spine)
	scap_supra_length	Maximum length of the supraspinous fossa
	scap_supra_length_90	Maximum length of the suprapinous fosssa (at 90 degree angle from spine)
	scap_infra_surf	Surface area of the infraspinous fossa
	scap_supra_surf	Surface area of the supraspinous fossa
	scap_breadth_infra	Maximum breadth of the scapula's infraspinous fossa (below the spine)
	scap_breadth_supra	Maximum breadth of the scapula's supraspinous fossa (above the spine)

3.2.1. Clavicle

clav_length: Maximum length of the clavicle. Measured from the distal (acromial) end to the proximal (sternal) end.
clav_thick_ap: Maximum antero-posterior thickness of the clavicle at midshaft. Midshaft was measured at 50% of the maximum length of the clavicle.
clav_thick_cc: Maximum cranio-caudal thickness of the clavicle at midshaft. Midshaft was measured at 50% of the maximum length of the clavicle
clav_torsion: Torsion of the distal clavicle relative to the proximal clavicle. This was measured as the intersection of a line of maximum length passing antero-posteriorly through the distal third of the clavicle (before the distal curvature), and a line of maximum length of the proximal (sternal) end of the clavicle, bisecting it into two equal halves. The obtuse angle is measured.
clav_angle_dist_ant: Distal angle of the clavicle (2D) in ventral view[1].
clav_angle_dist_sup: Distal angle of the clavicle (2D) in cranial view[1].
clav_angle_prox_ant: Proximal angle of the clavicle (2D) in ventral view[1].
clav_angle_prox_sup: Proximal angle of the clavicle (2D) in cranial view[1].
clav_freecurv_dist: Distal curvature of the clavicle in 3D[1].
clav_freecurv_prox: Proximal curvature of the clavicle in 3D[1].[1]

3.2.2. Humerus

hum_length: Maximum length of the humerus from the head of the humerus to the distal epicondyles of the humerus.
hum_torsion: Humeral torsion. Defined as the obtuse angle formed between the orientation of the humeral head and the orientation of the distal condyles of the humerus. This angle is measured using the intersection, viewed from the cranial perspective, of a line drawn through the centre of the humeral head dividing it into anterior and posterior halves, and a line passing through the centre of the capitulum

[1] See the next section and Chapter 6 for a detailed description on how these measurement protocols.

and trochlea (as defined by Krahl and Evans 1945; Rhodes 2006; Cowgill 2007; see Chapters 3, 4 and 5 for further details).

3.2.3. Scapula

scap_height: Maximum scapular height. Measured between the inferior and the superior angles of the scapula.
scap_breadth_spine_glen: Maximum breadth of the scapular body where the spine attaches to the body of the scapula. Measured from below the glenoid fossa to the medial border of the scapula where the spine meets the medial border.
glen_angle_latborder: Angulation of the glenoid fossa relative to the lateral border of the scapula. I report the acute angle (Haile-Selassie et al. 2010).
glen_angle_medborder: Angulation of the glenoid fossa relative to the medial border of the scapula (measured as the line from the inferior to the superior angle). I report the obtuse angle.
glen_angle_spine: Angulation of the glenoid fossa relative to the scapular spine.
glenoid_angle_bodyspine: Angulation of the glenoid fossa relative to body of the scapula where the scapular spine meets the body.
glen_version: Angulation of the glenoid fossa relative to the body of the scapula in transverse plane. Measured on the posterior side (as defined by Bokor et al. 1999; Nyffeler et al. 2003).
spine_angle_latborder: Angulation of the scapular spine relative to the lateral border of the scapula.
spine_angle_medborder: Angulation of the scapular spine relative to the medial border of the scapula (measured as the line from the inferior to the superior angle).
scap_spine_length: Maximum length of the scapular spine. Measured from the medial border of the scapula, where the spine meets the medial border, to the tip of the acromion.
scap_infra_length: Maximum length of the scapula's infraspious fossa. Measured between the inferior angle and the medial border of the scapula where the spine meets the medial border.

scap_infra_length_90: Maximum length of the scapula's infraspious fossa measured at a 90-degree angle from the scapular spine to the medial border of the scapula.
scap_supra_length: Maximum length of the scapula's supraspinous fossa. Measured between the superior angle and the medial border of the scapula where the spine meets the medial border.
scap_supra_length_90: Maximum length of the scapula's supraspinous fossa measured at a 90-degree angle from the scapular spine to the lateral border of the scapula.
scap_infra_surf: Maximum surface area of the scapula's infraspinous fossa.
scap_supra_surf: Maximum surface area of the scapula's supraspinous fossa.
scap_breadth_infra: Maximum breadth of the scapular body at the infraspinous fossa. Measured between the lateral and medial borders of the scapula below the spine.
scap_breadth_supra: Maximum breadth of the scapular body at the supraspinous fossa. Measured between the lateral and medial orders of the scapula above the spine.

3.3. Protocols for measuring surface areas, curvatures, torsion and angles

3.3.1. 3D curvatures

Curvatures were measured on the distal and proximal clavicle. The procedure for measuring curvatures was devised for the purposes of this study. Curvatures were measured using the curve fitting options 'Draw Curve' and 'Free Curve' in Geomagic 12.1 (figure 8). The two polylines are fitted such that they represent two arches of a circle, and their curvatures (k) are measured (in mm) as a function of the circle's radius (R):

$$k = 1 / \mathrm{R}$$

Details on how these measurement were collected and full protocol description can be found in Chapter 6.

3.3.2. Angles

Angles were measured on the humerus to determine torsion, on the clavicle to determine both torsion and 2D proximal and distal angles of the clavicle, and on the scapula, to determine the angulations of the scapular spine and glenoid fossa relative to each other and to the scapular borders. In all cases, the angles were measured by drawing lines through the segments of interest – for example, a line drawn through the centre of the humeral head dividing it into anterior and posterior halves, and a line passing through the centre of the capitulum and trochlea, for measuring humeral torsion –, and measuring the angle at the intersection of those lines. These lines are first drawn in a 3D environment (either Geomagic Suite 12.1 or Amira 3.1); the bone is then oriented in the plane of interest and the image is transferred to tpsDigs as a 2D image. The angles are estimated in tpsDigs using the 'Measure Angle' function, as the intersection of these lines. More details about how these measurements are obtained for individual bones can be found in Chapters 3 and 4.

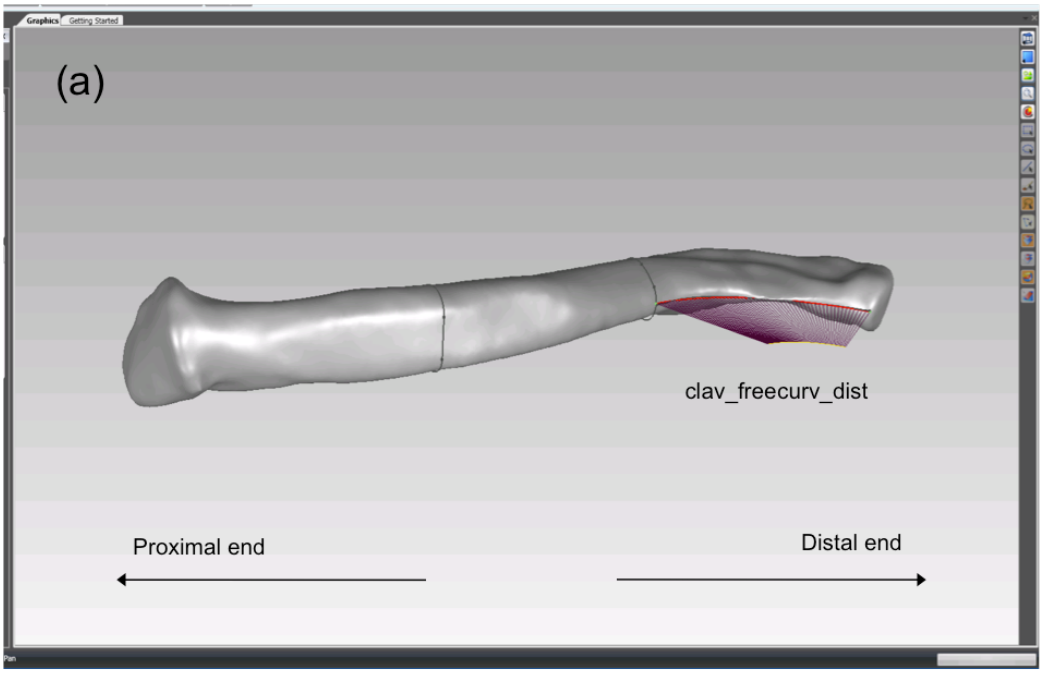

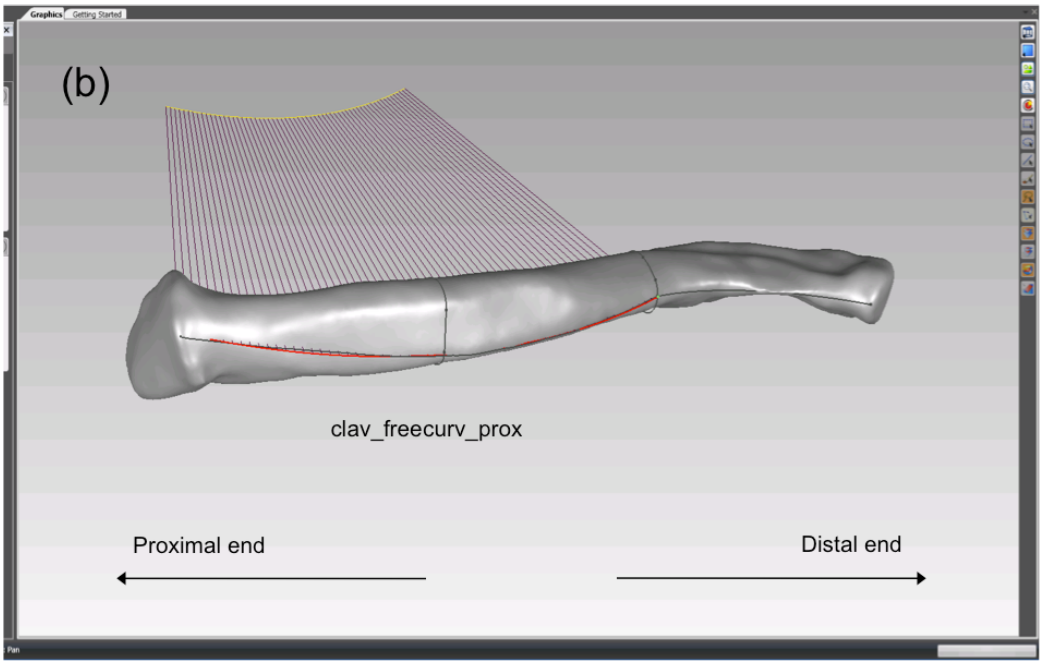

Figure 8 – 3D surface scan of an adult human left clavicle (ventral view) with the fitted distal (a), and proximal (b) profile curves. The profile curves are obtained from the reference polyline using the 'Edit Curve' function in Geomagic 12.1 (see figure 10). The profile curves represent arches of a circle; using the 'Analyse Curve' function in Geomagic Suite 12.1, the curvature measurements for both curves are calculated as a function of each circle's radius (in mm).

3.3.3. Surface areas

Surface areas of the supraspinatus and infraspinatus foassae of the scapula were measured in Geomagic 12.1. These areas were delineated using an automated function ('Extract Curve' function), which detects object contours and extracts curvatures based on these contours. In order to standardize the procedure across scapulae (figure 9a), the 'curvature sensitivity' setting was set to 80, the 'separator sensitivity' set to 10, and the 'minimum area' set to 100mm^2. These settings were found to correctly identify the relevant borders and isolate the two areas of interest across specimens, and produced reproducible results (see table 2). Once the contours are identified (figure 9b), the curves are extracted using the 'Compute Curve' and 'Extract Curve' functions (figure 9c). The curves are then converted to boundaries (using the 'Convert to Boundaries' function) (figure 9d), which allow to select the isolated areas via the 'Select Bounded Component' tool (figure 9e,f), and compute the surface area using the 'Compute Area' measuring tool.

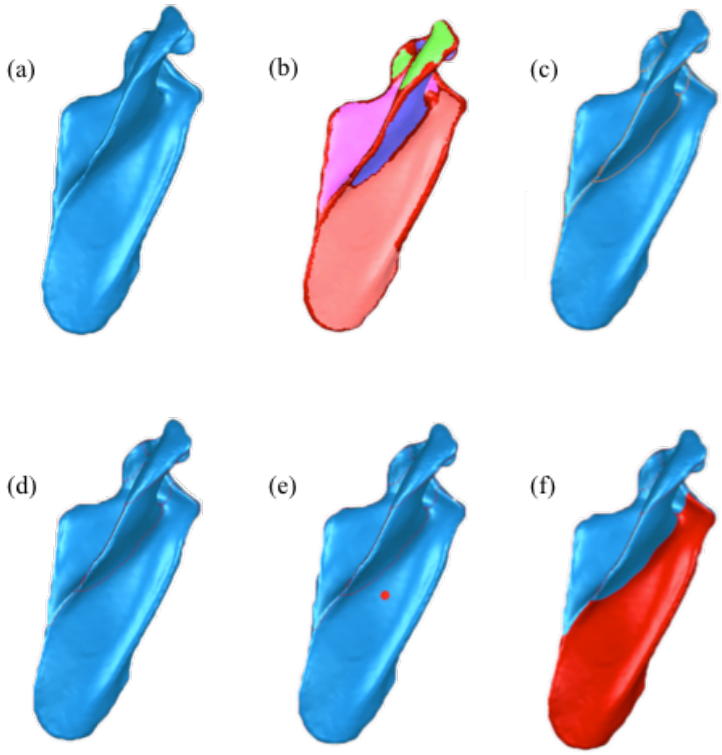

Figure 9 - 3D surface scan of a right *Hylobates lar* scapula showing the procedure to calculate surface areas of the supraspinous and infraspinous fossae. See text for detailed description.

3.4. Error

Intraobserver error was estimated following Tim White's procedure for estimating error (White et al. 2011) – it reports the percentage difference between repeated measurements in relation to 10 averaged repeat measurements (table 2). For every measurement, intraobserver error is approximately 2 to 10 times smaller than the average differences between specimens.

4. Ontogeny

In order to quantify ontogenetic changes in the development of the shoulder, all individual specimens were either of known age (in the case of humans) or were aged using relative dental ages (all hominoids and *Macaca fascicularis*). Hence, my sample only includes individual non-human primates for which radiographic information on the dentition is available. These were either generously provided by Prof. Christopher Dean (UCL), Dr. Julia Boughner (University of Saskatchewan) and Dr. Wendy Dirks (Newcastle University), or collected for the purpose of this study in the case of the orangutans (at the Zoologische Staatssammlung München & Staatssammlung für Anthropologie und Palaeoanatomie München, and at the Natural History Museum, London).

4.1. Dentition

For the purpose of this study, the goal was not to establish precise ages in years, which would require combining imaging data with histological data for each individual specimen, but rather to rank the individuals according to growth stages, from birth to adulthood, in order to obtain an ontogenetic series. For this reason,

Table 2 – Error table. The percentage differences for repeat measurements reports the mean differences between repeated measurements in relation the 10 averaged repeat measurements. The percentage difference for the total sample measures the average differences between adult human individuals.

Measurement	Sample	*N*	Mean difference (%)	Standard deviation
clav_length	Total	42	8.894	21.482
	Remeasurements	10	0.127	0.206
clav_thick_ap	Total	42	16.911	1.783
	Remeasurements	10	6.790	0.295
clav_thick_cc	Total	42	16.163	1.599
	Remeasurements	10	3.475	0.482
clav_torsion	Total	42	23.734	28.196
	Remeasurements	10	16.575	1.406
clav_dist_ant	Total	42	3.402	5.392
	Remeasurements	10	1.281	1.491
clav_dist_sup	Total	42	4.324	4.533
	Remeasurements	10	0.971	0.665
clav_prox_ant	Total	42	2.776	4.355
	Remeasurements	10	1.233	1.633
clav_prox_sup	Total	42	2.512	4.233
	Remeasurements	10	0.957	1.576
clav_freecurv_dist	Total	42	24.817	0.006
	Remeasurements	10	3.007	0.001
clav_freecurv_prox	Total	42	17.684	0.001
	Remeasurements	10	1.758	0.000
hum_length	Total	42	4.755	12.032
	Remeasurements	10	0.063	0.153
hum_torsion	Total	42	3.805	4.463
	Remeasurements	10	1.030	1.625
scap_height	Total	42	7.816	7.379
	Remeasurements	10	0.093	0.164
scap_breadth_spine_glen	Total	42	6.306	4.527
	Remeasurements	10	0.783	0.535
glen_angle_latborder	Total	42	3.279	3.278
	Remeasurements	10	0.657	0.661
glen_angle_medborder	Total	42	31.744	2.328
	Remeasurements	10	10.612	0.587
glen_angle_spine	Total	42	3.445	2.336
	Remeasurements	10	1.235	0.716
glenoid_angle_bodyspine	Total	42	3.376	2.395
	Remeasurements	10	3.962	2.370

Table 2 cont'd – Error table. The percentage differences for repeat measurements reports the mean differences between repeated measurements in relation the 10 averaged repeat measurements. The percentage difference for the total sample measures the average differences between adult human individuals.

Measurement	Sample	*N*	Mean difference (%)	Standard deviation
glen_version	Total	42	4.269	2.490
	Remeasurements	10	2.676	2.165
latborder_spine_angle	Total	42	10.250	3.024
	Remeasurements	10	2.013	0.414
spine_angle_medborder	Total	42	2.872	2.127
	Remeasurements	10	0.420	0.230
scap_spine_length	Total	42	7.175	6.298
	Remeasurements	10	0.222	0.266
scap_infra_length	Total	42	7.834	5.873
	Remeasurements	10	0.476	0.276
scap_infra_length_90	Total	42	8.121	6.062
	Remeasurements	10	2.024	2.998
scap_supra_length	Total	42	10.207	3.503
	Remeasurements	10	1.072	0.374
scap_supra_length_90	Total	42	13.294	4.364
	Remeasurements	10	1.559	0.449
scap_infra_surf	Total	42	16.275	814.359
	Remeasurements	10	0.461	64.646
scap_supra_surf	Total	42	17.077	336.361
	Remeasurements	10	2.196	84.189
scap_breadth_infra	Total	42	11.483	5.537
	Remeasurements	10	3.498	1.269
scap_breadth_supra	Total	42	6.823	4.465

Dean and Wood's (1981) atlas method is considered to be an adequate indicator of relative ages applicable to all apes, and sufficiently detailed for obtaining an ontogenetic series for each ape taxon (figure 10). This method allows splitting the sample into equal time spans, rather than the great jumps of unequal time represented by eruption stages alone, for a more accurate representation of ontogenetic change (Dean and Wood 1981; Boughner and Dean 2008).

The atlas method was developed by Dean and Wood (1981) as part of a study focusing on the cranial base of fossil hominids from East and South Africa, and involved the construction of a growth series of the three genera of apes (*Pongo, Pan and Gorilla*) to build a chart, or 'atlas'. This was devised by tracing the developing teeth from one quadrant of the upper jaw and one quadrant of the lower jaw for juvenile specimens collected at the Natural History Museum in London and the Powell-Cotton Museum in Kent. This chart can be used to assign specimens a relative dental developmental age ranging from 0 – 11 years. Dean and Wood's (1981) 'atlas method' for assigning Approximate Relative Dental Aging scores (ARDA) was used on my bonobo, chimpanzee, gorilla, and orangutan samples. The great ape dentition was scored by identifying stages of dental formation, from X-ray images of the mandibular dentition, for each specimen. Because this information is non-existent for gibbons, I also created an atlas for the gibbon dentition based on Dean and Wood's (1981) method and protocol. The gibbon atlas was created in collaboration with Prof. Christopher Dean (UCL) and Dr. Wendy Dirks (Newcastle University) and is described in detail below. The macaque dentition was scored using Swindler's (1985) chart of *Macaca* dental development. The human samples consist of individuals of known age (Molleson et al. 1993; Cardoso 2005). In humans, studies have shown that methods based on mineralization stages of dental formation, and radiographic images produce estimated ages within 0.52 ($\pm$ 0.62) years for deciduous teeth and 0.57 ($\pm$ 0.42) years for permanent teeth, of the chronological age (Liversidge and Molleson 1999; Liversidge 2005). I consider this sufficient evidence that the human and primate samples can be adequately compared to each other despite the differences in aging methods.

The *Pan trogoldytes,* and *Gorilla gorilla* and *Pongo pygmaeus* X-rays are from Dean and Wood's (1981) study and were collected from specimens at the Natural History Museum in London and the Powell-Cotton Museum in Kent. The *Pan paniscus* X-rays belong to Dr. Julia Boughner (Boughner and Dean 2008; Boughner et al. 2012) and were collected at the Koninklijk Museum voor Midden-Afrika, Tervuren. The *Macaca fascicularis* and *Hylobates lar* X-rays belong to Dr. Wendy Dirks (Newcastle

University) the Department of Anthropology at New York University and the Universität Zürich Anthropological Institute and Museum (Dirks 1998, 2003; Dirks and Bowman 2007). Additional I collected extra *Pongo* X-rays at the Zoologische Staatssammlung München & Staatssammlung für Anthropologie und Palaeoanatomie München, and at the Natural History Museum, London.

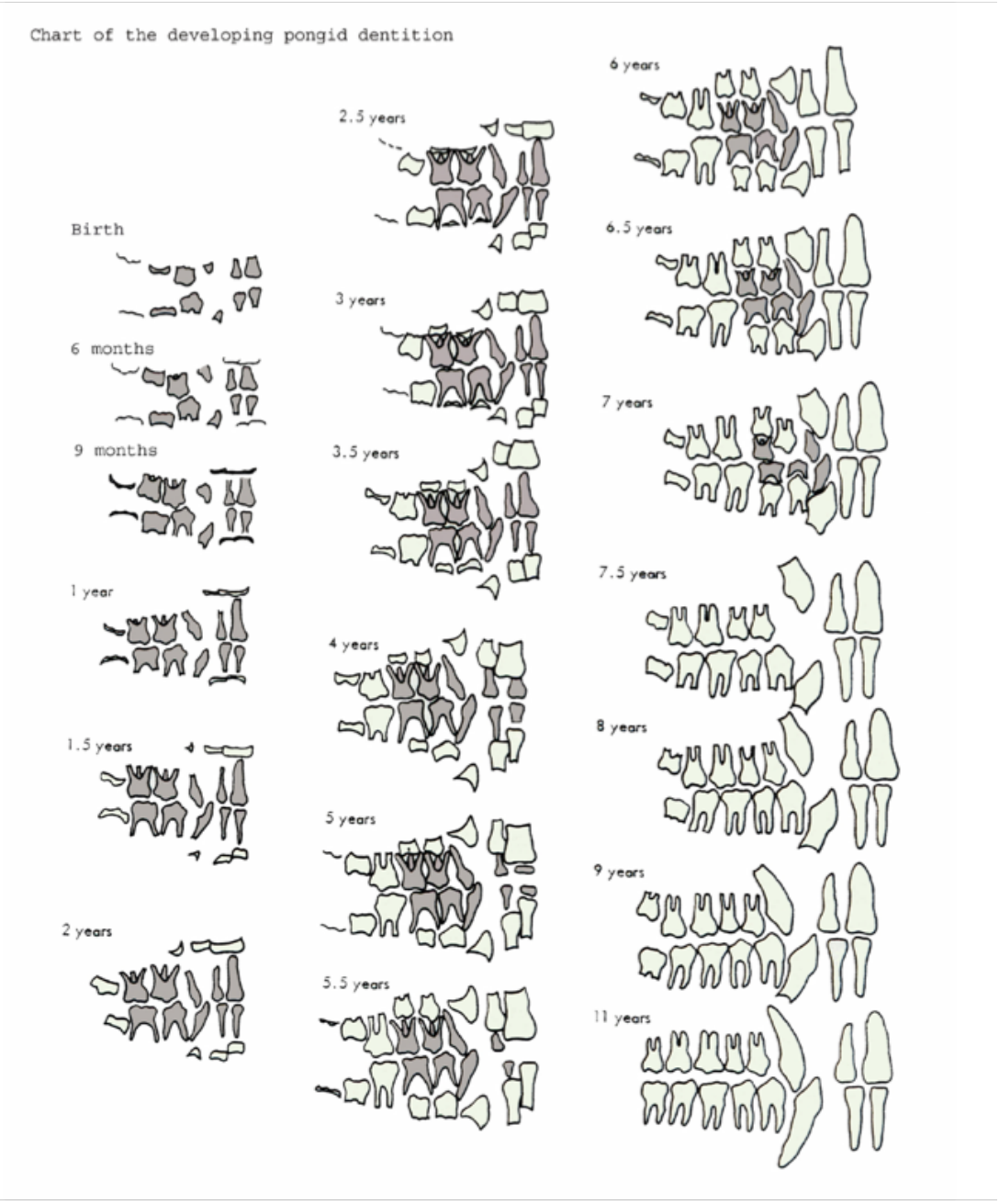

Figure 10 – Atlas of great ape dental development (from Dean and Wood, 1981).

4.1.1. Atlas of gibbon dental development

Because an atlas of dental development does not presently exist for gibbons, one was created for the purpose of this study. This was done in collaboration with Prof. Christopher Dean (UCL) and Dr. Wendy Dirks (Newcastle University), both of whom generously provided the X-rays and histological sections, and helped design the protocol for the atlas. The goal was to provide a chronological time scale for the developing dentition of *Hylobates lar* (based on Dean and Wood's [1981] atlas method). We used a combination of cross-sectional radiographic data of 18 juvenile gibbon mandibles and histological sections of three lower molars (M_1, M_2 and M_3), one lower premolar (P_4) and one lower canine from individuals with histologically derived ages at death (AS1627, from the Zurich collection, NYU008 and NYU029 from the Department of Anthropology at New York University [Dirks 1998]). The P_3 was too damaged to be included in the study, and the incisors (I_1, I_2) were left out because, unlike the molars, premolars and canines, they develop very quickly after birth and therefore are the least informative teeth in the mandible. In the future however, these can be added to the atlas to refine some of the earlier stages of dental formation.

The *Hylobates lar* X-rays as well as the histological information were obtained at the Universität Zürich Anthropological Institute and Museum and the Department of Anthropology at New York University by Dr. Wendy Dirks during the course of her PhD in 1996. Based on the X-rays, 8 separate stages of tooth mineralization were identified for all teeth. Growth increments in the crown and root of histological sections of each tooth were used to determine the age for each of these 8 stages. When information on all teeth is combined, 11 separate stages of mandibular dental formation were identified across all 18 X-rays, which provided a time-scale of postnatal dental development spanning from 0.42 yrs to $\geq$ 8 yrs.

4.1.1.1. Protocol

In order to create the atlas, the first step involved inspecting the 18 X-rays to determine what stages of tooth mineralization could be easily and realistically observed for each tooth across specimens. From these observations, 10 stages of tooth formation with 8 stages of tooth mineralization were established: empty crypt, crown initiation, crown initiation + ¼, crown initiation + ½, crown initiation + ¾, crown completion, root initiation + ¼, root initiation + ½, root initiation + ¾, and root completion (with apex closed). The first two stages: empty crypt and crown initiation were however, not used to age the specimens (figure 11).

The next step involved identifying the corresponding stages in the histological sections of three lower molars (M_1, M_2 and M_3), one lower premolar (P_4) and one lower canine from individuals with histologically derived ages at death (AS1627, NYU008 and NYU029) (see Dirks [1998] for details on how age at death was derived). Transmitted polarized light microscopy was used to analyze the thin sections using an Olympus BX51 microscope mounted with a QImaging Micropublisher 3.3 RTV camera. Images from the microscope were transmitted to a Macintosh computer equipped with image processing software, Improvision Openlab 5.0.2. Finally, individual images taken at the same magnification were standardized to the same enlargement size and merged together using Adobe Creative Suite 5 (Dirks 1998) (figure 12). The crown and root sections for each tooth were then divided into quarters and the Striae of Retzius – daily incremental growth lines – between these quarters were manually counted when it was possible; when this was not possible, formation time was determined by measuring along an enamel prism from the enamel dentine junction (EDJ) to the enamel surface and dividing by the average daily enamel secretion rate, calculated from the distances between adjacent cross striations (figure 13). This allowed obtaining an age in days for each of the 8 stages/quarters of tooth mineralization, for each tooth – from which an age in years was then derived (table 3).

Finally, the corresponding age (in years) was assigned to each tooth (M_1, M_2 and M_3, P_4, C) for each X-ray. The ages of all teeth with incomplete development were averaged and an Approximate Relative Dental Age (ARDA) was assigned to each mandible/specimen. Based on the 18 X-rays, 11 stages of mandibular dentition formation spanning from birth to adulthood could be easily identified and aged using this method. I therefore used this information to design the final atlas: containing 11 stages with a corresponding age in years (figure 14). This in turn allows for assigning approximate relative dental ages (ARDA) to individual lar gibbon specimens in the absence of known age at death and/or histological information, in a way that is comparable to Dean and Wood's (1981) great ape atlas (figure 15). Future work should include histological data for the remaining mandibular dentition (I_1, I_2, P_3) thus increasing the resolution of the method.

Stage	Description	X-ray
Crypt Empty	Large sphere with no visible signs of tooth mineralization	
Crown Initiation	Visible signs of mineralization (one or more cusps)	
Crown ¼	Approximately one quarter of the tooth crown is mineralized	
Crown ½	Approximately half of the tooth crown is mineralized	
Crown ¾	Approximately three quarters of the tooth crown is mineralized	
Crown Complete	The crown is visibly complete but no root is visible	
Root ¼	Approximately one quarter of the root is complete	
Root ½	Approximately half of the root is complete	
Root ¾	Approximately three quarters of the root is complete	
Root Complete with Apex Closed	Root is complete and the apex is closed	

Figure 11 – Dental development in gibbons with descriptions of the stages of tooth development/ mineralization that can be identified based on the X-ray images.

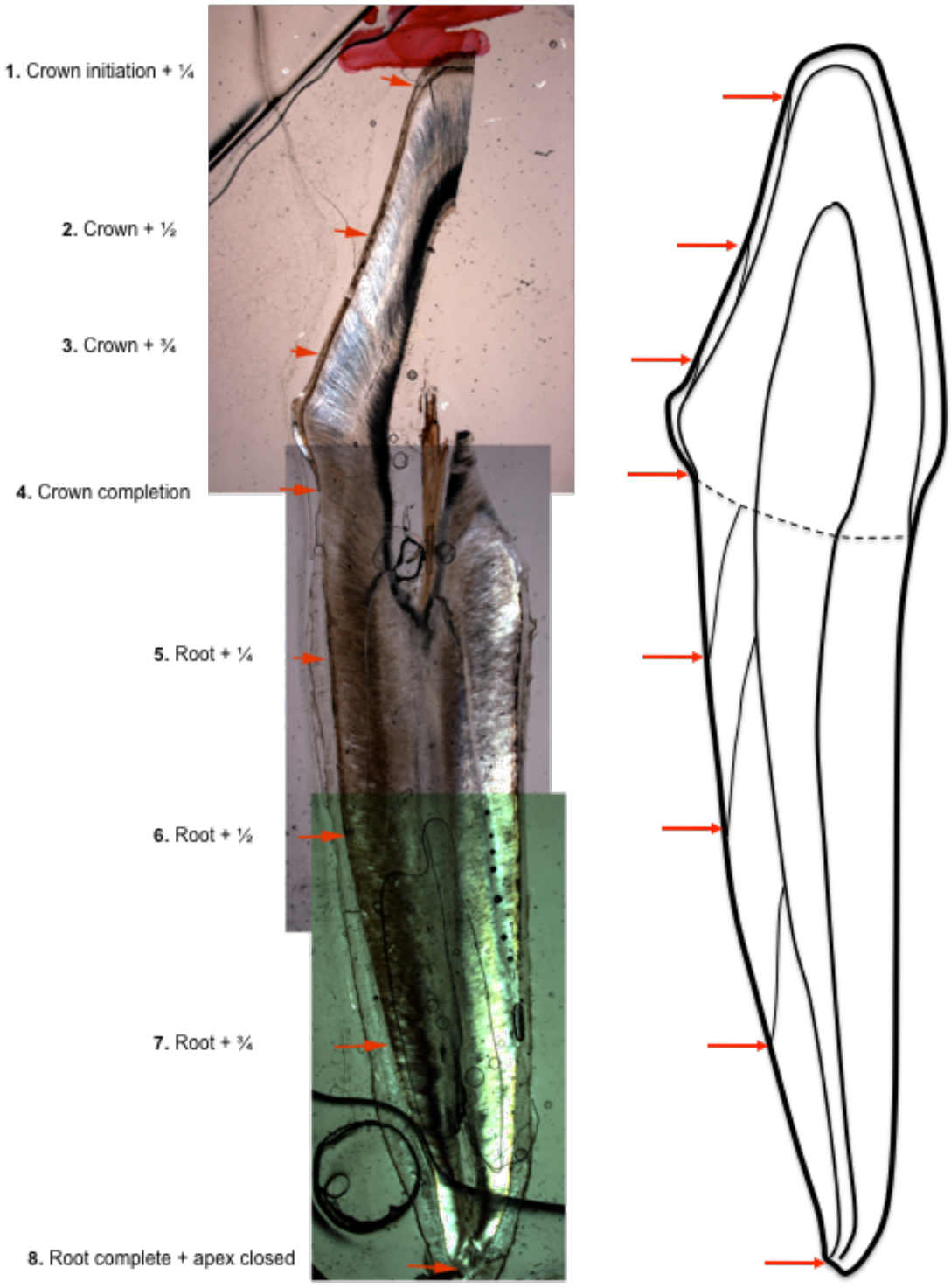

Figure 12 – Tooth section of the lower left canine (NYU11). Left: composite image of the histological tooth section merged in Photoshop CS5; right: drawing of the tooth section showing direction of the Striae of Retzius on the enamel (crown), and dentine (root). The red arrows indicate the stages of tooth mineralization that were used in this study.

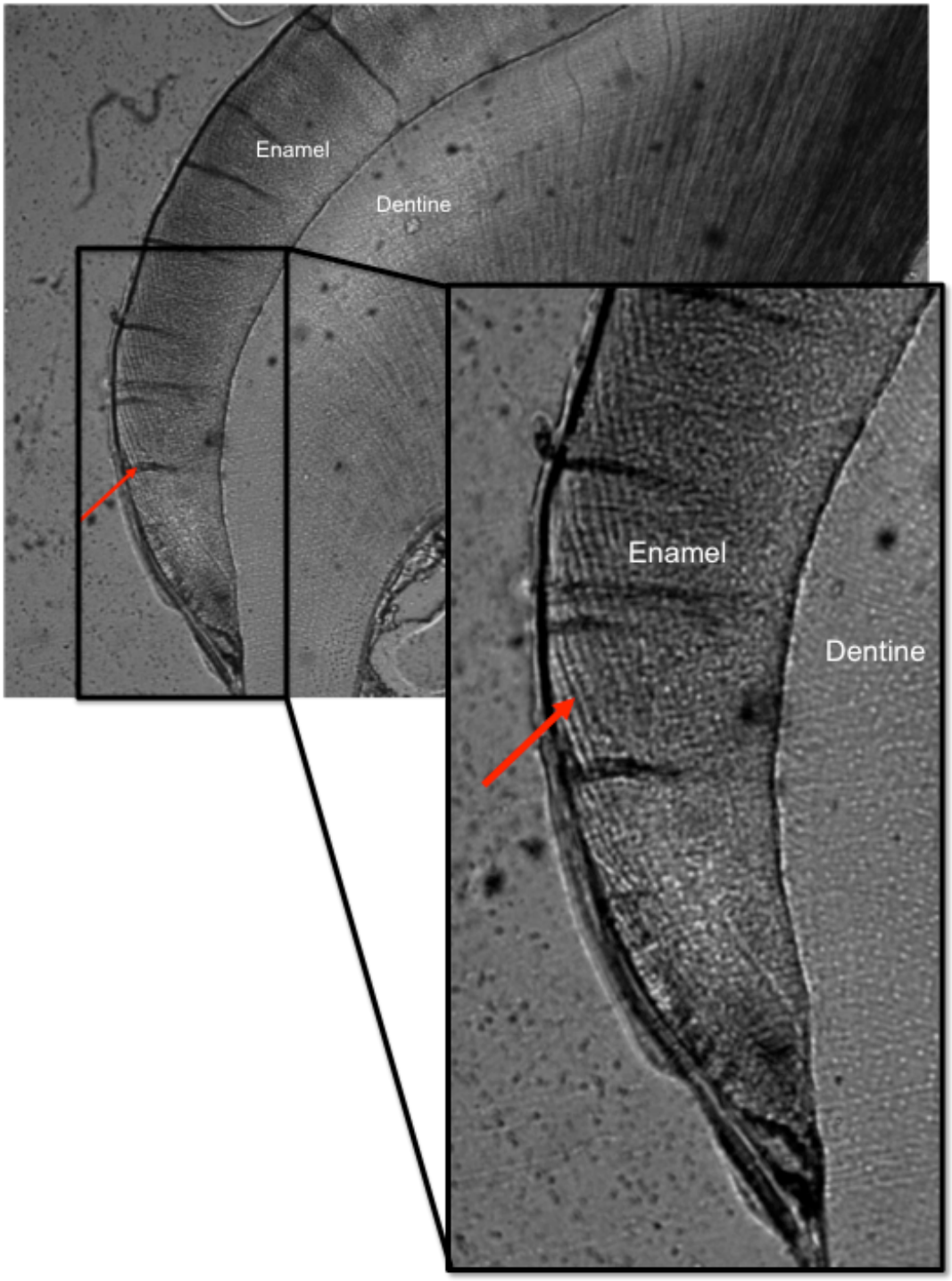

Figure 13 – Tooth section of the lower left P_4 (NYU0029). The image shows the buccal cusp at the base of the crown. The red arrows indicate the Striae of Retzius – daily increment lines – that were counted between each stage.

Table 3 – Table with age in days (and years) for each tooth mineralization stage, for each tooth.

Tooth	Specimen	Crown initiation + ¼	Crown initiation + ½	Crown initiation + ¾	Crown completion
Canine	NYU11	272 (0.74 yrs)	688 (1.87 yrs)	1016 (2.77 yrs)	1268 (3.46 yrs)
Premolar (P4)	NYU0029	538 (1.46 yrs)	686 (1.88 yrs)	815 (2.22 yrs)	967 (2.65 yrs)
Molar (M1)	AS1627	83 (0.23 yrs)	193 (0.53 yrs)	211 (0.58 yrs)	399 (1.08 yrs)
Molar (M2)	NYU0029 (crown)	432 (1.17 yrs)	528 (1.45 yrs)	730 (2 yrs)	890 (2.44 yrs)
	NYU008 and AS1627 (root)				
Molar (M3)	NYU0029 and AS 1627	922 (2.53 yrs)	982 (2.68 yrs)	1126 (3.07 yrs)	1170 (3.20 yrs)

Tooth	Specimen	Root initiation + ¼	Root initiation + ½	Root initiation + ¾	Root completion
Canine	NYU11	1555 (4.25 yrs)	1789 (4.90 yrs)	2728 (7.46 yrs)	3320 (9.09 yrs)
Premolar (P4)	NYU0029	1138 (3.12 yrs)	1206 (3.30 yrs)	1290 (3.52 yrs)	1362 (3.72 yrs)
Molar (M1)	AS1627	512 (1.40 yrs)	640 (1.74 yrs)	720 (1.93 yrs)	834 (2.27 yrs)
Molar (M2)	NYU0029 (crown)	938 (2.57 yrs)	1050 (2.88 yrs)	1150 (3.15 yrs)	1262 (3.46 yrs)
	NYU008 and AS1627 (root)				
Molar (M3)	NYU0029 and AS 1627	1250 (3.41 yrs)	2146 (5.88 yrs)	-	-

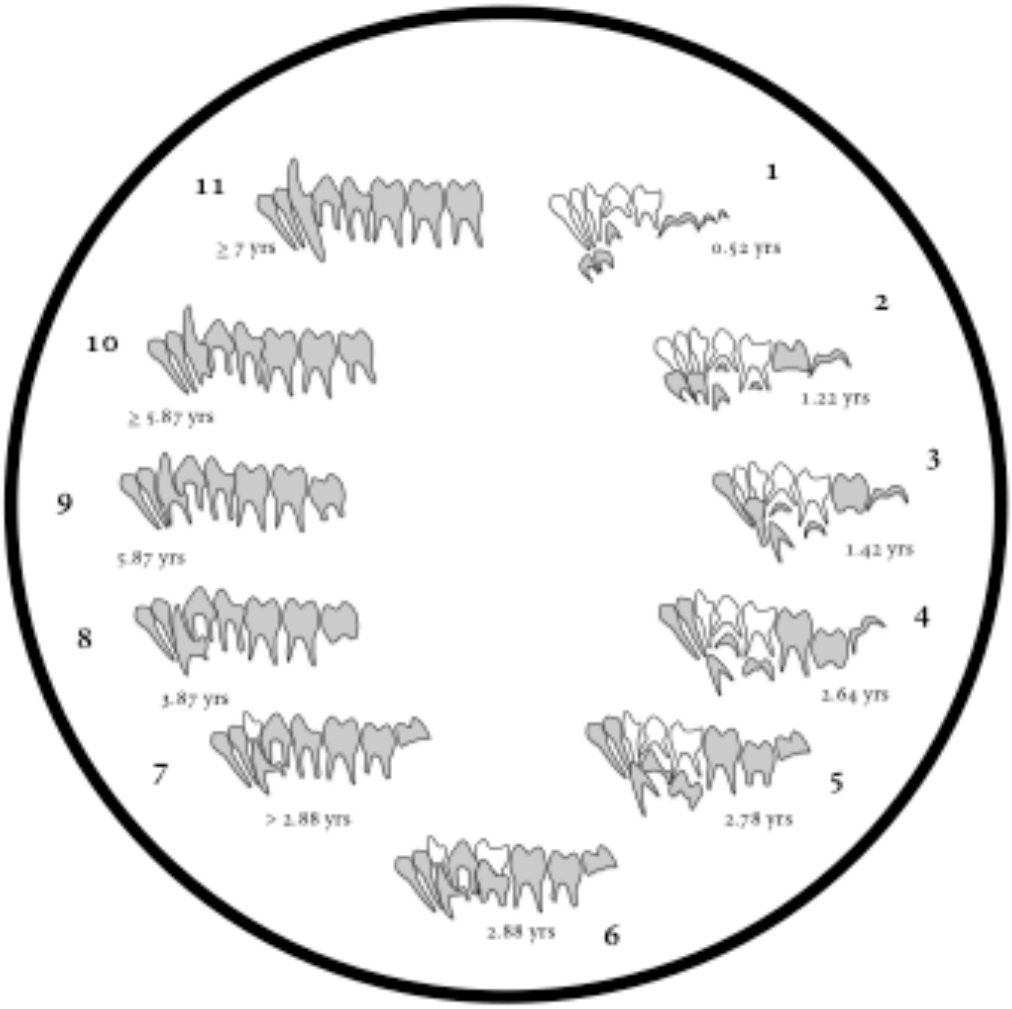

Figure 14 – Atlas of the developing lar gibbon dentition with Approximate Relative Dental Ages (ARDAs) attributed to each stage (deciduous teeth in white and permanent teeth in grey). 11 stages of mandibular tooth formation were identified based on the X-rays. Ages for each stage are based on the averaged ages of individual developing/incomplete teeth.

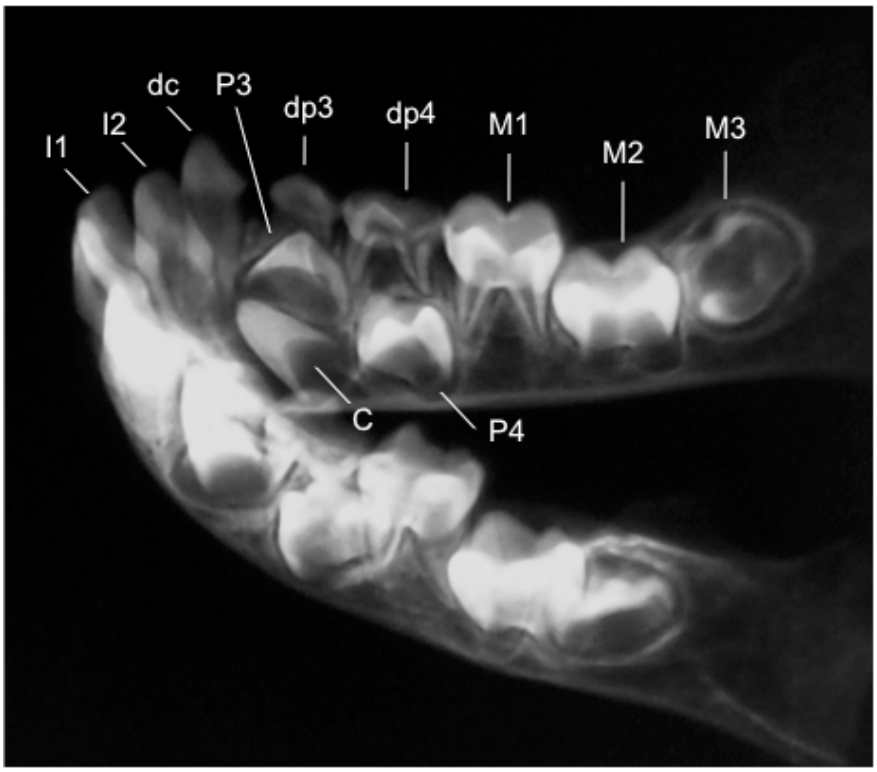

Figure 15 – X-ray of the mandibular dentition of AS1639 exemplifying how the atlas can be used. Based on the atlas, this specimen is at Stage 5 in its dental development, and therefore estimated to be about 2.86 years old.

5. Analysis

All statistical analyses (ontogenetic, phylogenetic, as well as within- and between-species differences) were conducted using R version 2.12.2 (R Core Development Team, 2011). The present study is innovative in that it uses growth curves to compare ontogenetic trajectories in the growth of the shoulder girdle between hominoid species. Additionally, this study is also innovative in its use of a new phylogenetically-integrated method – 'Independent Evolution' – to quantify evolutionary change along branches of a phylogenetic tree (Smaers and Vinicius 2009; Smaers et al. 2012).

5.1. Ontogeny: the use of Gompertz growth curves

Gompertz growth curves were fitted to the data using a self-starting three parameter Gompertz function in R version 2.12.2 (2011). The Gompertz function is a sigmoid

function developed for time series, and therefore temporally describes growth through successive phases of rapid, decaying, and asymptotic growth (Horton et al. 1998). I used a self-starting parameter rather than pre-defining a starting value (at x = 0) because in many of the samples the number of very young individuals close to birth was too small to provide a realistic estimate of the value at x = 0. The SSgompertz function estimates three parameters: the asymptotic value (Asym), the value at x=0 (b2), and a numeric parameter relating to the rate of growth (b3), for each distribution.

Usage in R: `SSgompertz(x, Asym, b2, b3)`

Arguments:

`x` : a numeric vector of values at which to evaluate the model (i.e. the data)
`Asym` : a numeric parameter representing the asymptote
`b2` : a numeric parameter related to the value of the function at `x` = 0
`b3` : a numeric parameter related to the scale of the `x` axis

Equation: $y(x)=Asym*\exp(-b2*b3^{x})$

Studies have shown that the overall process of skeletal maturation proceeds along a trajectory adequately predicted by this function (Horton et al. 2008), and therefore it is one of the most commonly used functions in studies of human growth and development as well as skeletal growth in mammals (Laird 1967; Jolicoeur 1985; Jolicoeur et al. 1988; German and Meyers 1989; Fiorello and German 1997; Humphrey 1998, 1999; Calzada et al. 1997; Read and Tolley 1997; Ramos et al. 2000; Koppe et al. 2000; Farmer and German 2004; Galatius 2005, 2010; Gonzalez et al. 2010; Valverde et al. 2010; Galatius and Goldin 2011; Galatius et al. 2011, 2012).

Because the atlas method for aging specimens according to dental formation does not permit aging individuals past M3 root completion, the same dental stage is attributed to all dentally adult individuals. In order to better fit a Gompertz model through the

samples and allow a comparison with humans (for which adult ages are known), adult individual points (for non-human primates) I attributed random ages up to a maximum of 40 years (figure 16 & table 4).

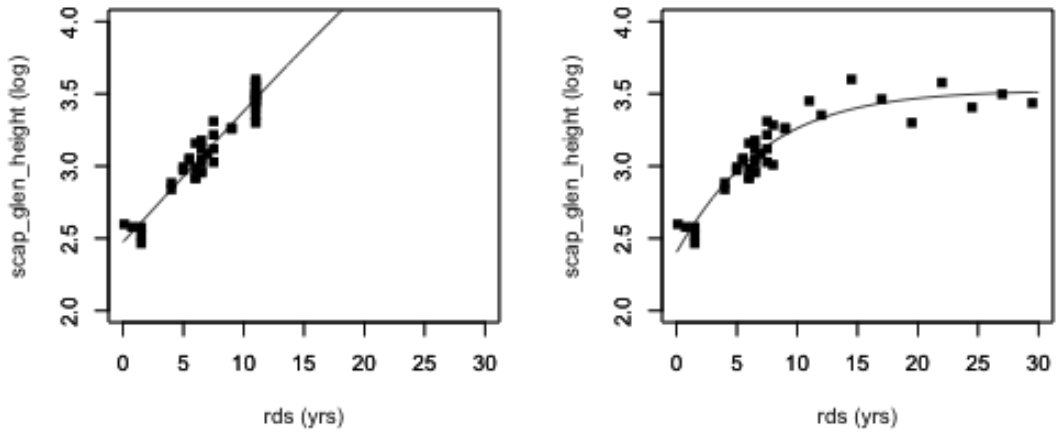

Figure 16 – Gompertz curve of glenoid fossa height in *Pan troglodytes*: with actual ARDA scores (left), and 'extended' adult scores ARDA scores (right). The Gompertz model cannot be fitted to this distribution (see table 4).

Table 4 – Gompertz parameter for *Pan troglodytes* glenoid fossa height growth models showing estimated value at growth completion (log) (Asymptote), estimated value at birth (b2), estimated rate of growth (b3), and the Residual Standard Error.

Species	Asymptote	Gompertz b2	Gompertz b3
P. troglodytes	7.607 (± 5.793)	1.123 (± 0.747)	0.968 (± 0.025)
P. troglodytes extended ages	3.523 (± 0.037)	0.382 (± 0.023)	0.851 (± 0.013)

5.2. Phylogeny: 'Independent evolution' and PGLS regressions

The study of shoulder morphology benefits greatly from being studied within a phylogenetic framework because much debate exists over whether the shared similarities in shoulder anatomy in hominoids are a product of shared ancestry or rather have evolved more recently in parallel. In order to discern clade-specific patterns in the hominoid shoulder girdle morphology, I use a phylogenetically-integrated approach that quantifies evolutionary changes along individual branches of an independently-derived (molecular-based) phylogeny. This method, 'Independent Evolution', developed by Dr. Smaers (Smaers and Vinicius 2009; Smaers et al. 2012, 2013), highlights processes of phenotypic change occurring across individual

branches of a phylogeny and therefore has the potential to identify processes such as convergence and mosaic evolution within the skeleton (figure 17). This approach moves away from direct species comparisons by (1) utilizing independently estimated (molecular) phylogenies to identify which morphological signals dominate the evolution of an anatomical module (e.g., humeral torsion) and (2) by inferring the timing and rate of evolutionary changes along individual lineages. By quantifying evolutionary changes along individual branches of the tree of life, this approach allows robust inferences of instances of independent evolution and provides a useful framework to help interpret fossil morphology. The primate phylogeny was taken from the 10k Trees Project (version 3) (Arnold and Nunn 2010). Fossil primates, when they are used, are placed onto the phylogeny according to published information (this is discussed and described in detailed in Chapter 5).

The appeal of incorporating phylogenetic information into morphological comparisons is especially evident when considering taxonomic groups and/or anatomical areas where homoplasies may be prevalent – which is the case with the hominoid shoulder. Indeed, the lack of congruence between phylogenetic trees based on molecular data and those based on morphological data has been a major topic of discussion over the last two decades (Begun 2007; Cannon and Manos 2001; Caumul and Polly 2005; Collard and O'Higgins 2002; Collard and Wood 2000; Collard and Wood 2001; Collard and Wood 2007; David and Laurin 1996; Frost et al. 2003; Klingenberg and Gidaszewski 2010; Leinonen et al. 2006; Neustupa and Skaloud 2007; Singleton 2002; Young 2008). Reconstructing trees from morphology assumes a clear association between morphological and evolutionary diversity, an assumption that is highly problematic when considering homoplasies, and in cases of mosaic evolution. Moreover, the lack of congruence between morphometric evolution and genetic differentiation results from the process of adaptation itself (Brehm et al. 2001; Cardini and Elton 2008; González-José et al. 2008; Hoekstra et al. 2004; Lockwood et al. 2004; Lycett and Collard 2005; MacLeod and Forey 2002; Michaux et al. 2007; Monteiro 2000; Naylor and Adams 2001; Polly 2001; Rohlf 2002; Zelditch et al. 1995); since understanding processes of adaptation is the primary goal of comparative

biology, rather than ‘removing’, ‘controlling’ or ‘accounting’ for a phylogenetic signal, a better alternative is to ‘map’ the morphological traits onto the phylogeny itself, thereby highlighting processes of adaption (including homoplasies) occurring across the branches of a phylogeny.

Phylogenetic Generalized Least Squares (PGLS) with likelihood-fitted Lambda are also performed using the package ‘Caper’ (Orme et al. 2012) in R version 2.12.2 (2011). Fort these analyses I use a sample of 6 hominoid species (species mean values of adult specimens only): *Homo sapiens* (n=42), *Gorilla gorilla* (n=12), *Pan troglodytes* (n=12), *Pan paniscus* (n=8), *Pongo pygmaeus* (n=7), *Hylobates lar* (n=10).

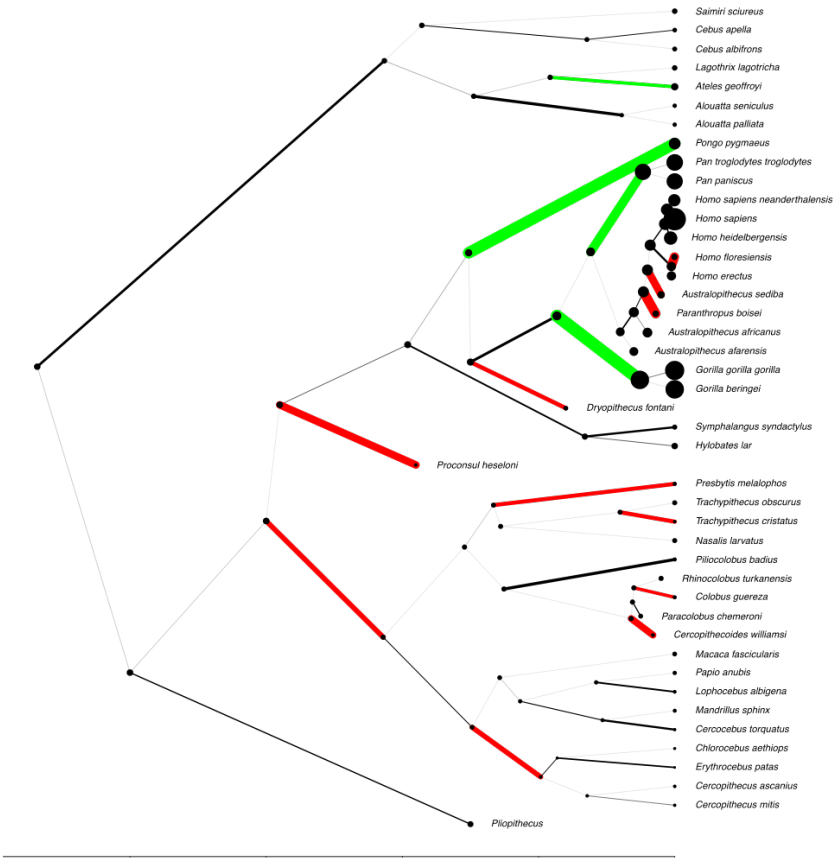

Figure 17 – Example of rates of evolution for a particular trait plotted along individual branches of an independently-derived (molecular-based) phylogeny, and estimated ancestral values plotted at the ancestral nodes and tips (red: decreases in the trait; green: increases in the trait; thickness of branch corresponds to extent of increase/decrease; size of black circles corresponds to size of the variable). The variable in this case is humeral torsion. Fossils are placed onto the tree according to published information (Kivell et al, 2011; Begun et al, 1997, 2012).

6. Behavioural data

For this study it is important to consider not only the differences in locomotion between hominoid species but the influence of body size on locomotion, and more importantly the influence of changing body size during ontogeny on locomotion.

Indeed, research has demonstrated that differences in body size influence locomotion, both in adult individuals, as well as throughout ontogeny (Bell 1971; Jarman 1974; Kleiber 1975; Chivers and Hladik 1984; Milton 1984; Fleagle 1985; Harvey et al, 1987; Doran 1997). For example, it is well established that larger animals are more terrestrial than smaller animals and when in an arboreal habitat, larger animals tend to either use larger substrates or perform different locomotor activities than smaller animals (Napier, 1967; Cartmill, 1974; Cartmill & Milton, 1977; Fleagle, 1985; Fleagle & Mittermeier, 1980; Crompton, 1984; Cant, 1992; Doran, 1993a; Hunt, 1994; Gebo & Chapman, 1995; McGraw, 1996). Perhaps with the exception of *Pongo* (see for example Thorpe et al 2009), hominoid primates show these same trends, for example the larger mountain gorilla is more terrestrial than the common chimpanzees (Schaller, 1963; Tuttle & Watts, 1985; Doran, 1996), and the female western lowland gorilla is more arboreal than its male counterpart (Remis 1995). Studies have also confirmed that there are changes in locomotion in primates and African ape primates during ontogeny (Rawlins, 1976; Rose, 1977; Crompton, 1983; Tuttle & Watts, 1985; Schaller, 1963; Goodall, 1968; Fossey, 1979). Doran (1997), for example, finds that mountain gorillas undergo dramatic changes in locomotor behaviour during ontogeny, with the frequency of quadrupedalism increasing and the frequency of climbing, suspensory behaviour and bipedalism all decreasing through ontogeny. The same author also finds that chimpanzees and gorillas of similar sizes (although widely disparate ages) perform very similar locomotor activities (Doran 1997), and an earlier study by the same author (Doran 1992a) demonstrates that the trends in positional behavioural development in chimpanzees and bonobos are similar, providing strong evidence for a link between locomotion and body size.

6.1. Pan troglodytes

Chimpanzees and humans likely diverged 10-5 million years ago, about 2 million years after the divergence of gorillas (12-7 Mya) (Wilkinson et al. 2011). Individuals of this species weigh between 47-60kg (Jungers and Susman 1984) and are moderately dimorphic (M/F = 1.27) (Leigh and Shea 1995). Studies have determined that *Pan troglodytes* reaches locomotor independence at around 5 years of age. Based on Doran's (1997) observations of chimpanzees in the wild from Tai Forest, Ivory Coast, the locomotor development in this species is as described in table 5. It is possible however, that body size differences within a species can also be correlated with differences in locomotor behaviour (Doran 1993a,b), and some studies have indicated that females spend more time resting above ground than do males, and when they are in the trees, both sexes differ in their locomotor and postural activities, height and substrate preference, and in the type of activity performed on some substrates (Doran 1993a,b).

Table 5 – Locomotor activities by age groups in chimpanzees (taken from Doran 1997).

Age Classes (months and years)	Locomotion
Infant 1 (0-6 months)	Dependent on mothers until 5 months, then engage in climbing, one/ two-handed arm-hanging, aided bipedalism
Infant 2 (6-23 months)	More frequent suspensory behaviour than at any other time in life Climbing and arm swinging; some palmigrade quadrupedalism
Infant 3 (2-5 years)	Shift to quadrupedalism: adept knuckle-walkers at this stage. Decrease in climbing, suspensory behaviour and bipedalism
Juveniles (5 to 11 years)	Proficient knuckle-walkers

6.2. Pan paniscus

Bonobos are thought to have split from the common chimpanzee lineage between 1 and 2 million years ago (Caswell et al. 2008). It is possible that the formation of the Congo River between 1.5 to 2 million years ago led to this speciation since bonobos live south of the river, whereas common chimpanzees live north of the river (Caswell et al. 2008). Bonobos are morphologically very similar to common chimpanzees, with a few key differences in their anatomy, social systems and sexual behaviours (Zihlman and Cramer 1978; Kano 1992; deWaal et al 1997; Boesch et al 2002; Hare et al 2012). The crania and mandibles of bonobos are quite distinct from those of chimpanzees, and they exhibit lower levels of craniodental sexual dimorphism than chimpanzees (Cramer 1977; Zihlman and Cramer 1978). Their body mass however, can be greater or equal to that of chimpanzees (adult body mass between 25kg to over 50kg [Rahm 1967; Napier and Napier 1967]). Bonobos also have a more slender build than chimpanzees, with longer thighbones, heavier thigh muscles and longer feet (Myers Thompson 2002). The shoulder anatomy is the same for bonobos and common chimpanzees, but *Pan paniscus* scapulae are relatively narrower than those of *Pan troglodytes* (Shea 1986), and their clavicles are relatively much shorter with a more extensive articular surface for the head of the humerus (McHenry and Corruccini 1983).

With regards to their locomotor ontogeny, both bonobos and chimpanzees follow the same general trends in locomotor behavior, as observed by Doran (1992, 1993a) and the same table of locomotor ontogeny may therefore be used for bonobos. However, a few differences do exist. Studies have shown that for all age classes bonobos are more arboreal than *Pan troglodytes* and that pygmy chimpanzee juveniles are more suspensory than their common chimpanzee counterparts (Doran 1992,1993a).

6.3. Gorilla gorilla

Chimpanzees and gorillas likely diverged between 12-7 Mya (Wilkinson et al. 2011). The species used in the present project is the western lowland gorilla (*Gorilla gorilla*

gorilla). The average body size for an adult male gorilla is 170 kg, and 70kg for a female (Jungers and Susman 1984), which means they are extremely dimorphic in their body mass. Sexual body mass dimorphism in gorillas is largely a consequence of differences in the duration of growth: male and female gorilla growth curves diverge at approximately 6-7 postnatal years, and while female growth ceases at approximately 9.5-10 years of age, males continue growth beyond this age, until about 12 years of age (Leigh and Shea 1996). Interestingly, despite their large size, lowland gorillas are like chimpanzees in terms of substrate use and positional behaviour, and more distinct from the ecologically specialized mountain gorillas than commonly believed (Remis 1995). However, due to their larger size gorilla males are at the upper body size limits which allow the use of arboreal substrates, so their behaviours are more cautious than those of females and other apes. Remis (1995) in fact shows that females use suspensory postures more frequently than males. Unlike for mountain gorillas, there is no data on locomotor development throughout growth for the lowland gorilla.

6.4. Pongo pygmaeus

Orangutans split from the African ape clade around 25-14 million years ago (Wilkinson et al. 2011). Currently, it is thought that Bornean and Sumatran orangutans constitute two distinct species (*Pongo pygmaeus* in Borneo and *Pongo abelii* in Sumatra), which are thought to have diverged about 1.1 million years ago – however, the level of variation does not approach that witnessed within other hominoid genera such as *Pan* (Campbell et al. 2007). The current project will only include Bornean orangutans.

Orangutans are the largest habitually arboreal mammal (Cant, 1987a; Thorpe and Crompton, 2006; Thorpe et al 2009), and they possess postcranial traits that are adapted for their complex arboreal environment, including long forelimbs with hook-like hands, short hindlimbs with hand-like feet, and highly flexible hip and shoulder joints (Fleagle, 1988; MacLatchy, 1996; Delgado and van Schaik, 2000; Manduell et

al 2011). The literature on orangutan locomotion is vast and studies suggested that while they exhibit a large repertoire of locomotor behaviour, they are predominantly characterized by orthograde suspensory locomotion: whereby the body is orthograde with the head superior, and various combinations of all four appendages are used to grasp supports in different ways, with suspension by the forelimbs from above (Cant, 1987b; Thorpe and Crompton, 2005, 2006; Thorpe et al., 2007a,b, 2009). Being one of the largest hominoid species, males can range in body weight from 34 kg to 90kg, and females can range in weight from 32kg to 45kg (Eckhardt, 1975).

Orangutans are one of the most sexually dimorphic species of mammals with adult males reaching on average 2.0 to 2.3 times the size of adult females (Leigh and Shea 1995). Orangutans males appear to have indeterminate growth, meaning that they carry on growing throughout their lives in both body mass (Leigh and Shea 1995) and cranial size (Balolia et al. 2013). The species is also exceptional in that there are two morphologically distinct types of adult males: one is large and fully developed with secondary sexual characteristics including large cheek flanges, and the second type which is smaller and does not have developed secondary sexual characteristics (Utami Atmoko and van Hoff 2004).

Given the extensive sexual and age-related dimorphism in orangutans (adult males weighing approximately twice as much as adult females and perhaps three times as much as adolescents), (Rodman, 1984), the relative congruence found in the locomotor behaviour of different age-sex categories is rather surprising (Thorpe and Crompton 2005). However, observations on feeding in northern Sumatra have shown that positional behaviour during feeding does vary between males and females, with males using larger branches than females and greater frequency of above branch postures (sitting and standing) than females, who employ suspensory under-branch postures more often (Cant 1987). Sugardjito and van Hooff (1986) also report significant differences in locomotor repertoire and in use of different canopy levels during travel for adult males, adult females, and adolescents.

There have currently been no studies focusing on the ontogeny of locomotor development in orangutans, similar to those performed on gorillas and chimpanzees. The data in table 7 have been derived from a study on the development of ecological independence in immature Sumatran orangutans, which includes some references to locomotor behaviour/independence.

Table 7 – Locomotor activities by age groups in orangutans (taken from van Adrichem et al. 2006).

Age Classes (years)	Locomotion
0 - 2 years	Mostly clinging to mother
2 - 3 years	Large drop in proportion of time spent clinging to mother and increase in the proportion of time spent moving. Move more independently
6 - 8 years	Nutritional and locomotor independence but daily contact with mother (ecologically dependent)
11 years	Independent travel alone

6.5. Hylobates lar

There are 4 genera and 12 species of gibbons, all small arboreal apes that inhabit the rain forests of eastern and southeastern Asia (Campbell et al. 2007). MtDNA studies suggested that the split of great apes and gibbons occurred 15–20 million years ago, with the four gibbon genera originated 7-8 million years ago (Schrago and Russo 2003; Raaum et al. 2005; Matsui et al. 2009; Matsudaira and Ishida 2010; Thinh et al. 2010). Lar gibbons, weighing on average 4.4 to 7.6 kg, have the broadest north to south distribution and diverged into subspecies at about 1–0.5 million years ago (Thinh et al. 2010). Gibbons are much smaller than any other hominoids and therefore are commonly referred to as lesser apes. As a group they are very similar in skeletal anatomy and more readily differentiated based on pelage and vocalizations (Campbell

et al. 2007). They are almost exclusively arboreal, and use a specialized mode of locomotion called brachiation; therefore, they exhibit a suite of morphological adaptations that are unique to them: extremely long forearms, highly mobile shoulder joints and long hook-like hands (Campbell et al. 2007). Gibbons are also unique in that they are sexually monomorphic: both sexes are the same size, with long saber-like canines (Campbell et al. 2007).

Gibbons (and siamangs) are skilled brachiators and 50–80% of their travelling time is spent using this specialised mode of locomotion (Fleagle, 1974, 1976; Andrews & Groves, 1976; Carpenter, 1976; Hollihn, 1984; Preuschoft & Demes, 1984; Tuttle, 1986; Takahashi, 1990). Brachiation is the 'bimanual progression along or between overhead structures for a distance of several metres without the intermittent use of other types of positional behaviour and without support by the hind limbs or tail' Hollihn (1984), and according to this definition, the hylobatids are the only true brachiators. The highly suspensory mode of locomotion of gibbons has contributed to some specialized anatomical features of the shoulder (i.e., well-developed scapular spine, long forearms relative to both humerus and body size, axially elongated scapulae and curvature of the clavicle) (Aiello and Dean 1990; Voisin 2006). The shoulder flexors, extensors, rotator muscles, elbow flexors and wrist flexors and especially the elbow flexors of gibbons are more powerful, compared with those of non-specialized brachiators (Michilsens et al 2009). However, within gibbons there appears to be no quantitative differences between gibbon species in both forelimb anatomy and muscle dimensions (Michilsens et al 2009).

There are currently no data on ontogeny of locomotion for lar gibbons, or for any other hylobatid.

6.6. Homo sapiens

Homo sapiens, anatomically modern humans, originated in Africa about 200,000 years ago, and are the only living species in the *Homo* genus and the only habitual

bipedal primates in Hominidae. *Homo sapiens* are the only habitually bipedal primate, with numerous morphological adaptations that resulted from this mode of locomotion. We are a sexually dimorphic species, with males possessing on average larger body masses: 86.6kg, versus 74.4kg in females (United States averages from 1999-2002; Ogden et al, 2004). However, we lack canine dimorphism, which implies a social structure with greater levels of male-male cooperation (e.g., Plavcan and Van Schaick, 1997; Plavcan, 2000).

Differences between non-human apes and human pectoral girdles are mainly found on the scapula and clavicle and suggest that the human arm is adapted for use in a lowered position and less powerful in a raised position (i.e., the glenoid fossa faces laterally, not cranially, and the clavicle lacks the cranial twist of the apes) (Aiello and Dean 1990).

Table 8 – Locomotor activities by age groups in modern humans (taken from Rose and Gamble 1994; Payne and Isaacs 2005).

Age Classes (months and years)	Locomotion
12 weeks	Control of head
4 months	Can lift head upright and hold trunk on extended arms
6 months	Independent sitting
8 – 10 months	Crawling/Begin to walk by holding onto things
10 – 17 months	Independent walking pattern
2 – 6 years	Gradual changes occur within each gait parameter, enabling child to progressively assume a more adult-like style of walking
7 years	Adult-like walking pattern

6.7. Macaca fascicularis (outgroup)

The fossil record indicates that macaques diverged from other papionids about 7 million years ago in Northern Africa and invaded Eurasia at about 5.5 million years ago via the Near East before branching into several phyletic lineages (Campbell et al. 2007).

Long tailed or crab eating macaques (*Macaca fascicularis*) have the highest degree of arboreality of all macaque species and are found in southeast Asia from Burma to the Philippines and southward through Indochina, Malaysia, and Indonesia. In Thailand, this species occurs in evergreen, bamboo, and deciduous forests. They are sexually dimorphic in size, with males weighing on average 4.8 to 7 kg and females weighing 3 to 4 kg, or approximately 69% of the average male weight (Wolfheim 1983).

The shoulder anatomy of macaques is quite different from that of great apes in several key aspects: the scapula is elongated mesio-distally instead of cranio-caudally, the glenoid faces laterally, not cranially, the clavicle is short and the humerus has low degrees of torsion (averaging 123 degrees according to Krahl 1945, and lower than any hominoid), and has lesser and greater tubercles that rise above the head (Aiello and Dean 1990). In many respects this is a quadrupedal morphology. However, when compared to *Papio*, a closely related clade of terrestrial quadrupeds, the scapular morphology of the less terrestrial macaque has a scapular configuration similar to more acrobatic primates capable of running, hopping, arm-swinging and suspension (Kimes et al. 1981). Even within two closely related species of macaques, the more terrestrial *Macaca nemestrina*, and the predominantly arboreal *Macaca fascicularis*, differences in shoulder morphology have been reported, namely related to the length of the scapula and length of the clavicle (Rodman 1979).

There is no detailed information about ontogeny of locomotion in *Macaca fascicularis*.

– Chapter 3 –

The ontogeny of humeral torsion in hominoid primates

1. Introduction

Hominoid primates share a number of features of shoulder morphology (e.g., dorsally placed scapulae, elevated humeral torsion, and cranially directed glenoid fossae), that have generally been associated with use of the upper limb in overhead postural and locomotor activities (Miller 1933; Ashton and Oxnard 1963, 1964; Oxnard 1963, 1967; Ashton et al. 1971, 1976; Roberts 1974; Andrews and Groves, 1976; Larson, 1988). In particular, high degree of humeral torsion (i.e., the medial displacement of the head of the humerus in relation to the shaft and distal epiphyses) has been interpreted as an accommodation to the dorsal repositioning of the scapula on a transversely widened rib cage – an upper body configuration that is characteristic of living hominoids (Larson 1998; Young 2003). Indeed, hominoids have the most dorsally positioned scapula among anthropoid primates (Corruccini and Ciochon 1976; Larson 1988; Chan 2007a,b), and the humeral head is therefore more medially oriented to articulate with a laterally oriented glenoid cavity (Larson 1996). In quadrupedal monkeys, on the other hand, the humeral head faces posteriorly to articulate with a ventrally oriented glenoid fossa (Larson 1996; Rein et al. 2011). These modifications in hominoid shoulder morphology have been associated with increased mobility at the glenohumeral joint, and the degree of humeral torsion is therefore viewed as a significant diagnostic characteristic in the interpretation of locomotor abilities in fossil primates (Begun 1992a, b, 1994; Larson, 1996).

Humeral torsion has been extensively studied in primate skeletons and is particularly well documented in humans (Martin 1933; Inman and Abbott 1944; Evans and Krahl 1945; Krahl and Evans 1945; Krahl 1947; Napier et al. 1959; Krahl 1976; Sarmiento

1985; Larson 1988, 1996, 1998, 2007a,b, 2009; Larson et al. 2007). It was previously considered to be a static, phylogenetic trait that varied slightly between sexes, sides, and populations (Krahl 1945; Krahl and Evans 1945; Edelson 1999, 2000) because variation within and between human groups in very young individuals suggests that there is a genetic component to this feature (Cowgill 2007). However, recent analysis of humeri from multiple human populations indicates that increases in upper limb activity prior to skeletal maturity lead to differences in humeral torsion values, and that this trait is therefore also a correlate of function (Krahl 1976; Cowgill 2007). Specifically, studies have established that torsion develops over time in the proximal epiphysis of the humerus (where 80% of humeral growth takes place [(Pritchett 1991]) as a result of repetitive rotational stresses, which lead to the deformation of the epiphyseal cartilage, thus resulting in reduced torsion (Mair et al. 2004; Murachovsky et al. 2010; Thomas et al. 2012; Wyland et al. 2012) (figure 1). Although the exact timing of the cessation of humeral torsion development is unknown (Cowgill 2007), it is thought to occur at the time of epiphyseal fusion, which occurs between the ages of 16 and 20 years in humans (Edelson 2000).

Because it appears to have both a phylogenetic base (primary rotation of the humerus happens *in utero*) and a functional base (secondary torsion of the humerus occurs during ontogeny and correlates with activity patterns) (Krahl and Evans 1945), humeral torsion has thus been of particular interest in discussions of hominoid, and in particular great ape, locomotor ancestry (Larson 1988, 1996, 1998; Larson 2007a,b; Larson et al. 2007). Indeed, along with the fusion of the *os centrale*, a synapomorphy of African apes and humans to the exclusion of Asian apes and most other primates (Corruccini 1978; Kivell and Begun 2007), the high degrees of humeral torsion in African apes and humans is considered by some to be a shared derived character and evidence for a knuckle-walking stage in human evolution – because it permits the arms to more effectively move in a parasagittal plane (Washburn 1967; Richmond and Strait 2000; Richmond et al. 2001; Begun 2004). Others, however, consider that humeral torsion in humans is an independently acquired characteristic that reflects upper limbs used for manipulation and the need to maintain the hands in front of the

body (Larson 1988, 1998; Larson 2007b); in gorillas and chimpanzees, high degrees of humeral torsion would have evolved, perhaps also independently, as a means to maintain the arms in a sagittal plain as a requirement for knuckle-walking (Larson, 1998, 2007a,b). Indeed, in her studies of humeral torsion in anthropoid humeri, Larson (1996, 1998; Larson et al. 2007) found that the degree of torsion in *A. afarensis*, *A. africanus, Homo floresiensis and Homo erectus* is lower than the degree of torsion found in either extant African apes or modern humans and according to the author, these results suggest that modern humans and African apes evolved their similar high degree of humeral torsion independently, and thus do not support the proposal that early hominids evolved from a knuckle-walking ancestor.

However, studies have shown that there is significant variation in the degree of humeral torsion between modern human populations (Edelson 1999; Cowgill 2007). Furthermore, the small sample sizes obtained from the fossil record do not allow us to form a clear picture of variation in this trait, and the incomplete elements from which these measurements of humeral torsion are derived are prone to have a significant margin of error rendering comparisons with modern human samples difficult (Richmond et al. 2001; Begun 2007). Therefore, the present chapter aims at tackling the issue of homoplasy versus homology in humeral torsion using a different method which takes into account variation within and across species and age classes: ontogeny. The present research thus investigates whether humeral torsion is a shared derived character or on the contrary, an independently acquired trait in the different hominoid lineages by comparing the ontogenies of humeral torsion in hominoid primates (*Hylobates lar, Pongo pygmaeus, Pan troglodytes, Pan paniscus, Gorilla gorilla, Homo sapiens*) and *Macaca fascicularis*, the assumption being that homologous characters will arise through similar developmental processes, while characters that are homoplastic will arise through different developmental processes (e.g., Gould 1977; Wray 1994; Hall 1999, 2007; Lieberman 1997, 2000; Lockwood 1999; Lockwood and Fleagle 1999).

The present project constitutes the first comprehensive comparison of humeral torsion across hominoid species from an ontogenetic perspective.

2. Materials and Methods

2.1. Sample

Humeral torsion was measured on left humeri (or right humeri when the left was not present or damaged) of *Macaca fascicularis* (n=20), *Hylobates lar* (n=24), *Pongo pygmaeus* (n=22), *Pan paniscus* (n=22), *Pan troglodytes* (n=43), *Gorilla gorilla* (n=39) and *Homo sapiens* (n=97) of all ages (0 to 70 years in humans; 0 to 13+ years in apes; 0 to 7+ in *Macaca*). A standard three-parameter Gompertz model was fitted to the distributions using the self-starting function SSgompertz in R version 2.12.2 (2011). The Gompertz function estimates three parameters: the asymptotic value (Asym), the value at x=0 (b2), and a numeric parameter relating to the rate of growth (b3), for each distribution. Additionally, analysis of variance (ANOVA) tests were employed to test for differences between age categories (based on dental age) across species. Boxplots were also employed to visualize the data by species and age category. Age categories were based on dental age and were defined as: 'infants', represented by individuals prior to M1 eruption (7 years for humans, 3.5 years for great apes, and 1.75 for macaques and gibbons), 'juveniles', represented by individuals prior to M3 eruption (18 years for humans, 11 for great apes, 7 years for macaques and 8 years for gibbons), and 'adults', represented by individuals with erupted M3s (Smith 1989). Further details on how the measurements were collected, on how individual specimens were aged, and on the Gompertz function, can be found in the Materials and Methods Chapter.

2.2. Measurement

The humeral torsion angle is the obtuse angle formed between the orientation of the humeral head and the orientation of the distal condyles of the humerus (figure 18). This angle is measured using the intersection, viewed from the cranial perspective, of

a line drawn through the centre of the humeral head dividing it into anterior and posterior halves, and a line passing through the centre of the capitulum and trochlea (as defined by Krahl and Evans 1945; Rhodes 2006; Cowgill 2007; see figure 18 legend for details). Because these are not present or are only partially fused in the juvenile population, the distal axis in immature, unfused humeri was defined as the transverse axis of the distal metaphyseal surface, bisecting the axis into two equal halves (as defined by Cowgill 2007) (figure 18b). With regards to the proximal axis, a similar issue arises since the humeral head is unfused in immature individuals. In this case, the proximal metaphyseal surface was used and the axis was defined as the line passing through the maximum diameter of the metaphyseal surface, and bisecting it into two even segments (as defined by Cowgill, 2007) (figure 18a). Discrepancies

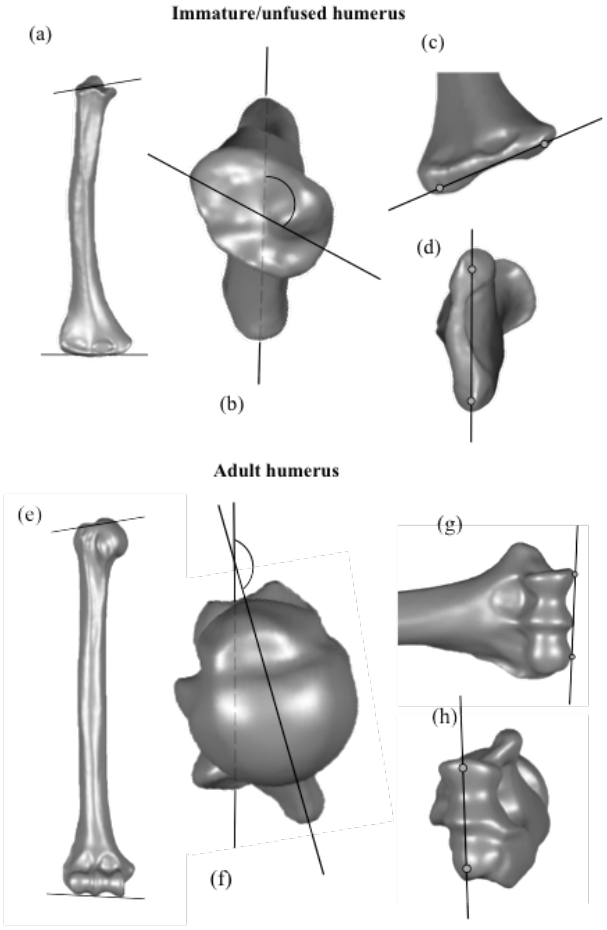

Figure 18 – Above: mmature gorilla right humerus in (a) anterior, (b) cranial, (c,) anterior, and (d) distal view, showing the proximal and distal axes used for measuring humeral torsion. The distal axis is formed by line passing through the maximum diameter of the metaphyseal surface, and bisecting it into two even segments (c) and (d). Below: adult gorilla right humerus in (a) anterior, (b) cranial, (c) anterior, and (d) distal view, showing the proximal and distal axes used for measuring humeral torsion. The distal axis is formed by a line passing through the centre of the distal-most points of the trochlea and capitulum (c) and (d).

between the two methods of defining the proximal axis and distal axis were measured on juvenile specimens who still retained clear lines of fusion (this was only the case in very few specimens). Differences between the two methods produced measurement error that ranged from 3% to 5% of the total measurement, falling below the average torsion differences between individual specimens at 5–9% (measurement error was calculated using White et al's [2011] procedure for estimating error on osteological material; see table 9). Intraobserver error was also calculated for both fused and unfused humeri of all species; intraobserver error did not exceed 4.6% in any sample, which is consistently below the average differences (in percent) between individual specimens (which exceeded 5.8% in all samples) (table 9).

Table 9 – Table of error measurements and total differences between individuals in the primate samples. The percentage difference for the total sample measures the mean differences between each measurement to the average humeral torsion value for each species. The percentage difference for repeat measurements reports the mean differences between repeated measurements in relation the three averaged repeat measurements (for mature and immature specimens). The average differences between individuals are greater than the differences between repeat measurements in each sample.

Sample	Species	N	Mean differences (%)	Standard deviation
Remeasurements	*H. sapiens*	3	0.573	0.529
Mature individuals (fused humeri)	*P. troglodytes*	3	1.917	1.483
	P. paniscus	3	3.822	2.452
	G. gorilla	3	0.654	0.728
	P. pygmaeus	3	4.602	3.234
	H. lar	3	0.778	0.599
	M.fascicularis	3	2.187	1.047
Remeasurements	*H. sapiens*	3	1.453	1.449
Immature individuals (unfused humeri)	*P. troglodytes*	3	2.740	2.466
	P. paniscus	3	0.497	0.309
	G. gorilla	3	0.163	0.091
	P. pygmaeus	3	0.893	0.419
	H. lar	3	3.622	2.873
	M.fascicularis	3	4.123	2.218
Total samples	*H. sapiens*	97	7.559	9.808
Average differences between individuals	*P. troglodytes*	45	6.774	8.008
	P. paniscus	23	5.805	6.623
	G. gorilla	42	8.024	7.85
	P. pygmaeus	24	6.923	7.712
	H. lar	24	8.536	6.959
	M.fascicularis	21	6.375	5.138

Discrepancies between the present study and the literature exist, as shown in table 10, however, for the most part, the variation in torsion measurements across studies is smaller than the variation within species in the adults of the present study (table 11). Indeed, adult humeral torsion values are very variable, with gorilla values for example ranging from 145 to 175 degrees. The same is true for the other species in the sample, with standard deviations ranging from 6.93 (in *Macaca*) to 12.2 (for *Pongo*). Additionally, the literature for humeral torsion in adult humans is vast and studies report humeral torsion values from as low as 115 to as high as 175 degrees (Leal and Checcia 2006).

Table 10 – Table showing mean humeral torsion values (adults) in the present study compared to those reported in the literature. Maximum differences between studies are reported in the last column.

Species	Present study	Krahl (1976)	Larson (1996)	Rein et al (2011)	Max Diff (°)
Homo sapiens	168.5 (n=42)	164	145 (n=40)	168.1 (n=20)	23.5
Pan troglodytes	152.6 (n=12)	146	143 (n=40)	132.9 (n=20)	19.7
Pan paniscus	151.5 (n=8)	-	-	-	-
Gorilla gorilla	160.2 (n=12)	161	145 (n=40)	133.7 (n=20)	26.5
Pongo pygmaeus	136 (n=13)	140	107 (n=31)	115.3 (n=20)	23.1
Hylobates lar	111.9 (n=10)	134	107 (n=31)	115.3 (n=20)	22.1
Macaca fascicularis	101.4 (n=10)	123	95 (n=27)	94.3 (n=10)	21.8

Table 11 – Table of mean torsion, minimum torsion and maximum torsion values found in the present study (adults). Differences between minimum and maximum torsion values are reported. This illustrates the spread of the distribution in torsion values in the present study and shows that within-species differences in torsion in the current study are on average bigger than the differences in torsion between studies.

Species	Mean torsion (°)	Min torsion (°)	Max torsion (°)	Max-Min torsion (°)
Homo sapiens	168.5	149.18	180	30.82
Pan troglodytes	152.6	137.29	168.48	31.19
Pan paniscus	151.5	137.74	161.37	23.63
Gorilla gorilla	160.2	143.31	175.03	31.72
Pongo pygmaeus	136	106.17	156.7	50.53
Hylobates lar	111.9	103.28	119.14	15.86
Macaca fascicularis	101.4	98.08	101.65	3.57

3. Results

3.1 Humeral torsion differences between adults

Boxplots of adult humeral torsion values show an increase in torsion from macaques to humans, with the African apes (gorillas, chimpanzees and bonobos) and humans showing the highest levels of torsion among the hominoids (figure 19). ANOVAs further show that there are significant differences between all species at the $p<0.05$ level ($F=116$, $df=6$, $p<0.000$). TukeyHSD post-hoc tests reveal that these differences exist between all species except between the non-human African apes, and between gibbons and macaques ($p>0.05$) (table 12).

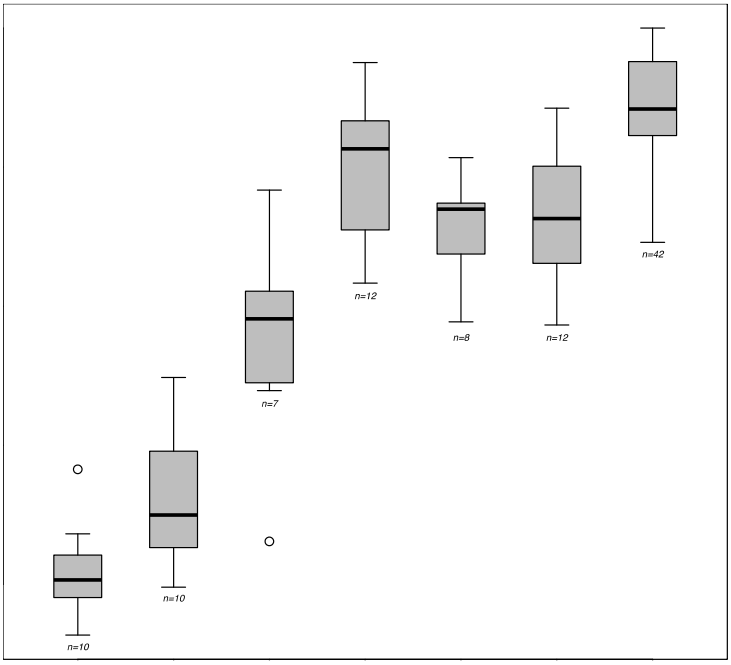

Figure 19 – Boxplot of adult humeral torsion values in adult hominoid species and *Macaca fascicularis*. Means are significantly different between species except between African ape species (excluding humans) and between gibbons and macaques ($p<0.05$) within a 95% confidence interval. Boxes represent the upper and lower quartile ranges, the black lines, the means, and the whiskers, the highest and lowest values within 1.5 times the interquartile range of the upper and lower quartiles; the circles represent outliers.

3.2. Ontogeny of humeral torsion: differences between age categories

First, the samples were divided into age categories (infant, juvenile, adult). ANOVA results show significant differences between all age classes in the human, gorilla and chimpanzee (*P. troglodytes*) samples at the p<0.05 level (*H. sapiens*: F=62.254, df=2, p<0.000; *G. gorilla*: F=6.9697, df=2, p=0,002; *P. troglodytes*: F=17.597, df=2, p<0.000). TukeyHSD post-hoc tests show that these differences exist between all age classes in the human sample, and between infants and juveniles, but not between juveniles and adults, for the gorilla and chimpanzee samples (figure 20, table 13).

Table 12 – Tukey's HSD post-hoc test for the ANOVA test of between species differences (adult specimens). Significant values (within a 95% confidence interval) marked in bold (diff: difference between means; lwr/upr: lower and upper bounds of the mean within a 95% CI).

Species		diff	lwr	upr	p-adj
G. gorilla (12)	*H. sapiens (42)*	8.306	1.365	15.247	**0.009**
G. gorilla (12)	*H. lar (10)*	-48.283	-58.492	-38.074	**0.000**
G. gorilla (12)	*M. fascicularis (9)*	-58.824	-69.033	-48.615	**0.000**
G. gorilla (12)	*P. paniscus (8)*	-8.761	-19.834	2.313	0.218
G. gorilla (12)	*P. troglodytes (12)*	-7.623	-17.212	1.967	0.214
G. gorilla (12)	*P. pygmaeus (13)*	-25.461	-37.113	-13.810	**0.000**
H. sapiens (42)	*H. lar (10)*	-56.589	-66.133	-47.045	**0.000**
H. sapiens (42)	*M. fascicularis (9)*	-67.130	-76.674	-57.586	**0.000**
H. sapiens (42)	*P. paniscus (8)*	-17.067	-27.530	-6.603	**0.000**
H. sapiens (42)	*P. troglodytes (12)*	-15.928	-24.807	-7.050	**0.000**
H. sapiens (42)	*P. pygmaeus (13)*	-33.767	-44.841	-22.694	**0.000**
H. lar (10)	*M. fascicularis (9)*	-10.541	-22.671	1.589	0.133
H. lar (10)	*P. paniscus (8)*	39.523	26.656	52.389	**0.000**
H. lar (10)	*P. troglodytes (12)*	40.661	29.047	52.275	**0.000**
H. lar (10)	*P. pygmaeus (13)*	22.822	9.455	36.189	**0.000**
M. fascicularis (9)	*P. paniscus (8)*	50.064	37.197	62.930	**0.000**
M. fascicularis (9)	*P. troglodytes (12)*	51.202	39.588	62.816	**0.000**
M. fascicularis (9)	*P. pygmaeus (13)*	33.363	19.996	46.730	**0.000**
P. paniscus (8)	*P. troglodytes (12)*	1.138	-11.242	13.519	1.000
P. paniscus (8)	*P. pygmaeus (13)*	-16.700	-30.738	-2.662	**0.009**
P. troglodytes (12)	*P. pygmaeus (13)*	-17.839	-30.739	-4.939	**0.001**

In contrast, ANOVAs show no statistically significant differences between age categories in the other apes (Asian apes and bonobos), suggesting that in these species torsion levels remain constant throughout growth, or that ontogenetic changes are not adequately captured by the present data and categorisation. In macaques, a t-test shows significant changes between the juveniles and the adults ($p<0.000$), with adults appearing to have lower torsion values than juveniles. There are no infant specimens for this sample.

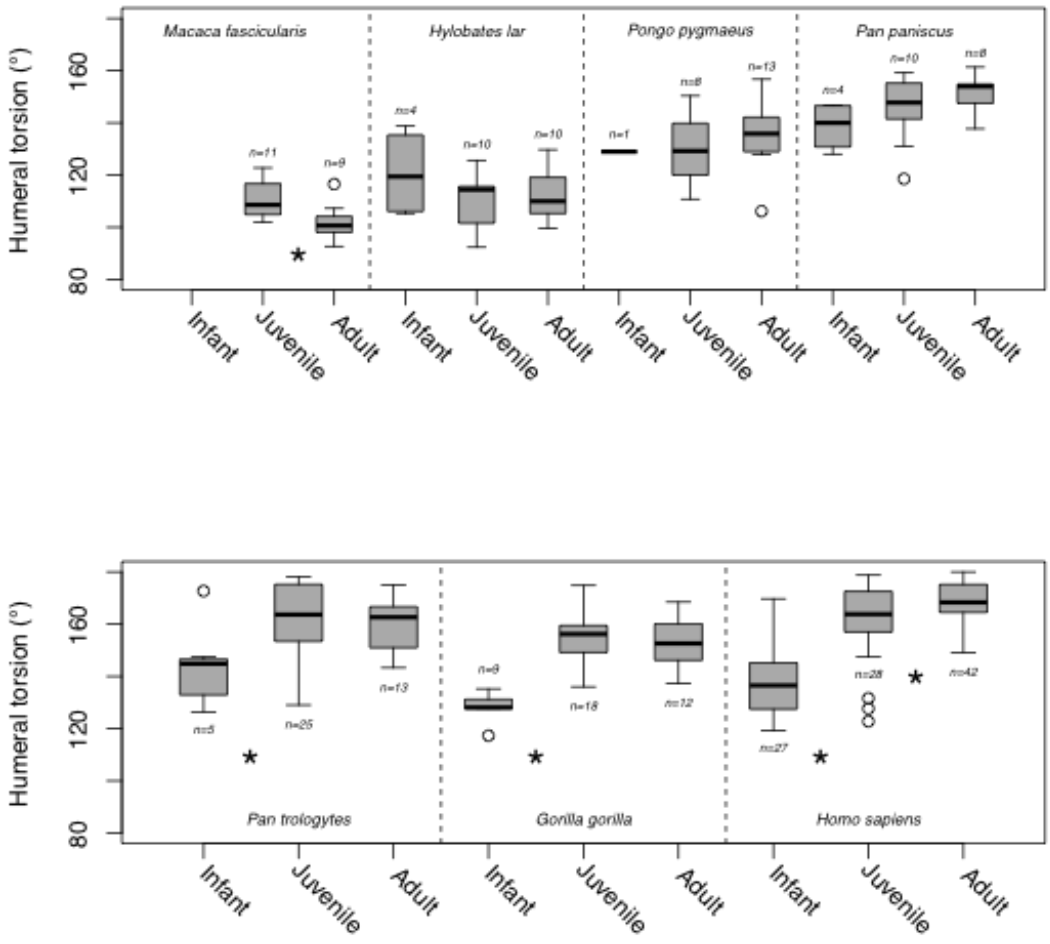

Figure 20 – Boxplot of humeral torsion values in hominoid species and Macaca fascicularis by age categories: infant (birth to M1 eruption), juvenile (M1 eruption to M3 eruption), adult (post M3 eruption). Asterisks mark significant differences between adjacent age categories within 95% confidence interval ($p<0.05$). Boxes represent the upper and lower quartile ranges, the black lines, the means, and the whiskers, the highest and lowest values within 1.5 times the interquartile range of the upper and lower quartiles. The circles represent outliers.

3.3. Ontogeny of humeral torsion: fitting the Gompertz model

The Gompertz model fits all species' distributions (on logged and non-logged values), except for the Asian apes' (figure 21 & 22; table 14).

Table 13 – Tukey's HSD post-hoc test for the ANOVA test of differences between age categories within species. Significant values (within a 95% confidence interval) marked in bold (diff: difference between means; lwr/upr: lower and upper bounds of the mean within a 95% CI).

Species	Age Categories		diff	lwr	upr	p-adj
P. troglodytes	Infant (5)	Juvenile (25)	27.465	16.135	38.796	**0.000**
	Infant (5)	Adult (12)	24.714	12.403	37.025	**0.000**
	Juvenile (25)	Adult (12)	-2.751	-10.874	5.371	0.690
G. gorilla	Infant (9)	Juvenile (18)	18.899	5.989	31.808	**0.003**
	Infant (9)	Adult (12)	17.381	3.437	31.324	**0.012**
	Juvenile (18)	Adult (12)	-1.518	-13.303	10.266	0.947
H. sapiens	Infant (27)	Juvenile (28)	23.792	16.495	31.088	**0.000**
	Infant (27)	Adult (42)	30.767	24.094	37.44	**0.000**
	Juvenile (28)	Adult (42)	6.975	0.375	13.576	**0.036**

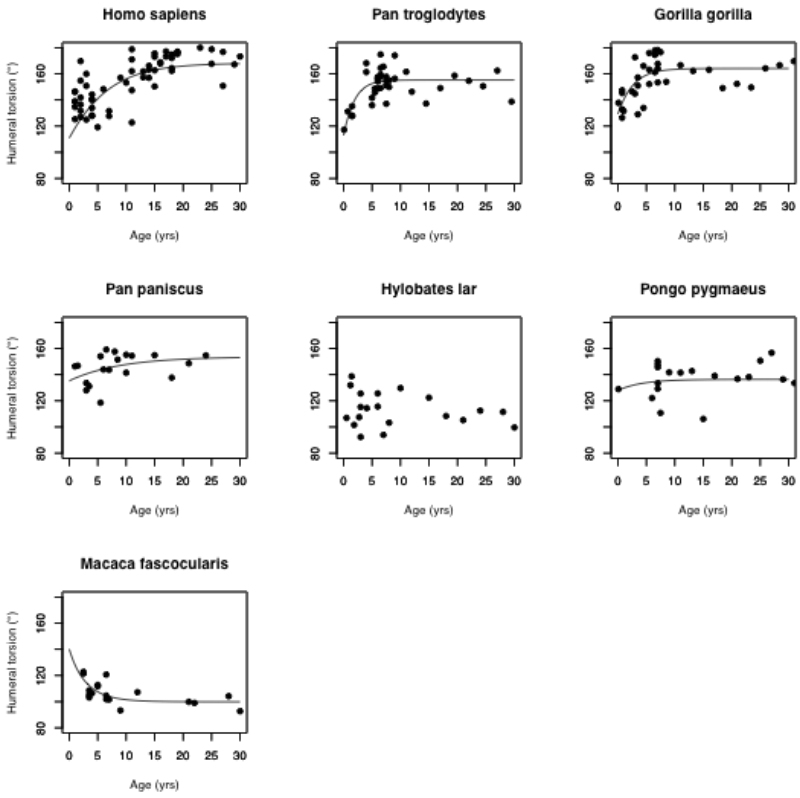

Figure 21 – Gompertz curves of humeral torsion development in hominoid species and *Macaca fascicularis* on non-logged values.

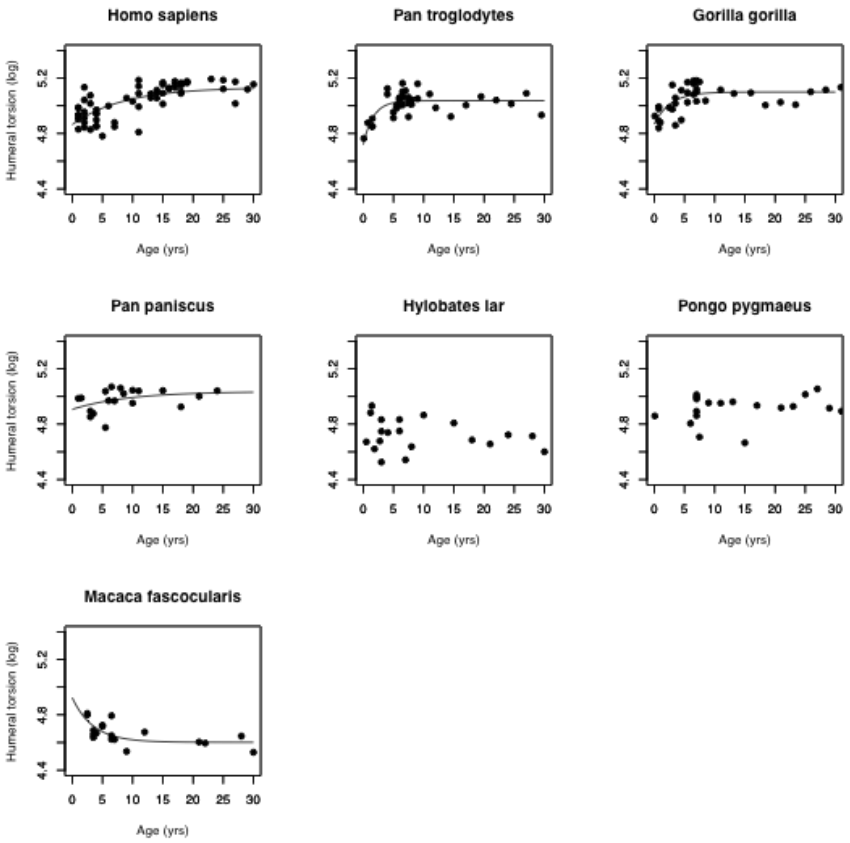

Figure 22 – Gompertz curves of humeral torsion development in hominoid species and *Macaca fascicularis* on logged values ($\log_e$).

The growth curves indicate that humeral torsion in humans reaches full adult value just after M3 eruption (Smith, 1989); African apes attain their adult values before M3 eruption, except in bonobos, whose torsion seems to develop later, around M3 eruption; macaques finish developing torsion around M3 eruption (~8 years) (figure 23).

However, because humans mature more slowly than their ape relatives – about half as fast, with adulthood occurring around 11 years in apes, and around 18 in humans (Smith and Tompkins, 1995) –, in order to better understand how humans compare to

Table 14 – Gompertz parameters showing estimated value at growth completion (log) (Asymptote), estimated value at birth (b2), estimated rate of growth (b3), and the Residual Standard Error.

Measurement	Species	Asymptote	Gompertz	Gompertz	RSE	DF
Humeral torsion (°)	*Homo sapiens*	168.156 (±2.415)	0.417 (±0.081)	0.842 (±0.036)	10.89	50
	Pan troglodytes	155.253 (±2.165)	0.319 (±0.078)	0.562 (±0.137)	9.688	39
	Gorilla gorilla	164.074 (±3.697)	0.237 (±0.055)	0.664 (±0.138)	11.80	36
	Pan paniscus	153.601 (±6.035)	0.127 (±0.060)	0.888 (±0.117)	10.34	19
	Hylobates lar	-	-	- -	-	-
	Pongo pygmaeus	-	-	- -	-	-
Humeral torsion	*Homo sapiens*	5.124 (±0.015)	0.080 (±0.013)	0.850 (±0.035)	0.07	50
	Pan troglodytes	5.045 (±0.015)	0.063 (±0.013)	0.575 (±0.126)	0.06	37
	Gorilla gorilla	5.098 (±0.025)	0.047 (±0.010)	0.681 (±0.134)	0.08	36
	Pan paniscus	5.034 (±0.044)	0.026 (±0.012)	0.894 (±0.114)	0.07	19
	Hylobates lar	-	-	- -	-	-
	Pongo pygmaeus	-	-	- -	-	-

the African apes, the human growth curve was scaled to match the ape growth curves (figure 24). Doing so highlights the differences between the human and the chimpanzee and gorilla curves, with the bonobos appearing slightly derived in comparison. Here, chimpanzees, gorillas increase torsion at a similar rate, with chimpanzees and gorillas reaching their final values slightly earlier (before M3 eruption) than humans (after M3 eruption). Bonobos on the other hand seem to increase torsion much more slowly, and reach their final values around M3 eruption – although the lack of young individuals in the sample may be partially responsible for this pattern (figure 24).

ANOVA tests performed between species at each age category (infant, juvenile, adult) further show a lack of significant differences between any of the species at infancy ($F=2.7602$, $df=4$, $p=0.06$), but significant differences between the juveniles ($F=42.272$, $df=5$, $p<0.000$) and adults ($F=69.013$, $df=5$, $p<0.000$) of each species within 95% confidence interval (see also table 15). These results indicate that hominoids exhibit similar torsion levels at birth (between ~110° and 135°), with differences arising as a product of growth, after M1 eruption.

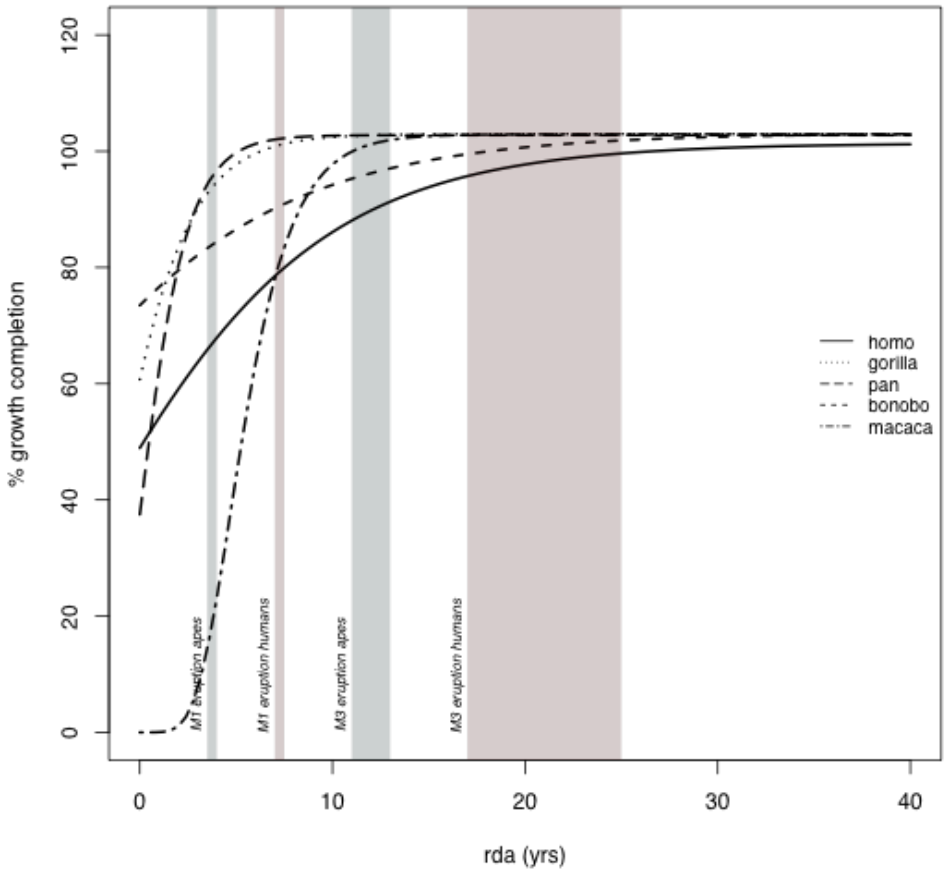

Figure 23 – Gompertz curves of humeral torsion development in hominoid species and *Macaca fascicularis* on non-logged values, with M1 and M3 eruption indicated for great apes (grey) and humans (red). The *Macaca fascicularis* growth curve follows the opposite pattern from the hominoid growth curves.

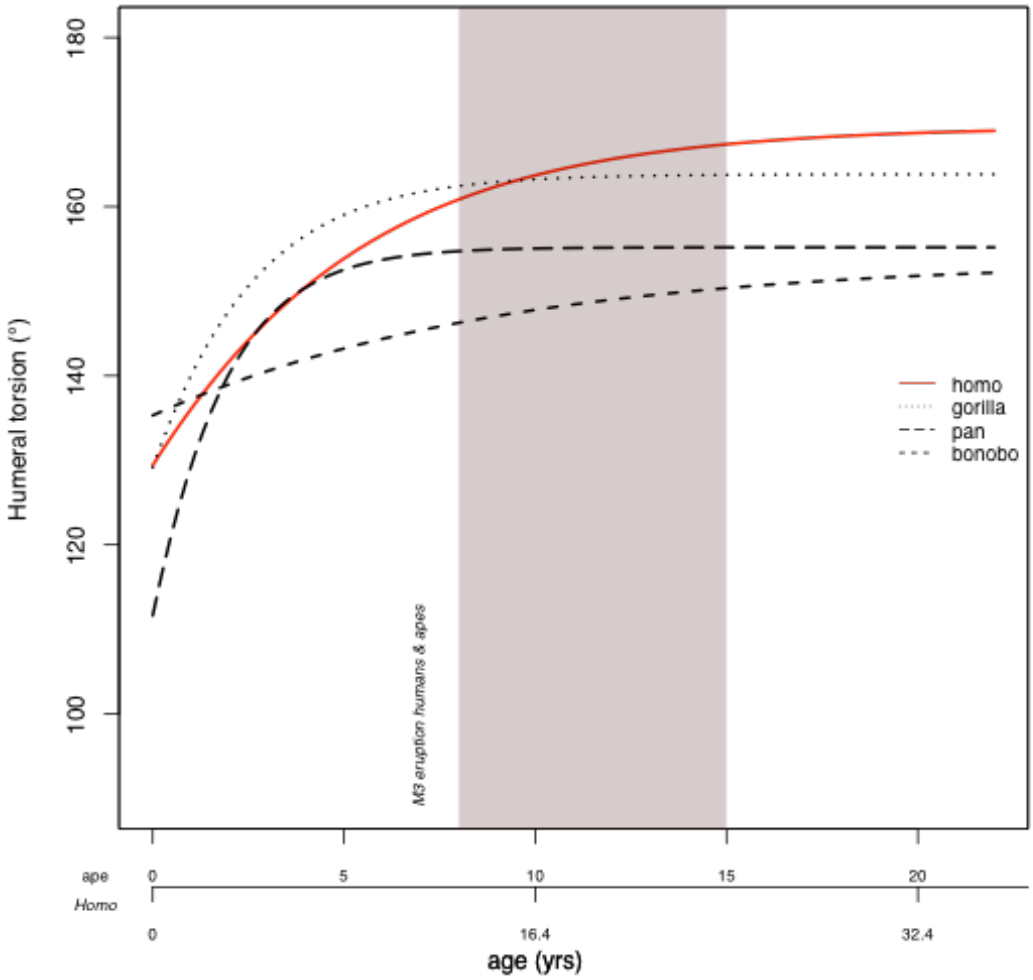

Figure 24 – Gompertz curves of humeral torsion development in hominoid species on non-logged values, with M3 eruption indicated for apes humans (red). The human x axis was 'scaled' to aproximate the African ape life histories (African apes attain adulthood around 11 years of age; humans at around 18 years of age).

3.4. Humeral torsion and growth completion

Torsion values were then converted to percentages representing levels of growth completion – 100% growth completion was calculated as the average adult value for each species. Gompertz growth curves were then derived from these percentages (figure 25). Overall, results suggest that humeral torsion at birth is 40%-60% complete in all species except macaques and bonobos. In the latter, torsion is ~70% complete at birth, and in macaques, it is 0% complete. In macaques, torsion is estimated to be underdeveloped at birth compared to the other species, but develops rapidly and attains its final value around adulthood (~8 yrs) (figure 25). However, values at birth are likely underestimated due to the absence of very young individuals in the sample. Moreover, there is a remarkable similarity between the chimpanzee and gorilla patterns, as seen by the largely overlapping curves, with growth being completed between M1 and M3 eruption (figure 25). Humans on the other hand show a much slower growth rate in torsion development, likely due to their slower life histories, with growth being completed around M3 eruption (figure 25). Curiously, the bonobos also develop more slowly, thus deviating slightly but noticeably from the pattern seen in chimpanzees and gorillas – but with no significant differences between bonobos and chimpanzees in torsion (table 12). When the human growth curve is scaled to the African ape curves (figure 25), this pattern becomes even more evident – with torsion development in chimpanzees and gorillas finishing well before M3 eruption, unlike humans, who continue developing torsion for relatively longer period of time. The bonobos again appear to slightly deviate from this pattern with torsion developing at a much slower pace, and with values at birth being at ~70% of their final adult values (figure 25).

Table 15 – Tukey's HSD post-hoc test for the ANOVA test of differences between species, within age categories. Significant values (within a 95% confidence interval) marked in bold (diff: difference between means; lwr/upr: lower and upper bounds of the mean within a 95% CI).

Age Class	Species		diff	lwr	upr	p-adj
Juveniles	*G. gorilla (18)*	*H. lar (10)*	-49.479	-64.222	-34.736	**0.000**
	G. gorilla (18)	*M. fascicularis (13)*	-50.884	-64.162	-37.606	**0.000**
	G. gorilla (18)	*P. paniscus (10)*	-16.089	-29.773	-2.405	**0.012**
	G. gorilla (18)	*P. troglodytes (25)*	-6.389	-17.115	4.336	0.507
	G. gorilla (18)	*P. pygmaeus (4)*	-31.600	-53.236	-9.964	**0.001**
	H. lar (10)	*M. fascicularis (13)*	-1.405	-17.526	14.717	1.000
	H. lar (10)	*P. paniscus (10)*	33.391	16.933	49.848	**0.000**
	H. lar (10)	*P. troglodytes (25)*	43.090	28.996	57.183	**0.000**
	H. lar (10)	*P. pygmaeus (4)*	17.879	-5.610	41.368	0.237
	M.fascicularis (13)	*P. paniscus (10)*	34.795	19.636	49.955	**0.000**
	M.fascicularis (13)	*P. troglodytes (25)*	44.494	31.941	57.048	**0.000**
	M.fascicularis (13)	*P. pygmaeus (4)*	19.284	-3.315	41.882	0.138
	P. paniscus (4)	*P. troglodytes (25)*	9.699	-3.283	22.681	0.256
	P. paniscus (4)	*P. pygmaeus (4)*	-15.511	-38.351	7.328	0.358
	P. troglodytes (5)	*P. pygmaeus (4)*	-25.211	-46.410	-4.011	**0.011**
Adults	*G. gorilla (12)*	*H. lar (10)*	-48.283	-60.058	-36.509	**0.000**
	G. gorilla (12)	*M. fascicularis (9)*	-60.507	-72.633	-48.381	**0.000**
	G. gorilla (12)	*P. paniscus (8)*	-9.381	-21.156	2.393	0.193
	G. gorilla (12)	*P. troglodytes (12)*	-7.623	-18.849	3.604	0.355
	G. gorilla (12)	*P. pygmaeus (8)*	-24.193	-35.201	-13.184	**0.000**
	H. lar (10)	*M. fascicularis (9)*	-12.224	-24.859	0.411	0.063
	H. lar (10)	*P. paniscus (8)*	38.902	26.604	51.200	**0.000**
	H. lar (10)	*P. troglodytes (25)*	40.661	28.886	52.435	**0.000**
	H. lar (10)	*P. pygmaeus (8)*	24.090	12.524	35.657	**0.000**
	M.fascicularis (9)	*P. paniscus (8)*	51.126	38.491	63.761	**0.000**
	M.fascicularis (9)	*P. troglodytes (12)*	52.885	40.759	65.011	**0.000**
	M.fascicularis (9)	*P. pygmaeus (8)*	36.314	24.390	48.239	**0.000**
	P. paniscus (8)	*P. troglodytes (12)*	1.759	-10.016	13.533	0.998
	P. paniscus (8)	*P. pygmaeus (8)*	-14.812	-26.378	-3.245	**0.005**
	P. troglodytes (12)	*P. pygmaeus (8)*	-16.570	-27.579	-5.562	**0.001**

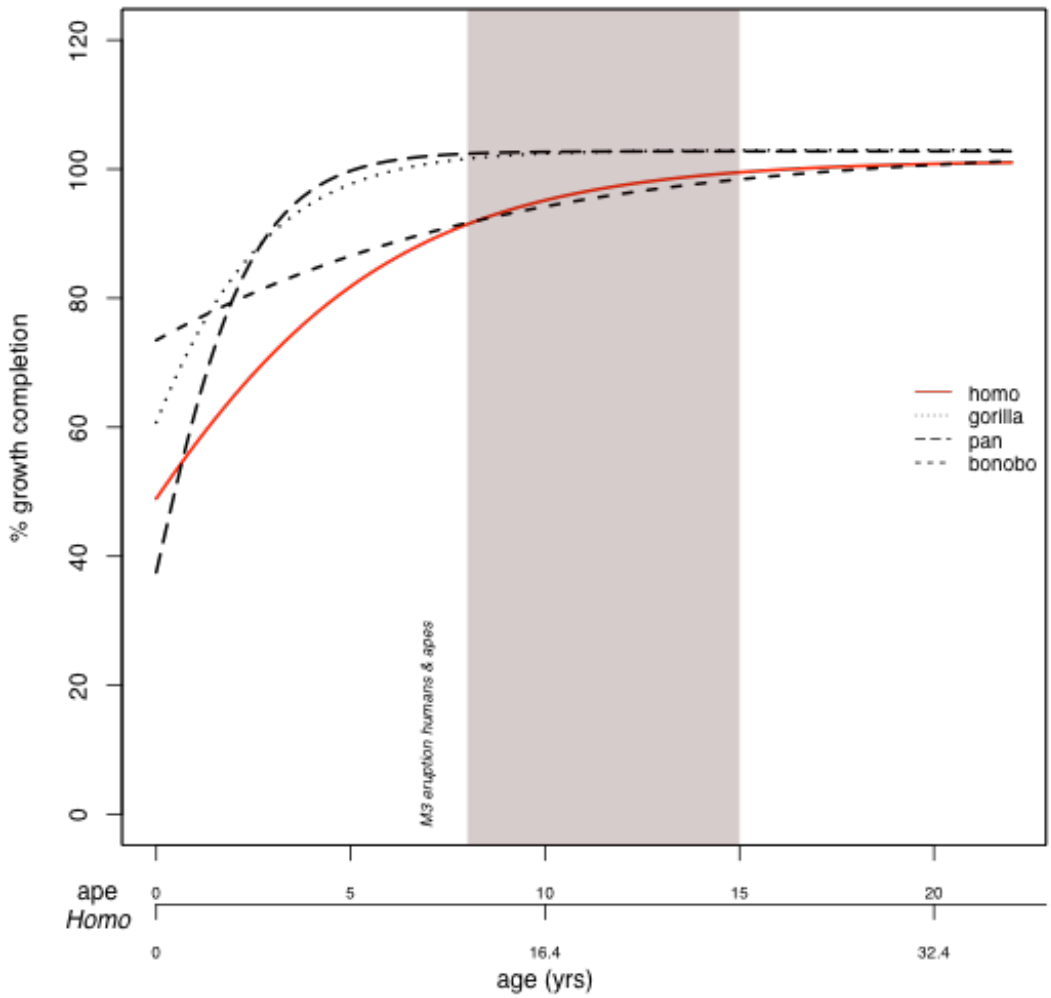

Figure 25 – Gompertz curves of humeral torsion development in hominoid species with M3 eruption indicated for apes humans (red). The values were converted to percentages represented growth completion. The human x axis was 'scaled' to approximate the African ape life histories (African apes attain adulthood around 11 years of age; humans at around 18 years of age).

4. Discussion

4.1. Humeral torsion in hominoid primates: evolution and developmental mechanism

The present study shows that, like in humans, humeral torsion develops through ontogeny in at least *Pan*, *Gorilla* and *Macaca fascicularis*, and is thus the first study to establish this. My results show that torsion ceases its development around adulthood (M3 completion/eruption) at the time of epiphyseal fusion (Krahl and Evans, 1945; Schultz 1956; Krahl 1947, 1976; Edelson, 1999) (figures 21 & 22); moreover, results suggest that there may be no differences in torsion values between species at birth, but significant differences between species in adulthood (table 12 &

13), suggesting that differences in torsion arise through ontogeny via diverging developmental trajectories in the different lineages.

Overall, my results show three major trends in the development of torsion in hominoids and *Macaca fascicularis*: (1) African apes and humans increase their humeral torsion values throughout growth, (2) Asian apes maintain low levels of torsion throughout growth, and (3) macaques reduce their humeral torsion throughout growth (figure 21 & 22). These results support the notion that there is a phylogenetic component to humeral torsion, because these three trends match the phylogenetic distances between species: *Macaca* < Asian apes < African apes < humans (Evans and Krahl 1945; Krahl 1976). On the other hand, because this trait develops throughout ontogeny with no apparent differences between species at birth, and because there is evidence of individual variation within populations (figure 21 & 22), results also support the notion that there is a functional element associated with torsion that is likely related to locomotor and/or postural behaviours, with some of the more orthograde suspensory species having lower torsion than the more terrestrial pronograde species: gibbons < chimpanzees < gorillas and humans. Additionally, there may also be some relationship with size and life-history, since the larger, slower growing species develop higher torsion, and the smaller, faster growing species maintain low torsion: macaques and gibbons < gorillas and humans. The results thus suggest that size, phylogenetic distance and locomotion may all contribute to humeral torsion: at the onset, the amount of torsion in hominoids seems to be genetically determined, with changes in torsion arising subsequently, as a product of changes in body size and divergent locomotor habits between species and between individuals.

It is known that in humans, differences in torsion arise via the opposite actions of the medial and lateral rotators on the head of the humerus, which varies between individuals and groups, prior to epiphyseal fusion (Krahl and Evans 1945; Edelson 2000; Cowgill 2007). Although the natural tendency is for humeral torsion to increase throughout ontogeny (Cowgill 2007), in athletes and more active populations, increased activity of the medial rotators (subscapularis, pectoralis major, latissimus dorsi, and teres major) in relation to the lateral rotators (infraspinatus and teres

minor), limits the development of torsion, thus resulting in relatively lower torsion in these individuals (Cowgil 2007), and in fact, Krahl (1947) reports a correlation between the strengths of these muscles and the degree of torsion in the corresponding humeri. This explains why professional athletes such as baseball or tennis players have relatively lower torsion on the playing arm compared to the non-playing arm (Pieper 1998; Crockett et al. 2002; Osbahr et al. 2002; Whiteley et al. 2008, 2010; Taylor et al. 2009; Myers et al. 2009; Schwab and Blanch 2009), why females tend to possess higher torsion than males (Krahl and Evans 1945), and why individuals with brachial plexus injuries in which the medial rotators are unopposed by the lateral rotators, have posteriorly oriented humeral heads (i.e., very low torsion) (Codine et al. 1997; Waters et al. 1998; Van Der Sluijs et al. 2002; Pöyhiä et al. 2005; Cowgill, 2007).

Interestingly, the types of activities that produce these imbalances between medial and lateral rotators and, as a result decreased torsion, are overhead movements, in particular, throwing movements (Pieper 1998; Crockett et al. 2002; Osbahr et al. 2002; Reagan et al. 2002; Rhodes and Knüsel 2005; Sabick et al. 2005; Rhodes 2006; Whiteley et al. 2008, 2010; Taylor et al. 2009; Myers et al. 2009; Schwab and Blanch 2009; Rhodes and Churchill 2009; Roach et al. 2012). It is possible then, that the same mechanism that explains within-species differences in human torsion, also explains between-species differences in hominoid torsion, since the species that use the most overhead movements, the gibbons and orangutans, are the ones who exhibit the lowest torsion among hominoids. The fact that chimpanzees have less torsion compared to the more terrestrial gorillas (figure 19), and that lowland gorillas have less torsion than the more terrestrial mountain gorillas (Inouye 2003), also supports this notion. Moreover, evidence from orangutans shows that captive, predominately quadrupedal individuals have substantially higher torsion than their wild counterparts, a difference which is attributed to locomotor behavioural differences during growth (Sarmiento 1985). If this is true, then the observation that torsion remains constant throughout growth in the Asian apes while increasing in African apes and humans, could be explained by the presence of relatively more powerful medial rotators,

compared to lateral rotators, in Asian apes, which would act to maintain a posteriorly oriented humeral head throughout growth – by stopping the otherwise natural progression towards higher torsion. Larson (1988), for example, notes that in gibbons the subscapularis acts as a powerful medial rotator, and EMG results show this muscle is more active in gibbons than in chimpanzees who also engage in suspensory activities. Similarly, Oishi et al. (2008, 2009) find that the force-generating capacity of the subscapularis (a medial rotator) is significantly larger in orangutans, than in chimpanzees, while Zihlman et al (2011) find no differences between rotator cuff muscles between gorillas and orangutans, but marked differences in the size of the latissimus dorsi (a medial rotator), between these species, with the latissiumus dorsi in orangutans comprising more than 50% of the major trunk muscles. Larson (1988) hypothesizes that the greater recruitment of the subscapularis in gibbons is necessary to overcome the effects of a lateral-facing elbow caused by low torsion, but perhaps an alternative explanation is that the recruitment of the subscapularis (along with the other medial rotators) in gibbons acts to maintain the low degree of torsion by stopping the medial rotation of the humeral head, which in turn keeps the elbow in a more lateral-facing position. It is possible that the same occurs in *Pongo*, albeit to a lesser degree because orangutans are not committed brachiators, although still almost exclusively arboreal, with substantial involvement of overhead movements (MacKinnon 1974; Cant 1987; Delgado and Van Schaik 2000; Thorpe and Crompton, 2005, 2006). The faster life histories of gibbons compared to African apes and humans may also be in part responsible for the lower degrees of torsion in this species, because this means the humeral head in gibbons is exposed to rotational forces for less time prior to fusion. However, this does not explain the presence of relatively low humeral torsion in *Pongo*, whose life histories are similar to that of African apes (Wich et al. 2004; Kelley and Schwartz 2010), supporting the notion that low torsion is actively maintained throughout growth in these species. This explanation would also account for the slower torsion development seen in the present bonobo sample – although there are no significant differences in torsion between chimpanzees and bonobos at any stage (also reported by Inouye, 2003), bonobos do engage in higher frequencies of suspensory and arm-swinging behaviour than

chimpanzees throughout life (Doran 1992; Doran 1993), which may be responsible for slower rates of torsion increase (figure 21-23). In contrast, chimpanzees and gorillas are adult-like in their locomotion pattern (mostly quadrupdedal) by 4 years of age (Doran 1997), which coincides with M1 eruption in great apes (Kelley and Schwartz 2010), and is also when torsion appear to start stabilizing (figure 21-23).

The idea that lateral-facing elbows are suited to suspensory behaviours and brachiation has indeed been proposed by Larson (1988); the author describes how all apes engage in a characteristic form of arm-swinging in which the body undergoes 180 degrees of rotation around the supporting hand. This results in extreme rotation of the forelimb at the end of the support phase whereby the humerus is laterally rotated at the shoulder in such a way that the cubital fossa (the inner elbow) faces superiorly (Avis 1962; Larson 1988). The chimpanzees, who have relatively high humeral torsion, must then hypersupinate the foream to achieve the full range of rotation around the supporting arm, while gibbons, who have relatively low torsion and thus more laterally-facing elbows, do not (Larson 1988). Although chimpanzees engage in brachiation, the adaptation seems particularly relevant for the gibbons, who spend 50–80% of their travelling time brachiating (Fleagle 1974; Fleagle 1976; Andrews and Groves, 1976; Carpenter, 1976; Hollihn 1984; Preuschoft and Demes 1984; Tuttle 1986; Takahashi 1990), and for the orangutans, who spend about 40% of their time engaging in suspensory locomotion and 25% engaging in vertical climbing (Thorpe and Crompton 2006). The idea that the elbow joint is under selection due to the use of suspensory behaviours is further supported by other lines of evidence which show that in gibbons and orangutans the elbow appears to be more powerful than in other hominoids, the elbow flexors especially are more powerful compared with those of non-specialized brachiators suggesting that elbow muscles are particularly important for a brachiating/suspensory lifestyle (Usherwood et al. 2003; Oishi et al. 2008, 2009; Michilsens et al. 2009).

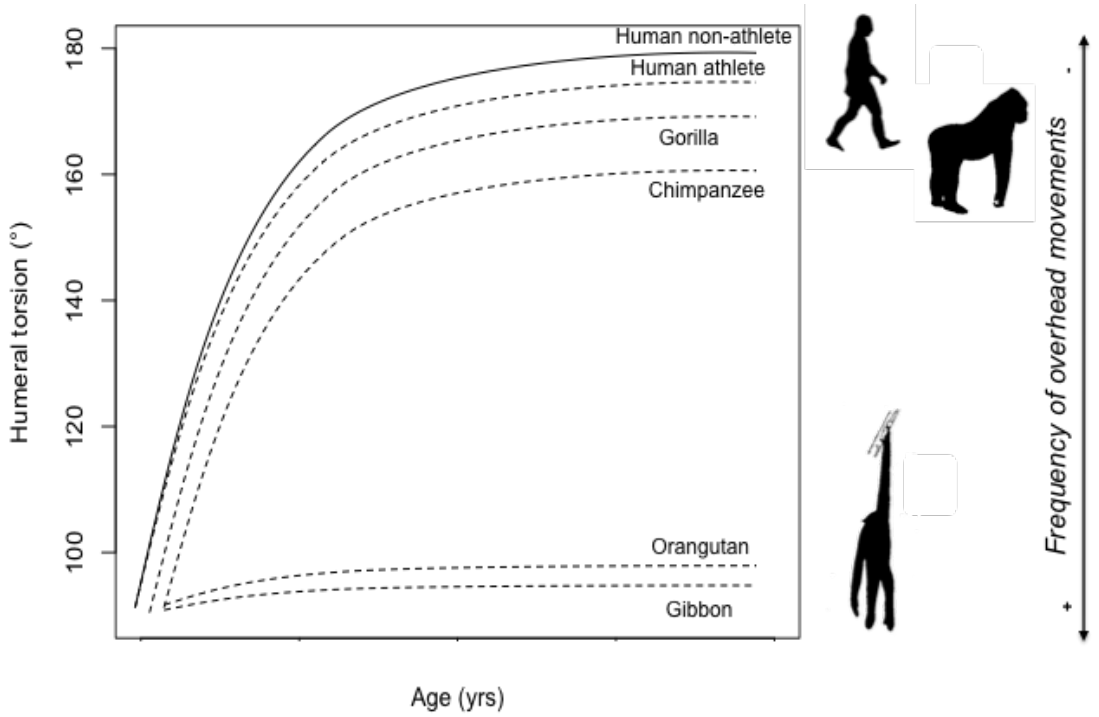

Figure 26 – Schematic representation of the suggested scenario for the evolution of torsion in the hominoid clade. Low torsion in the suspensory gibbon and *Pongo* lineages suggests a common ancestor that had low torsion and suspensory locomotion/frequent overhead behaviours; high torsion in African apes and humans suggests a common ancestor with less suspensory locomotion/ frequent overhead behaviours.

Overall, it seems that elbow positioning may indeed be an important adaptation for brachiation and more generally, suspension, in hominoids as suggested by Larson (1988), and that low humeral torsion, rather than simply being an accommodation to the dorsal repositioning of the scapula (Larson, 1988, 1993, 1996), may in fact be a consequence of the need to maintain the elbows in a lateral set necessary to a orthograde suspensory lifestyle in the hominoid clade (figure 26 & 27). Low torsion would thus be conserved throughout ontogeny in the more orthograde suspensory hominoids via the greater action of the medial rotators of the shoulder, thus stopping the natural medial rotation of the humeral head. In the absence of such frequencies of overheard movements, torsion would then be free to complete its medial rotation until fusion – and indeed humans, who are committed bipeds with long life histories, often reach full torsion levels of 180° (Krahl and Evans 1945; Krahl 1976; Edelson 1999; figure 19 present study). Additionally, because evidence suggests that the natural tendency is for torsion to increase with growth (and thus for the elbows to move inwards/medially), it is possible that high torsion, rather than being an adaptation for

quadrupedal locomotion and knuckle-walking in African apes, is rather a consequence of the decreased importance of orthograde suspensory behaviours or more generally, frequent overhead movements, in these lineages. The slower development of torsion in bonobos compared to the less suspensory chimpanzees (present study), the higher degrees of torsion in captive orangutans (Sarmiento 1985), and the lower degrees of torsion of lowland gorillas compared to the more terrestrial mountain gorillas (Inouye 2003), may support this suggestion.

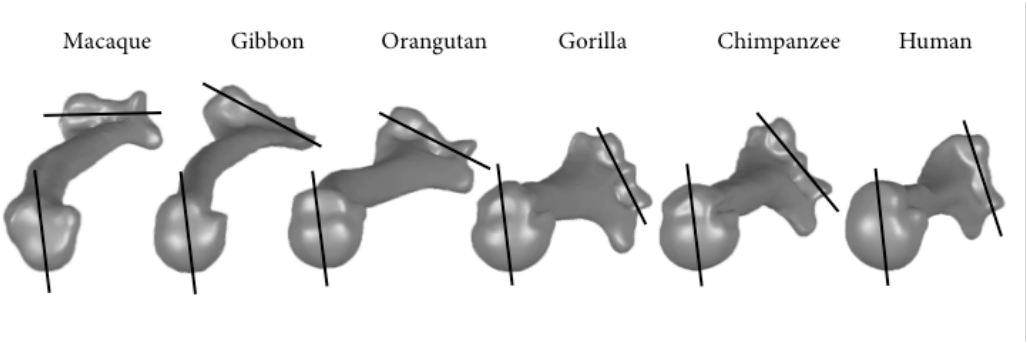

Figure 27 – Cranial view of humeral torsion angles in the left humerus of hominoids and *Macaca fascicularis* illustrating the orientation of the elbow joint in relation to orientation of the proximal humeral head (shown in the same orientation for all species). The gibbon and orangutan elbow joint is more laterally oriented than the other hominoid species.

Because low torsion is assumed to be the primitive condition in hominoid apes, high torsion has typically been viewed as the functionally significant condition (Larson, 1988; Gebo 1998), ascribed to the possible knuckle-walking ancestry of African apes and humans (Richmond et al. 2001; Begun 2004; Begun et al. 2007; Venkataraman et al. 2013). However, the underlying ontogenetic patterns leading to humeral torsion in the different hominoid lineages challenge this notion by suggesting that low torsion may be actively maintained via a developmental mechanism in hominoids. By viewing this trait under this ontogenetic framework, differences in torsion between species and between individuals can be explained without the need for recurring homoplasies or speculations about the origins of knuckle-walking. Under this perspective, elevated torsion would simply result from a reduced level of muscular activity resulting in a higher constraint on the development of humeral torsion due to decreases in frequency of orthograde suspensory/climbing behaviours, and thus would not be associated to the emergence of knuckle-walking locomotion *per se* as is currently proposed (Larson 1996, 1988; Richmond et al. 2001; Begun 2004; Larson et

al. 2007). The low torsion in fossil hominins would also be explained under this framework, by the likely more active lifestyles in *Homo erectus* and Neanderthals, and/or the importance of suspension and climbing in australopithecins, as has in fact been recently suggested (Green and Alemseged 2012; Venkataraman et al. 2013).

I should note however, that even though humeral torsion seems to be a developmentally plastic trait, it is likely to be genetically constrained up to a certain extent, since human athletes who engage in repetitive overhead movements throughout life (such as baseball pitchers for example), do not reach low levels of torsion in the range of *Pongo* or *Hylobates* (e.g., Crockett et al. 2002; Reagan et al. 2002; Whiteley et al. 2010), nor do captive quadrupedal orangutans develop torsion levels comparable to those of African apes (Sarmiento 1985). Further evidence on torsion differences between wild and captive apes would be useful to understand the extent of plasticity in this trait in non-human hominoids; information on the ratios of medial-to-lateral rotator muscle strength in non-hominoids and their relationship to torsion would also help confirm my suggestions. Additionally, information on the degree of humeral head torsion in human swimmers and gymnasts, and populations who engage in regular climbing activities such as the Twa from Uganda (Venkatraman et al. 2013), would be useful to understand whether overhead movements aside from throwing also produce relatively low torsion.

4.2. Ontogenetic patterns reveal clade-specific patterns in primate humeral head torsion

In macaques, on the other hand, whose scapulae are laterally positioned on a deep and narrow thorax, the low degrees of torsion allow for the elbows to face forward (cranially), thus permitting the arms to move in a parasagittal plane (Sarmiento 1985; Chan 2007; Rein et al. 2011). Therefore, while in the quadrupedal hominoids, it is high torsion that allows for the arms to move in a parasagittal plane, in the quadrupedal *Macaca*, it is low torsion that allow for this to happen. This explains the differences in the ontogenetic trajectories of humeral torsion between African apes

and *Macaca* – due to differences in scapular position between these clades, humeral head rotation follows opposite directionalities in these species in order to achieve similar forearm positioning (figure 28). On the other hand, the inverse also appears to be true – i.e. that relatively higher torsion in monkeys is related to suspension while in hominoids it is related to quadrupedalism –, as the highly suspensory atelines have relatively higher torsion than the quadrupedal ceboids and cercopithecoids (Larson 1996), with torsion levels that are in fact comparable to those seen in the highly suspensory hylobatids (ranging 105° to 123° in atelines according to Larson, 1988 and Gebo, 1996) (figure 29). Indeed, *Ateles* is said to converge on the hominoid pattern, especially on the hylobatid pattern, in many features of shoulder morphology including in degree of humeral torsion (Larson 1998; Young 2003).

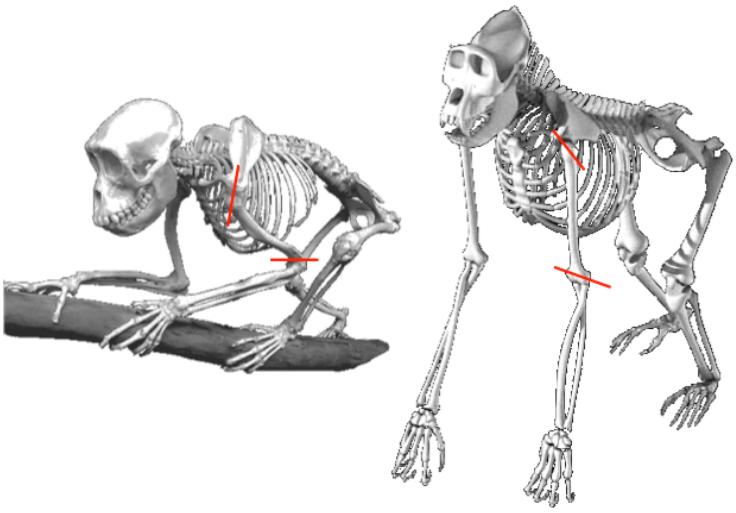

Figure 28 – *Macaca fascicularis* (left) and *Gorilla* (right) skeletons showing the proximal and distal axes of the humerus (red). Note the low torsion in *Macaca* and the high torsion in *Gorilla* despite the use of quadrupedal locomotion; this likely results from differences in shoulder configuration between clades (laterally facing scapula in *Macaca*, and dorsally oriented scapula in *Gorilla* and hominoids).

This explains why *Macaca* and *Hylobates* both have relatively low torsion values even though they have completely different locomotor repertoires, as low torsion appears to serve opposite purposes in both species and clades. As a result, predicting the locomotion of extant species based on humeral torsion across clades may be problematic, as is the case in Rein et al's (2011) study of skeletal correlates of quadrupedalism and climbing in the anthropoid forelimb. In this sense, it may be more suitable to build clade-specific predictive models for locomotor types when

using humeral torsion. This has important implications for predicting locomotion from humeral torsion in fossil primates, especially in cases where information about scapular positioning is unavailable, or when phylogenetic position is contentious. This is particularly relevant for stem hominoids because these are expected to possess a combination of 'ape-like' and 'monkey-like' traits, as has been found in the forelimb of Miocene primates such as such as *Proconsul, Afropithecus, Equatorius, Sivapithecus* and *Pliopithecus vindobonensis* (e.g., Zapfe 1958,1960; Pilbeam and Simons 1971; Corruccini et al. 1976; Rose 1989, 1994, 1997; Ward 1998, 2007; Pilbeam et al. 1990; Begun 1992a, b, 2010; Moyà-Solà and Köhler 1996; Larson 1998; Ward et al. 1999; MaClatchy et al. 2000; Nakatsukasa et al. 2003; Moyà-Solà et al. 2004, 2009; Ishida et al. 2004; Dunsworth 2006; Nakatsukasa et al. 2007; Suwa et al. 2007; Kunimatsu et al. 2007). Moreover, given the humeral torsion patterns described in the present study (with increasingly higher torsion developing in the most recently diverged hominoid species and decreasing torsion in *Macaca*) (figure 21 & 22), I would expect stem hominoids to possess relatively low degrees of torsion, as is the case for *Proconsul* and *Pliopithecus* (Larson 1996). However, because of their phylogenetic position at the stem of the hominoid lineage and given the inverse relationship between torsion and quadrupedalism in the two clades – with low torsion relating to suspension in hominoids and to quadrupedalism in cercopithecines –, it is difficult to make predictions about *Proconsul* and *Pliopithecus* locomotion based on humeral torsion alone. Indeed, Rein et al's (2011) predictive models yield contradictory information regarding the degree of quadrupedalism in *Proconsul* and *Pliopithecus*, namely, the predictive model based on torsion suggests that *Pliopithecus* was less quadrupedal than *Proconsul*, while the predictive model based on the olecranon process suggests this species was highly quadrupedal like *Proconsul*.

Further studies on the ontogeny of humeral torsion in cercopithecines and platyrrhines should explore whether differences in the development of this trait also exist between species with divergent locomotor types in these clades, in particular, between the brachiating atelines and the quadrupedal cercopithecoids.

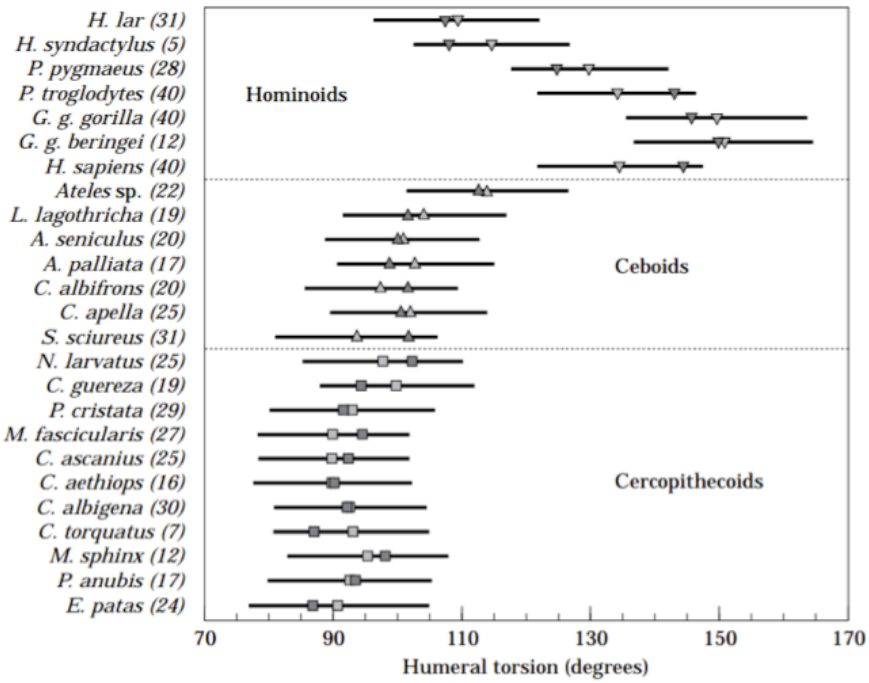

Figure 29 – Predicted mean torsion values (based on proximal landmarks of the humerus, see Larson 1996 for details) (light shaded symbols) plus 95% confidence intervals for those predicted values (black bars), and actual mean values for humeral torsion for each species (dark shaded symbols); taken from Larson (1996). This shows the inverted relationship between torsion and suspensory behaviour in the hominoid and monkey clades: more suspensory apes have relatively lower torsion (i.e. *Hylobates lar*), while more suspensory monkeys (i.e. *Ateles*) have relatively higher torsion.

4.3. Growth and development of humeral torsion: homology or homoplasy?

The variation in the developmental timing and expression of humeral torsion between hominoid species in this study indicates divergent ontogenetic trajectories in torsion within the hominoid clade that match the phylogenetic distances between species with, on the one hand, the Asian apes maintaining relatively low degrees of torsion throughout ontogeny and, on the other hand, the African apes and humans increasing their humeral torsion throughout ontogeny. However, the absence of significant differences in torsion values at birth between hominoid species suggests a common origin to this trait, with differences in torsion arising subsequently, as a product of changes in body size and divergent locomotor habits between species and between individuals. Differences between the *Macaca* and hominoid torsion ontogenies further highlight divergent evolutionary patterns of torsion development between these clades, likely related to anatomical differences in shoulder configuration.

Unfortunately, it is not possible to estimate whether torsion in *Macaca* infants is comparable to that of infant hominoids since the youngest individuals in the sample are ~2,5 years, but the ontogenetic patterns leading to torsion differences within the hominoid clade, suggest that there is a common developmental mechanism underlying these differences in these species.

Given this scenario of torsion development whereby the more recently diverged and terrestrial species (African apes) have relatively higher torsion than the more distantly diverged suspensory ones (Asian apes), and assuming my interpretations about the developmental mechanisms driving humeral torsion are correct, my results are compatible with the notion that the relatively high levels of torsion of African apes and humans is a homology. On the other hand, because my results also support that humeral torsion is a highly developmentally plastic trait, and because more closely related hominoid species also share similar modes of locomotion, these results are equally compatible with the notion that the relatively high degrees of torsion in African apes and humans are the result of parallel evolution, arising as a consequence of decreased orthograde suspensory behaviours/increased terrestrial quadrupedalism, in the various hominoid lineages (extant and extinct).

Indeed, since *Pongo* and *Hylobates* are the first two lineages to diverge, and because both are almost exclusively arboreal with relatively low degrees of torsion, my own results on humeral torsion are compatible with the notion that the ancestral hominoid morphotype was a suspensory ape, and that the high levels of torsion in African apes and humans are homologous, arising once, in the LCA of African apes and humans, due to the decreased importance of orthograde suspensory/climbing behaviours, in combination with increased body size and longer life history (figure 30). Because the vast majority of the features supporting a climbing hypothesis are also consistent with the knuckle-walking hypothesis (Thorpe and Crompton 2006; Thorpe et al. 2007; Crompton and Thorpe 2007; Crompton et al. 2008), these results are compatible with the notion that knuckle-walking evolved once, from a climbing ancestor, as a means for an ape to travel terrestrially while maintaining climbing adaptations (Tuttle and

Basmajian 1974; Richmond et al. 2001). In fact, because quadrupedal knuckle or fist walking is a behaviour found in all the large apes (Young 2003), Young (2003) argues that it is an efficient solution for animals that need to retain arboreal suspensory capabilities. This scenario would thus place knuckle walking as the mode of locomotion from which human bipedalism arose.

However, the problem with this scenario is that it does not explain the low levels of torsion in early hominins, which is the main reason why the high levels of torsion in African apes and humans are hypothesized to have evolved in parallel (Larson, 1996, 1998, 2007a,b). Moreover, because of *Hylobates'* small body size and highly derived brachiating specializations, this species' morphology is likely to be secondarily derived since its divergence from a more generalized suspensory ancestor (Cartmill 1985; Young 2003), and therefore, postcranially, this species may make a poor representative of the hominoid ancestral morphotype even though it is the first hominoid to diverge (Groves 1972; Ruvolo 1997; Roos and Geissmann 2001). My own results also suggest that distinguishing the Asian apes and the African apes on the basis of torsion is misleading, since within the Asian apes, gibbons and orangutans show significant differences in adult humeral torsion, with gibbons exhibiting very low levels of torsion comparable to those of *Macaca fascicularis,* and with *Pongo* showing significant differences in adult torsion with African apes (and humans), with intermediate levels of torsion between that of gibbons and that of African apes. What the Asian apes do seem to have in common is the fact that torsion remains essentially stable throughout ontogeny, unlike in African apes who increase torsion throughout growth (and who do not significantly differ in their adult humeral torsion levels, table 12). These results indicate that the way by which torsion develops is similar within the Asian apes and also within the African apes, but this can be attributed to the high levels of developmental plasticity in torsion and the similar modes of locomotion in these species rather than to a homologous origin. It is thus equally possible that low torsion in gibbons and *Pongo* results from parallel evolution of suspensory behaviours as suggested by Larson (1998), and that that the high levels of torsion of African apes and humans are also the result of parallelism – a scenario which would explain the

low levels of torsion in early hominins and which is consistent with the suggestion that knuckle-walking may have evolved independently in the various hominoid lineages (Kivell and Schmitt 2009; Begun and Kivell 2011; *contra* Richmond and Strait 2000, Richmond et a. 2001). The Miocene hominoid fossil record supports multiple instances of independent evolution of specialized suspensory adaptations (e. g., *Morotopithecus, Oreopithecus, Dryopithecus*, or *Pongo*) (Begun, 2007), and the presence of knuckle-walking features in the hind limb, humerus, and wrist bones of *Sivapithecus* (Begun and Kivell, 2011), also supports the case of independent evolution of knuckle-walking.

These results thus support that the mechanism by which torsion is achieved appears to be homologous to all hominoids, as indicated by the clade specific differences that seem to exist between *Macaca fascicularis* and the hominoids, and that activity after birth dictates the amount of torsion levels in adulthood, within phylogenetic constraints, but these results cannot support either the independent or homologous evolution of this trait in African apes and humans, and whichever the scenario, it is unlikely that humeral torsion can be used as direct evidence in support of one over the other.

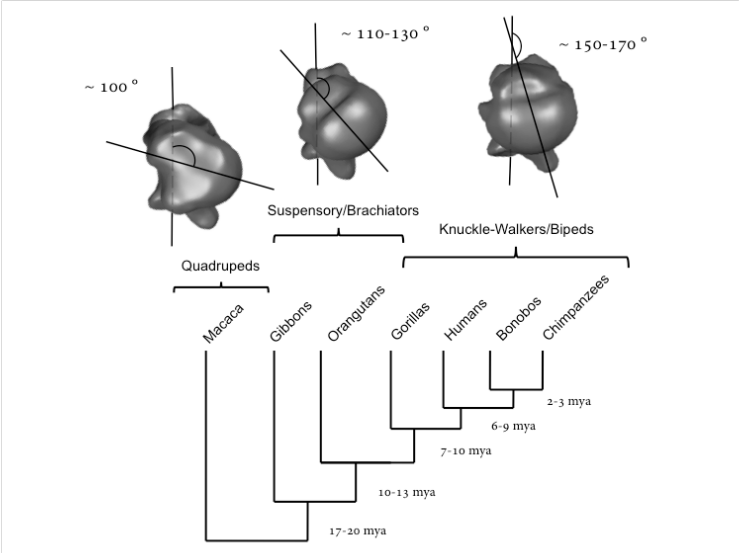

Figure 30 – Phylogenetic relationships between hominoid species and *Macaca fascicularis* (not scaled), illustrating how degrees of torsion match phylogenetic relationships, size and locomotor types. Note the increased torsion in the more recently diverged, large-bodied, quadrupedal species.

5. Conclusion

The present study aimed to determine whether humeral torsion in hominoid primates is a shared derived character or, on the contrary, an independently acquired trait in the different hominoid lineages by studying its ontogenetic development. This study was based on the assumption that homologous characters arise through similar developmental processes, while characters that are homoplastic arise through different developmental processes, and it thus takes into account variation within and across species and age classes.

My results show that humeral torsion in non-human hominoid primates develops throughout ontogeny and ceases around adulthood, and is the first study to establish this. This study shows that differences in the timing and expression of torsion between species appear with growth and match remarkably well with on the one hand (a) species locomotor repertoire, phylogenetic relationships, size and life history, and on the other hand, (b) changing locomotor patterns through life in the different species. Bonobos for example seem to develop torsion more slowly throughout life, compared to chimpanzees and gorillas, which is congruent with their more suspensory lifestyles (Doran 1992, 1993, 1997). Chimpanzees and gorillas, on the other hand, adopt fully adult locomotor patterns by the age of 4 years (Doran 1997), which coincides with M1 emergence, and cessation of torsion development. Additionally, Asian apes, who are committed orhograde suspensory apes maintain low torsion throughout growth, which supports the notion that lateral-facing elbows are important for highly arboreal lifestyles (Larson 1988), while humans, whose upper limbs are free from locomotor contraints, are the only hominoid species that reach the full range of humeral head rotation at 180 degrees.

Perhaps one of the most interesting results, however, is the find that macaques develop torsion in an entirely opposite way to that of hominoids: by reducing torsion throughout growth rather than increasing it. I suggest that humeral head rotation follows opposite directionalities in these species in order to achieve similar forearm

positioning due to differences in scapular positioning. Although I cannot confirm this, I suspect that torsion levels at birth in this species should be in the range of that of infant hominoids, as is predicted by the Gompertz models. If this is true, this suggests a deeper evolutionary inheritance to this trait, with differences in torsion arising as a result of divergent shoulder configurations between monkey and hominoid clades, most likely due to thoracic expansion and dorsal repositioning of the scapula in hominoids (Larson 1996; Chan 2007a,b; Kagaya 2008, 2010). Most crucially, these divergent patterns between *Macaca* and hominoids indicate opposite relationships between torsion and locomotion in these clades, with relatively high torsion in hominoids relating to terrestrial quadrupedalism, and relatively low torsion relating to orthograde uspensory behaviours, while in New World and Old World monkeys it is relatively low torsion that relates to terrestrial quadrupedalism and relatively high torsion that related to orthograde suspensory behaviours. This has important implications for the interpretation of locomotion from fossil postcranial remains, and particularly so for stem hominoid fossils who are expected to present a mosaic of shoulder characteristics that are both ape-like and monkey-like. I propose that predictive models for locomotor types based on humeral torsion should be clade-specific, and interpretations should preferentially not be made without additional information about scapular positioning and/or thoracic shape.

Finally, I propose that it is low torsion, rather than high torsion that is the functionally significant condition in hominoids, and that this trait is related to suspension/climbing behaviours, or more generally, to any locomotor behaviours involving frequent use of the arms in overhead movements/postures. For this reason my results can neither support nor reject the independent or shared derivation of knuckle-walking in hominoids, and instead suggest that high torsion in African apes and humans arises as a by-product of decreased frequencies of orthograde suspensory/climbing activities and by consequence, the greater importance of terrestrial quadrupedal locomotion – but not knuckle-walking specifically – in African apes and humans.

In sum, this study shows (1) that there is no evidence for interspecific differences in torsion in hominoids at birth, (2) that there are interspecific differences in torsion in adult hominoids, but (3) also large amounts of intraspecific variation in torsion in all hominoid species throughout growth. Therefore, these results suggest that humeral torsion is a highly plastic trait that reflects individual behaviour, but operating within phylogenetic constraints. This phylogenetic component is most likely determined by selection for specific patterns of locomotor and postural behaviour – which given the lack of inter-specific differences at birth, appears to have acted primarily on post-natal development –, but modulated by the underlying anatomy of the thorax and shoulder girdle. Future work should include an increased sample of very young individuals and a broader intraspecific sample.

– Chapter 4 –

The evolution of humeral torsion in hominoids – a phylogenetically integrated, comparative analysis of humeral torsion in hominoid primates

1. Introduction

The evolution of biological traits is better understood when framed within a phylogenetic perspective because a phylogenetic framework is essential in 1) assessing evolutionary trends, 2) inferring changes in rates of evolution, and 3) ascertaining whether observed similarities result from common descent or were acquired independently (Revell et al. 2008; Sakamoto and Ruta 2012). Therefore, phylogenetic methods for statistical analysis of morphological data, which address the issue of non-independence of data points (Blomberg and Garland 2002; Blomberg et al. 2003; Garland Jr et al. 2005; Revell et al. 2008), have become widely accepted in recent years (O'Meara et al. 2006; Smaers and Vinicius 2009; Jombart et al. 2010; Ivanović et al. 2012; Revell 2012; Sakamoto and Ruta 2012; Smaers et al. 2011, 2012). Furthermore, improvements in computing, namely the development of multifunctional packages designed for R (R Development Core Team 2011), such as 'ape' (Analysis of Phylogenetics and Evolution [Paradis et al. 2004]), 'geiger' (Harmon et al. 2008), 'adephylo' (Jombart et al. 2010), 'phangorn' (Schliep 2011), and 'phytools' (Revell 2012), have facilitated and popularized the application of phylogenetic methods.

The appeal of incorporating phylogenetic information into morphological comparisons is especially evident when considering taxonomic groups and/or anatomical areas where homoplasies are prevalent. Indeed, the lack of congruence in many cases between phylogenies inferred from molecular data versus phylogenies

inferred from morphological data, and/or between those inferred using phenetic versus cladistic approaches, has been a major topic of discussion over the last two decades (David and Laurin 1996; Collard and Wood 2000; Collard and Wood 2001; Cannon and Manos 2001; Collard and O'Higgins 2002; Singleton 2002; Frost et al. 2003; Caumul and Polly 2005; Leinonen et al. 2006; Begun 2007; Collard and Wood 2007; Neustupa and Skaloud 2007; Young 2008; Klingenberg and Gidaszewski 2010). Reconstructing trees from morphology assumes a clear association between morphological and evolutionary diversification, an assumption that is highly problematic when considering homoplasies, and in cases of mosaic evolution. Moreover, the lack of congruence between morphometric evolution and genetic differentiation results from the process of adaptation itself (Zelditch et al. 1995; Monteiro 2000; Brehm et al. 2001; Naylor and Adams 2001; MacLeod and Forey 2002; Rohlf 2002; Hoekstra et al. 2004; Lockwood et al. 2004; Lycett and Collard 2005; Michaux et al. 2007; Cardini and Elton 2008; González-José et al. 2008; Polly 2001). Since understanding processes of adaptation is the primary goal of comparative biology, rather than 'removing', 'controlling' or 'accounting' for a phylogenetic signal, a better alternative is to 'map' the morphological traits onto the phylogeny itself, thereby highlighting processes of adaption (including homoplasies) occurring across the branches of a phylogeny.

The study of shoulder morphology and, in particular, humeral torsion benefits greatly from being studied within a phylogenetic framework because much debate exists over whether the shared similarities in shoulder anatomy in hominoids are a product of shared ancestry or rather have evolved more recently in parallel (Washburn 1967; Richmond and Strait 2000; Richmond et al. 2001; Begun 2004; Larson 1996, 1998, 2007, 2009, 2013; Larson et al. 2007). This is especially true in the case of African apes and humans, who share a number of similarities in shoulder morphology such as dorsally placed scapulae, elevated humeral torsion, and S-shaped clavicles (Miller 1933; Ashton and Oxnard 1963,1964; Oxnard 1963, 1967; Ashton et al. 1971, 1976; Roberts 1974; Larson 1988). Additionally, the fact that African apes share similar locomotor repertoires (i.e. knuckle-walking), has led to the suggestion that knuckle-

walking is the locomotor habit from which bipedalism arose (Washburn 1967; Richmond and Strait 2000; Richmond et al. 2001; Begun 2004). The discovery of Miocene and Plio-pleistocene fossils, which exhibit a mix of ancestral and derived traits has, however, cast some doubt over this suggestion of shared ancestry (Larson 1996, 2007, 2009, 2013; Larson et al. 2007). For example, *Sivapithecus* is most likely an ancestor of *Pongo* but exhibits a postcranial anatomy reminiscent of that of African apes, and the australopithecine scapula morphology is more similar to that of *Gorilla*, even though australopithecines are more closely related to humans and chimpanzees (Young 2003; Alemseged et al. 2006; Begun and Kivell 2011).

The degree of humeral torsion in extant and extinct hominoids has been at the centre of this debate for over a decade, because it is thought that this trait caries both a phylogenetic signal and a locomotor signal (Krahl and Evans 1945) – with relatively higher degrees of torsion in the more closely related African apes and humans being generally associated with movement of the arms in a parasagittal plane (such as in knuckle-walking and manipulation) (Washburn 1967; Richmond and Strait 2000; Richmond et al. 2001; Begun 2004). However, the presence of elevated humeral torsion in extant great apes is directly at odds with the low degrees of torsion found in the Miocene and Plio-pleistocene hominid fossil record, leading to the suggestion that the high degrees of torsion shared, for example, between the great apes and humans arose in parallel in the individual lineages due to their independently acquired locomotor requirements (Larson 1996, 2007, 2009, 2013; Larson et al. 2007). Under this scenario, knuckle-walking would have arisen independently in gorillas and chimpanzees, and thus would not be the locomotor behaviour from which bipedalism arose. These conflicting interpretations regarding the varying degrees of humeral torsion in extant and extinct hominoids reveal its potential in reconstructing locomotor ancestry in the homoinoid clade.

The high degrees of intra-specific variation in humeral torsion in hominoids (see Chapter 3) however, confound its use as a diagnostic character of both phylogenetic relationships and locomotor habits; this is because humeral torsion is a highly plastic

trait, which has been shown to vary widely across human groups (athletes versus non-athletes), populations, sexes and sides (Krahl and Evans 1945; Edelson 1999; Pieper 1998; Crockett et al. 2002; Osbahr et al. 2002; Cowgill 2007). For example, in the great apes, the average within-species range of variation is comparable to the range of species means, showing that within-species differences can be substantially more elevated than between-species differences (table 16; figure 31). Moreover, torsion has been shown to increase with age in hominoids and therefore is highly developmentally plastic (Chapter 3). This is problematic not only when performing cross-species comparisons, but also highlights the problem with establishing effective comparisons between extant species and single fossil values (many times estimated on incomplete and/or immature fossils).

Table 16 – Table of mean torsion, minimum torsion and maximum torsion values found in the present study (adults). Differences between minimum and maximum torsion values are reported. This illustrates the spread of the distribution in torsion values in the present study.

Species	Mean torsion (°)	Min torsion (°)	Max torsion (°)	Max-Min torsion (°)
Homo sapiens	168.5	149.18	180	30.82
Pan troglodytes	152.6	137.29	168.48	31.19
Pan paniscus	151.5	137.74	161.37	23.63
Gorilla gorilla	160.2	143.31	175.03	31.72
Pongo pygmaeus	136	106.17	156.7	50.53
Hylobates lar	111.9	103.28	119.14	15.86
Macaca fascicularis	101.4	98.08	101.65	3.57

In order to understand whether torsion is more likely to have evolved as a result of shared ancestry (homology) or functional convergence (homoplasy) in the hominoid clade, the present study analyses humeral torsion within a phylogenetic framework and taking into account intraspecific variation. I use the method of 'Independent Evolution' (IE) (Smaers and Vinicius 2009; Smaers et al. 2012, 2013), which is a variable-rates method for estimating rates of evolution across individual branches of a phylogenetic tree, and a re-sampling technique (Smaers, unpublished), that takes into account the adult variation within each sample. I also incorporate fossil torsion values, allowing for the uncertainty associated with these single torsion measurements by attributing standard deviations and deriving distributions from which values are computationally re-sampled.

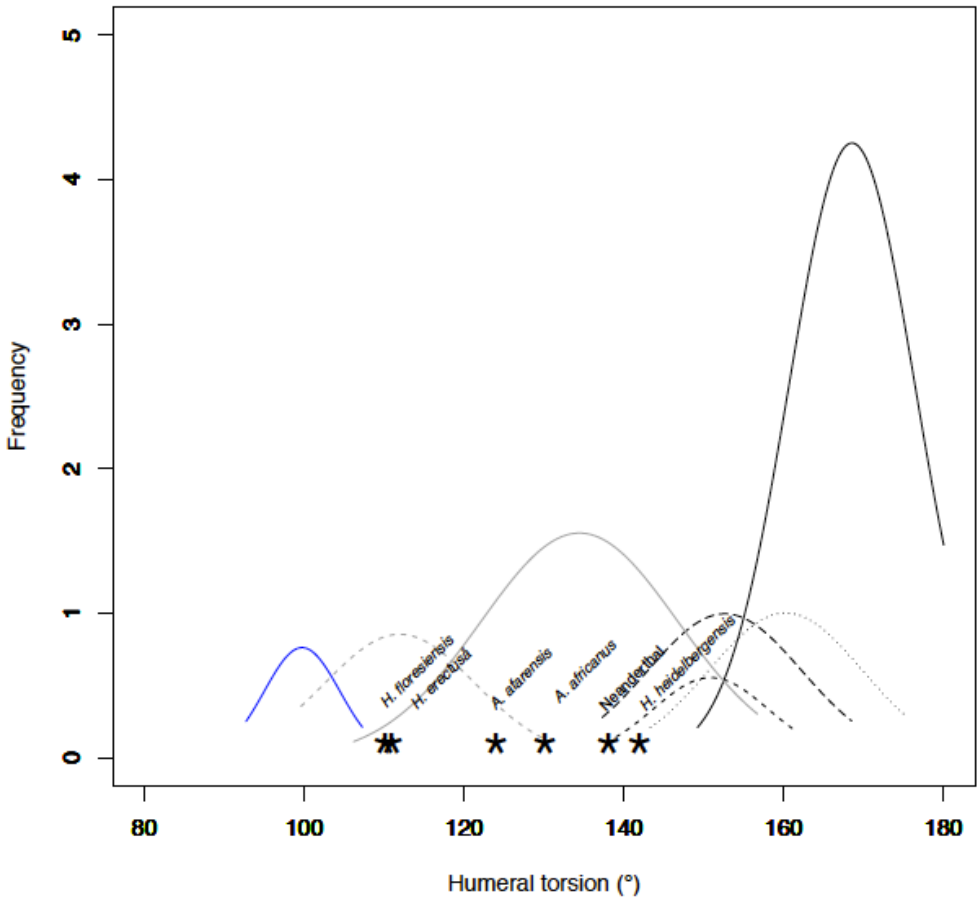

Figure 31 – Absolute frequency distribution of humeral torsion in hominoid primates (solid black line: *H. sapiens*; dotted line: *G. gorilla*; long dashed line: *P. troglodytes*; small dashed line: *P. paniscus*; gray solid line: *P. pygmaeus*; gray dashed line: *H. lar*) and *Macaca fascicularis* (solid blue line). Asterisks show hominin fossil values. The figure illustrates how hominin fossil values fall outside the range of variation for my human sample, and most fall outside the range of variation of my African ape sample.

2. Materials and Methods

2.1. Independent evolution

I use a phylogenetically-integrated approach that quantifies evolutionary changes along individual branches of an independently-derived (molecular-based) phylogeny. This method, 'Independent Evolution' (Smaers and Vinicius 2009; Smaers et al. 2012, 2013), highlights processes of phenotypic change occurring across individual branches of a phylogeny and therefore has the potential to identify processes such as convergence and mosaic evolution within the skeleton. This approach moves away

from direct species comparisons by (1) utilizing independently estimated (molecular) phylogenies to identify which morphological signals dominate the evolution of an anatomical module and (2) by inferring the timing and rate of evolutionary changes along individual lineages. By quantifying evolutionary changes along individual branches of the tree of life, this approach allows robust inferences of instances of independent evolution and provides a useful framework to help interpret fossil morphology. I apply this method to a phylogeny of 44 primate species, which includes extant New World Monkeys (n=7), extant Old World Monkeys (n=15) and extant hominoids (n=8). I also include 14 fossil species (*Homo neanderthalensis*, *Homo heidelbergensis, Homo floresiensis, Homo erectus, Paranthropus boisei, Australopithecus africanus, Australopithecus afarensis, Australopithecus sediba, Dryopithecus fontani, Proconsul heseloni, Rhinocolobus turkanaensis, Paracolobus chemeroni, Cercopithecoides williamsi, Pliopithecus* sp.). The extant primate phylogeny is taken from the 10k Trees Project (version 3) (Arnold and Nunn 2010). Fossil species are placed onto the phylogeny following the best solution given the divergence dates of the molecular phylogeny. My own data on humeral torsion is used for the hominoid species and *Macaca fascicularis*. For all other species (NWMs and OWMs), torsion measurements are taken from the literature: from Larson (1996) and Rein (2011). Fossil torsion values are taken from Larson (1996, 2007), Rhodes and Churchill (2009), Churchill et al. (2013), and Lordkipanidze et al. (2007).

2.2. Re-sampling

In order to incorporate uncertainty due to intra-specific variation into the analysis, the ancestral values are estimated using IE in combination with a new re-sampling approach developed by Dr. Smaers (unpublished). This approach consists of two steps: (1) defining a sample of values for each species; (2) running analyses across all different combinations of values across species. For the first step, the standard deviation of torsion was computed for those species for which different values per species were available (18 out of 30 extant species). This standard deviation averaged 9 ± 2 (figure 32). For some species, however, values for only one specimen were

available. To define an equal sample of values for each species, 1000 values were drawn from a normal distribution with a mean equal to the species average measurement and a standard deviation of 9 ± 2. At the end of this first step, each species is allocated 1000 values for torsion (with an average value of the average torsion measurement from the literature and a standard deviation of 9). Secondlly, in order to include intraspecific variation, analyses were repeated for all possible combinations of values across species. For example in the case of 2 species X and Y with values A and B for X and C and D for Y, the analysis is repeated using values A and C, A and D, B and C, B and D. Because an exhaustive sampling (such as in this example) is not feasible for larger samples, a separate sampling was performed that draws 10,000 different combinations from all possible combinations. Final results are based on this set of 10,000 results. The ancestral values for each node and associated estimated mean rates of evolution were thus obtained (using IE) by running 10,000 iterations across individual samples.

This approach produces two types of results crucial to the comparative phylogenetic analysis of torsion: 1) graphs showing the estimated mean ancestral values with associated estimated mean rates of evolution, and 2) graphs showing the estimated standard deviation associated to the estimated mean ancestral values and rates of evolution. These last graphs allow identifying the branches and nodes where the most uncertainty (attributed to intraspecific variation) exists.

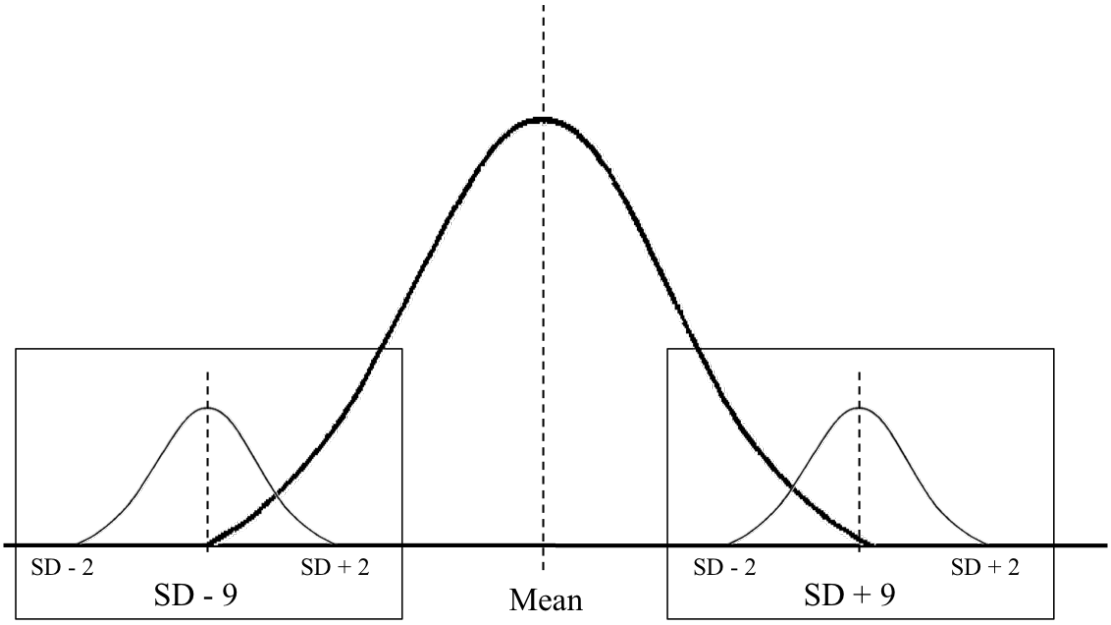

Figure 32 – A mean standard deviation of 9 was applied to all species. This mean standard deviation was calculated based on 18 extant species distributions. The standard deviation of this mean standard deviation was also calculated (± 2). The re-sampling code in IE ran 1000 iterations between samples, creating distributions of 1000 values with standard deviations 9 ± 2 for each sample/species. For each iteration, the code first randomly selects a standard deviation to be applied to each species sample within this 9 ±2 parameter, and then selects values in each sample within this distribution. The process is repeated in each iteration.

2.3. Measurements

The humeral torsion angle is formed between the orientation of the humeral head and the orientation of the distal condyles of the humerus (see Materials and Methods Chapter and Chapter 3 for further details). This angle is measured using the intersection, viewed from the cranial perspective, of a line drawn through the centre of the humeral head dividing it into anterior and posterior halves, and a line passing through the centre of the capitulum and trochlea (as defined by Evans and Krahl 1945; Kate 1968; Rhodes 2006; Shah et al. 2006; Cowgill 2007; see Chapter 3, figure 18 legend for details). Discrepancies between the present study and the literature exist (table 10 & 11, Chapter 3), and are likely due to differences in methodology, in particular with choice of references for the proximal and distal axes. However, for the most part, the variation in torsion measurements across studies is smaller than the variation within species in the adults of the present study (table 10 & 11, Chapter 3). Indeed, adult humeral torsion values are very variable, with gorilla values for example

ranging from 145 to 175 degrees. The same is true for the other species in the sample, with standard deviations ranging from 6.93 (in *Macaca*) to 12.2 (for *Pongo*). Additionally, the literature for humeral torsion in adult humans is vast and studies report humeral torsion values from as low as 115 to as high as 175 degrees (Leal and Checcia 2006) (see Chapter 3 for details).

3. Results

IE was applied to two separate primate phylogenies: one including only extant species (30 species) and one also containing 14 primate fossils (*Homo neanderthalensis*, *Homo heidelbergensis, Homo floresiensis, Homo erectus, Paranthropus boisei, Australopithecus africanus, Australopithecus afarensis, Australopithecus sediba, Dryopithecus fontani, Proconsul heseloni, Rhinocolobus turkanaensis, Paracolobus chemeroni, Cercopithecoides williamsi, Pliopithecus* sp.). My results show that when only extant species are included, humeral torsion is estimated to be largely a homology in great apes (figure 33), with an increase in torsion estimated to occur in the branch leading to the great apes after the split with the gibbon lineage, and additional slight increases in torsion further occurring on individual African ape and human lineages.

However, when fossils are included in the analysis, humeral torsion is estimated to be a homoplasy, with major increases in torsion estimated to occur on the individual branches leading to the *Pongo, Pan, Gorilla* and *H. sapiens* lineages (figure 34). In both analyses however, the estimated ancestral values for the hominoid clade and the immediate ancestors of all hominoid species are almost identical (for example, the ancestral hominoid values in both models vary within 1-3^{o}: 116.3^{o} in the 'extant only' analysis, and 115^{o} in the fossil analysis), attesting to the stability of these results (figures 33 & 34; See Appendix 2 for table with all the ancestral estimates). Additionally, my results indicate instances of parallelism in the low levels of torsion between *Dryopithecus* and *Proconsul* as well as *P. boisei, A. sediba* and *H.*

floresiensis – although there are high degrees of uncertainty associated to the estimates in the latter three species (figure 37).

Because some of the fossil specimens are problematic in terms of their humeral torsion estimates, I tested the reliability and stability of the results by removing two of the most problematic fossils: *Homo erectus* (KNM-WT 15000) and *Homo floresiensis* (LB1/50). *Homo floresiensis* presents a suite of characters, both cranially and postcranially, that appear to be derived and unlike any other hominin species (Brown et al. 2004), to the point that for many years it was debated whether this was a pathological specimen (Argue et al. 2006, 2009; Falk et al. 2007; Hershkovitz et al. 2007; Baab et al. 2013). The low degrees of torsion in this specimen are but one of many shoulder traits that make this specimen unique (Larson et al. 2007, 2009), and therefore there is a real possibility that the inclusion of *Homo floresiensis* in the analysis is introducing some bias. Furthermore, *Homo erectus* (KNM-WT 15000) is also a problematic fossil, because humeral torsion in this specimen is measured on a juvenile individual (~8years old), with unfused proximal and distal humeral epiphyses, and therefore torsion levels are expected to be low (Leakey and Walker 1989; Walker and Leakey 1993; Lordkipanidze et al. 2007; Larson 2007). However, my results show that including and excluding the two most problematic specimens does not affect the outcome of the analysis, and humeral torsion is, in all cases, (where fossils are incorporated into the analysis) estimated to be homoplastic within hominins (figure 35). Additionally, in both analyses (where fossils are included) the estimated ancestral values for the hominoid clade and the immediate ancestors of all hominoid species are again almost identical (for example, the ancestral hominoid values in both models, again, vary within 1-3^{o}: 115^{o} when all fossils are considered, and 114.4^{o} when *H. erectus* are removed), attesting to the stability of these results (figures 34 & 35).

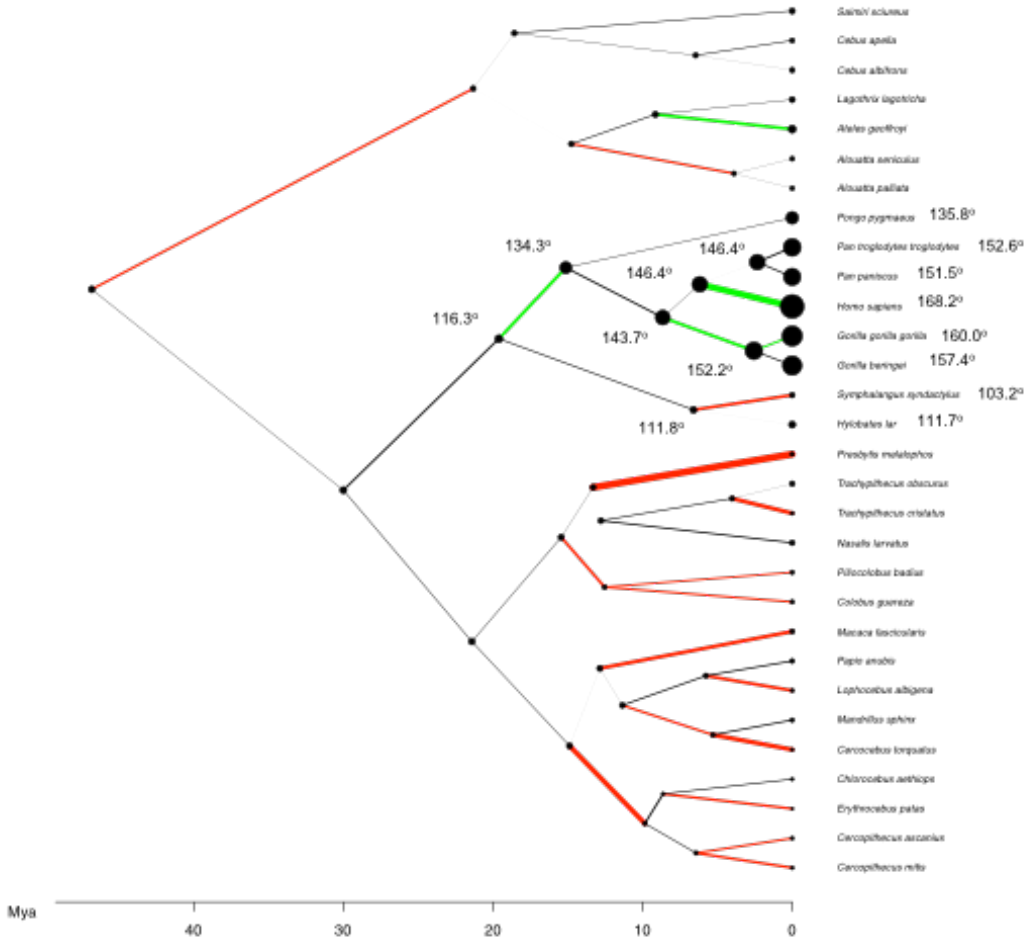

Figure 33 – Phylogenetic tree of extant primates only, with estimated mean ancestral nodes and tips (black circles with estimated nodal values indicated for the hominoids), and estimated mean rates of evolution (coloured branches). The thickness of the circles corresponds to the amount of torsion; the thickness of the branches represents the amount of change from one ancestral node to the next (green: increases in torsion; red: decreases in torsion; threshold: 1.1 SD away from the mean - chosen to maximize visual clarity and used consistently across all analyses). See Appendix 2 for detailed list of ancestral node estimates.

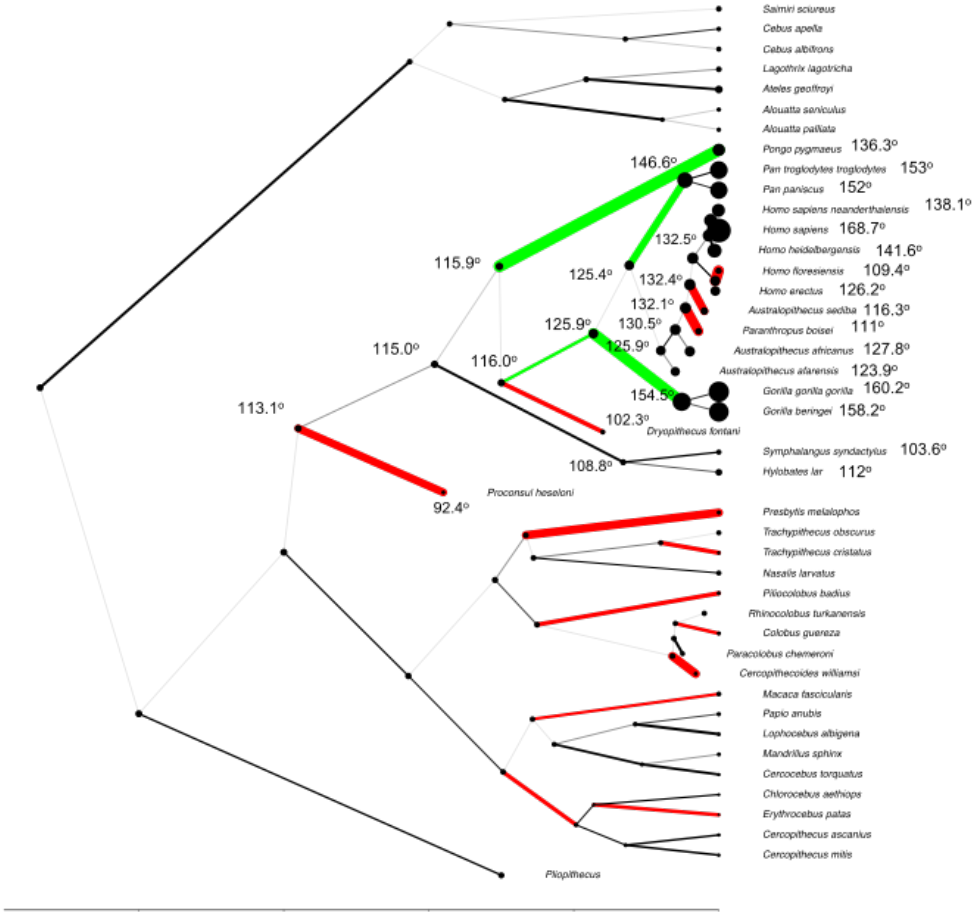

Figure 34 – Phylogenetic tree of extant and extinct primate species, showing estimated mean ancestral nodes and tips (black circles with estimated nodal values indicated for the hominoids), and estimated mean rates of evolution (coloured branches). The thickness of the circles corresponds to the amount of torsion; the thickness of the branches represents the amount of change from one ancestral node to the next (green: increases in torsion; red: decreases in torsion; threshold: 1.1 SD away from the mean - chosen to maximize visual clarity and used consistently across all analyses). See Appendix 2 for detailed list of ancestral node estimates.

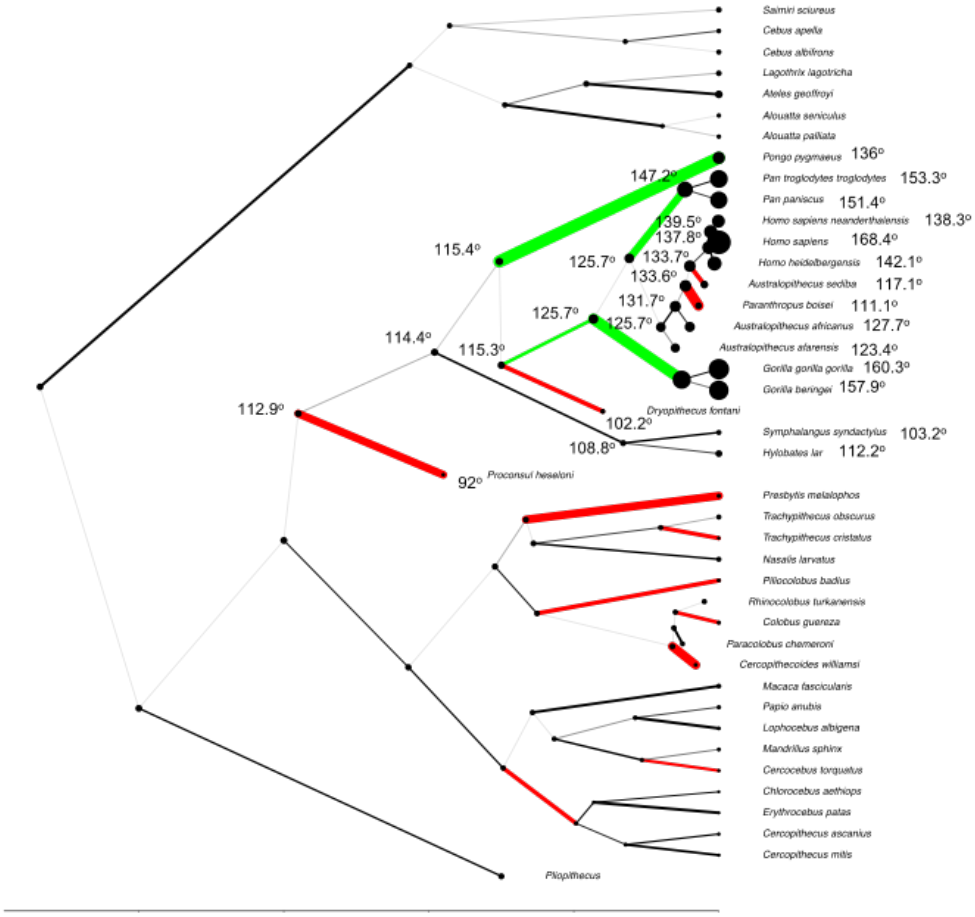

Figure 35 – Phylogenetic tree of extant and extinct primate species (without *H. floresiensis* or *H. erectus*), showing estimated mean ancestral nodes and tips (black circles with estimated nodal values indicated for the hominoids), and estimated mean rates of evolution (coloured branches). The thickness of the circles corresponds to the amount of torsion; the thickness of the branches represents the amount of change from one ancestral node to the next (green: increases in torsion; red: decreases in torsion; threshold: 1.1 SD away from the mean - chosen to maximize visual clarity and used consistently across all analyses). See Appendix 2 for detailed list of ancestral node estimates.

Additionally, when looking at the graphs of standard deviations for the estimated ancestral nodal and branch values (for both the 'extant only' analysis and the analyses that include the fossils), the estimated values for the hominoids tend to be quite stable (with low SD) (figures 36 & 37). In contrast, OWM and hominin estimates tend to have greater associated SD and therefore greater uncertainty associated to them (figures 36 & 37). In particular, *A. sediba, P. boisei* and *H. floresiensis* seem to have higher degrees of uncertainty associated to them than all other fossil hominins (figures 37 & 38). Additionally, when fossils are included, the estimates for *Pongo* become less reliable, with greater SD values associated to its estimates (figures 37 & 38).

4. Discussion

4.1. The inclusion of fossil data and intra-specific variation in phylogenetic analyses

The present study enables phylogenetic analyses to implement phylogenetic trait plasticity, intra-specific variation and measurement uncertainty derived from incomplete fossil specimens, into the phylogenetic analysis. The study is also innovative in that it allows us to quantify and visualise the amount and degree of uncertainty in the estimated values for individual nodes and branches, thus providing us with a sense of the reliability of the results (figures 36-38). Overall, my results show very clearly that including fossils into the analysis substantially changes the predictions regarding the evolution of humeral torsion in hominoids: from a homology, when considering extant species only, to a homoplasy, when fossils are included (figures 33 & 34). This highlights an important issue: that shared derived features in extant hominoids can be a poor indicator of common inheritance of those features, particularly when dealing with highly plastic traits, and that the inclusion of fossil data in phylogenetic analyses can highlight otherwise hidden evolutionary patterns (Smaers et al. 2012). Interestingly however, in both analyses (with and without fossils), the estimated nodal values for the hominoid ancestor and those for the immediate ancestors of each hominoid species are essentially identical (within

1-3º) – for example, the estimate for the ancestral hominoid torsion value is virtually the same in both analyses (115º with fossils; 116.3º without fossils) even though I have

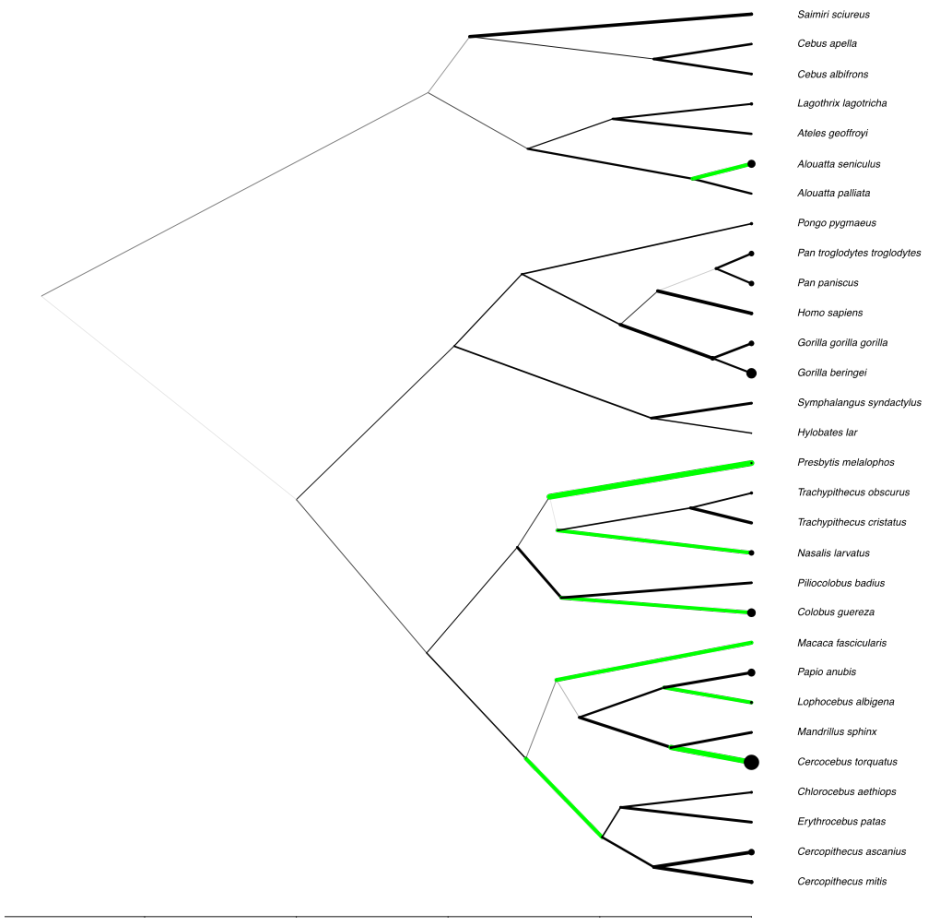

Figure 36 – Phylogenetic tree of extant primates only, with standard deviations associated to the estimated ancestral nodes and tips (black circles), and to the estimated mean rates of evolution (coloured branches). The thickness of the circles corresponds to the size of the standard deviation associated to the estimated nodal value; the thickness of the branches represents the size of the standard deviation associated to the estimated rate of evolution between nodes (green: branches with absolute rates of evolution above 0.095 with SD values between 5 and 14). The graphs indicate instances where ancestral estimates are heavily influenced by intraspecies variability. Rates here refer to changes in the standard deviation of rates across simulations. See Appendix 2, figure 1, table 1.

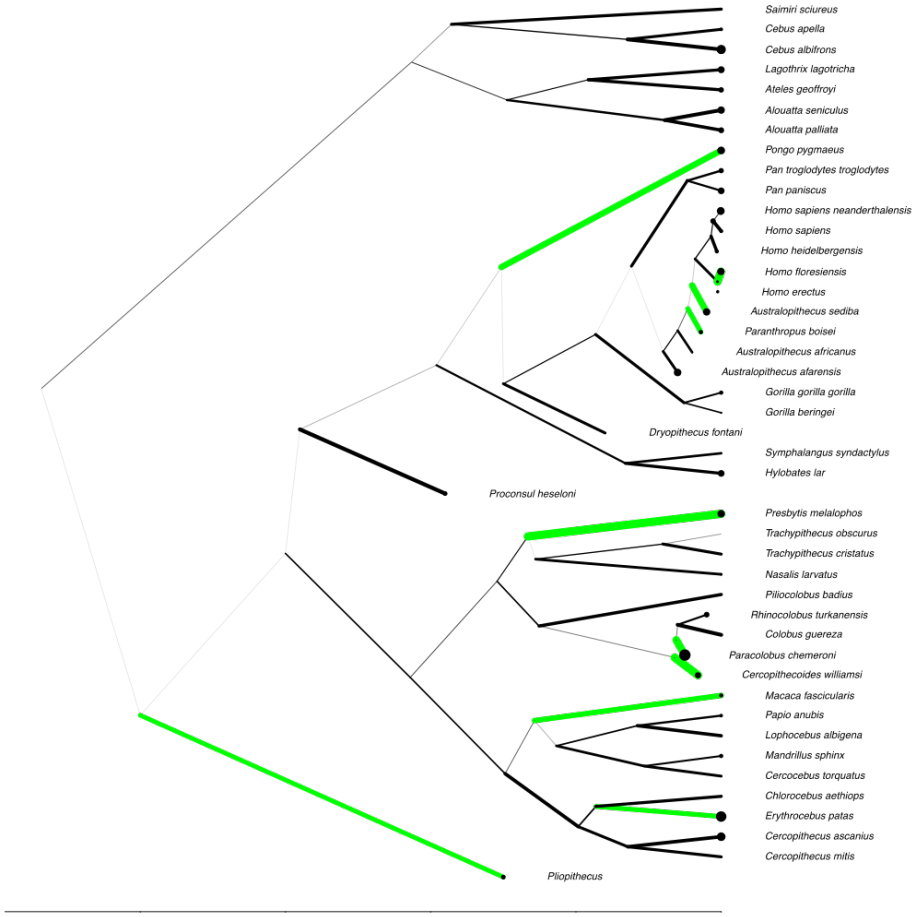

Figure 37 – Phylogenetic tree of extant and extinct primate species, showing standard deviations associated to the estimated ancestral nodes and tips (black circles), and to the estimated mean rates of evolution (coloured branches). The thickness of the circles corresponds to the size of the standard deviation associated to the estimated nodal value; the thickness of the branches represents the size of the standard deviation associated to the estimated rate of evolution between nodes (green: branches with absolute rates of evolution above 0.120 with SD values between 9 and 13). The graphs indicate instances where ancestral estimates are heavily influenced by intraspecies variability. Rates here refer to changes in the standard deviation of rates across simulations. See Appendix 2, figure 2 and table 2.

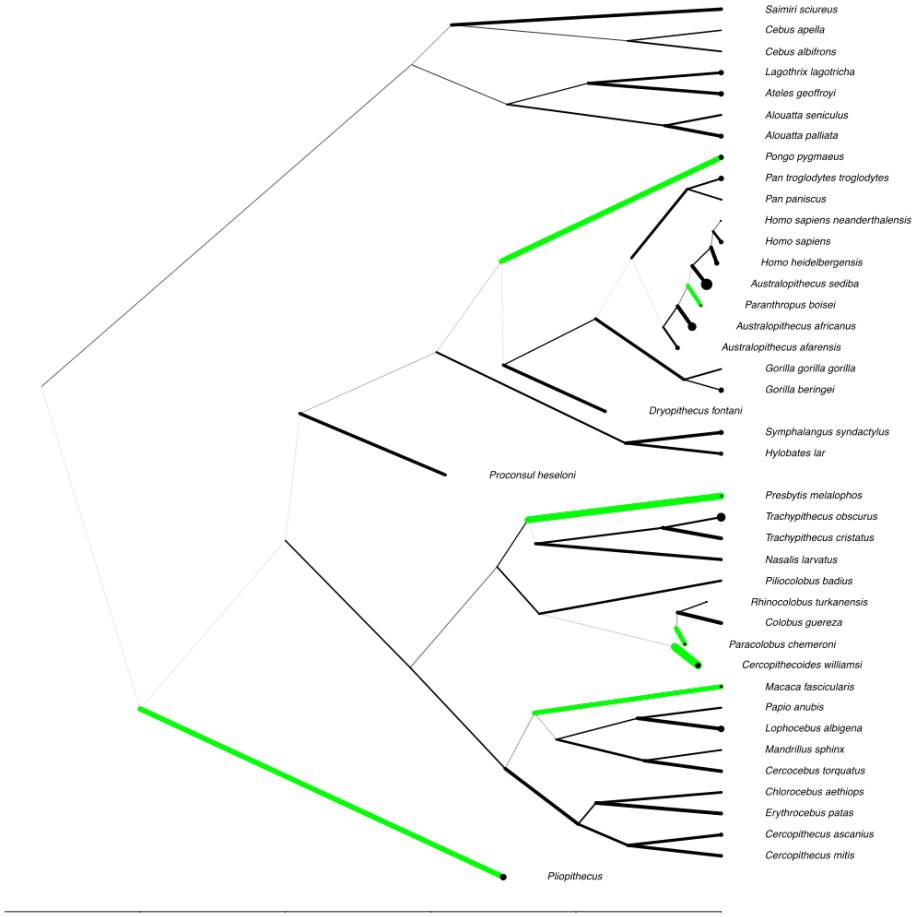

Figure 38 – Phylogenetic tree of extant and extinct primate species showing standard deviations associated to the estimated ancestral nodes and tips (black circles), and to the estimated mean rates of evolution (coloured branches). The thickness of the circles corresponds to the size of the standard deviation associated to the estimated nodal value; the thickness of the branches represents the size of the standard deviation associated to the estimated rate of evolution between nodes (green: branches with absolute rates of evolution above 0.103 with SD values between 7 and 11). The graphs indicate instances where ancestral estimates are heavily influenced by intraspecies variability. Rates here refer to changes in the standard deviation of rates across simulations. See Appendix 2, figure 3 and table 3.

included 10 fossil species to the analysis, all with relatively low torsion (figure 34) –, which attests to the stability of the results (figures 34 & 35). What the inclusion of fossil data does do is push back the timing and rate at which torsion increases in the different hominoid branches, and by consequence suggests that the elevated levels of humeral torsion in the extant apes are a homoplasy, while early fossil hominins retain the ancestral torsion levels of the LCA of hominoids (figure 34). This indicates that estimating ancestral states based only on extant data doesn't necessarily produce unrealistic results, but that without the fossil data, specific information regarding the detailed evolutionary processes shaping these traits within the hominoid clade is lost. These results corroborate Smaers et al's (2012) observation that fossil specimens can add valuable information to reconstructions of phylogenetic relationships and macroevolutionary patterns by providing primary data on the tempo of evolution (by introducing chronological depth into a sample). On the other hand, my results show that the inclusion of fossils into the analysis can increase the uncertainty of the ancestral estimates (ancestral values and rates of evolution) within the hominoid clade (figures 36-38). This is appears to be the case for the hominins, in particular *A. sediba, P. boisei* and *H. floresiensis*.

Overall this study shows that phenotypic plasticity and phylogenetic significance are not necessarily mutually exclusive concepts, since the incorporation of phylogenetic trait plasticity largely corroborates our understanding of the evolution of humeral torsion based on single fossil values (e.g., Larson 1996). Furthermore, this study also agrees with Smaers' et al (2012) finding that exclusion of fossil taxa may yield misleading reconstructions of the evolutionary patterns and mechanisms leading to the diversity observed in the modern taxa.

I caution however, that creating a distribution based on the standard deviations of intra-specific variation in the extant species assumes that the fossil values are representative of the sample mean and thus risks shifting the distribution into values that were never part of the extinct species variation. Future work should therefore focus on addressing this issue. On the other hand, because all of the early hominin

fossils show considerably lower torsion than later hominins and modern humans, it is not unreasonable to assume that they are indeed representative of the species mean.

4.2. The evolutionary significance of humeral torsion in hominoid primates

Overall, this study suggests that high humeral torsion in hominoids is a homoplastic trait independently derived in extant great apes and modern humans and low humeral torsion largely a retained ancestral trait in early hominins (figure 34). On the whole, this confirms Larson's (Larson 2007, 2009, 2013; Larson et al. 2007) suggestion that the elevated levels of humeral torsion in African apes and humans are not a product of shared ancestry but have evolved more recently in parallel, as a result of the need to maintain the arms in parasagittal plane due to independently acquired locomotor requirements (such as in knuckle-walking and manipulation). These results further indicate that the high levels of developmental plasticity in humeral torsion do not necessarily confound interpretations of the overall evolutionary significance of the low levels of early hominin humeral torsion as suggested by Richmond et al (2001). Richmond et al (2001) specifically question (1) the accuracy with which torsion can be determined from the preserved morphology (see Larson 1996) – and suggest that fossil hominin humeri may be more African-apelike, or more orangutan-like, than their torsion estimates suggest –, as well as (2) the functional/phylogenetic significance of early hominin humeral torsion given that torsion is developmentally plastic. These results go some way towards answering these concerns by showing that despite considerable amounts of overlap between extant and extinct species' estimates, humeral torsion in early hominins is sufficiently distinct from that of extant great apes and humans, and therefore humeral torsion is best explained as a parallelism between the great apes and humans, and a symplesiomorphic character in early hominin species.

These results are thus compatible, on the one hand, with the suggestion (1) that quadrupedalism, and more specifically knuckle-walking (in chimpanzees and gorillas) evolved in parallel in the great ape lineages, possibly as a result of increased climatic

and ecological instability during the Miocene (Hill 1995; Kivell and Schmitt 2009; Begun and Kivell 2011), and on the other hand, (2) that the very high degree of torsion of modern humans is a recently derived condition, resulting from the need to maintain the shoulders in sagittal plain for manipulation (as suggested by Larson 2007). These results are thus consistent with other lines of evidence, which also support the idea that knuckle-walking may have arisen in parallel in the African ape lineages (Larson 1998; Dainton et al. 2001; Dainton and Macho 1999; Orr 2005). In particular, Kivell and Schmitt's (2009) study on the ontogeny of the wrist in chimpanzees and gorillas suggests that knuckle-walking is not the same biomechanical phenomenon in both species – an idea which is also supported by existing African ape locomotor data (Jenkins and Fleagle 1975; Tuttle and Watts 1985; Doran 1992, 1993a,b, 1997; Doran and Hunt 1996; Remis 1995; Inouye 1994; Wunderlich and Jungers 2009) –, and thus likely arose via different pathways in both lineages. The Miocene hominoid fossil record certainly makes the case for multiple instances of independent evolution of specialized suspensory adaptations (e.g., *Morotopithecus, Oreopithecus, Dryopithecus*, or *Pongo*) (Begun 2007), and the presence of knuckle-walking features in the hind limb, humerus, and wrist bones of *Sivapithecus* (Begun and Kivell 2011), similarly supports the case of independent evolution of knuckle-walking. However, *Pongo*'s high levels of torsion, which also converges on this pattern, suggest that humeral torsion in great apes is perhaps not indicative of knuckle-walking *per se*, but of more generalized terrestrial behaviours, which include *Pongo*'s characteristic 'fist-walking' (Tuttle 1967). Evidence from orangutans shows that captive, predominately quadrupedal individuals have substantially higher torsion than their wild counterparts (Sarmiento 1985). This is in line with the idea that knuckle-walking may be an effective means for apes to travel terrestrially while maintaining climbing adaptations (Tuttle and Basmajian 1974; Richmond et al. 2001), and for this reason, may have evolved multiple times in different ape lineages. More importantly, however, these results suggest that humeral torsion is not diagnostic of knuckle-walking specifically, but rather of more general quadrupedal postures in apes, and thus the high degrees of torsion in modern humans should not be taken as evidence for a knuckle-walking stage in human evolution.

My results also strongly support the notion that the high levels of humeral torsion in modern humans – a pattern that converges on the African ape form – evolved, in fact, very recently (figure 34) (Larson 2007). These high levels of torsion in modern humans are likely associated both (1) to a reconfiguration of the shoulder anatomy in *Homo sapiens* (Larson 2007), and (2) to reduced levels of activity (namely, use of the limbs in locomotion) in this lineage, compared to all other of hominoid/hominin species (Krahl and Evans 1945; Krahl 1976; Edelson 1999). These results are in line with Larson's (2007) suggestion that a dorsally placed scapula with a lateral facing glenoid fossa, as seen in modern humans, requires torsion to be relatively elevated in order to maintain a sagittal functioning of the elbow joint.

Interestingly, these results also show instances of parallelism in torsion between *Dryopithecus* and *Proconsul,* with both species showing very low levels of torsion (figure 34). Given my interpretations about the functional significance of humeral torsion in hominoids (Chapter 3), these results are consistent with the presence of suspensory/climbing behaviours in both species. While this is most likely the case for *Dryopithecus* (Begun 1992), it contradicts our current understanding of *Proconsul* as an arboreal quadruped (Cartmill and Milton 1977; Begun et al. 1994; Rose 1994; Larson and Stern 2006). However, my own ontogenetic analyses indicate that humeral torsion has an inverse relationship to suspension and quadrupedalism in the hominoid and monkey clades due to the lateral placement of the scapula in monkeys and the dorsal placement in hominoids (Chapter 3). Therefore, while in the quadrupedal hominoids, it is high torsion that allows for the arms to move in a parasagittal plane, in the quadrupedal *Macaca*, it is low torsion that allow for this to happen. On the other hand, the inverse also appears to be true – i.e. that relatively higher torsion in monkeys is related to suspension while in hominoids it is related to quadrupedalism –, as the highly suspensory atelines have relatively higher torsion than the quadrupedal ceboids and cercopithecoids (Larson 1996). As a result, the convergence in torsion between *Dryopithecus* and *Proconsul* in the current analysis may in fact be associated to opposite locomotor strategies in both species: suspension/climbing *in Dryopithecus*

and arboreal quadrupedalism in *Proconsul*. Given these results, and our current knowledge of stem hominoids' morphology, it is not possible to ascertain whether the low levels of torsion estimated for the LCA of hominoids in my analyses (115° – 116.3°; figures 33 & 34) are more consistent with a suspensory/climbing or rather an arboreal quadrupedal common ancestor, although they support an arboreal/semi-arboreal ancestry for apes. This agrees with the notion that postcranial specializations in individual living ape lineages arose after the divergence from either a suspensory ancestor (Cartmill 1985; Young 2003), or more generally, from an ancestor engaging in upright (orthograde) truncal postures (Thorpe and Crompton 2006; Thorpe et al. 2007; Crompton and Thorpe 2007; Crompton et al. 2008); whichever the scenario, this highlights the importance of considering clade-specific patterns as well as information about scapular positioning and/or thoracic shape when making inferences about locomotion based on humeral torsion.

Conversely, the present results suggest that low torsion is likely a symplesiomophic trait in early hominins. Indeed, my analyses reconstruct the LCA of hominoids to have had low torsion (115° – 116.3°; figures 33 & 34), a condition that would have been retained in the early hominins. Although the low torsion in these early fossil hominins is consistent with the notion that they were either predominantly or partially arboreal (e.g., Green and Alemseged 2012; Larson 2007; Larson 2009; Larson 2013; Venkataraman et al. 2013), their mosaic shoulder configuration, which exhibits a mix of primitive and derived features (primitive: short clavicle, cranially directed glenoid, low to modest humeral torsion; derived: dorsal scapula) has been the source of continuing debate, with some researchers viewing the primitive features as phylogenetic 'baggage' retained in the absence of selective pressures against them (Day 1978; Lovejoy 1978, 1988 ; Ohman 1986; Latimer and Lovejoy 1989; Latimer 1991), and others considering the persistence of features as an indication of continuing function (e.g., Stern 2000; Larson 2007). However, a recent analysis of scapular morphology in *A. afarensis* (Green and Alemseged 2012) provides support for the hypothesis that its locomotor repertoire included a substantial amount of climbing, and recent evidence based on the shoulder anatomy of *A. sediba* (cranially

oriented glenoid fossa and scapular spine, short clavicle, low humeral torsion) also suggests the presence of continued climbing behaviours (Churchill et al. 2013). Based on my own findings on the ontogenetic development of torison (Chapter 3) the low levels of torsion in early hominins may also be diagnostic of a life spent (or partially spent) in the trees, because low torsion is actively maintained throughout ontogeny in more suspensory species via the greater action of the medial rotators of the shoulder; this stops the natural medial rotation of the humeral head and consequently keeps the lateral set to the elbows necessary for a suspensory/climbing lifestyle (Larson 1988). These results are in line with our current understanding of African paleoclimate from the last 6-8Myr after the divergence from the LCA (Cerling et al. 2011), which places the LCA in a wooded environment, with hominin habitats becoming progressively less wooded after the divergence from the LCA (Reed 1997; Behrensmeyer et al. 1997; Potts 1998; Bobe et al. 2002; Demenocal 2004). This is also in line with recent behavioural data collected on modern human populations who engage in frequent climbing (Venkatraman et al. 2013), which hypothesises the existence of strong ecological incentives for climbing in *Au. afarensis*, such as foraging, resting and sleeping, or escape, all of which are linked with climbing and use of trees by savannah-living primates (Washburn and Devore 1961; Tuttle 1981; Susman et al. 1984; Venkatraman et al. 2013).

Interestingly, relatively low levels of torsion seem to persist with the emergence of *Homo* (*H. erectus, H. heidelbergensis,* Neanderthals), albeit to a lesser degree (with lower values than modern humans, but higher values than the australopithecines), which my results predict is a symplesiomorphic trait with the early hominins (figure 34). This is intriguing given the marked differences in size, anatomy, habitat and locomotor repertoire between early hominins and early *Homo*. It is clear that relatively low torsion in these species cannot be attributed to the continued exploitation of arboreal substrates, but more likely results from the more active lifestyles in these species, when compared to modern humans, associated with the advent of more sophisticated hunting and tool technologies – including throwing in Neanderthals (Gjerdrum et al. 2003; Rhodes and Churchill 2009). This notion is

supported by modern human evidence, which indicates that higher levels of upper limb activity, including throwing, lead to a significant reduction in humeral head torsion values (Pieper 1998; Crockett et al. 2002; Osbahr et al. 2002; Whiteley et al. 2008, 2010; Taylor et al. 2009; Myers et al. 2009; Schwab and Blanch 2009). Larson (2007), however, suggests that relatively low torsion in these species cannot be attributed to activity alone, since the amount of reduction in torsion that has been associated to range of external rotation at the shoulder in humans is relatively small (10^{o} – 15^{o}), and is therefore unlikely to explain the very low torsion values observed in early *Homo* (~126^{o} in *H. erectus* and ~138^{o} in Neanderthals, versus ~168^{o} in humans; figure 34). It is possible that differences in the morphology and positioning of other shoulder elements such as the orientation and length of the clavicle and position of the scapula on the thorax may play an important role in torsion reduction. Indeed, Larson (2007) suggests that there is a shift in the anatomical configuration of the shoulder with the emergence of the genus *Homo,* with the scapula changing from being positioned high on the thorax with a cranially oriented glenoid fossa (such as in australopithecines), to being positioned lower on the thorax with more laterally facing glenoid fossae. According to the author, this reconfiguration requires torsion to stay low in order to allow for the sagittal functioning of the elbow joint necessary for manipulation (Larson 2007). Conversely, the shift to a dorsally positioned scapula with a laterally facing glenoid fossa and an elongated clavicle, as seen in modern humans, requires torsion to be relatively elevated in order to maintain this same sagittal functioning of the elbow joint (Larson 2007) – a pattern that, for this reason, converges on the African ape's. Larson's (2007) observation that differences in the positioning of the scapula on the hominin thorax influences humeral torsion levels is interesting given my own interpretations about the effect of scapular positioning on torsion differences between the monkey and hominoid clades (Chapter 3). This suggests that slight differences in scapular positioning and glenoid fossa orientation between species, within the hominoid clade, may similarly be (at least partially) responsible for the parallel evolution in torsion between great apes and humans. This certainly emphasizes the importance of considering the shoulder girdle as a whole when making inferences about locomotion based on humeral torsion.

It is important to note, however, that these analyses indicate a level of uncertainty associated to the estimates of *P. boisei, A. sediba* and *H. floresiensis* (figure 37). These are also the species that are estimated to show some degree of parallelism in their decreased torsion levels (figure 34). It is likely that with better samples this uncertainty would be resolved, and/or that these parallelisms would disappear. The uncertainty associated to *Pongo* when the fossils are included likely reflects the large range of variation present within this species (as well as their large amounts of sexual dimorphism) and its overlap with many of the fossil values, (figure 31). Increasing the sample size for this species should clarify this pattern.

5. Conclusion

In the present study, I applied a phylogenetically-integrated approach that quantifies evolutionary changes along individual branches of a phylogeny, to look at the evolutionary processes shaping humeral torsion in the hominoid clade, in combination with a re-sampling technique that takes into account the adult variation within each sample. Incorporating intra-specific variation into the analyses allowed taking into account the developmental plasticity of humeral torsion, which have long hampered interpretations of the functional/phylogenetic significance of early hominin humeral torsion (e.g., Richmond et al. 2001). Overall, my results suggest that despite the large amounts of intraspecific variation, levels of humeral torsion in early hominins are sufficiently distinct from that of extant great apes and humans, and therefore this trait is best explained as a symplesiomorphic character in early hominin species, and a parallelism between the great apes and humans. This shows that phenotypic plasticity and phylogenetic significance are not necessarily mutually exclusive concepts, since the incorporation of phylogenetic trait plasticity largely corroborates our understanding of the evolution of humeral torsion based on single fossil values.

My results also show that the inclusion of fossil data substantially changes the results from a homology in great apes and humans (when only extant species are considered)

to homoplasy in these species (when fossils are included), which highlights the importance of incorporating fossil data into phylogenetic analyses. This emphasizes an important issue: that shared morphological features in extant hominoids can be a poor indicator of common inheritance of those features, and that the inclusion of fossil data in phylogenetic analyses highlights otherwise hidden evolutionary patterns.

In evolutionary terms, these results support the notion of parallel evolution of terrestrial quadrupedalism in the great apes, and specifically, the parallel evolution of knuckle-walking in the *Gorilla* and *Pan* stem lineages. Conversely, my results estimate that the low levels of torsion in early hominins are a symplesiomorphic trait in the species and are retained from the LCA of hominoids. These results thus support the notion of an arboreal origin to the great ape lineages – a scenario that does not require a knuckle-walking stage in human evolution (Stern 1975; Rose 1991; Thorpe et al. 2007; Kivell and Schmitt 2009). However, because high levels of torsion are also found in *Pongo*, who are not knuckle-walkers, my results also support that torsion should not be discussed in the context of knuckle-walking specifically (Kivell and Schmitt 2009). My results also support that the high levels of torsion seen in modern humans are recently derived, possibly as a result of a reconfiguration of the shoulder girdle anatomy in this lineage (Larson 2007).

Finally, functionally, these results suggest that although the mechanism by which torsion arises is the same across the different hominoid lineages, and although there is convergence in this trait between great apes and humans, its functional significance differs between lineages: (1) in great apes high torsion is associated to the locomotor requirements related to terrestrial quadrupedalism, while in humans it arises via the relaxed selection on the upper limbs as locomotor structures; (2) the low levels of torsion in australopithecines are likely related to the retention of suspensory/climbing behaviours, while in *H. erectus*, *H. heidelbergensis* and Neanderthals they are likely explained by the more active lifestyles in these species and confirm my own observations (Chapter 3) on torsion being influenced by the positioning of the scapula on the thorax, both across primate clades and within the hominoid clade.

– Chapter 5 –

Bilateral asymmetry of humeral torsion and length in African apes and humans

1. Introduction

Approximately 90% of modern humans display a preference for right-hand use (McGrew and Marchant 1996), a trait that is generally considered unique to this species (Porac and Coren 1981; Raymond and Pontier 2004). Interest in the evolution of handedness is rooted in its implications for brain hemispheric specialization and, more specifically, for the evolution of language and complex tool production (Corballis 2003; Hopkins et al. 2007), with a potential co-evolutionary link between the two (Sherwood et al. 2007; Hopkins and Nir 2010; Stout and Chaminade 2012; but see Hopkins and Cantalupo 2004). In humans, habitual lateralization of behaviours, possibly associated to this cerebral lateralization, has been shown to produce skeletal asymmetries, and a number of osteological studies have established an association between lateralized mechanical loads and bone remodelling (e.g. Ruff and Hayes 1983; Steele 2000a,b; Lazenby 2002; Stock and Pfeiffer 2004). In particular, upper limb asymmetries have been well documented in the skeleton of Homo sapiens with numerous studies showing how asymmetric loads influence upper limb morphology in human populations and professional athletes (Roy et al. 1994; Trinkaus et al. 1994; Kontulainen et al. 2002; Lazenby et al. 2002, 2008; Rhodes and Knüsel 2005; Shaw and Stock 2009a,b; Shaw 2011). Bilateral asymmetries in the upper limbs of great apes are, however, less well documented, even though these are potentially informative about the origins of functional lateralization in humans and non-human primates. Indeed, the question of whether non-human primates exhibit individual or population-level functional laterality remains unclear and controversial: behavioural studies, for example, suggest that handedness in great apes can in some

instances reach exclusive use of one arm (e.g., right arm: Humle and Matsuzawa 2009; Meguerditchian et al. 2010; Llorente et al. 2011; left arm: Parnell 2001; Lonsdorf and Hopkins 2005), but this pattern seems to be strongly dependent on factors such as age, sex, task complexity, setting and posture (e.g. Byrne and Byrne 1991; McGrew and Marchant 1997; Byrne 2004; Hopkins and Cantalupo 2005; Lonsdorf and Hopkins 2005; Marchant and McGrew 2007; Pouydebat et al. 2010; Hopkins et al. 2011), and overall, these species do not exhibit the overwhelming right-hand bias across a wide range of everyday tasks so evident in humans (McGrew and Marchant 1997, 2001; Cashmore et al. 2008).

Studies on upper limb asymmetries in great apes seem to agree that behavioural lateralization is present in these species, but to a lesser extent than in humans and with no strong right-side directionality. Specifically, Drapeau (2008) finds that humans are more asymmetric than African apes in the development of musculoskeletal markers of both fore- and hindlimb, reflecting the relatively greater asymmetry in limb use in humans and the more symmetric use in apes, and suggests that this reflects comparatively more moderate handedness in apes during manipulative activities. Schultz (1937) also finds that there is no tendency for the right arm to be longer in apes, and finds that the degree of length asymmetry in apes is half that of humans, while Sarringhaus et al (2005) actually find left-side biases in total subperiosteal area of humeral diaphyses in the common chimpanzees (but right-side biases in the same measurement for the second metacarpal), which they relate to behavioural laterality linked to precision and power. Additionally, Morbeck et al (1994), describe greater bone mineralization in the right humeri in Gombe chimpanzee skeletons, but no clear association between these asymmetries and hand preferences, while Carlson (2006) finds that overall forelimb muscle mass is statistically biased to the left, but that only the manual digital muscles retain a statistically significant bias when muscle groups are considered individually.

In humans, upper limb asymmetries are well documented for external measurements such as lengths and diaphyseal breadths as well as cross-sectional properties (Ruff

1987; Ruff et al. 1993; Stock and Pfeiffer 2001; Auerbach and Ruff 2006; Shaw and Stock 2011), and these have been used to infer behavioural lateralizations in past populations (Churchill and Formicolla 1997; Pearson et al 2006; Shaw et al. 2012). Notably, humeral length and humeral torsion have both been found to show bilateral asymmetries in human samples. A number of studies show that humans tend to exhibit longer right humeri than left (Schultz 1937; Latimer and Lowrance 1965; Steele and Mays 1995; Sladek et al. 2007) and that this asymmetry increases throughout ontogeny (Stirland 1993; Blackburn 2011). For example, Steele and Mays' (1995) study of upper limb lengths of the mediaeval Wharram Percy cemetery population finds a pattern of bilateral asymmetry in adult humeral length that is very similar to that for reported handedness in the modern British population, with 81% showing longer right humeri. However, because humans show relatively little bilateral asymmetry in humeral lengths compared to other features, such as cross-sectional geometry (Trinkaus et al. 1994; Auerbach and Ruff 2006), some uncertainty exists about whether these occur as a consequence of mechanical stimuli or of intrinsic genetic/hormonal factors, and therefore whether they can be linked to behavioural lateralization at all (Jolicoeur 1963; Stirland 1993; Trinkaus et al. 1994; Steele and Mays 1995). The presence of length asymmetries in human foetuses (Pande and Singh 1971; Bareggi et al. 1994), suggests that this may be the case, but ultrasound evidence also indicates that 85% of human foetuses at 10 weeks of gestational age move their right arm more than their left arm (Hepper et al. 1998; Steele 2000b), raising the possibility that, although partly congenital, asymmetries in humeral length may be further enhanced by preferential use of the right arm, which may commence early in development and continue throughout growth (Stirland 1993). It is unclear, however, whether this pattern is unique to humans or whether it is shared with African apes. If asymmetries in humeral length favouring the right side do indeed exist in chimpanzees and gorillas, which do not exhibit a clear population-level right handedness (McGrew and Marchant 2001; Cashmore et al. 2008), it would support that length asymmetries are mostly independent of function lateralization in African apes and humans, and that this pattern in humans is part of a general ape trend.

Adult humeral torsion values in humans develop during growth in the proximal epiphysis (where 80% of humeral growth takes place [Pritchett 1991]) as a result of repetitive rotational stresses, which lead to the deformation of the epiphyseal cartilage, thus resulting in reduced torsion values (Mair et al. 2004; Murachovsky et al. 2010; Wyland et al. 2012; Thomas et al. 2012). Although the exact timing of the cessation of humeral torsion development is unknown (Cowgill 2007), it is thought to occur at the time of epiphyseal fusion, between the ages of 16 and 20 (Krahl 1947; Edelson 2000). While the natural process is for humeral torsion to increase throughout ontogeny, increased activity of the medial rotators (subscapularis, pectoralis major, latissimus dorsi, and teres major) relative to that of the lateral rotators (infraspinatus and teres minor), limits the development of torsion, thus resulting in relatively lower torsion in these individuals (Cowgill 2007) – Krahl (1947) for example reports a correlation between the relative strengths of these muscles and the degree of torsion in the corresponding humeri. This may explain why professional athletes such as baseball or tennis players have relatively lower torsion on the playing arm compared to the non-playing arm (Pieper 1998; Crockett et al. 2002; Osbahr et al. 2002; Whiteley et al. 2008, 2010; Taylor et al. 2009; Myers et al. 2009; Schwab and Blanch 2009), and why individuals with brachial plexus injuries in which the medial rotators are unopposed by the lateral rotators, have posteriorly oriented humeral heads (i.e., very low torsion) (Codine et al. 1997; Waters et al. 1998; Van Der Sluijs et al. 2002; Pöyhiä et al. 2005; Cowgill, 2007). Conversely, no statistically significant differences were found between right and left arms in non-athlete control groups (Pieper, 1998; Crockett et al., 2002). Furthermore, anthropological studies have reported lower degrees of torsion in physically active populations, such as Melanesians and Australian Aborigines (Martin 1933) and that males possess relatively lower torsion than females (Krahl and Evans 1945; Edelson 1999). Given these observations, it seems reasonable to assume that increased activity (i.e., more vigorous use of) one arm relative to the other during ontogeny, will lead to decreased torsion in the dominant arm relative to the non-dominant arm. An earlier study has shown the presence positive correlation between bilateral asymmetry and age in humans when adults are included in the regression, but the relationship disappeared when adults

were removed from the analysis (Cowgill 2007). The author suggests that this is due to relatively smaller available sample sizes for the sub-adults (Cowgill, 2007).

Although asymmetries of humeral measurements (including length and torsion) have been used to investigate activity patterns in archaeological samples, such as the emergence of projectile weaponry in Neanderthal and archaic Homo sapiens (Gjerdrum et al. 2003; Rhodes and Churchill 2009), little work has been published directly comparing the bilateral asymmetry of the humerus between humans and our closest ape relatives. The purpose of the present article is thus to report the magnitude and directionality of asymmetries in humeral length and torsion in humans and two species of African apes (Gorilla gorilla and Pan troglodytes), in order to test the expectations that: (a) African apes lack population-level directionality in either measurement in line with the reported absence of strong population-level behavioural lateralization; (b) humans show strong right-side directionality in both measurements in line with previous studies and reported degrees of population-level lateralization (McGrew and Marchant 2001; Cashmore et al. 2008); (c) there are no sex differences in asymmetry for either measurement, with the possible exception of gorillas, where high levels of sexual body size dimorphism are associated with sex differences in locomotor patterns (Doran 1993; Remis 1995).

2. Materials and Methods

2.1 Sample

Measurements were collected for 40 adult Pan troglodytes (14 males, 26 females) and 40 adult Gorilla gorilla (20 males, 20 females) from the Powell-Cotton museum (UK). All individuals are wild-shot specimens from central Africa with erupted M3s. The human sample consists of 40 adults (20 males and 20 females, between 19 and 70 years old) from modern cemeteries in Lisbon (dating 1880 to 1975).

Humeral torsion and maximum length of the humerus were measured on left and right humeri for each individual. Measurements were taken from 3D surface scans collected with a Handyscan 3D EXAscan (by Creaform). The surface scans were collated and cleaned using Geomagic Suite 12.1, and the measurements were taken using Amira.

2.2. Measurements

The humeral torsion angle is the obtuse angle formed between the orientation of the humeral head and the orientation of the distal condyles of the humerus (figure 39a, b, c, d). This angle is measured using the intersection, viewed from the cranial perspective, of a line drawn through the centre of the humeral head dividing it into anterior and posterior halves, and a line passing through the centre of the capitulum and trochlea (as defined by Krahl and Evans 1945; Rhodes 2006; Cowgill 2007; see figure legend for details).

Humeral lengths were measured as the maximum distance between the humeral head and the distal condyles (figure 39e).

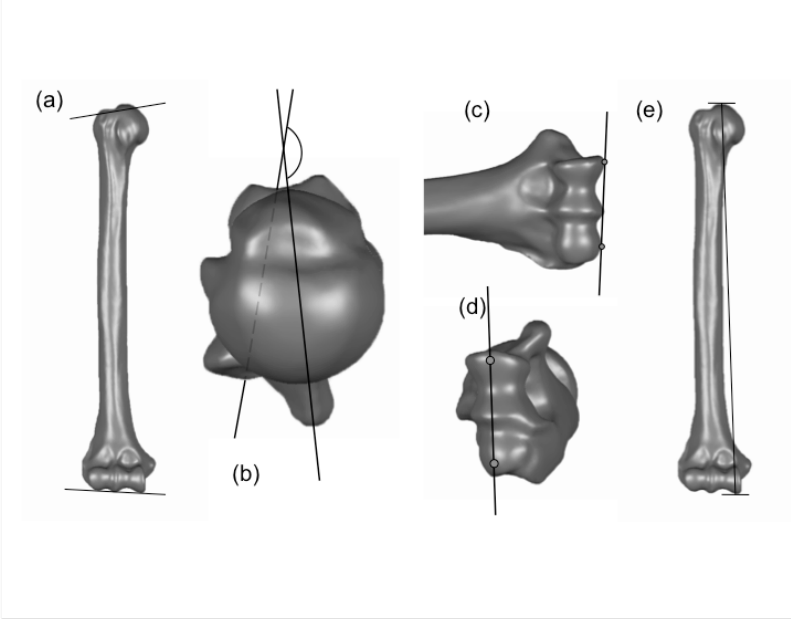

Figure 39 – Adult gorilla right humerus (3D) in anterior (a) and cranial (b) view showing the proximal and distal axes used for measuring humeral torsion; the distal axis is formed by a line passing through the centre of the distal-most points of the trochlea and capitulum (c) and (d). This was preferred to a line passing through the epicondyles because these were frequently damaged in the human collections. Figure 39e illustrates the line of maximum humeral length.

2.3. Reporting asymmetry scores

Asymmetries in humeral torsion and humeral length were calculated using a published method for reporting asymmetries in the postcranial skeleton (Steele and Mays 1995; Auerbach and Ruff 2006; Auerbach and Raxter 2008). For each individual the differences between the torsion/length of right and left elements of a pair were calculated and standardized by the mean torsion/length of left and right elements. Two measurements of asymmetry were obtained; both are reported as percentages:

• Directional asymmetry (DA): which indicates whether the asymmetry favours the right or the left side, was calculated by subtracting the left (L) measurement from the right (R), and dividing it by the average of left and right measurements:

$$DA\% = (R-L)/ [(R+L)/2] \times 100$$

• Absolute asymmetry (AA): which indicates the magnitude of the asymmetry ignoring directionality, was also reported. It resembles the DA calculation except that it uses the unsigned values of the difference between left and right measurements:

$$AA\% = (|R-L|)/[(R+L)/2] \times 100$$

Because of the nature of humeral torsion development, lower relative torsion on a humerus has been linked to higher relative activity levels; therefore, a negative %DA score indicates a right arm bias. The opposite is true of humeral length, however, where longer relative length of the right humerus has been linked to right biases; thus it is a positive %DA score that indicates a right arm bias. %AA and %DA values close to zero indicate symmetry.

2.4. Calculating Bilateral Asymmetry

Statistical analyses were performed using R version 2.12.2 (2011). Paired t-tests were conducted on torsion/length values for each sample. Humeral torsion values in the three samples were plotted against humeral lengths using Reduced Major Axis (RMA) linear regressions (using the package 'Smatr', [Warton et al 2011]). Unlike linear measurements, symmetry values, which were expressed in percentages (%AA and %DA), failed to conform to a normal distribution based on frequency distributions. Nonparametric tests were therefore applied to these scores: Kruskal-Wallis tests – as a nonparametric equivalent of ANOVA – as well as Mann-Whitney U-tests – a nonparametric equivalent of the two-sample t-test – with Hochberg post-hoc corrections were applied to test for significant differences of %AA and %DA scores between species and between sexes (at 95% confidence interval). Additionally, a chi-square test for equivalency was employed to test whether frequencies of right/left directional asymmetries are higher than expected (i.e. significantly different from a 50%-50% distribution). %AA and %DA values which scored 3 times above the interquartile range of the rest of the scores (i.e. extreme outliers) were excluded from the analyses (Wilcox 2001). This resulted in two values being removed from each analysis.

Since slight side biases (i.e. deviations from zero) may not be biologically significant (Auerbach and Ruff 2006; Auerbach and Raxter 2008; Cashmore 2009), I also test whether %DA and %AA scores are significantly different from 0% using a one-sample Wilcoxon Signed Rank Test – the nonparametric equivalent of the one-sample t-test. Significant deviations from 0% in %DA are interpreted as evidence for population-level lateralization. Significant deviations from 0% in %AA in the absence of significant deviations from 0% in %DA are interpreted as evidence for individual-level lateralization where the distribution of %DA is non-normal (as is the case in the present study).

2.5. Repeatability of measurements

To assess the repeatability of asymmetry scores, the average percentage difference between three repeated measurements was calculated using White et al's (2011) procedure for estimating error on osteological material (table 17). Results indicate that in all cases the average difference between repeated measurements is small compared with the average difference between right and left sides (1.8-6.5 times smaller for humeral torsion and 15 to 108 times smaller for humeral length).

3. Results

3.1 Humeral Length

Gorillas and chimpanzees are evenly distributed in left and right humeral lengths (gorilla: 24 longer right/16 longer left; chimpanzee: 17 longer right/23 longer left). Humans, in contrast, show a distinct population bias towards longer right humeri, with only 6 out of 40 individuals displaying relatively longer left humeri. Paired t-

Table 17 – Comparison of asymmetry values with measurement error for humeral torsion and length. The percentage difference for the total sample measures the mean difference between right and left sides of a pair of elements in relation to the averaged left and right measurements (length and torsion). The percentage difference for repeat measurements reports the mean difference between repeated measurements in relation to the three averaged repeat measurements (length and torsion).

Measurement	Species	Sample	*N*	Mean difference (%)	Standard deviation
Humeral Torsion	*G. gorilla*	Total	40	3.30	2.530
		Remeasurements	3	0.82	0.427
	P. troglodytes	Total	40	3.16	2.217
		Remeasurements	3	1.69	0.885
	Homo sapiens	Total	40	4.67	4.413
		Remeasurements	3	0.72	0.522
Humeral Length	*G. gorilla*	Total	40	0.60	0.519
		Remeasurements	3	0.04	0.074
	P. troglodytes	Total	40	0.65	0.655
		Remeasurements	3	0.01	0.018
	H. sapiens	Total	40	1.08	0.775
		Remeasurements	3	0.01	0.016

tests, with sexes pooled, reveal that the right humerus is significantly longer than the left humerus in the human sample, but not in the apes (table 18). When the sexes are considered separately, both male and female humans have significantly longer right humeri than left (table 19). Chi-square tests also show that the proportion of longer right humeri is significant in humans, and female gorillas (chi-square scores: p=0.000, male humans; p=0.014, female humans; p=0.000, total humans; p=0.014, female gorillas) (see also table 19). One-sample Wilcoxon Signed Rank tests further show that %AA is significantly different from 0% in all three samples, but that only humans have %DA scores which deviate significantly from 0% (table 20). Additionally, humans are significantly different from the apes in both absolute and directional length asymmetries (Kruskal-Wallis for between species differences: p=0.005, absolute asymmetry; p=0.000, directional asymmetry) (see also table 21). Furthermore, humans show some evidence for sex differences in length directional asymmetry (p=0.052), which may reach reach statistical significance with larger sample sizes (table 22). Absolute asymmetry (%AA), however, was found to differ significantly between male and female humans (table 22) – females being more lateralized than males (table 23) – though in both cases the asymmetry favours the right (table 23). The same pattern was not found within the apes, whose levels of directional and absolute asymmetry did not significantly differ between sexes (table 23). Finally, only humans showed right-side directionality in length asymmetry (tables 18, 19 & 24; see also figure 2).

Table 18 – Pairwise t-test of left and right humeral torsion and humeral length values in humans, chimpanzees and gorillas, with sexes pooled.

Measurement	Species	Mean (Left / Right)	*P-value*	*t*	*N*
Humeral torsion	*Gorilla gorilla*	158.0 / 159.7	0.154	-1.455	39
	Pan troglodytes	149.1 / 148.2	0.419	-1.101	39
	Homo sapiens	165.7 / 162.0	0.024	2.077	40
Humeral length	*Gorilla gorilla*	407.0 / 406.0	0.086	1.754	40
	Pan troglodytes	299.1 / 299.0	0.631	0.483	40
	Homo sapiens	300.8 / 304.2	0.000	-5.530	40

Table 19 – Pairwise t-test of left and right humeral torsion and humeral length values in humans, chimpanzees and gorillas, by sex. Italicised indicates significantly biased directional asymmetry values based on a chi-square test ($p < 0.05$).

Measurement	Species	*Sex*	Mean (Left / Right)	*P-value*	*t*	*N*
Humeral torsion	*Gorilla gorilla*	M	159.3 / 159.0	0.843	0.200	20
		F	156.9 / 160.3	0.022	-2.510	19
	Pan troglodytes	M	150.0 / 150.5	0.804	-0.254	14
		F	148.5 / 147.0	0.273	1.123	25
	Homo sapiens	M	167.6 / 163.5	0.093	1.762	20
		F	163.5 / 160.6	0.144	1.517	20
Humeral length	*Gorilla gorilla*	M	437.8 / 437.2	0.354	0.949	19
		F	379.8 / 379.2	*0.317*	1.027	20
	Pan troglodytes	M	298.7 / 298.7	0.943	0.072	14
		F	299.5 / 299.2	0.628	0.490	26
	Homo sapiens	M	315.0/317.0	*0.001*	-3.993	19
		F	288.0 / 291.7	*0.000*	-5.389	20

3.2. Humeral torsion

In both African ape species, 20 individuals present lower torsion on the right humerus and 20 lower torsion on the left humerus while in the humans, 25 individuals have lower torsion on the right humerus and 15 lower torsion on the left humerus. Paired t-tests (with sexes pooled) reveal that right torsion is significantly lower than left torsion in humans but not in the apes (table 18). When the sexes are considered separately, this pattern is no longer observed in humans, and in gorillas, the females but not the males show significant differences between right and left torsion, with females presenting lower torsion on the left than on the right (table 19 & 24). However, $\chi 2$ tests show that the proportion of lower right or left torsion is not significant in any sample ($p>0.05$). Mann-Whitney U tests further show that %AA is significantly different from 0% in all three species, but that only humans have %DA scores that deviate significantly from 0% (table 20). However, Kruskal-Wallis tests show no significant differences in absolute or directional asymmetry between species (Kruskal-Wallis for between species differences: $p=0.577$, absolute asymmetry; $p=0.105$, directional asymmetry). Additionally, absolute asymmetry was not found to be sexually dimorphic for any of the three species, but directional asymmetry was found to differ significantly between male and female gorillas (table 23), with the data

suggesting less torsion in the right humeri of males and left humeri of females (table 23). Although the differences between sexes are not significant in chimpanzees, male and female %DA scores are biased in opposite directions (males have less humeral torsion on the left and females less humeral torsion on the right) (table 23). Results also show that in all three species, torsion asymmetries are more pronounced than length asymmetries (figure 40), and RMA regressions show no relationship between the two measurements in either sample (figure 41).

Table 20 – One sample Wilcoxon Signed Rank Test probability of AA and DA values being 0% (symmetry) (at 95% CI). V corresponds to the Wilcoxon signed rank statistic (the sum of ranks assigned to the differences with positive sign).

	Measurement	Species	*P-value*	*V*	*N*
Humeral Torsion	AA Asymmetry	*Gorilla gorilla*	0.000	780	39
		Pan troglodytes	0.000	780	39
		Homo sapiens	0.000	780	40
	DA Asymmetry	*Gorilla gorilla*	0.361	456	39
		Pan troglodytes	0.503	341	39
		Homo sapiens	0.031	251	40
Humeral Length	AA Asymmetry	*Gorilla gorilla*	0.000	780	39
		Pan troglodytes	0.000	820	40
		Homo sapiens	0.000	741	39
	DA Asymmetry	*Gorilla gorilla*	0.176	292	39
		Pan troglodytes	0.899	420	40
		Homo sapiens	0.000	675	39

Table 21 – Mann-Whitney U-tests, with Hochberg post-hoc correction, of absolute and directional asymmetry of lengths between samples.

	Absolute Asymmetry (%)			*Directional Asymmetry* (%)			
Species	*P-value*	*W*	*P-adjust.*	*P-value*	*W*	*P-adjust.*	*N*
Chimp - Gorilla	0.868	797.5	0.868	0.398	693.5	0.399	c(40), g(39)
Gorilla - Human	0.005	477.5	0.013	0.000	275.0	0.000	g(39), h(39)
Human - chimp	0.006	504.5	0.013	0.000	342.0	0.000	h(39), c(40)

Table 22 – Mann-Whitney U tests testing for differences between males and females in absolute and directional asymmetry of humeral torsion (outliers removed) and humeral length for all three samples.

Measurement	Score	Species	*P-value*	*W*	*N*
Humeral torsion	*Absolute Asymmetry*	*Gorilla gorilla*	0.684	205	M (20), F (19)
		Pan troglodytes	0.377	144	M (14), F (25)
		Homo sapiens	0.841	192	M (20), F (20)
	Directional Asymmetry	*Gorilla gorilla*	0.047	119	M (20), F (19)
		Pan troglodytes	0.289	212	M (14), F (25)
		Homo sapiens	0.798	190	M (20), F (20)
Humeral length	*Absolute Asymmetry*	*Gorilla gorilla*	0.569	169	M (19), F (20)
		Pan troglodytes	0.138	129	M (14), F (26)
		Homo sapiens	0.022	102	M (19), F (20)
	Directional Asymmetry	*Gorilla gorilla*	0.727	203	M (19), F (20)
		Pan troglodytes	0.856	189	M (14), F (26)
		Homo sapiens	0.052	114	M (19), F (20)

Table 23 – Table of mean absolute asymmetry (AA) and mean directional asymmetry (DA) of humeral torsion (outliers removed) and humeral length in the gorilla, chimpanzee and human samples. For directional asymmetry values, negative DA scores in torsion and positive DA scores in length indicate right side biases.

Measurement	Species	*Absolute Asymmetry* (%)			*Directional Asymmetry* (%)		
		Total	Males	Females	Total	Males	Females
Humeral torsion	*G. gorilla*	3.314	3.391	3.235	0.905	-0.283	2.157
	P.trog.	3.170	2.725	3.423	-0.521	0.164	-0.905
	H. sapiens	4.669	4.838	4.499	-2.213	-2.567	-1.858
Humeral length	*G. gorilla*	0.602	0.570	0.632	-0.171	-0.174	-0.167
	P.trog.	0.648	0.438	0.760	-0.066	-0.008	-0.100
	H. sapiens	1.076	0.767	1.387	0.937	0.658	1.219

4. Discussion

4.1. Length asymmetries versus torsion asymmetries

Overall, results suggest that humans are unique in presenting population-level right side directionality in both humeral torsion and humeral length (tables 18 & 20).

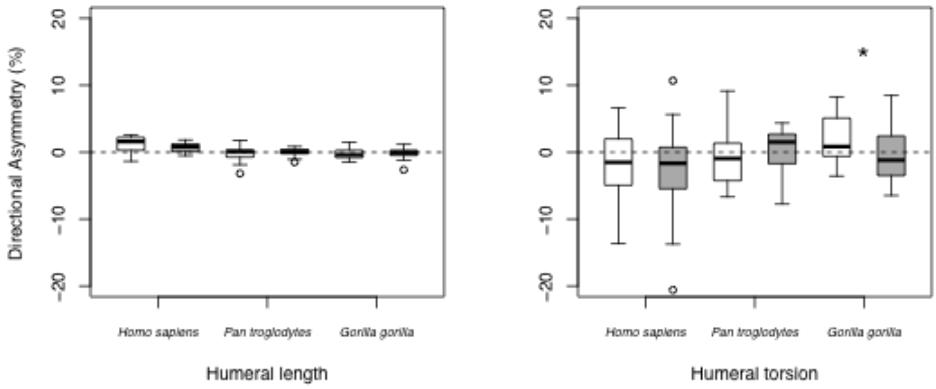

Figure 40 – Box-plots of directional asymmetries (%DA) for humeral torsion (a) and humeral length (b) in humans, chimpanzees and gorillas. Shaded boxes: males; open boxes: females. Significant difference (95% CI) between gorilla sexes marked with asterisk (at p=0.052 humans show evidence for sex differences in length DA%). Boxes represent the upper and lower quartile ranges, the black lines, the means, and the whiskers, the highest and lowest values within 1.5 times the interquartile range of the upper and lower quartiles. The circles represent outliers within 3 times the interquartile range of the upper and lower quartiles.

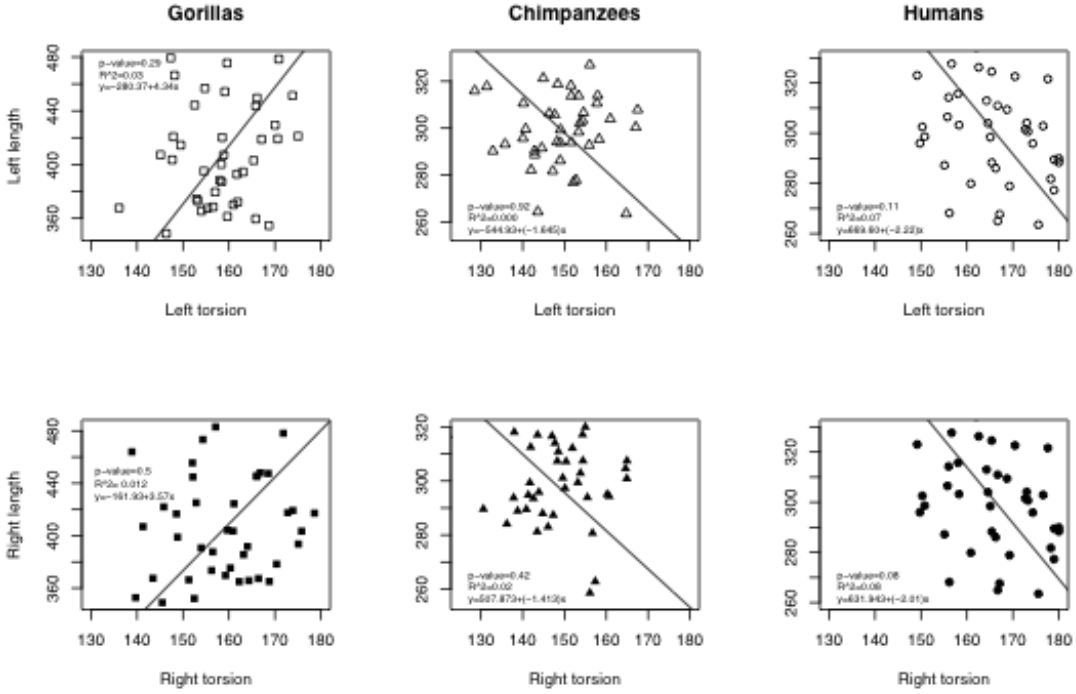

Figure 41 – RMA linear regressions of left and right humeral torsion against left and right humeral length, respectively, in gorillas (N=40), chimpanzees (N=40) and humans (N=40).

However, length asymmetries (%AA) are less pronounced than torsion asymmetries in all three species (~2.6-4.5% for torsion versus ~0.3-1.4% for length; see table 23 & figure 40). Indeed, torsion asymmetry scores (%AA) in the present study are comparable to the highest scoring variable in Auerbach and Ruff's (2006) study of 780 Holocene adult humans (mid-shaft diaphyseal diameter in limb long bones), while length asymmetry scores for humans are almost identical in both studies (mean %AA scores for present study: 1.1%; Auerbach and Ruff 2006: 1.5%). These authors hypothesize that the more constrained ranges of asymmetry in length reflect a greater genetic control over this variable – the assumption being that, because genetic constraint results in equal expression of bilateral traits, more plastic traits exhibit greater magnitudes of asymmetry than traits that are more genetically constrained. If this is correct, these results also suppose that torsion is more sensitive to environmental plasticity, and lengths more genetically constrained. This seems to be in line with previous studies, which suggest that lengths are less sensitive to mechanical stimuli than other traits (Steele and Mays 1995; Steele 2000b; Auerbach and Ruff 2006).

However, while the strength and shape of cross-sectional morphology has been associated with bone responses to loading regimes throughout life (Ruff 1990; Ruff et al. 1993; Stock and Pfeiffer 2001; Matsumura 2002, 2010; Lieberman et al. 2003; Shaw and Stock 2009a,b; Marchi 2007, 2008), humeral torsion does not continue to develop past fusion of the proximal epiphysis (Krahl 1976). I postulate that it is the degree of sensitivity of the epiphyseal cartilage to biomechanical stimuli, as well as its speed of response and the timing of epiphyseal growth during formative adolescence (90% of epiphyseal growth occurs between 11 and 20 years of age in humans [Osbahr et al. 2002]), that are responsible for these asymmetries. Furthermore, these results also show that there is no correspondence between length asymmetries and torsion asymmetries, not even in humans who are right-side dominant for both measurements (figure 40). This indicates a lack of correlation between asymmetry in bone lengths and asymmetry in humeral torsion, suggesting a

decoupling between limb variables in response to mechanical stimuli, in line with previous studies (Ruff 2003; Auerbach and Ruff 2006). Nevertheless, if differences in degree of genetic constraint were the only factor, a correlation would still be expected, albeit reflecting an allometric rather than isometric relationship between variables. The observation that no such relationship exists suggests otherwise.

4.2. Humeral length asymmetries in humans and African apes

Only humans show a population-level bias towards longer right humeri (tables 18 & 24), and the present results show that humans are significantly different from the apes in magnitude (%AA) and directionality (%DA) of this asymmetry (table 21). These results are in line with Schultz (1937) who found no tendency for the right arm to be longer in apes, and that the degree of length asymmetry in apes is half that of humans. Interestingly, and in contrast to the current results, subperiosteal area of humeral diaphysis has been found to be left-biased in a sample of common chimpanzees (Sarringhaus et al. 2005), suggesting sample-specific differences in lateralization and/ or that variation in humeral length and subperiosteal area are the consequence of different mechanisms. I also report significant differences in absolute asymmetry (and near-significance in directionality) in length between human males and females, with females being more asymmetric than males (table 23). These results are also in agreement with previous studies, which show that females are more likely than males to have longer bones in the right forelimb (Steele 2000a,b; Auerbach and Ruff 2006). Although I cannot exclude the possibility that behavioural differences between sexes are in part responsible for this pattern (Ruff 1987; Weiss 2009), the fact that similar asymmetries are found across human populations, and that the same pattern is not observed for humeral torsion, suggests otherwise. Some researchers have hypothesized that subtle asymmetries in length may be linked to bilateral differences in blood oxygen levels, potentially leading to unequal bone growth (Steele 2000a,b). Such innate factors would also help explain why, according to some research, human foetuses already exhibit heavier muscle and bone weights as well as greater lengths on the right arm in utero (Pande and Singh, 1971; Bareggi et al. 1994). Other studies,

however, have failed to confirm these patterns or even found the opposite to be the case, and more research will be needed to establish whether consistent biases already exist at foetal stages (Steele 2000a,b). Asymmetries in humeral length may be due to innate factors in non-human apes as well, but it is relevant to note nonetheless that unlike in humans, humeral length asymmetries are not significantly biased in any direction in the apes, making humans unique in exhibiting strong population-level right-side directionality in humeral lengths (with only 6 out of 40 individuals in the current sample presenting longer left humeri). These results suggest that this pattern in humeral length is unique to Homo sapiens and thus may have arisen after the Pan-hominin split possibly as a result of selective pressures for increased lateralization and towards right-side dominance.

4.3. Humeral torsion asymmetries in humans and African apes

These results indicate that humans are unique among the three species in showing significant right-side biases in directional asymmetry for humeral torsion (table 18, 20 & 24). However, chi-square tests show that the distribution of %DA frequencies is non-significant in either species (table 19), and that there are no significant differences in directionality (%DA) between species (table 21), suggesting that the relationship between humeral torsion and handedness is not straightforward, at least when considering modern populations and non-athletes. Interestingly, unlike for lengths, the magnitude (%AA) of torsion asymmetries is not significantly different between samples. The present study indicates that the amount of torsion asymmetry within individual chimpanzees and gorillas is statistically significant (table 20), and that it occurs in magnitudes not significantly different from those in individual humans, which suggests that African ape locomotion may produce forelimb lateralization. Although ape quadrupedal locomotion is considered to be largely symmetrical (Hildebrand 1967; Vilensky and Larson 1989), chimpanzees exhibit a tendency to angulate their torsos during quadrupedal gaits, either to the left or right (Larson and Stern 1987), and studies on both captive and wild chimpanzees have identified gait lateralization at the individual level (but not at the group-level)

(Marchant and McGrew 1996; Hopkins et al. 1997; Morcillo et al. 2006; Arcadi and Wallauer 2011). However, whether gorillas also exhibit similar lateralization is unknown, as are the effects that asymmetrical gait patterns might have on skeletal asymmetries (Carlson 2006).

The suggestion that locomotion, not just manipulatory activities, induces lateralization is interesting in the context of upper limb versus forearm asymmetries. Some studies suggest that upper limb asymmetries reflect only the more vigorous and power-based activities related to locomotion, and that forearm asymmetries (particularly, the hand) reflect the more fine tuned manual activities that we normally associate with handedness (Cashmore and Zakrewski 2011). Sarringhaus et al (2005), for example, find opposite directionalities in asymmetries of chimpanzees for total subperiosteal area of humeral diaphyses and second metacarpals (left for humerus and right for metacarpal). The possibility that there may exist opposite directionality between the proximal and distal segments of the upper limb, as suggested by Sarringhaus et al (2005), is interesting in light of Hunt's (1994) observations of chimpanzee feeding behaviours (individuals often hang from one arm for support, while using the opposite hand for manipulation). It is possible then, that biases in torsion asymmetry in apes reflect a preference for the support arm, rather than for the arm performing the manipulative task, but further studies on the effects of locomotion on torsional asymmetries in apes are needed to explore this. In humans, a contra-lateral relationship has also been described between clavicle lengths and humeral lengths (Auerbach and Raxter 2008; Mays et al 1999; Fatah et al 2012) and more recently, Cashmore and Zakrzewski (2011) also found differences in the expression of asymmetry between musculoskeletal markers in human hand bones and the humerus. If indeed different biomechanical factors influence proximal and distal upper limb segment morphologies, then the relationship between humeral torsion and handedness at the individual level may be less straightforward than previously hypothesized, and hand bone asymmetries may be better suited to address questions on handedness specifically. It is possible that, in humans, only repetitive strenuous activities, such as throwing, induce pronounced population-level asymmetries in humeral torsion that

actually correspond to population-level handedness patterns, as has been shown for athletes and physically active populations (Martin 1933; Edelson 1999; Osbahr et al. 2002). More studies on the directionality of asymmetries in the entire upper limb of apes and humans (particularly the hand) are needed, as are studies on the relationship between torsion, handedness and locomotion.

Furthermore, the magnitude and directionality of torsion asymmetries in male and female apes have opposite patterns (table 23), with significant differences between the male and female gorillas (table 23). Moreover, it is the female gorillas, and not the males who show significant differences between left and right torsion (table 19), being left lateralized for this trait (table 23). While differences in humeral torsion between male and female humans have been previously reported (Edelson 1999), there are no reported differences in directional asymmetry between sexes in humans, making this a unique ape trend. The possibility that males and females show different degrees and patterns of lateralization is intriguing, but consistent with other lines of evidence, such as behavioural observations that indicate the presence of locomotor differences between male and female gorillas (Doran 1993; Remis 2005). It has been suggested for example, that female gorillas use suspensory postures more frequently than males (Doran 1993), and that captive apes are left lateralized for infant cradling (Manning and Chamberlain 1991), which is possibly linked to brain hemispheric specialization and the processing of emotional cues by the right hemisphere (Manning et al. 1994). This is particularly interesting in light of the recent suggestion that anthropoid primate males and females have followed different hemisphere-specific evolutionary trends in the evolution of the prefrontal cortex (Smaers et al. 2012). It is possible, on the other hand, that differences in thoracic shape and scapular position, rather than behaviour, are responsible for this dimorphism (Larson 2007), but further studies are needed to explore this possibility. Due to the lack of significant differences in directional asymmetry in the current data for the gorilla males and for chimpanzees, as well as the lack of significance in left/right torsion frequencies in either sample, these interpretations must for now remain tentative, but future studies should explore the possibility of sexual differences in lateralization.

5. Conclusion

Overall, humans are unique in presenting a population-level right bias for both humeral length and torsion, consistent with population-level right-handedness, while the African apes show no significant directionality in either measurement. Additionally, length asymmetries are less pronounced than torsion asymmetries, which are elevated and comparable in magnitude, both across the current species sample and to other comparatively more environmentally plastic variables reported in the literature. These differences in asymmetry magnitude between length and torsion in all species support previous suggestions that lengths are more genetically constrained than other skeletal variables. Furthermore, divergent ape and human patterns in length asymmetry suggest that this may reflect, on the one hand, a need to maintain upper limbs of equal length and strength in apes due to locomotor constraints, and, on the other hand, the consequence of pronounced lateralization, related to population-level right handedness, in humans. For humeral torsion, species-level magnitudes of asymmetry were found to be comparable between humans and African apes, which suggests the presence of pronounced behavioural lateralization in the latter (in locomotion and/or other activities) as well as in the former, albeit at the individual rather than the species level.The current results, showing that species-level lateralization exists in humans but not apes, are in line with suggestions from behavioural studies that hand preference (laterality within subjects within tasks) and hand specialization (laterality within subjects across tasks) exist in non-human apes, but not population-level handedness (laterality across subjects and across tasks) (Marchant and McGrew 1991, 1996; McGrew and Marchant 1996). These results also indicate, however, that the relationship between humeral torsion/length and handedness specifically, is not straightforward, but rather the consequence of both developmental processes and patterns of behavioural lateralization.

– Chapter 6 –

A novel 3D protocol for analysing clavicle curvature: shedding light on the phylogeny, ontogeny, and functional morphology of the hominoid clavicle.

1. Introduction

Hominoids possess particularly mobile shoulder joints compared to most other primates (Avis 1962; Lewis 1971, 1974, 1985; Temerin and Cant 1983; Cant 1986; but see Chan 2007a,b). This mobility, which is achieved by a combination of glenohumeral and pectoral girdle movements (Chan 2008), is thought to be particularly crucial for large bodied animals like great apes to profit from a complex 3D arboreal environment in locomotion and feeding (Kagaya et al. 2010). The clavicle plays a central role in this mobility because it maintains a fixed distance between the acromion and the manubrium, like a 'spoke' (figure 42 & 43), thus ensuring that relative movement between these structures is arcuate (Jenkins 1974) – an arcuate excursion moves the shoulder through a greater range of positions, especially with regards to adduction-abduction, than would be possible if excursion were confined to a single (sagittal) plane as is the case in mammals with reduced or absent clavicles, such as ungulates and carnivores (Jenkins 1974; Ljunggren 1979) – indeed, excision of the clavicle in rats, for example, is accompanied by increased mobility of the shoulder girdle in the sagittal plane but loss of circular movement (Jenkins 1974). In mammals and, in particular, arboreal mammals, long clavicles are found together with a short mesiodistal and a long cranio-caudal scapular diameter, and with a relatively large transversal thoracic diameter, permitting a large range of movements in a three-dimensional environment (Oxnard 1973; Jenkins 1974; Ljunggren 1979). Accordingly, extant apes and humans, unlike other extant primates, possess a bent and elongated clavicle relative to their thoracic cage (Gebo 1996; Larson 1998; Schmitt and Lemelin 2002; Kagaya et al. 2010), which maintains the

scapula dorsally positioned and allows a wide range of shoulder movements (Chan 2007b; Kagaya et al. 2010) (figure 44).

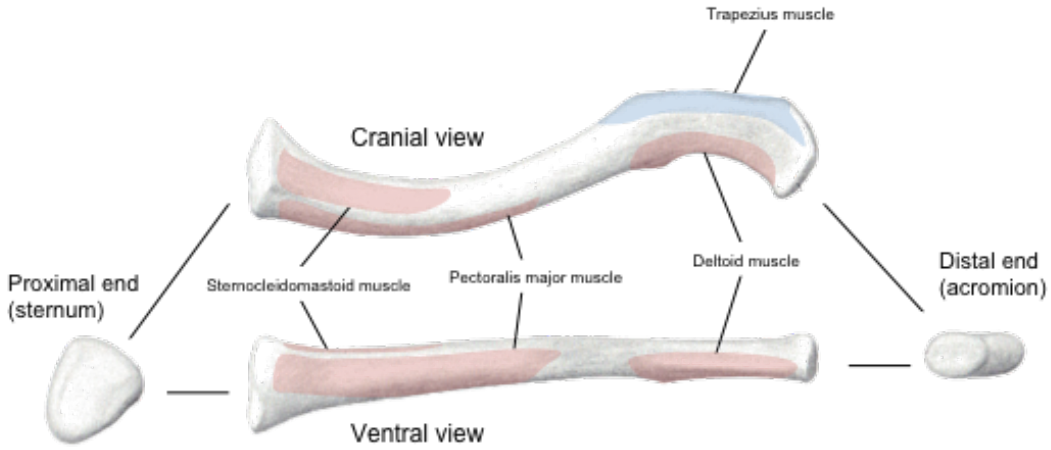

Figure 42 – Anatomy of the adult left human clavicle (in cranial and ventral views) showing muscle origins (red) and muscle insertions (blue). The medial two-thirds of the clavicle are approximately circular/triangular in cross section, a shape consistent with axial pressure or pull; its lateral third has a relatively flat cranial and caudal surface, a shape compatible with pull from muscles and ligaments (Ljunggren, 1979).

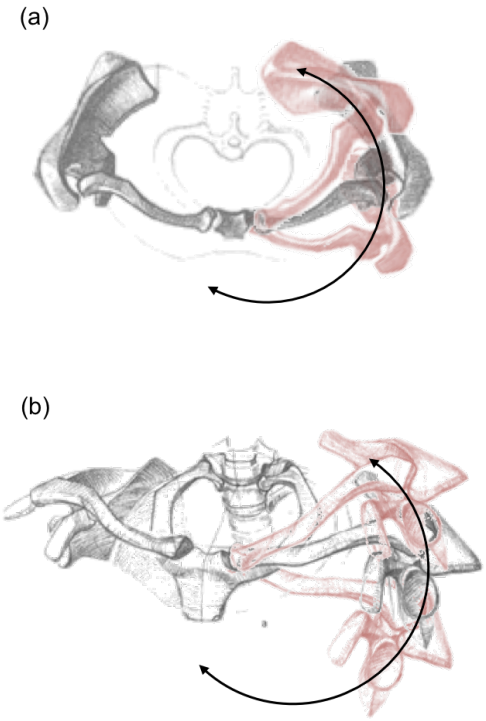

Figure 43 – The adult human shoulder at rest (gray) and in (a) retraction/protraction (red), (b) elevation/depression (red), illustrating the role of the clavicle as a 'strut': the clavicle allows the shoulder complex to move in an arcuate fashion (black circular arrows).

More importantly, the clavicle is an important shoulder joint stabilizer, particularly during overhead movements (Voisin 2006), because it acts as a compression-resistant 'strut' during weight-bearing and pulling movements, and keeps the shoulder complex distant from the rib cage during quadrupedal walking and suspension (Preuschoft et al. 2010). This stability results in part from the fact that the clavicle limits the amount of shoulder joint excursion; in humans, for example, removal of the clavicle results in negligible functional disturbances and increased range of motion, but leads to instability during weight support and pushing above head level because these movements cause pressure/tension in the longitudinal axis of the clavicle (Inman and Abbott 1944; Inman and Saunders 1946; Ljunggren 1979). This suggests that more than mobility, the clavicle is crucial in providing stability to the shoulder complex during elevation of the arm/shoulder (Inman and Abbott 1944; Inman and Saunders 1946).

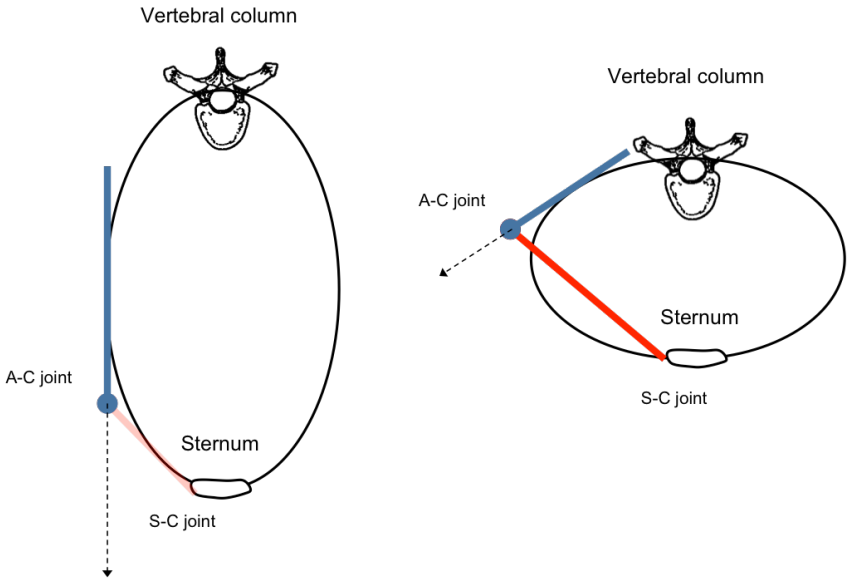

Figure 44 – Schematic representation (in cranial view) of the thorax (black circle), scapula (blue), and clavicle (red) in a quadrupedal mammal (left) versus a hominoid (right); In hominoids the long clavicle allows for a dorsally positioned scapula and a lateral facing glenohumeral joint (arrow), which facilitate a wide range of shoulder movements (namely circular movements), while in quadrupedal mammals, where the clavicle is reduced or absent, the glenohumeral joint faces more ventrally (arrow) limiting shoulder movement to the sagittal plane (A-C joint: acromioclavicular joint; S-C joint: sternoclavicular joint) (redrawn from Ljunggren, 1979).

However, the fundamental and most important function of the clavicle is related to the existence of its curvatures, as these are responsible for providing the necessary range of movement characteristic of the hominoid shoulder complex (Inman and Abbott

1944; Inman and Saunders 1946). The distal curvature is of particular importance because it permits the clavicle to act as a 'crankshaft', which allows the final half of scapular rotation to take place (Inman and Saunders 1946). In humans, loss of this distal curvature prohibits the full range of scapular rotation and interferes with complete shoulder elevation, causing increased shearing forces and consequently degenerative changes at the acromioclavicular joint (Inman and Saunders 1946; Ljunggren 1979). The proximal curvature in hominoids, on the other hand, allows for the scapula to be dorsally positioned all the while preventing obstruction of the thoracic inlet – which serves as the passage for several vital structures such as arteries, veins, lymph nodes and the brachial plexus (Jenkins et al. 1978; Chan 2008). In humans, excessive exaggeration of this curvature interferes with the axis of clavicular rotation, resulting in displacement of its sternal extremity and pain at the sternoclavicular joint (Inman and Saunders 1946).

Despite playing a central role in predicting and determining the range of motion at the shoulder girdle in hominoids, the clavicle's complex anatomy with its twisted S-shape appearance has made it a particularly challenging bone to analyse, and for this reason, it has remained seldom studied in a comparative context. Perhaps the most comprehensive cross-comparative analysis of clavicular curvatures in primates is offered by Voisin (2006); using traditional 2D methods, the author finds that the primate clavicles in his sample can be divided into three groups based on ventro-cranial curvatures, which according to the author are associated with scapular positioning, and into four groups based on cranio-caudal curvatures, which are thought to relate information about the parameters of arm elevation in primates (Voisin 2006).

Clavicle curvatures have typically been quantified via the assessment of the bone's proximal and distal curvatures when projected on two perpendicular planes, cranial and dorsal (Olivier 1951; Voisin 2006; Bachoura et al 2013). Olivier's method (1951) for example, estimates the middle arc of the curvatures as the proportion between the length of the chord and the height of the curvature, which is also the method used in

Voisin's (2006) study. The emergence of novel 3D methods in recent years, however, has prompted renewed interest in clavicle morphology, particularly in the medical field, with studies proposing a number of protocols for quantifying the curvatures of the clavicle in 3D, as an alternative to forcing its curvatures into two-dimensional planes which may not be as biologically relevant (Daruwalla et al. 2010; Fatah et al. 2012; Bachoura et al. 2013; Mathieu et al. 2013). Bachoura et al (2013), for example, estimate proximal and distal clavicle curvatures as the angles (in degrees) between the medial, middle and lateral segments of the clavicle in both axial and coronal planes using a 3D environment, while Fatah et al (2012) use a protocol for defining multiple segments based on clavicular contours, and then measure clavicular curvatures as the angles (in degrees) between these various segments. Both these studies were based on human clavicles.

In this chapter, I propose a new and more streamlined 3D protocol – which I refer to as 'freecurve' (based on the Geomagic Suite 12.1 function 'Free Curve') – for analysing clavicle curvatures across primate species. This protocol is devised as an alternative to forcing the clavicle into 2D planes, and thus yields two curvature measurements (distal and proximal), rather than the four measurements produced with the more traditional 2D methods (proximal cranial, proximal ventral, distal cranial, and distal ventral). The aim is to provide a simple and reproducible 3D protocol for assessing clavicular curvatures that can be applied to clavicles across species. This method should also be able to quantify curvature in fossil clavicles, which may be difficult to place in the 2D planes due to being damaged and/or incomplete. I also measure curvatures using a more traditional 2D approach in order to compare methods and to test whether/how methodological choices impact functional interpretations. Additionally, I analyse clavicular curvatures within both an ontogenetic and a phylogenetic framework, in order to address the absence to date of any such data and to understand how clavicular curvatures develop with growth; I also look at the relationship between these curvatures and 11 functionally significant variables of the other elements of the shoulder girdle (scapula and humerus) across hominoid species. The 11 measurements are: clavicle length, clavicle thickness

(antero-posterior and cranio-caudal), clavicle torsion, humeral torsion, angulation of the glenoid fossa relative to the lateral border of the scapula, orientation of the glenoid fossa relative to the medial border of the scapula, orientation of the scapular spine relative to the glenoid fossa, glenoid version, angulation of the spine relative to the lateral border of the scapula, angulation of the spine relative to the medial border of the scapula, and geometric mean of the shoulder (table 24; see Materials and Methods chapter for details). These measurements were chosen because they relate information about orientation of the scapular spine and the glenoid fossa (angles of the glenoid fossa and spine relative to the scapular body and humeral torsion), which have functional implications for genohumeral joint mobility and range of motion (e.g., Larson and Stern 1986; Larson et al. 1991; Inouye and Shea 1997; Haile-Selassie et al. 2010; Green and Alemseged 2012) as well as overall size/shape of the clavicle (thickness, length and torsion of the clavicle). This should ultimately contribute towards a better understanding of the clavicle's functional morphology in extant and possibly extinct hominoid species.

Table 24 – Table with the 12 shoulder variables plotted against clavicle curvatures.

Element	Measurement name	Measurement description
Clavicle	clav_length	Maximum length of the clavicle
	clav_thick_ap	Maximum thickness of the clavicle at midshaft (antero-posterior)
	clav_thick_cc	Maximum thickness of the clavicle at midshaft (cranio-caudal)
	clav_torsion	Clavicle torsion
	clav_angle_dist_ant	Distal angle of the clavicle (anterior/ventral view)
	clav_angle_dist_sup	Distal angle of the clavicle (superior/cranial view)
	clav_angle_prox_ant	Proximal angle of the clavicle (anterior/ventral view)
	clav_angle_prox_sup	Proximal angle of the clavicle (superior/cranial view)
	clav_freecurv_dist	Distal angle of the clavicle using 'freecurve' method
	clav_freecurv_prox	Proximal angle of the clavicle using 'freecurve' method
Humerus	hum_length	Maximum length of the humerus
	hum_torsion	Medial rotation of the humeral head over the humeral shaft
Scapula	scap_height	Maximum height of scapular body
	scap_breadth_spine_glen	Maximum breadth of the scapula from the glenoid fossa to where the long axis of the scapular spine and the vertebral border meet
	glen_angle_latborder	Angle of the glenoid fossa to the lateral border of the scapula
	glen_angle_medborder	Angle of the glenoid fossa to the medial border of the scapula
	glen_angle_spine	Angle of the glenoid fossa to the spine of the scapula
	glenoid_angle_bodyspine	Angle of the glenoid fossa to the scapular body below the spine
	glen_version	Angulation of the glenoid fossa relative to the body of the scapula in transverse plane. Measured on the posterior side.
	latborder_spine_angle	Angle of the scapular spine to the lateral border of the scapula
	spine_angle_medborder	Angle of the scapular spine to the medial border of the scapula

2. Materials and Methods

2.1. 'Freecurve' method for quantifying 3D curves

The 'freecurve' protocol was devised as an alternative to forcing the clavicle into 2D planes, which may not capture the true biological significance of its curvatures. Instead, here I estimate these curvatures by fitting two polylines (proximal and distal) through four homologous landmarks on the ventral surface of the clavicle (the distal polyline is fitted through two landmarks, and the proximal polyline, through three landmarks), using the curve fitting options 'Draw Curve' and 'Free Curve' in Geomagic 12.1. The two polylines are fitted such that they represent arches of two circles, and their curvatures (k) are measured (in mm) as a function of each circle's radius (R):

$$k = 1 / \mathrm{R}$$

Because smaller circles have smaller radii, they bend more sharply and thus have a higher curvature (values closer to 1); conversely, larger circles have bigger radii and thus less curvature (values closer to 0 mm).

These fitted curves are therefore less constrained from adhering to particular pre-defined planes of view (figure 45), and are allowed to move freely between landmarks, across the ventral aspect of the clavicle (hence the name 'freecurve'). Using this protocol, two curvature measurements are produced (distal and proximal), rather than the four measurements produced with the more traditional 2D methods.

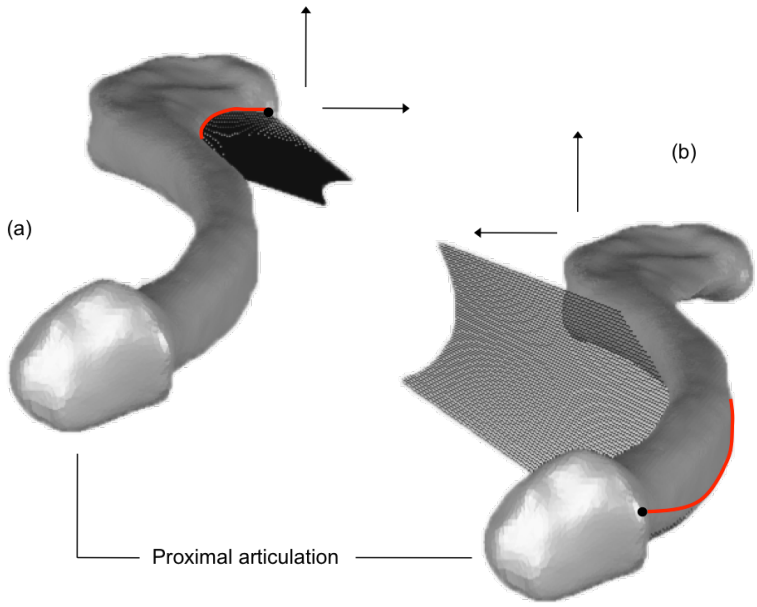

Figure 45 – 3D surface scans of an adult human left clavicle (sternal view) showing the distal (a) and proximal (b) 'freecurves'. The figure illustrates how, using this protocol, the curvatures are less constrained from adhering to 2D planes. The curvatures are measured (in mm) as a function of the circle's radius, rather than angles expressed in degrees.

2.2. Procedure

Using Geomagic Suite 12.1, the clavicle is oriented into cranial view, then, using a cylinder of best fit, the clavicle is divided into 3 slices of equal lengths (figure 46). Using the 'Draw Curve' function – which allows placing free-form lines on three-dimensional object surfaces –, the distal and proximal curvatures are captured by placing two lines (distal and proximal) between these slices on the ventral portion of the clavicle: (1) the distal line is placed on the distal third of the clavicle, between the ventral-most point of the acromial facet (figure 47a, landmark 1), and the point of intersection between the distal-most slice and the ventral-most point on the dividing plane between the distal and the central slices (figure 47a, landmark 2); (2) the proximal line is placed on the proximal two thirds of the clavicle, between the intersection of the distal-most dividing plane with the ventral-most portion of the clavicle (figure 47a, landmark 2), and the protuberance on the proximal ventral clavicle, between the attachments for the sternocleidomastoid muscle and the pectoralis major muscle (figure 47a, landmark 3); in order for this measurement to be consistent across species and specimens, the centre of this proximal line is also fixed

to a landmark where the proximal dividing plane intersects with the ventral-most portion of the clavicle (figure 47a, 4).

Once the lines are fitted onto the surface of the clavicle, they are converted into 'Free Curves' using the function by this name in Geomagic Suite 12.1. This converts the free-form lines into reference polylines from which a line-arc can be derived (figure 48a, blue line) – with the polyline endpoints corresponding to polygonal mesh points on the surface object (Attene et al. 2006; Botsch et al. 2007; Varady 2008). This function first computes a sequence of marker points that correspond to the endpoints of consecutive segments (figure 48, green points), from which a curve approximating the underlying segmented data points is then extracted (figure 48, orange lines). I selected an 'Adaptive' Control Point Layout (the default setting), which allows the software to optimize the number of control points to obtain this segmentation (Varady 2008). This reference polyline is then edited using the 'Edit Curve' function, the segmentation sensitivity is set to 0, and all remaining reference points (figure 48b, green points) are manually removed from the polyline, which allows to produce one continuous line – rather than several segmented lines – describing the curvatures (figure 48c, orange line).

The curvature values obtained are invariably positive, except in a few cases, where I manually assigned a negative value to the measurement to indicate that the curvature bends in the opposite direction than is expected. The proximal curvature is always expected to bend ventrally, and the distal curve to bend dorsally (figure 49), but in some instances this was not the case – this was particularly true in the gibbons, where the distal curvature bent ventrally rather than dorsally in some specimens.

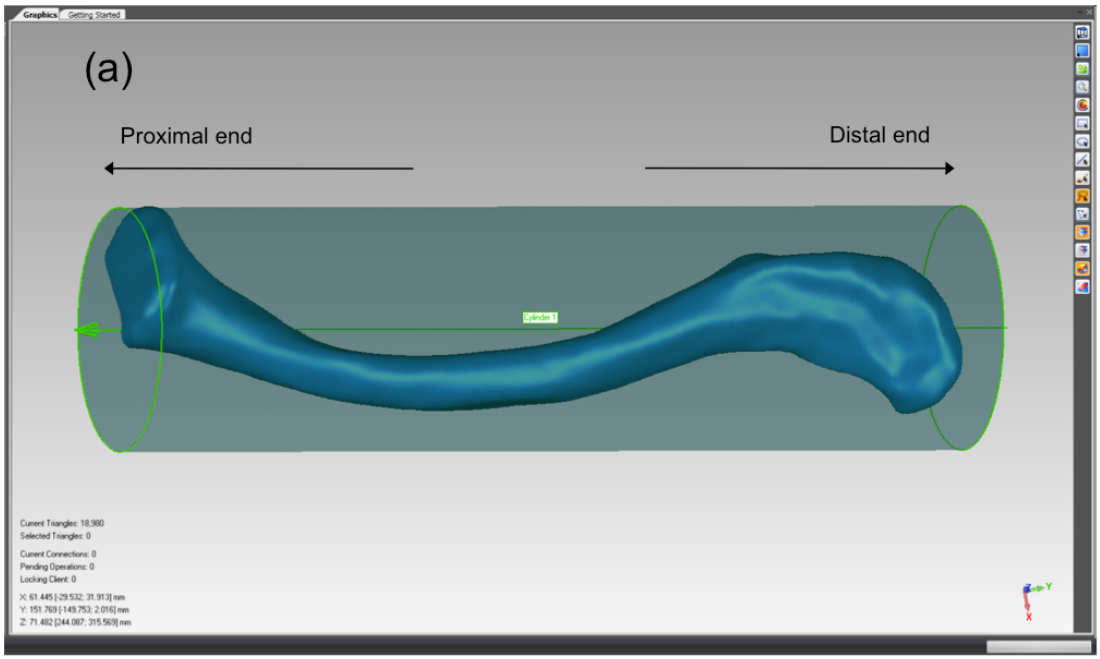

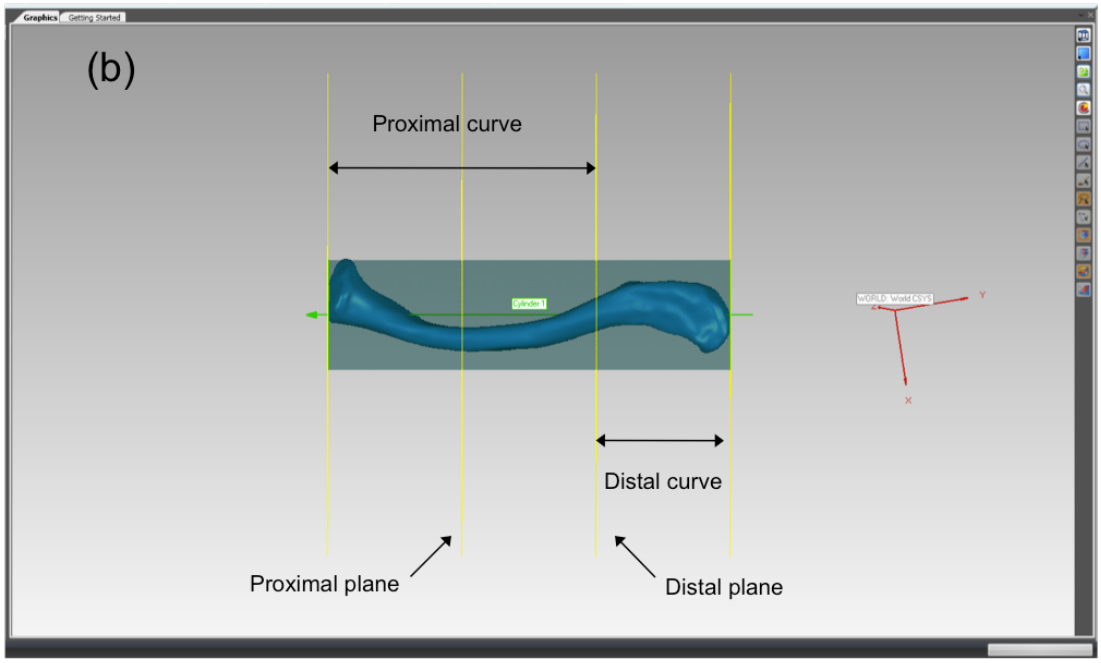

Figure 46 – 3D surface model of an adult human left clavicle (cranial view) with cylinder of best fit (a), and fitted equidistant dividing planes (b), in Geomagic Suite 12.1.

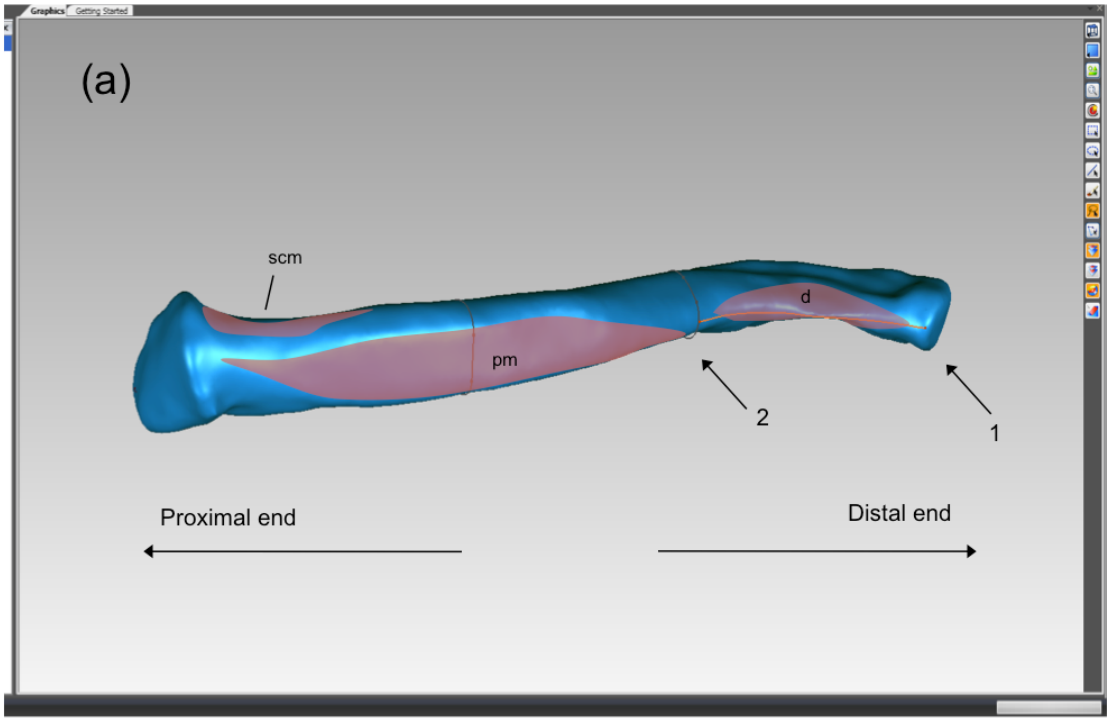

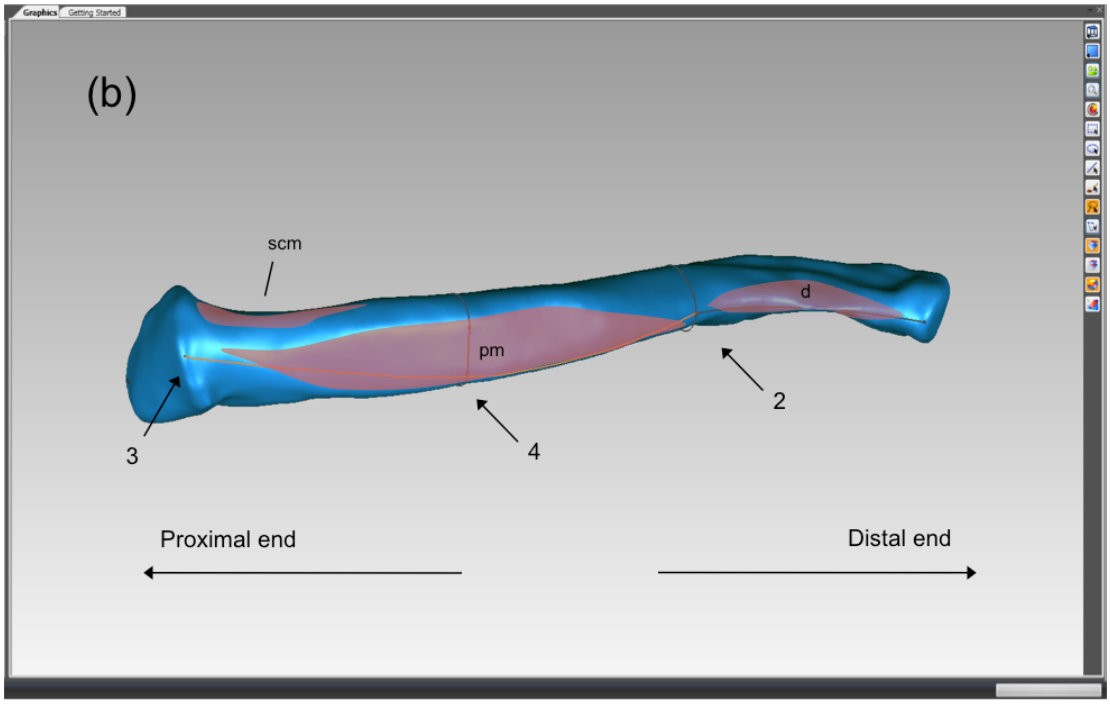

Figure 47 – 3D surface model of an adult human left clavicle (ventral view) with the fitted distal (a), and proximal (b) polylines (using the 'Draw Curve' function in Geomagic Suite 12.1). The attachments for the deltoid (d), pectoralis major (pm) and sternocleidomastoid (scm) muscles are indicated in red; the two black circles around the clavicle body represent the proximal and distal dividing planes. The landmarks used to draw the polylines are: the ventral-most point of the acromial facet (1), the intersection of the distal dividing plane with the ventral portion of the clavicle (2), the protuberance on the proximal ventral clavicle, between the attachments for the sternocleidomastoid muscle and the pectoralis major muscle (3), the intersections of the proximal dividing plane with the ventral portion clavicle (4).

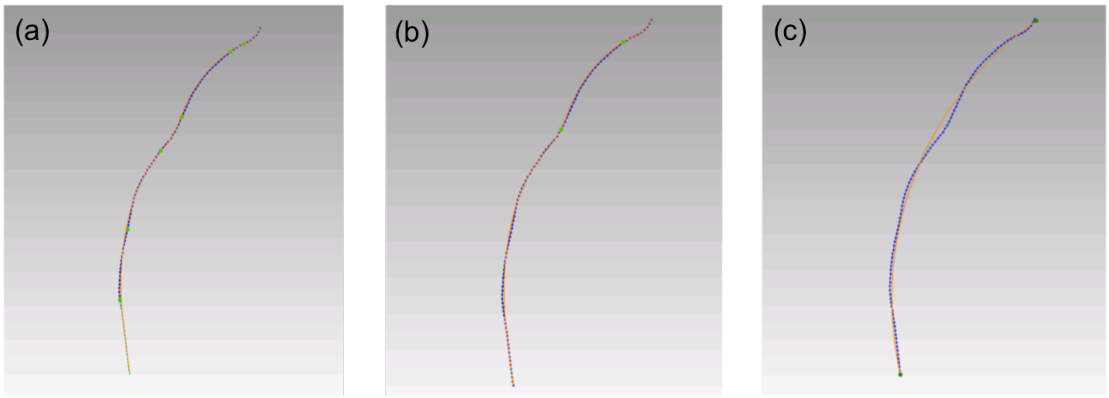

Figure 48 – Isolated reference polyline (blue line), and profile curve (orange line) fitted to the segmented reference polyline using the 'Edit Curve' function in Geomagic 12.1. The segmented reference polyline (a) contains multiple reference points (bright green) through which the profile curve is fitted. The segmentation sensitivity is then set to 0 (b) which reduces the number of reference points through which the profile curve is fitted; the remaining reference points are then manually removed (c), and the final profile curve is fitted to the distal-most and proximal most reference points (dark green), which correspond to the landmarks.

2.3. Traditional 2D curve measurements: clavicle angles

Clavicle curvatures have typically been measured via the assessment of the bone's proximal and distal curvatures when projected on two perpendicular planes, cranial and ventral (Olivier 1951; Voisin 2006; Bachoura et al. 2013). Therefore, here I also report clavicle angles calculated in this way by orienting the clavicle in both cranial and ventral views using a 3D environment (Geomagic Suite 12.1), and estimating the distal and proximal angles of the clavicle in both planes as the intersection of proximal, middle and distal lines in 2D (tpdDigs) (figures 50 & 51).

Using Geomagic Suite 12.1, the clavicle is first oriented into the cranial plane. Using a cylinder of best fit, the clavicle is divided into 10 dividing planes of equal length (figure 50) and the image is transferred to tpsDigs as a 2D image, where a series of 9 points are placed at the centre of the clavicle on each intersecting line (figure 51). The proximal and distal angles are then measured using the points of maximum angulation of the clavicle, by drawing three lines (proximal, middle and distal). The lines are selected in order to minimise the value of the angles that they define (in other words, to measure the maximum angulation). The angles are measured in 2D in tpsDigs at the intersection of these lines (figure 51). These steps are repeated with the clavicle in

ventral view. In the end, four angles (in degrees) are obtained: proximal cranial, distal cranial, proximal ventral, and distal ventral.

The angle measurements obtained are invariably ≤ 180°, since a measurement of 180° corresponds to a flat angle/curvature. However, values above 180° were attributed to those few angles that bent in the opposite direction than expected (i.e., to proximal angles that bent dorsally or cranially, and to distal angles that bent ventrally or caudally).

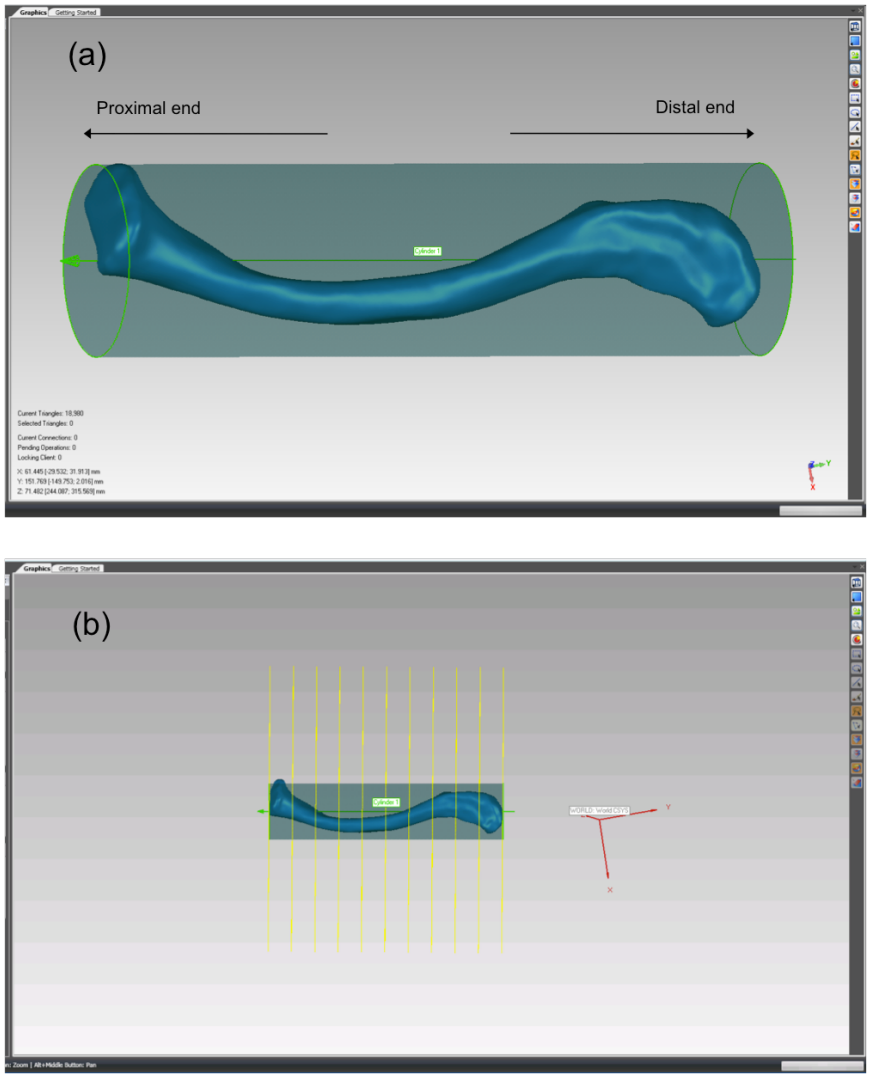

Figure 50 – 3D surface scan of an adult human left clavicle (cranial view) with cylinder of best fit (a), and fitted equidistant dividing planes (b), in Geomagic Suite 12.

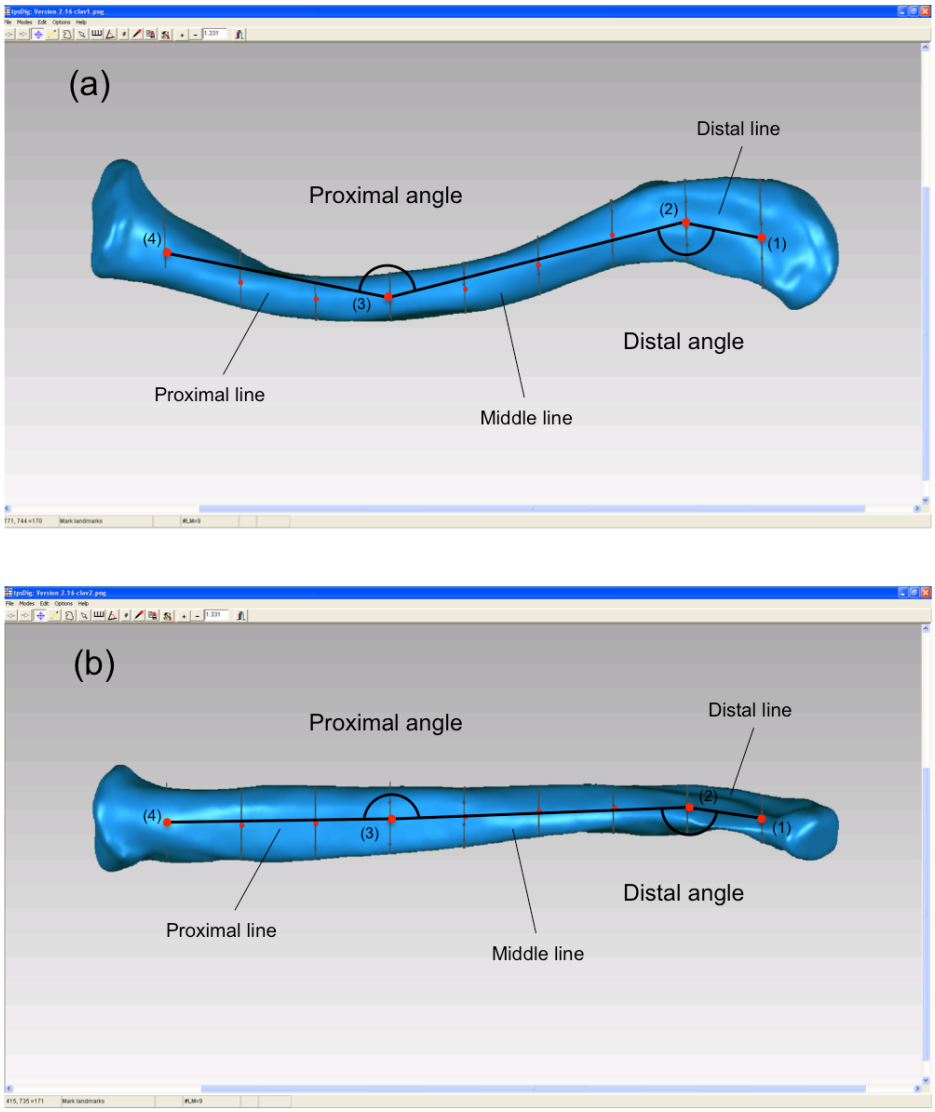

Figure 51 – 2D image of an adult human left clavicle, in cranial view (a) and ventral view (b), in tpsDigs; nine points (red) are placed at the centre of the clavicle, on the intersecting planes (black transverse lines). The distal and proximal angles of the clavicle are measured (in both planes) as the points of maximum angulation of the clavicle, at the intersection of the proximal, middle and distal lines (thick black lines connected to the red dots). These three lines are drawn from the distal-most (1) to the superior-most points (2) (distal line), from the superior-most (2) to the inferior-most points (3) (middle line), and from the inferior-most (3) to the proximal-most points (4) (proximal line).

2.4. Sample

Clavicle angles (2D) and curvatures (3D) were measured on left clavicles (right clavicles when the left was not present or damaged) of *Macaca fascicularis* (n=20), *Hylobates lar* (n=24), *Pongo pygmaeus* (n=25), *Pan paniscus* (n=23), *Pan troglodytes* (n=45), *Gorilla gorilla* (n=42) and *Homo sapiens* (n=97) of all ages (0 to 70 years in

humans; 0 to 13+ years in apes; 0 to 7+ years in *Macaca*). A standard three-parameter Gompertz model was fitted to the distributions using the self-starting function SSgompertz in R version 2.12.2 (2011). The Gompertz function estimates three parameters: the asymptotic value (Asym), the value of x at birth (b2), and a numeric parameter relating to the rate of growth (b3), for each distribution. We also performed regular PGLS regressions with likelihood-fitted Lambda using the package Caper in R (Orme et al, 2011) of adult hominoid clavicle angles/curvatures against 12 shoulder variables of the humerus, scapula and clavicle (which reflect scapular positioning, glenoid fossal orientation as well as overall size and shape of the clavicle; see Materials and Methods section for measurement descriptions), in order to understand the relationship between clavicle angles/curvatures and other functionally significant aspects of shoulder morphology across hominoid species. Additionally, analysis of variance (ANOVA) tests were employed to test for differences in proximal and distal clavicle angles between species, and between age categories within and across species. Boxplots were also employed to visualize the data by species and age categories. Age categories were defined as: 'infants', represented by individuals prior to M1 eruption (7 years for humans, 3.5 years for great apes, and 1.75 for macaques and gibbons), 'juveniles', represented by individuals prior to M3 eruption (18 years for humans, 11 for great apes, 7 years for macaques and 8 years for gibbons), and 'adults', represented by individuals with erupted M3s (Smith 1989). Further details on how the measurements were collected, on how individual specimens were aged, and on the Gompertz function, can be found in the Materials and Methods Chapter.

2.5. Error

Intraobserver errors for clavicle curvatures were conducted on human clavicles and estimated following Tim White's procedure for estimating error (White et al. 2011) – it reports the percentage difference between repeated measurements in relation to 10 averaged repeat measurements (table 1). For every measurement, intraobserver error is approximately 2 to 10 times smaller than the average differences between specimens.

Table 25 – Error table. The percentage differences for repeat measurements reports the proportional deviation between individual repeat measurements and the mean of all repeat measurements. The percentage difference for the total sample the proportional average deviation between individual measurements and the sample mean.

Measurement	Sample	*N*	Mean difference (%)	Standard deviation
clav_dist_ant	Total	25	3.402	5.392
	Remeasurements	10	1.281	1.491
clav_prox_ant	Total	25	2.776	4.355
	Remeasurements	10	1.233	1.633
clav_dist_sup	Total	25	4.324	4.533
	Remeasurements	10	0.971	0.665
clav_prox_sup	Total	25	2.512	4.233
	Remeasurements	10	0.957	1.576
clav_freecurv_dist	Total	25	24.817	0.006
	Remeasurements	10	3.007	0.001
clav_freecurv_prox	Total	25	17.684	0.001
	Remeasurements	10	1.758	0.0001

3. Results

3.1. Ontogeny

Gompertz growth curves generally did not fit the 2D distributions, but fit the 'freecurve' distributions, except in the case of the orangutans and macaques – the lack of very young individuals in these samples does not allow for the Gompertz curve to be fitted (figures 52 & 53; table 26). In the instances where the growth curves can be fitted, the Gompertz models indicate that the curvatures of the clavicle are more curved at birth and gradually flatten out with growth, reaching adult values after M3 eruption, around the time clavicle length reaches its adult values (figure 55).

Additionally, throughout growth, the 2D distal angles are consistently more acute across species than the proximal angle, except in gibbons, where the pattern seems to be inverted (i.e., the proximal angle is consistently more acute) (figures 52 & 53). Using the 'freecurve' method, both proximal and distal curvatures in gibbons show considerable overlap, unlike in the rest of the species, where the two ends of the clavicle show distinct and non-overlapping degrees of curvatures (figure 54).

When the samples are split into age categories, ANOVAs show some differences exist between age categories within species for the 2D angle measurements ($p>0.05$; see figure 56-59 & table 27), and clear differences between age classes (in particular between infants and juveniles/adults) across all species except *M. fascicularis* ($p>0.05$) for the 'freecurves' (figures 60 & 61 & table 27). These results suggest that overall, the clavicle in hominoids undergoes changes in angulation/curvature after infancy and that these are better captured by the 'freecurves' than the 2D angles. Curvatures generally tend to become flatter during infancy and the juvenile period, stabilizing into adult values after M3 eruption.

3.2. Linear regressions and PGLS

According to previous studies of the hominoid clavicle, the clavicle's curvature are thought to be associated with scapular positioning and shoulder joint mobility for overhead movements (e.g., Voisin 2006). Therefore, each clavicle curvature (3D) and angulation (2D) measurements were individually plotted against 12 other shoulder variables of the clavicle plus size of the shoulder (geometric mean), humerus and scapula, using Phylogenetic Generalized Least Squares (PGLS) regressions.

Results indicate that the proximal and distal curvatures/angles of the clavicle in both 2D and in 3D views correlate with different and non-overlapping variables, with the exception of clavicular thickness (cranio-caudal) and the orientation of the glenoid fossa relative to the scapular spine (table 28). In cranial view, the proximal angle (2D) of the clavicle is only significantly correlated with the size of the shoulder (geo_mean) ($p<0.05$) (table 28; figure 63), while the distal angle (2D) is significantly correlated with 3 out of these 12 variables ($p<0.05$): the distal 'freecurve' of the clavicle, humeral torsion, the angulation of the glenoid fossa relative to the scapular spine (table 28; figure 64).

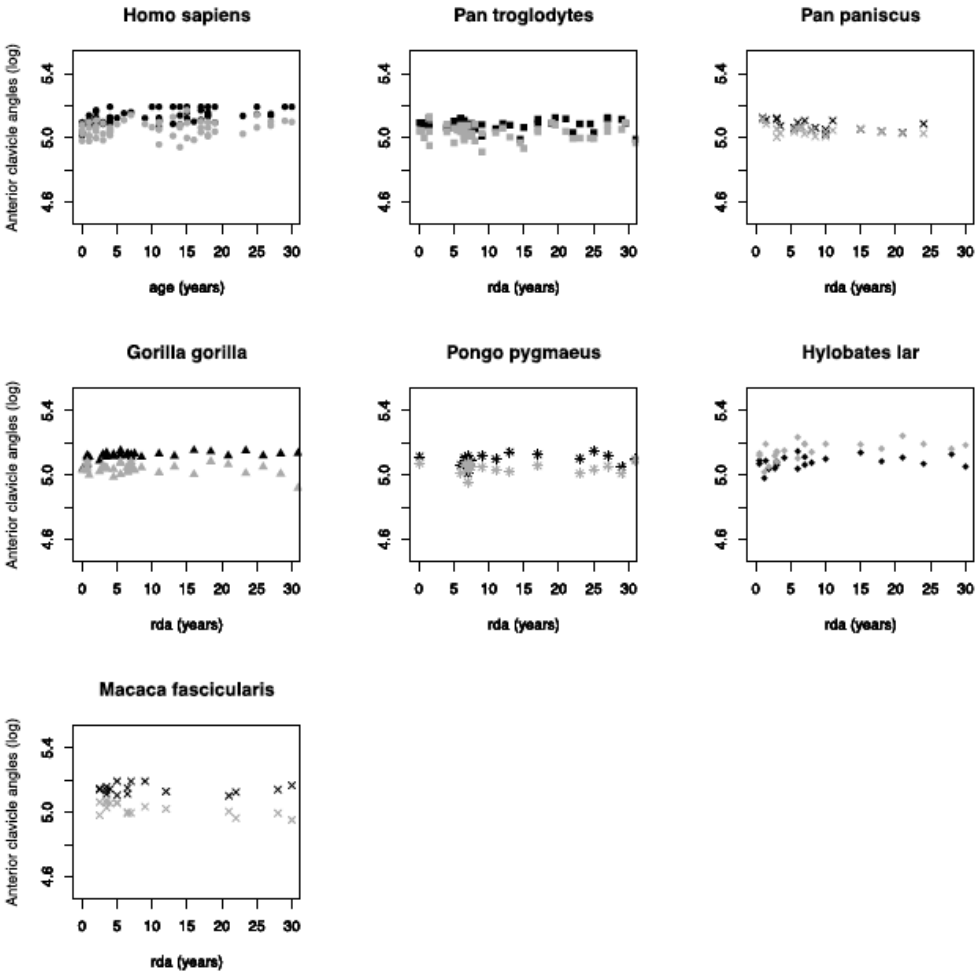

Figure 52 – Ontogeny of the distal (gray) and proximal (black) 2D angles (log) of the clavicle in ventral view (rda: relative dental ages).

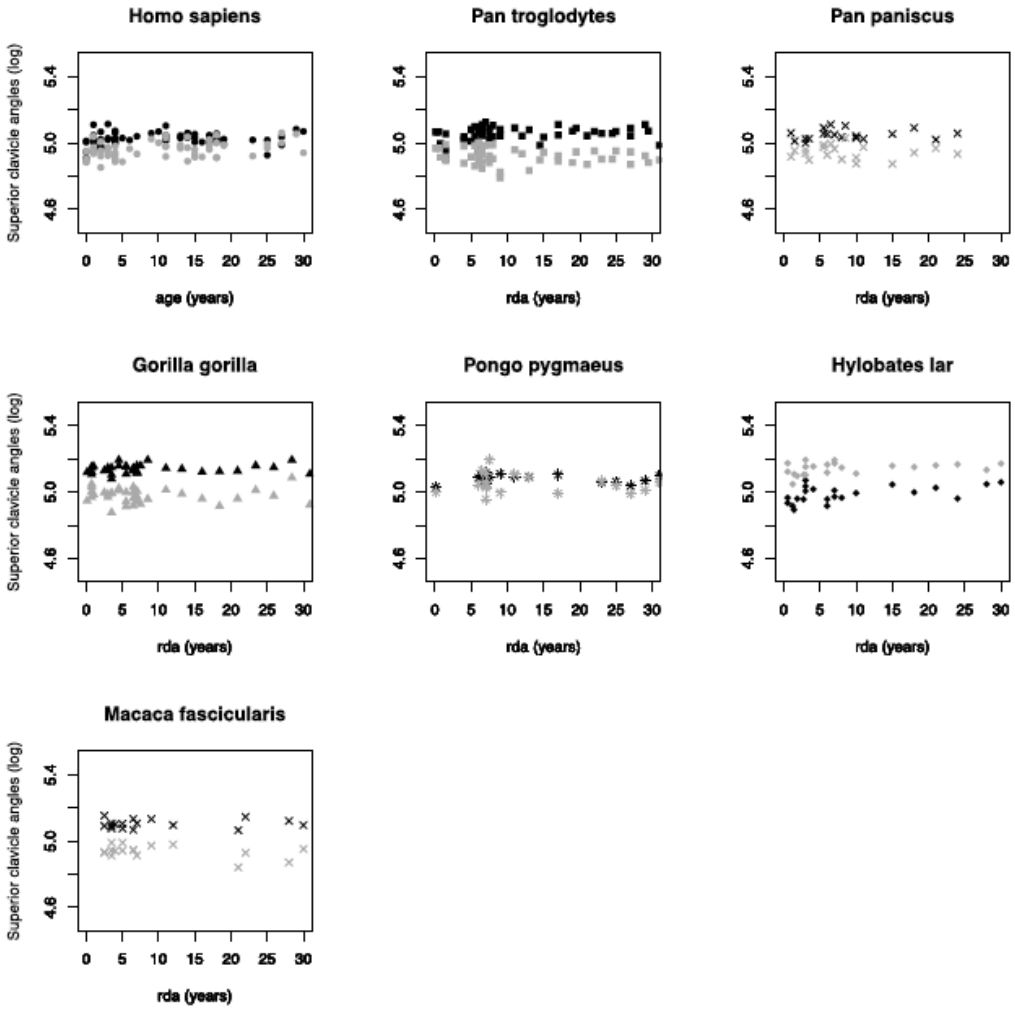

Figure 53 – Ontogeny of the distal (gray) and proximal (black) 2D angles (log) of the clavicle in cranial view (rda: relative dental ages).

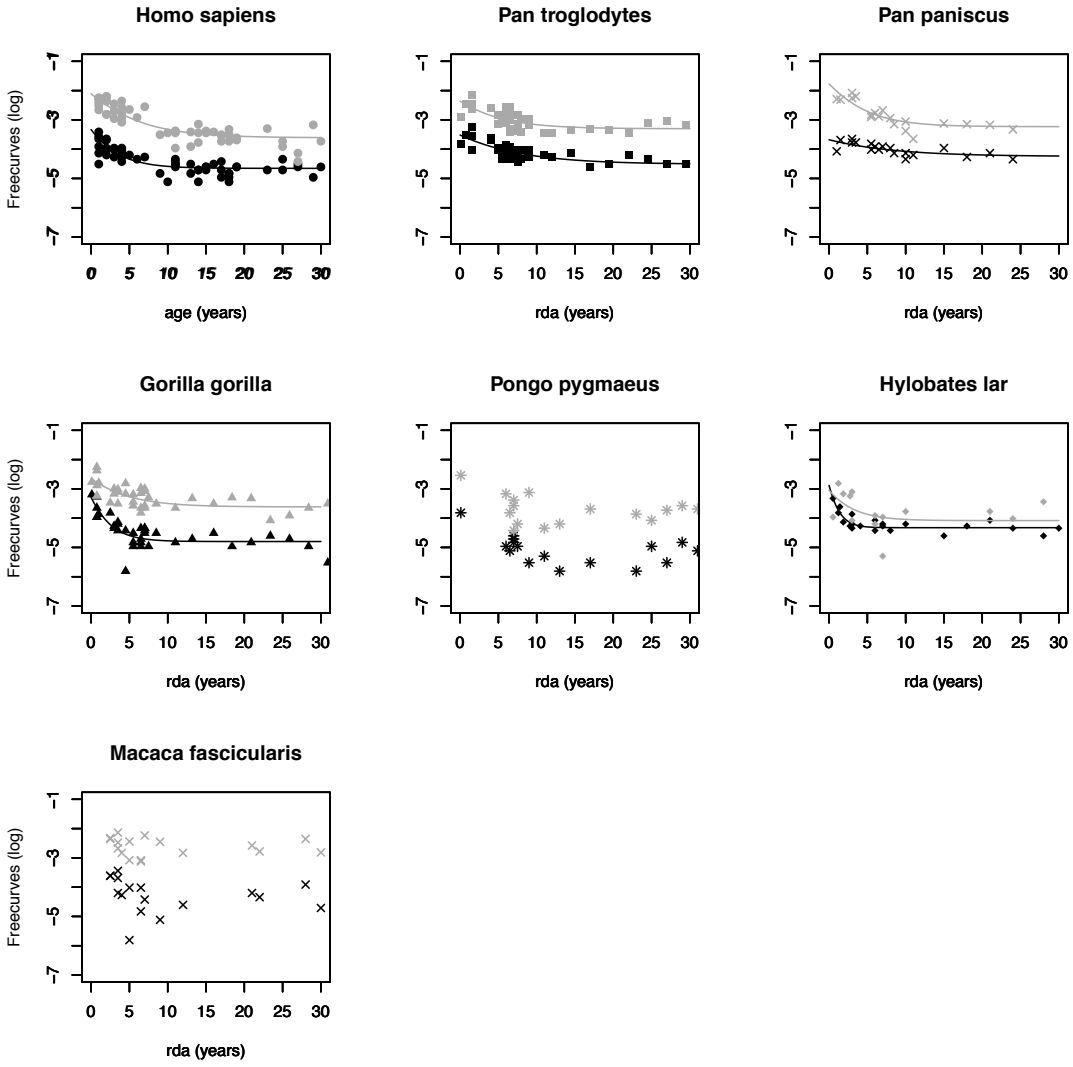

Figure 54 – Ontogeny of the distal (gray) and proximal (black) 'freecurves' (log) of the clavicle (rda: relative dental ages).

Table 26 – Gompertz parameter for the clavicle angle (2D)/curvature (3D) measurements showing estimated value at growth completion (log) (Asymptote), estimated value at x=0 (b2), estimated rate of growth (b3), and the Residual Standard Error.

Species	Measurement	Asymptote	Gompertz b2	Gompertz b3	RSE	DF
Homo sapiens	freecurve prox	-4.655 (±0.060)	0.335 (±0.038)	0.731 (±0.053)	0.284	85
	freecurve dist	-3.610 (±0.050)	0.538 (±0.065)	0.828 (±0.035)	0.341	85
Pan troglodytes	freecurve prox	-4.517 (±0.078)	0.250 (±0.030)	0.872 (±0.028)	0.183	39
	freecurve dist	-3.303 (±0.082)	0.334 (±0.060)	0.815 (±0.046)	0.235	39
Pan paniscus	freecurve prox	-4.247 (±0.082)	0.144 (±0.030)	0.883 (±0.054)	0.145	19
	freecurve dist	-3.232 (±0.094)	0.601 (±0.122)	0.782 (±0.054)	0.234	19
Gorilla gorilla	freecurve prox	-4.797 (±0.086)	0.377 (±0.060)	0.650 (±0.080)	0.329	36
	freecurve dist	-3.616 (±0.091)	0.311 (±0.055)	0.799 (±0.059)	0.284	36
Pongo pygmaeus	freecurve prox	-	-	-	-	-
	freecurve dist	-	-	-	-	-
Hylobates lar	freecurve prox	-4.326 (±0.044)	0.406 (±0.102)	0.434 (±0.098)	0.167	20
	freecurve dist	-4.082 (±0.240)	0.292 (±0.201)	0.713 (±0.278)	0.587	13
M. fascicularis	freecurve prox	-	-	-	-	-
	freecurve dist	-	-	-	-	-

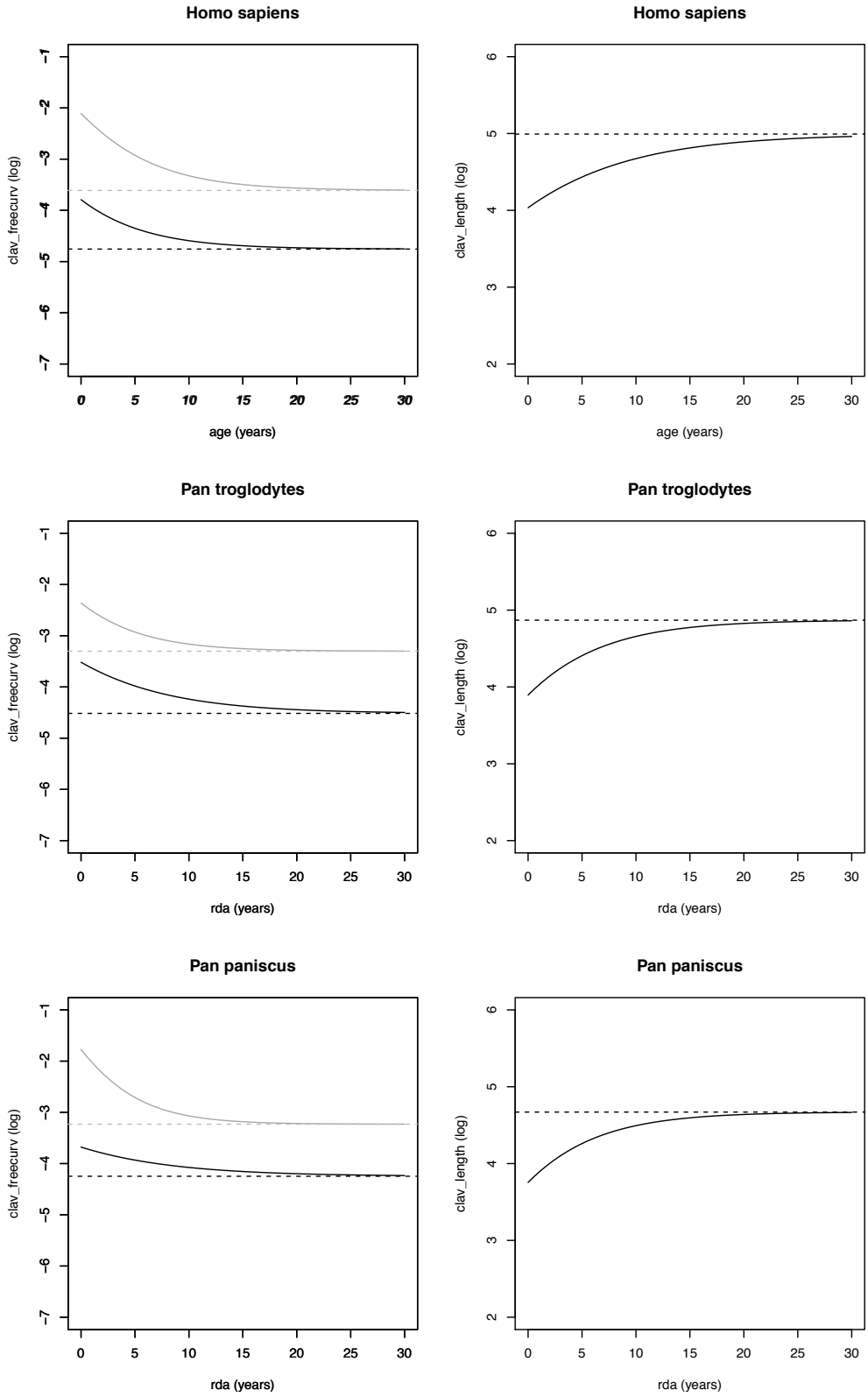

Figure 55 – Ontogeny of the distal (gray) and proximal (black) clavicle curvatures (log) and clavicle lengths (log), using 'freecurves' (rda: relative dental ages). The dashed line represents the asymptote and shows that clavicular curvatures stop developing around the same time as clavicular length.

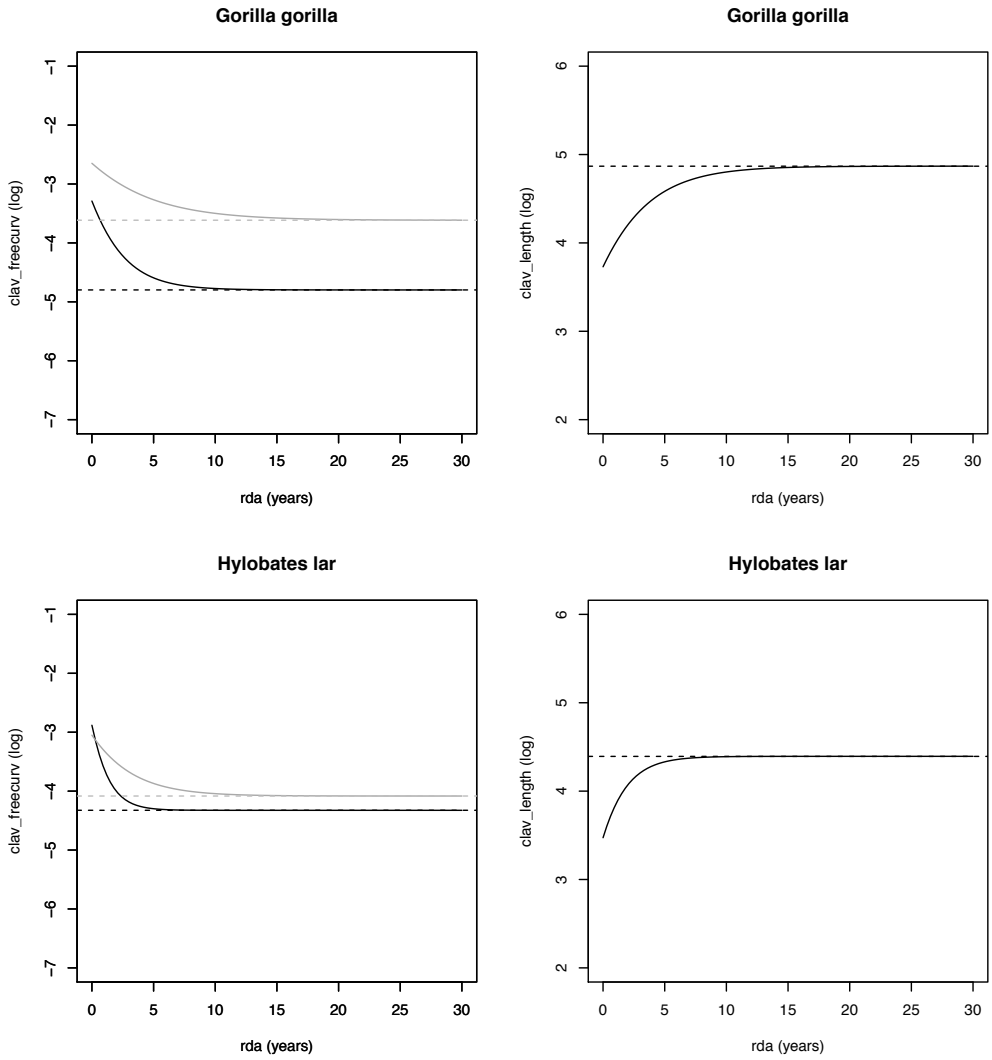

Figure 55 cont'd – Ontogeny of the distal (gray) and proximal (black) clavicle curvatures (log) and clavicle lengths (log), using 'freecurves' (rda: relative dental ages). The dashed line represents the asymptote and shows that clavicular curvatures stop developing around the same time as clavicular length.

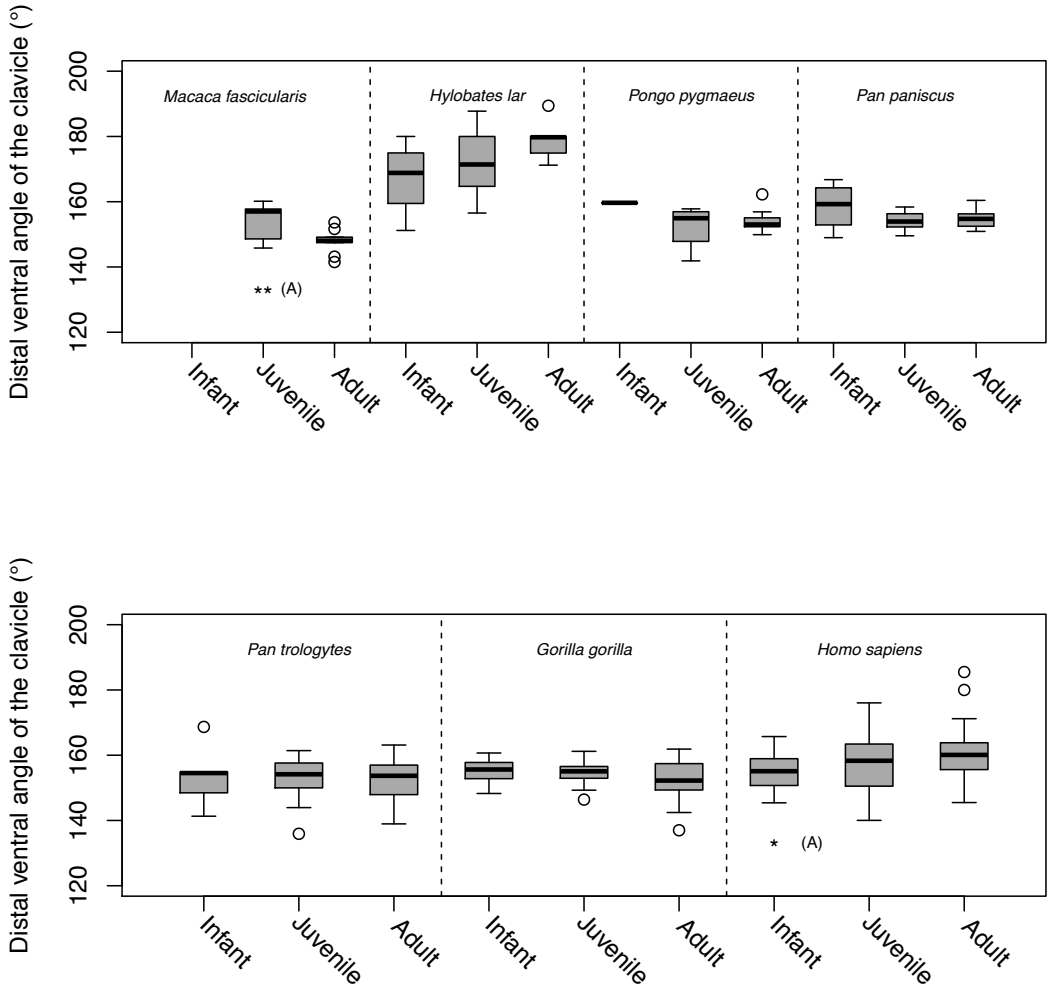

Figure 56 – Boxplot of distal ventral 2D clavicle angles (in degrees) in hominoids and *Macaca fascicularis* by age categories. Significant differences between age categories are marked with asterisks (p<0.001 ***; p<0.01 **; p<0.05 *). ANOVAs show there are no significant differences between age categories for *H. lar* (p = 0.05, df = 2, F value = 3.5825), *P. pygmaeus* (p = 0.05, df = 2, F value = 0.7541), *P. paniscus* (p = 0.178, df = 2, F value = 1.8805), *P. troglodytes* (p = 0.913, df = 2, F value = 0.0898), *G. gorilla* (p = 0.331, df = 2, F value = 1.141); there are significant differences between age categories for *H. sapiens* (p = 0.02, df = 2, F value = 31.8855). A t-test shows significant differences between age categories in *M. fascicularis* (p =0.005).

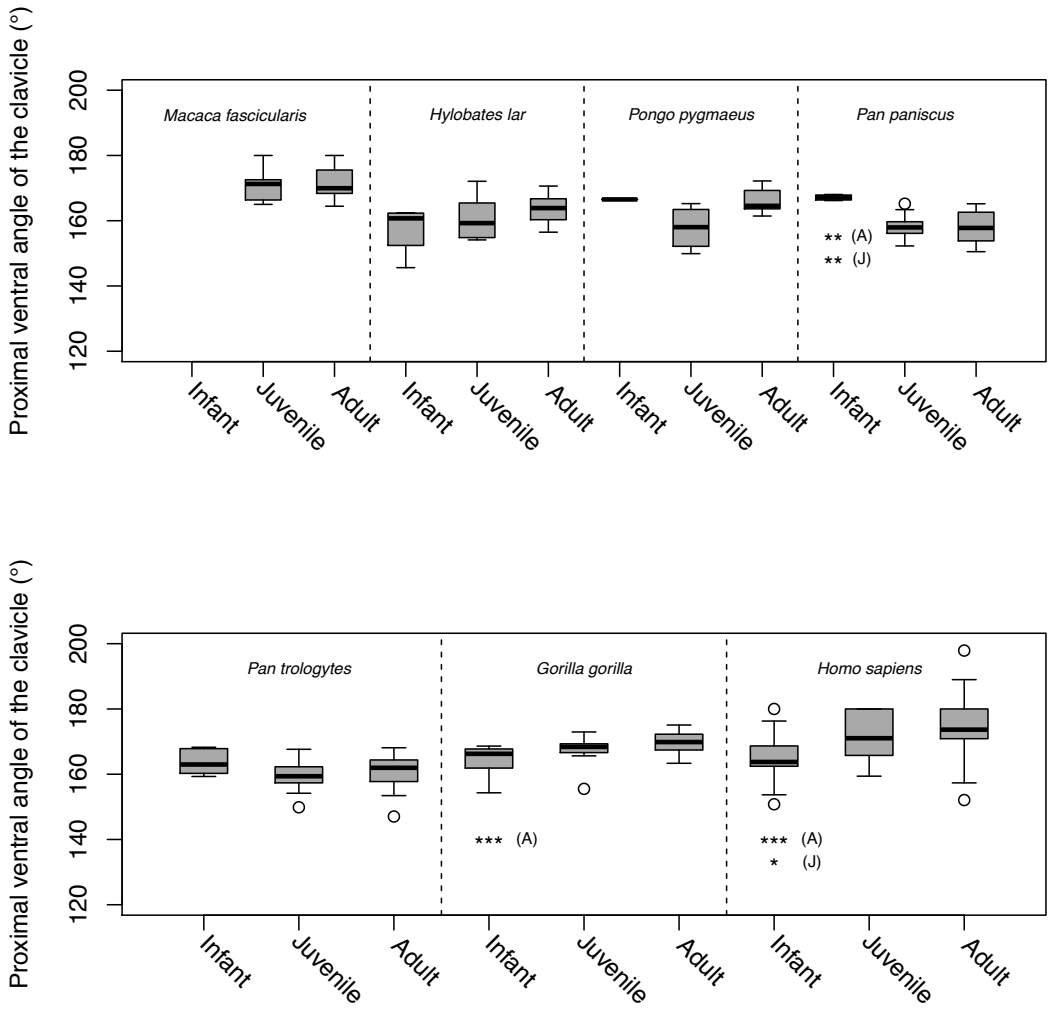

Figure 57 – Boxplot of proximal ventral 2D clavicle angles (in degrees) in hominoids and *Macaca fascicularis* by age categories. Significant differences between age categories are marked with asterisks ($p<0.001$ ***; $p<0.01$ **; $p<0.05$ *). ANOVAs show there are no significant differences between age categories for *H. lar* ($p = 0.169$, $df = 2$, F value = 1.9371), *P. pygmaeus* ($p = 0.072$, $df = 2$, F value = 3.5451), *P. troglodytes* ($p = 0.295$, $df = 2$, F value = 1.2597); there are significant differences between age categories for *P. paniscus* ($p = 0.003$, $df = 2$, F value = 7.7496), *G. gorilla* ($p = 0.006$, $df = 2$, F value = 5.6803), *H. sapiens* ($p = 0.000$, $df = 2$, F value = 12.122). A t-test shows no significant differences between age categories in *M. fascicularis* ($p = 0.678$).

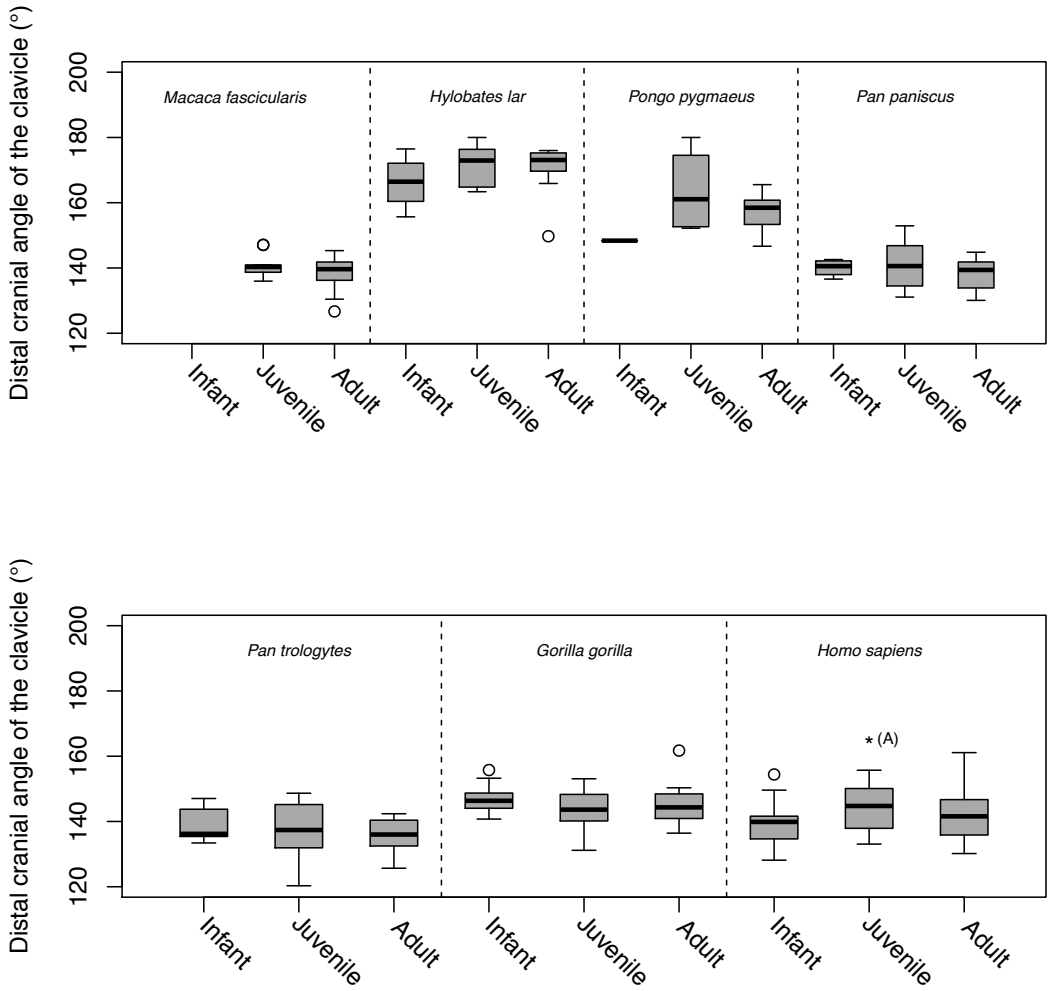

Figure 58 – Boxplot of distal cranial 2D clavicle angles (in degrees) in hominoids and *Macaca fascicularis* by age categories. Significant differences between age categories are marked with asterisks ($p<0.001$ ***; $p<0.01$ **; $p<0.05$ *). ANOVAs show there are no significant differences between age categories for *H. lar* ($p = 0.474$, df = 2, F value = 0.770), *P. pygmaeus* ($p = 0.337$, df = 2, F value = 1.2319), *P. paniscus* ($p = 0.636$, df = 2, F value = 0.4617), *P. troglodytes* ($p = 0.656$, df = 2, F value = 0.4254), *G. gorilla* ($p = 0.347$, df = 2, F value = 1.0861); there are significant differences between age categories for *H. sapiens* ($p = 0.030$, df = 2, F value = 3.6597). A t-test shows no significant differences between age categories in *M. fascicularis* ($p = 0.260$).

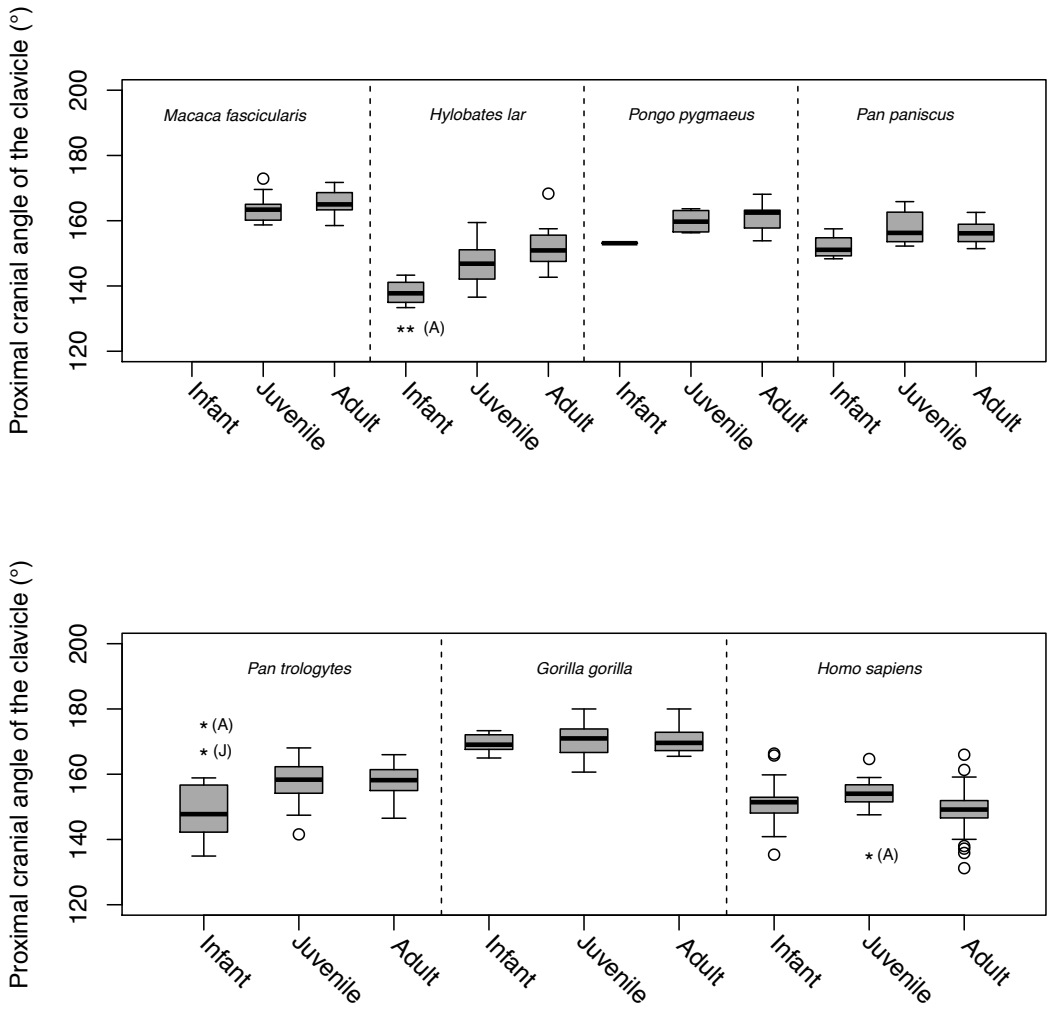

Figure 59 – Boxplot of proximal cranial 2D clavicle angles (in degrees) in hominoids and *Macaca fascicularis* by age categories. Significant differences between age categories are marked with asterisks ($p<0.001$ ***; $p<0.01$ **; $p<0.05$ *). ANOVAs show there are no significant differences between age categories for *P. pygmaeus* ($p = 0.307$, $df = 2$, F value = 1.3446), *P. paniscus* ($p = 0.122$, $df = 2$, F value = 2.3408), *G. gorilla* ($p = 0.857$, $df = 2$, F value = 0.155); there are significant differences between age categories for *H. lar* ($p = 0.009$, $df = 2$, F value = 5.9746), *P. troglodytes* ($p = 0.013$, $df = 2$, F value = 4.748), *H. sapiens* ($p = 0.004$, $df = 2$, F value = 5.9501). A t-test shows no significant differences between age categories in *M. fascicularis* ($p =0.482$).

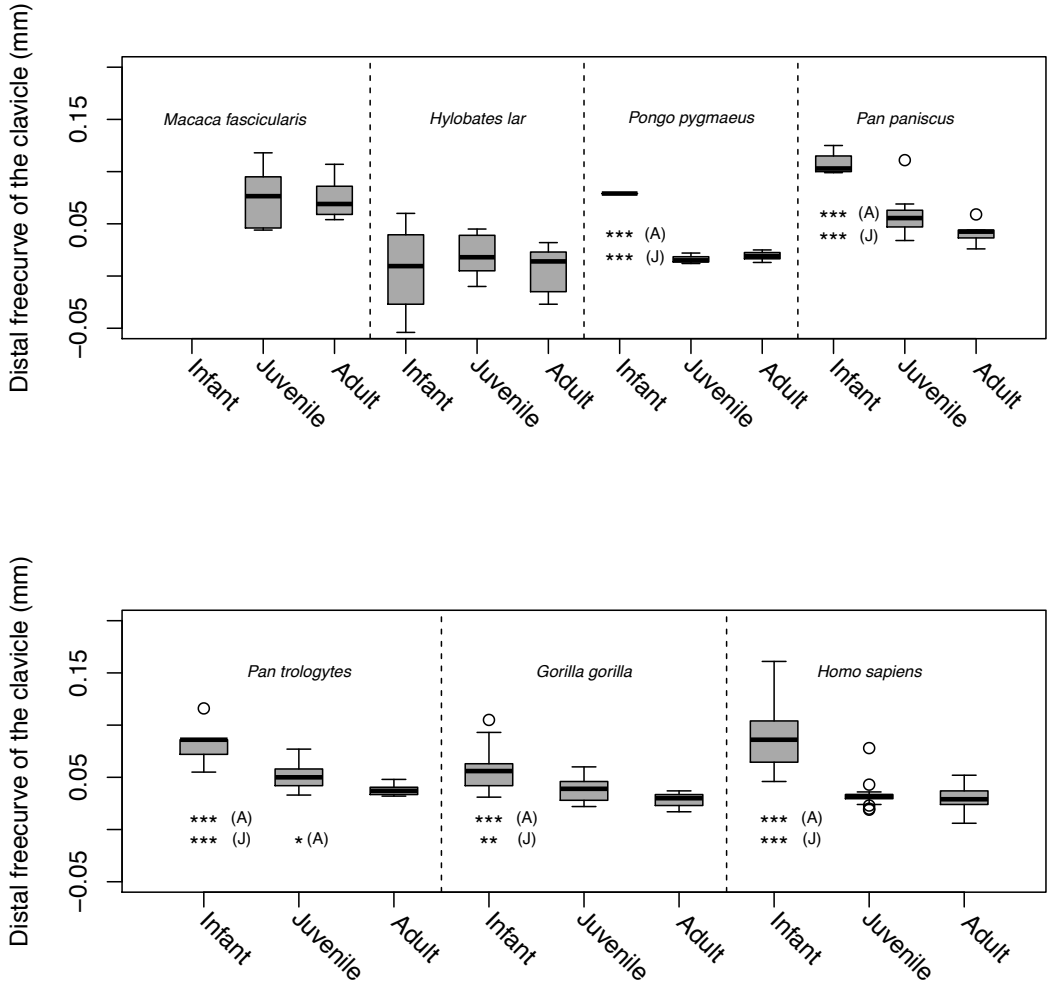

Figure 60 – Boxplot of distal 'freecurves' (in mm) in hominoids and *Macaca fascicularis* by age categories. Significant differences between age categories are marked with asterisks (p<0.001 ***; p<0.01 **; p<0.05 *). ANOVAs show there are significant differences between age categories for *H. lar* (p = 0.000, df = 2, F value = 35.408), *P. pygmaeus* (p = 0.000, df = 2, F value = 51.769), *P. paniscus* (p = 0.001, df = 2, F value = 9.2769), *P. troglodytes* (p = 0.000, df = 2, F value = 26.410), *G. gorilla* (p = 0.000, df = 2, F value = 25.637), *H. sapiens* (p = 0.000, df = 2, F value = 47.212). A t-test shows no significant differences between age categories in *M. fascicularis* (p =0.688).

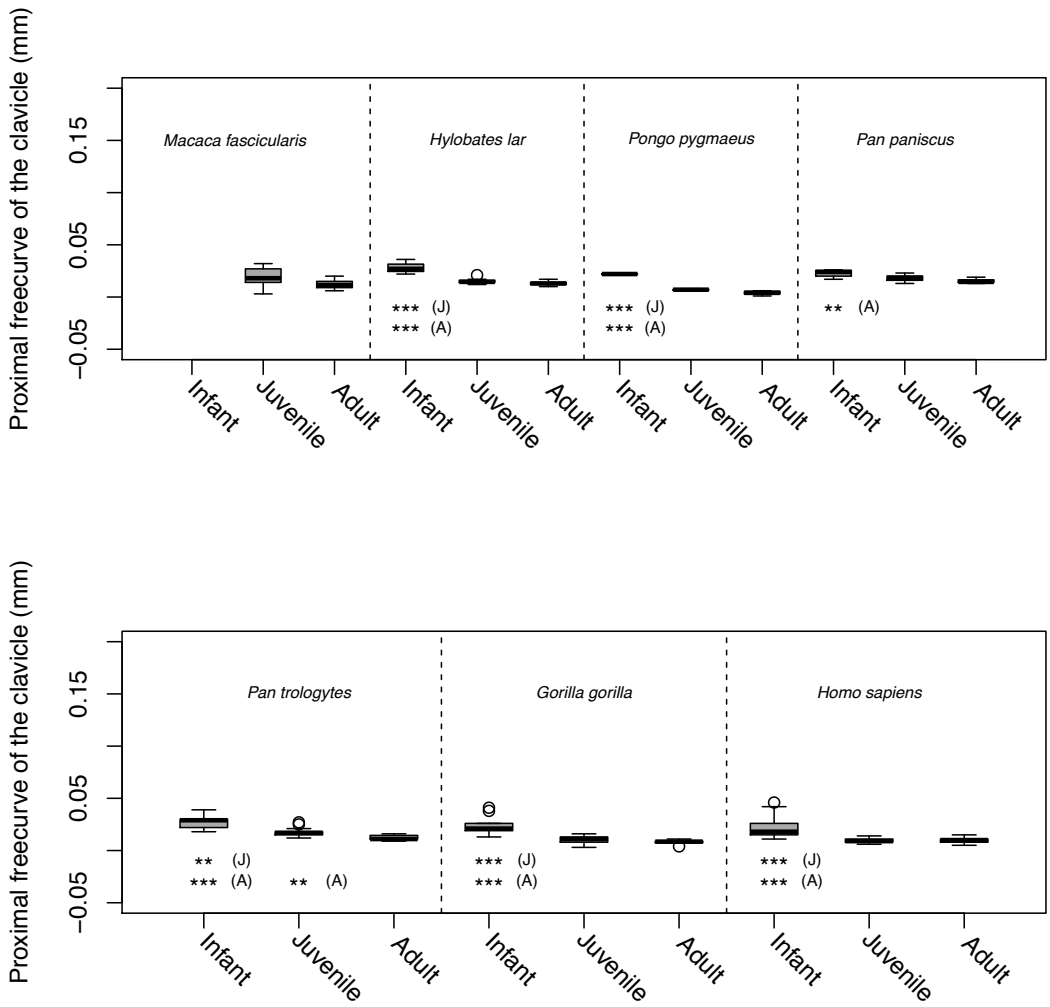

Figure 61 – Boxplot of proximal 'freecurves' (in mm) in hominoids and *Macaca fascicularis* by age categories. Significant differences between age categories are marked with asterisks (p<0.001 ***; p<0.01 **; p<0.05 *). ANOVAs show there are significant differences between age categories for *P. pygmaeus* (p = 0.000, df = 2, F value = 78.94), *P. paniscus* (p = 0.001, df = 2, F value = 22.605), *P. troglodytes* (p = 0.000, df = 2, F value = 20.346), *G. gorilla* (p = 0.000, df = 2, F value = 13.04), *H. sapiens* (p = 0.000, df = 2, F value = 99.229); there are significant differences between age categories for *H. lar* (p = 0.491, df = 2, F value = 0/7365), A t-test shows no significant differences between age categories in *M. fascicularis* (p =0.897).

Table 27 – Table of ANOVA TukeyHSD post-hoc results of differences between age categories within species, with adjusted p-values (p-adj) upper and lower bounds of the 95% confidence interval (lwr, upr), and difference between means (diff).

Measurement	Species	Age Categories		diff	lwr	upr	p-adj
clav_angle_prox_ant	*P. paniscus*	Infant (4)	Juvenile (10)	-8.693	-14.831	-2.554	**0.005**
		Infant (4)	Adult (8)	-9.103	-15.456	-2.749	**0.005**
		Juvenile (10)	Adult (8)	-0.410	-5.331	4.511	0.976
	G. gorilla	Infant (9)	Juvenile (18)	3.554	-0.221	7.330	0.068
		Infant (9)	Adult (12)	5.603	1.525	9.682	**0.005**
		Juvenile (18)	Adult (12)	2.049	-1.398	5.496	0.325
	H. sapiens	Infant (27)	Juvenile (24)	6.029	1.129	10.929	**0.012**
		Infant (27)	Adult (41)	8.971	4.620	13.322	**0.000**
		Juvenile (24)	Adult (41)	2.942	-1.465	7.349	0.255
clav_angle_prox_sup	*H. lar*	Infant (4)	Juvenile (10)	9.079	-1.152	19.310	0.088
		Infant (4)	Adult (10)	13.972	3.741	24.203	**0.007**
		Juvenile (10)	Adult (10)	4.893	-2.841	12.627	0.270
	Pan	Infant (5)	Juvenile (25)	9.445	1.712	17.178	**0.014**
		Infant (5)	Adult (12)	9.645	1.243	18.047	**0.021**
		Juvenile (25)	Adult (12)	0.200	-5.343	5.744	0.996
	H. sapiens	Infant (27)	Juvenile (24)	2.940	-1.318	7.197	0.232
		Infant (27)	Adult (41)	-2.569	-6.349	1.212	0.243
		Juvenile (24)	Adult (41)	-5.508	-9.337	-1.680	**0.003**
clav_angle_dist_ant	*H. lar*	Infant (4)	Juvenile (10)	4.103	-8.245	16.451	0.684
		Infant (4)	Adult (10)	11.647	-0.701	23.995	0.067
		Juvenile (10)	Adult (10)	7.544	-1.790	16.878	0.128
	H. sapiens	Infant (27)	Juvenile (24)	2.287	-2.822	7.396	0.537
		Infant (27)	Adult (41)	5.207	0.670	9.743	**0.020**
		Juvenile (24)	Adult (41)	2.920	-1.675	7.515	0.289
clav_angle_dist_sup	*H. sapiens*	Infant (27)	Juvenile (24)	5.341	0.633	10.049	**0.022**
		Infant (27)	Adult (41)	2.672	-1.509	6.852	0.285
		Juvenile (24)	Adult (41)	-2.669	-6.904	1.565	0.294
clav_freecurv_prox	*H. lar*	Infant (4)	Juvenile (10)	-0.013	-0.017	-0.008	**0.000**
		Infant (4)	Adult (10)	-0.015	-0.020	-0.010	**0.000**
		Juvenile (10)	Adult (10)	-0.002	-0.006	0.001	0.300
	P. pygmaeus	Infant (1)	Juvenile (3)	-0.015	-0.020	-0.010	**0.000**
		Infant (1)	Adult (8)	-0.018	-0.023	-0.013	**0.000**
		Juvenile (3)	Adult (8)	-0.003	-0.006	0.000	0.071
	P. paniscus	Infant (4)	Juvenile (10)	-0.004	-0.009	0.000	0.054
		Infant (4)	Adult (8)	-0.008	-0.012	-0.003	**0.001**
		Juvenile (10)	Adult (8)	-0.003	-0.007	0.000	0.068
	P. troglodytes	Infant (5)	Juvenile (25)	-0.010	-0.015	-0.006	**0.000**
		Infant (5)	Adult (12)	-0.015	-0.021	-0.010	**0.000**
		Juvenile (25)	Adult (12)	-0.005	-0.008	-0.002	**0.003**
	G. gorilla	Infant (9)	Juvenile (18)	-0.013	-0.018	-0.008	**0.000**
		Infant (9)	Adult (12)	-0.015	-0.021	-0.010	**0.000**
		Juvenile (18)	Adult (12)	-0.002	-0.007	0.003	0.507
	H. sapiens	Infant (27)	Juvenile (24)	-0.013	-0.016	-0.009	**0.000**
		Infant (27)	Adult (41)	-0.013	-0.016	-0.009	**0.000**
		Juvenile (24)	Adult (41)	0.000	-0.003	0.004	0.997

Table 27 cont'd – Table of ANOVA TukeyHSD post-hoc results of differences between age categories within species, with adjusted p-values (p-adj) upper and lower bounds of the 95% confidence interval (lwr, upr), and difference between means (diff).

Measurement	Species	Age	diff	lwr	upr	p-adj	Measurement
clav_freecurv_prox	*P. pygmaeus*	Infant (1)	Juvenile (3)	-0.063	-0.078	-0.047	**0.000**
		Infant (1)	Adult (8)	-0.060	-0.074	-0.046	**0.000**
		Juvenile (3)	Adult (8)	0.003	-0.006	0.012	0.639
	P. paniscus	Infant (4)	Juvenile	-0.049	-0.073	-0.024	**0.000**
		Infant (4)	Adult (8)	-0.066	-0.091	-0.041	**0.000**
		Juvenile (10)	Adult (8)	-0.018	-0.037	0.002	0.080
	P. troglodytes	Infant (5)	Juvenile	-0.032	-0.048	-0.016	**0.000**
		Infant (5)	Adult (12)	-0.045	-0.063	-0.028	**0.000**
		Juvenile (25)	Adult (12)	-0.013	-0.025	-0.002	**0.020**
	G. gorilla	Infant (9)	Juvenile	-0.022	-0.036	-0.008	**0.002**
		Infant (9)	Adult (12)	-0.032	-0.047	-0.016	**0.000**
		Juvenile (18)	Adult (12)	-0.010	-0.023	0.003	0.167
	H. sapiens	Infant (27)	Juvenile	-0.054	-0.065	-0.042	**0.000**
		Infant (27)	Adult (41)	-0.057	-0.067	-0.047	**0.000**
		Juvenile (24)	Adult (41)	-0.003	-0.014	0.008	0.787

In ventral view, the proximal angle (2D) is significantly correlated with the angulation of the spine relative to the lateral border of the scapula and the angulation of the glenoid fossa relative to the scapular spine ($p<0.05$) (table 28; figure 62), while the distal angle (2D) is significantly correlated with 5 of the 12 shoulder measurements plus shoulder size (geometric mean): clavicle thickness (antero-posterior and cranio-caudal), the angulation of the glenoid fossa relative to the scapular spine, and glenoid fossa version ($p<0.05$) (table 28; figure 65).

With regards to the 'freecurves', the proximal 'freecurve' is significantly correlated with clavicle length and clavicle thickness (cranio-caudal) ($p<0.05$) (table 28; figure 66), while the distal 'freecurve' is significantly correlated with the distal angle (2D) in cranial view, and the angulation of the glenoid fossa relative to the scapular spine ($p<0.05$) (table 28; figure 67).

A multiple linear regression analysis does show however that substantial collinearity exists between each angle (2D) and curvature (3D) measurements, as well as between angle (2D) and curvature (3D) measurements and other shoulder variables – with non-significant p-values for each regression ($p>0.05$) when more than one variable is added to the multivariate model.

Table 28 – Table of R square values and lambda values (parentheses) from the PGLS regressions of clavicle angles/curvatures against each other and 12 shoulder variables (of the clavicle, scapula and humerus). Significant PGLS results marked with asterisks (p<0.001 ***; p<0.01 **; p<0.05 *).

		2D angles				3D curvature	
		Cranial		Ventral		'Freecurves'	
Element	Measurement	Proximal	Distal	Proximal	Distal	Proximal	Distal
Clavicle	clav_length	0.427 (0)	0.083 (1)	0.092 (0)	0.645 (1)	**0.698 * (1)**	0.014 (1)
	clav_thick_ap	0.650 (0)	0.204 (1)	0.018 (0)	**0.751 * (1)**	0.456 (1)	0.024 (1)
	clav_thick_cc	0.511 (0)	0.079 (1)	0.067 (0)	**0.754 * (1)**	**0.740 * (1)**	0.022 (1)
	clav_torsion	0.010 (0)	0.000 (1)	0.133 (0)	0.097 (1)	0.322 (1)	0.140 (1)
	clav_angle_dist_ant	0.323 (0)	0.479 (1)	0.005 (0)	-	0.271 (1)	0.346 (1)
	clav_angle_dist_sup	0.038 (0)	-	0.056 (0)	0.479 (1)	0.051 (1)	**0.906 ****
	clav_angle_prox_ant	0.087 (0)	0.053 (1)	-	0.005 (1)	0.133 (1)	0.004 (1)
	clav_angle_prox_sup	-	0.012 (1)	0.087 (0)	0.318 (1)	0.302 (1)	0.014 (1)
	clav_freecurv_dist	0.022 (0)	**0.906 ****	0.001 (0)	0.661 (0)	0.054 (1)	-
	clav_freecurv_prox	0.251 (0)	0.051 (1)	0.170 (0)	0.271 (1)	-	0.054 (1)
Humerus	hum_torsion	0.202 (0)	**0.830 * (0)**	0.020 (0)	0.591 (1)	0.001 (1)	0.884 (0)
Scapula	glen_angle_latborder	0.002 (0)	0.047 (1)	0.575 (1)	0.038 (1)	0.001 (1)	0.335 (1)
	glen_angle_medborder	0.046 (0)	0.003 (1)	0.576 (0)	0.000 (1)	0.004 (1)	0.127 (1)
	glen_angle_spine	0.162 (0)	**0.836 * (1)**	0.032 (0)	**0.804 * (1)**	0.016 (1)	**0.842 ****
	glen_version	0.420 (0)	0.258 (1)	0.073 (0)	**0.906 ****	0.140 (1)	0.420 (1)
	latborder_spine_angle	0.058 (0)	0.024 (1)	**0.689 * (1)**	0.135 (1)	0.0845 (1)	0.302 (1)
	spine_angle_medborder	0.000 (0)	0.011 (1)	**0.731 * (0)**	0.003 (1)	0.040 (1)	0.108 (1)
Size	geo_mean	**0.849 ** (1)**	0.1578 (1)	0.016 (0)	**0.668 * (1)**	0.365 (1)	0.014 (1)

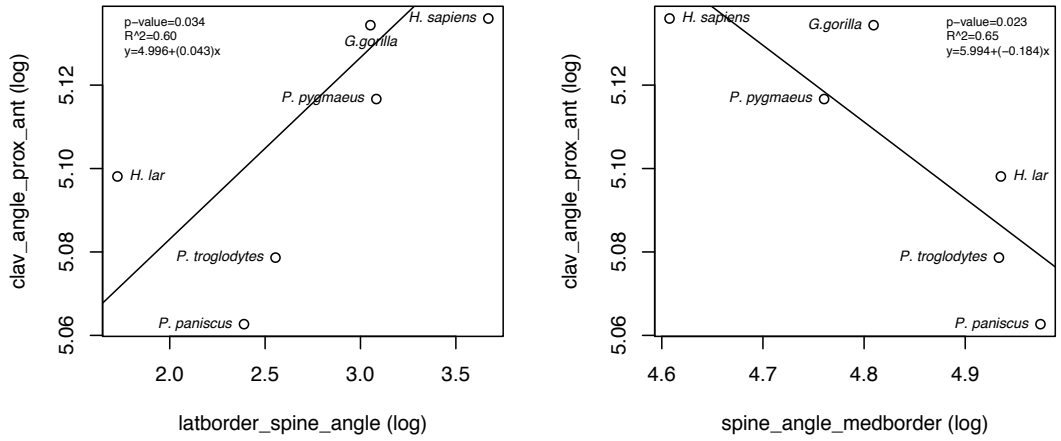

Figure 62 – PGLS regression of the proximal ventral angle of the curvature against significantly correlated shoulder variables (see table 28).

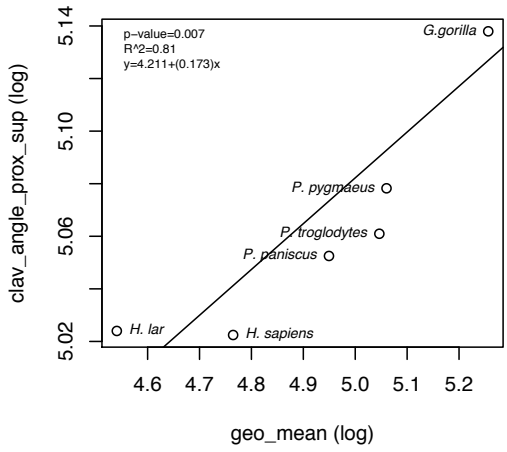

Figure 63 – PGLS regression of the proximal cranial angle of the curvature against significantly correlated variables (see table 28).

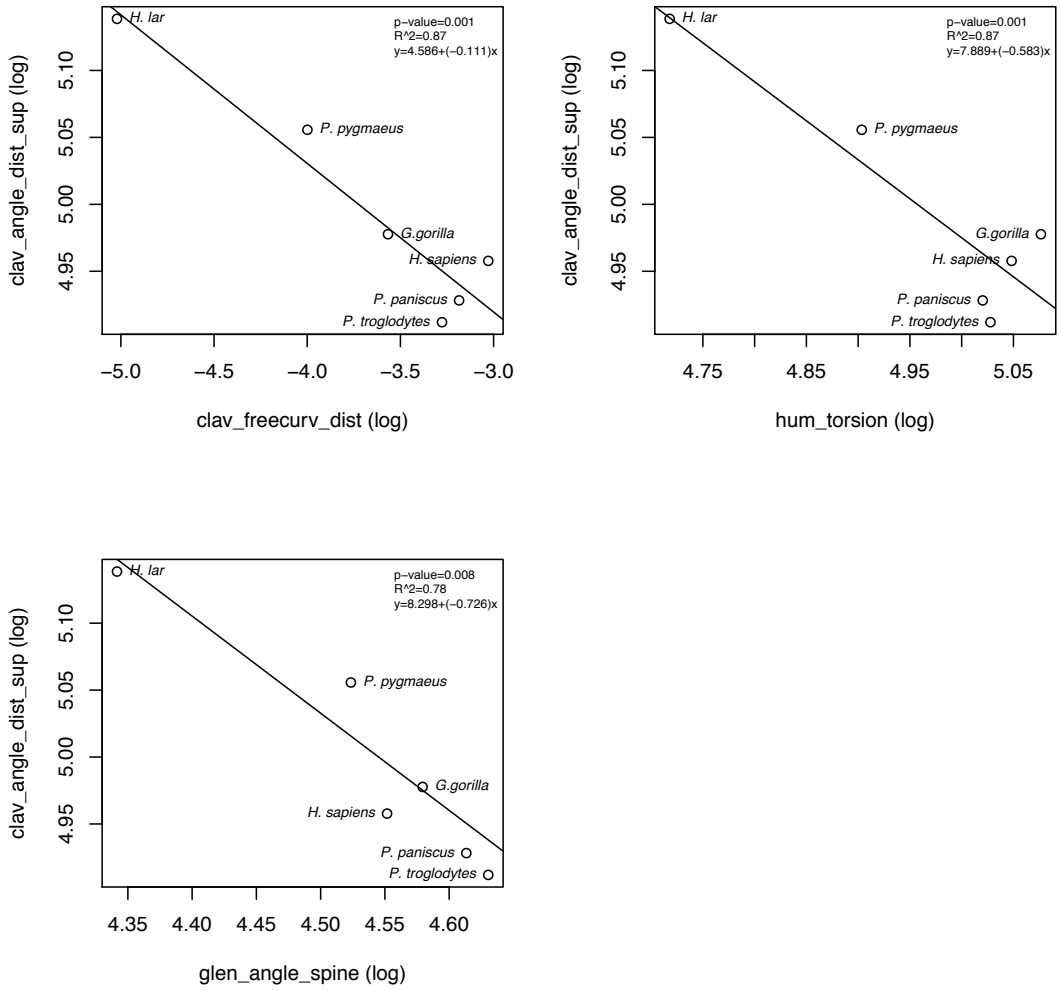

Figure 64 – PGLS regression of the distal cranial angle of the curvature against significantly correlated variables (see table 28).

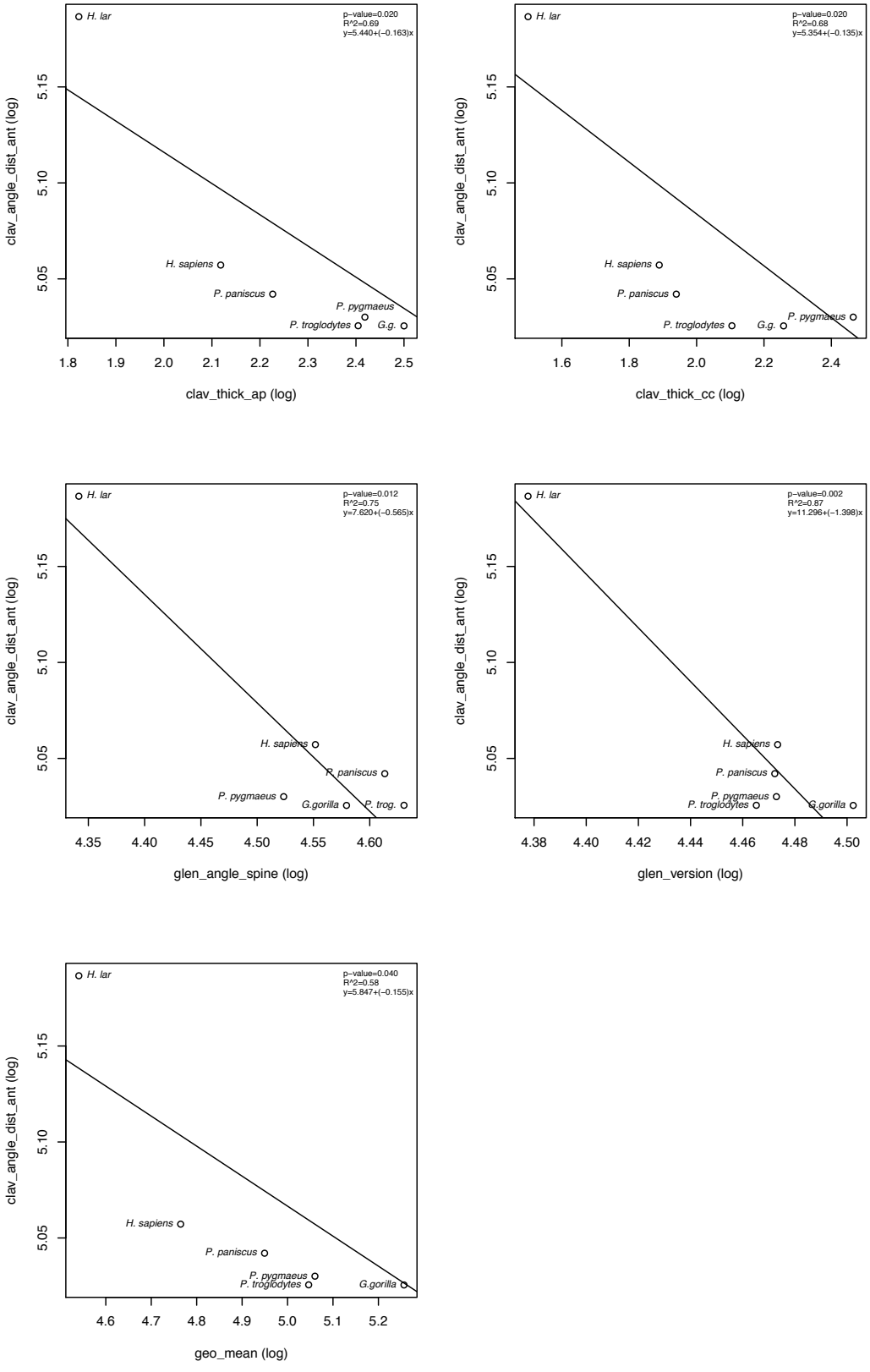

Figure 65 – PGLS regression of the distal ventral angle of the curvature against significantly correlated variables (see table 28).

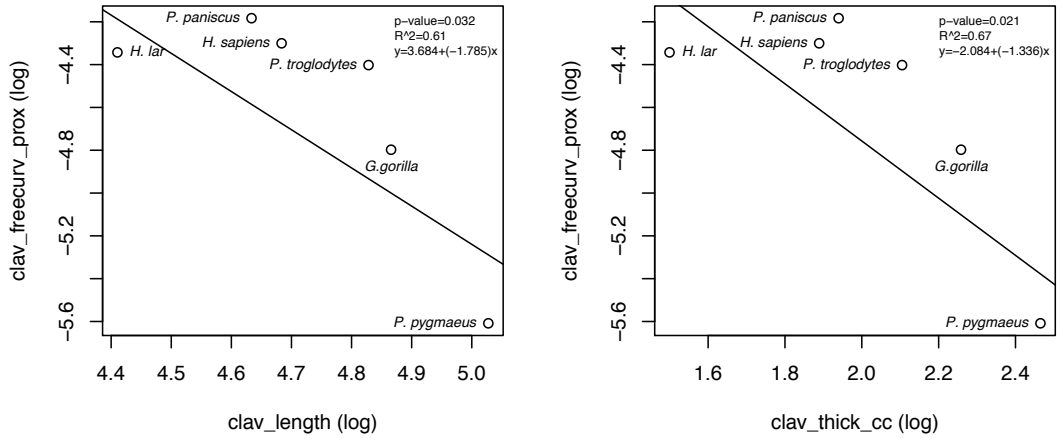

Figure 66 – PGLS regression of the proximal freecurve against significantly correlated variables (see table 28).

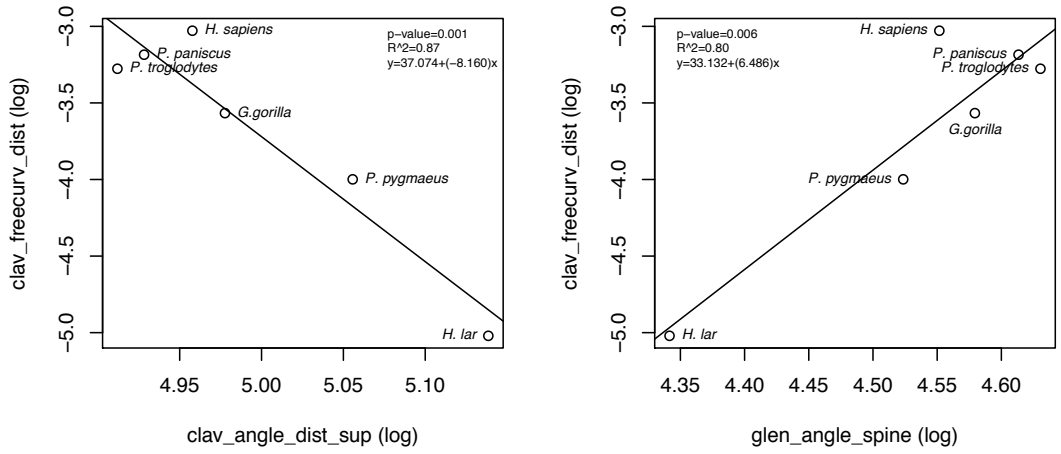

Figure 67 – PGLS regression of the distal freecurve against significantly correlated variables (see table 28).

3.3 Between-species differences in hominoids

Pairwise t-tests indicate that in both the 2D planes and in 3D, the distal and proximal curvatures do not significantly correlate with each other ($p>0.05$), suggesting relative independence between the proximal and distal morphologies of the clavicle across species (table 29). These results also show that the distal end of the clavicle (both in cranial and ventral planes, as well as in the 3D plane) is significantly more curved

than the proximal end ($p<0.05$), which is generally flatter across all species, with the exception of gibbons, which do not show significant differences between proximal and distal curvatures when using the 'freecurve' methodology ($p=0.33$) (table 29).

Table 29 – Pairwise t-tests of within species differences in proximal/distal angles (2D) and curvatures (3D).

Measurement	Species	P-value	*t*	df
Cranial view (2D)	*Homo sapiens*	0.000	6.190	40
	Pan troglodytes	0.000	13.487	14
	Pan paniscus	0.000	8.550	10
	Gorilla gorilla	0.000	14.254	14
	Pongo pygmaeus	0.018	2.833	10
	Hylobates lar	0.003	-4.124	9
	Macaca fascicularis	0.000	14.174	8
Ventral view (2D)	*Homo sapiens*	0.000	15.906	40
	Pan troglodytes	0.000	5.209	14
	Pan paniscus	0.026	2.609	10
	Gorilla gorilla	0.000	8.616	14
	Pongo pygmaeus	0.000	6.830	10
	Hylobates lar	0.000	-8.054	9
	Macaca fascicularis	0.000	11.121	8
Freecurves (3D)	*Homo sapiens*	0.000	-11.792	40
	Pan troglodytes	0.000	-13.547	14
	Pan paniscus	0.000	-11.460	10
	Gorilla gorilla	0.000	-6.175	14
	Pongo pygmaeus	0.000	-11.249	10
	Hylobates lar	0.332	1.026	9
	Macaca fascicularis	0.000	-11.657	8

Moreover, ANOVAs testing for across-species differences also show that in all cases, for all curvatures/angles, there are significant differences between species (proximal ventral 2D angle: $p=0.000$, $df=6$, $F=15.932$; proximal cranial 2D angle: $p=0.000$, $df=6$, $F=41.175$; distal ventral 2D angle: $p=0.000$, $df=6$, $F=27.742$; distal cranial 2D angle: $p=0.000$, $df=6$, $F=33.902$; proximal freecurve: $p=0.000$, $df=6$, $F=21.080$; distal freecurve: $p=0.000$, $df=6$, $F=35.192$; see table 30 for post-hoc tests). Interestingly, boxplots of adult curvatures (3D)/angles (2D) across species show that the proximal 'freecurves' are generally more constrained than the distal 'freecurves', which appear to be more variable across species (figure 68). However this pattern is not observed

when looking at the 2D curvatures, which show similar ranges of variation across species.

Additionally, the distal angles of the clavicle in 2D appear to be flatter in the more suspensory gibbons and orangutans, and more acute in the more terrestrial hominoids and in the macaques (figure 68). This pattern is less evident when considering the distal 'freecurves', which instead appear to separate the macaques, with more curved distal clavicles, from the hominoids, which exhibit comparatively flatter distal clavicles. The same is not observed in the proximal curvature of the clavicle across measurements (both 2D and 3D), with no discernible between-species pattern in clavicle curvature.

4. Discussion

4.1. 'Freecurves' versus traditional 2D angles: methodological considerations

Overall, the 'freecurve' methodology seems to yield a clearer ontogenetic signal with clearer distinctions between proximal and distal curvatures and between age groups, and a substantially more conservative phylogenetic relationship with other shoulder variables across species – with only two variables being phylogenetically significant (figures 52-54 table 26). Because the 'freecurve' protocol combines information on clavicular curvatures from both planes, it provides a more holistic approach to the analysis of the clavicle's curves, and therefore the results obtained using this methodology are likely more biologically relevant and better suited to tracking ontogeny. Conversely, the comparatively reduced number of correlations of the 'freecurve' curvatures with other variables suggests that the 2D curves may be better at tracking function.

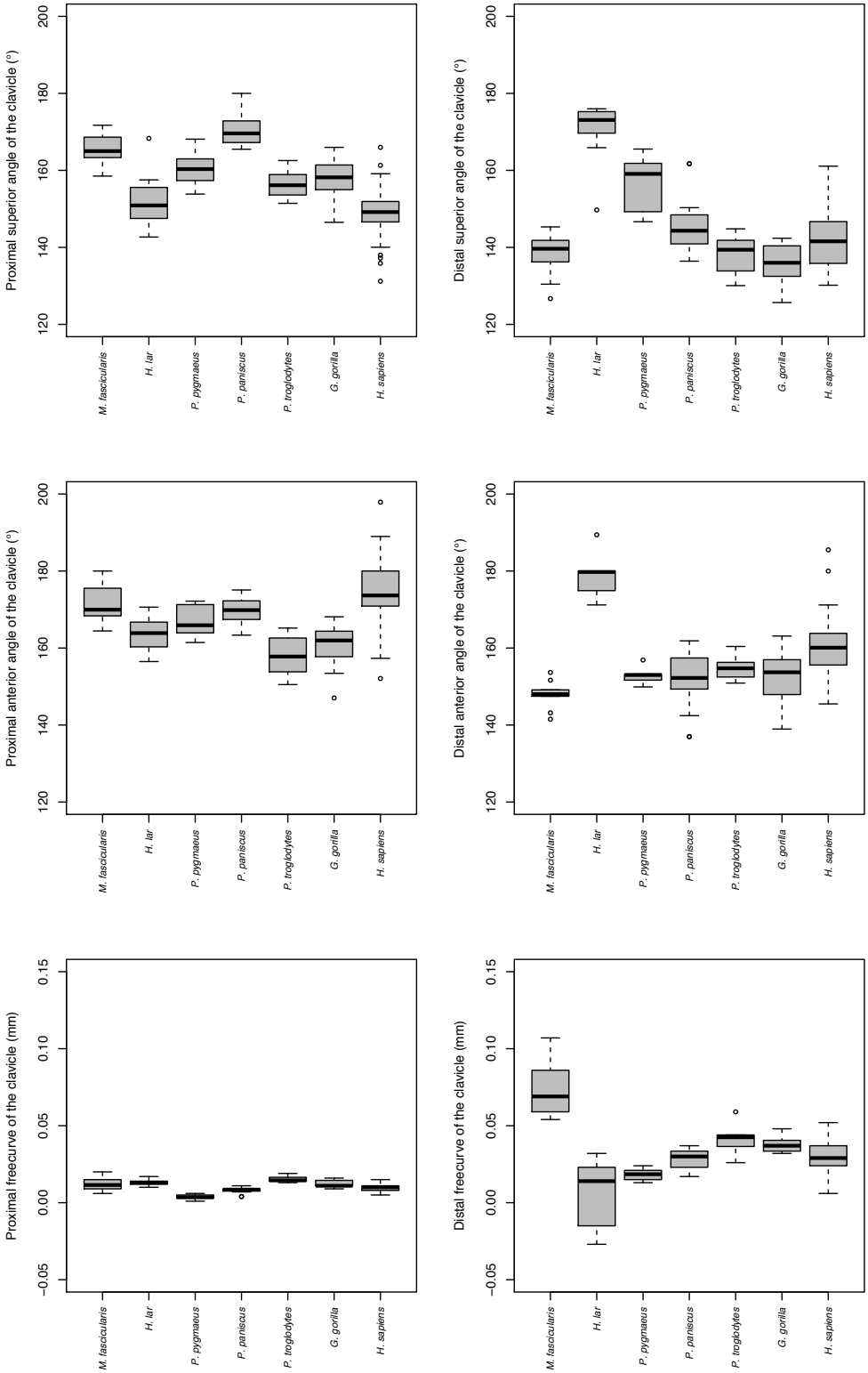

Figure 68 – Boxplot of clavicle angles (2D)/curvatures (3D) in adult hominoids and *Macaca fascicularis*. Boxes represent the upper and lower quartile ranges, the black lines, the means, and the whiskers, the highest and lowest values within 1.5 times the interquartile range of the upper and lower quartiles; the circles represent outliers within 3 times the interquartile range of the upper and lower quartiles.

Table 30 – Table of ANOVA TukeyHSD post-hoc results of between species differences in angles (2D) and curvatures (3D), with adjusted p-values (p-adj) upper and lower bounds of the 95% confidence interval (lwr, upr), and difference between means (diff).

Measurement	*Species*	diff	lwr	upr	p-adj
clav angle prox ant	*H. sapiens (41) - G. gorilla (15)*	4.717	0.075	9.358	**0.044**
	H. lar (10) - G. gorilla (15)	-6.047	-12.844	0.751	0.115
	M. fascicularis (9)- G. gorilla (15)	2.027	-4.771	8.824	0.972
	P. paniscus (11) - G. gorilla (15)	-11.743	-19.115	-4.370	**0.000**
	P. troglogytes (15) - G. gorilla (15)	-9.202	-15.587	-2.817	**0.001**
	P. pygmaeus (14) - G. gorilla (15)	-2.979	-11.222	5.264	0.931
	H. lar (10) - H. sapiens (41)	-10.763	-17.133	-4.394	**0.000**
	M. fascicularis (9) - H. sapiens (41)	-2.690	-9.060	3.679	0.864
	P. paniscus (11) - H. sapiens (41)	-16.459	-23.440	-9.479	**0.000**
	P. troglogytes (15) - H. sapiens (41)	-13.919	-19.846	-7.991	**0.000**
	P. pygmaeus - H. sapiens (41)	-7.696	-15.590	0.198	0.061
	M. fascicularis (9) - H. lar (10)	8.073	-0.003	16.149	0.050
	P. paniscus (11) - H. lar (10)	-5.696	-14.262	2.870	0.421
	P. troglogytes (15) - H. lar (10)	-3.155	-10.888	4.577	0.882
	P. pygmaeus - H. lar (10)	3.067	-6.259	12.393	0.955
	P. paniscus (11) - M. fascicularis (9)	-13.769	-22.335	-5.203	**0.000**
	P. troglogytes (15) - M. fascicularis (9)	-11.228	-18.961	-3.496	**0.001**
	P. pygmaeus - M. fascicularis (9)	-5.006	-14.332	4.320	0.674
	P. troglogytes (15) - P. paniscus (11)	2.541	-5.702	10.784	0.967
	P. pygmaeus - P. paniscus (11)	8.763	-0.990	18.517	0.108
	P. pygmaeus - P. troglogytes (15)	6.223	-2.807	15.252	0.377
clav angle prox sup	*H. sapiens (41) - G. gorilla (15)*	-21.713	-26.157	-17.269	**0.000**
	H. lar (10) - G. gorilla (15)	-18.351	-24.859	-11.844	**0.000**
	M. fascicularis (9)- G. gorilla (15)	-4.964	-11.472	1.543	0.257
	P. paniscus (11) - G. gorilla (15)	-13.953	-21.012	-6.895	**0.000**
	P. troglogytes (15) - G. gorilla (15)	-12.625	-18.738	-6.512	**0.000**
	P. pygmaeus (14) - G. gorilla (15)	-9.875	-17.767	-1.983	**0.005**
	H. lar (10) - H. sapiens (41)	3.362	-2.736	9.459	0.645
	M. fascicularis (9) - H. sapiens (41)	16.749	10.651	22.846	**0.000**
	P. paniscus (11) - H. sapiens (41)	7.760	1.077	14.442	**0.012**
	P. troglogytes (15) - H. sapiens (41)	9.088	3.413	14.763	**0.000**
	P. pygmaeus - H. sapiens (41)	11.838	4.281	19.395	**0.000**
	M. fascicularis (9) - H. lar (10)	13.387	5.655	21.119	**0.000**
	P. paniscus (11) - H. lar (10)	4.398	-3.803	12.599	0.675
	P. troglogytes (15) - H. lar (10)	5.726	-1.677	13.129	0.242
	P. pygmaeus - H. lar (10)	8.476	-0.452	17.405	0.074
	P. paniscus (11) - M. fascicularis (9)	-8.989	-17.190	-0.788	**0.022**
	P. troglogytes (15) - M. fascicularis (9)	-7.661	-15.064	-0.258	**0.038**
	P. pygmaeus - M. fascicularis (9)	-4.911	-13.839	4.018	0.648

Table 30 cont'd – Table of ANOVA TukeyHSD post-hoc results of between species differences in angles (2D) and curvatures (3D), with adjusted p-values (p-adj) upper and lower bounds of the 95% confidence interval (lwr, upr), and difference between means (diff).

Measurement	*Species*	diff	lwr	upr	p-adj
	P. troglogytes (15) - P. paniscus (11)	1.328	-6.563	9.220	0.999
	P. pygmaeus - P. paniscus (11)	4.078	-5.259	13.416	0.844
	P. pygmaeus - P. troglogytes (15)	2.750	-5.895	11.395	0.962
clav angle dist ant	*H. sapiens (41) - G. gorilla (15)*	8.352	3.325	13.380	**0.000**
	H. lar (10) - G. gorilla (15)	26.609	19.246	33.971	**0.000**
	M. fascicularis (9)- G. gorilla (15)	-4.314	-11.677	3.048	0.576
	P. paniscus (11) - G. gorilla (15)	2.540	-5.445	10.526	0.962
	P. troglogytes (15) - G. gorilla (15)	0.012	-6.904	6.928	1.000
	P. pygmaeus (14) - G. gorilla (15)	0.698	-8.230	9.627	1.000
	H. lar (10) - H. sapiens (41)	18.257	11.358	25.156	**0.000**
	M. fascicularis (9) - H. sapiens (41)	-12.666	-19.565	-5.767	**0.000**
	P. paniscus (11) - H. sapiens (41)	-5.812	-13.372	1.749	0.249
	P. troglogytes (15) - H. sapiens (41)	-8.340	-14.761	-1.920	**0.003**
	P. pygmaeus - H. sapiens (41)	-7.654	-16.204	0.896	0.111
	M. fascicularis (9) - H. lar (10)	-30.923	-39.671	-22.175	**0.000**
	P. paniscus (11) - H. lar (10)	-24.068	-33.347	-14.790	**0.000**
	P. troglogytes (15) - H. lar (10)	-26.597	-34.973	-18.221	**0.000**
	P. pygmaeus - H. lar (10)	-25.910	-36.012	-15.809	**0.000**
	P. paniscus (11) - M. fascicularis (9)	6.855	-2.424	16.133	0.293
	P. troglogytes (15) - M. fascicularis (9)	4.326	-4.050	12.702	0.712
	P. pygmaeus - M. fascicularis (9)	5.013	-5.089	15.114	0.749
	P. troglogytes (15) - P. paniscus (11)	-2.529	-11.457	6.400	0.979
	P. pygmaeus - P. paniscus (11)	-1.842	-12.406	8.722	0.998
	P. pygmaeus - P. troglogytes (15)	0.687	-9.094	10.467	1.000
clav angle dist sup	*H. sapiens (41) - G. gorilla (15)*	-3.228	-8.517	2.061	0.528
	H. lar (10) - G. gorilla (15)	25.335	17.589	33.080	**0.000**
	M. fascicularis (9)- G. gorilla (15)	-6.722	-14.468	1.023	0.134
	P. paniscus (11) - G. gorilla (15)	-6.997	-15.398	1.404	0.169
	P. troglogytes (15) - G. gorilla (15)	-9.229	-16.505	-1.954	**0.004**
	P. pygmaeus (14) - G. gorilla (15)	11.778	2.385	21.170	**0.005**
	H. lar (10) - H. sapiens (41)	28.563	21.305	35.820	**0.000**
	M. fascicularis (9) - H. sapiens (41)	-3.494	-10.752	3.763	0.775
	P. paniscus (11) - H. sapiens (41)	-3.769	-11.723	4.185	0.787
	P. troglogytes (15) - H. sapiens (41)	-6.001	-12.755	0.753	0.116
	P. pygmaeus - H. sapiens (41)	15.005	6.010	24.000	**0.000**
	M. fascicularis (9) - H. lar (10)	-32.057	-41.260	-22.854	**0.000**
	P. paniscus (11) - H. lar (10)	-32.332	-42.093	-22.570	**0.000**
	P. troglogytes (15) - H. lar (10)	-34.564	-43.375	-25.753	**0.000**
	P. pygmaeus - H. lar (10)	-13.557	-24.184	-2.931	**0.004**

Table 30 cont'd – Table of ANOVA TukeyHSD post-hoc results of between species differences in angles (2D) and curvatures (3D), with adjusted p-values (p-adj) upper and lower bounds of the 95% confidence interval (lwr, upr), and difference between means (diff).

Measurement	*Species*	diff	lwr	upr	p-adj
	P. paniscus (11) - M. fascicularis (9)	-0.275	-10.036	9.487	1.000
	P. troglogytes (15) - M. fascicularis (9)	-2.507	-11.318	6.304	0.978
	P. pygmaeus - M. fascicularis (9)	18.500	7.873	29.126	**0.000**
	P. troglogytes (15) - P. paniscus (11)	-2.233	-11.625	7.160	0.991
	P. pygmaeus - P. paniscus (11)	18.774	7.661	29.888	**0.000**
	P. pygmaeus - P. troglogytes (15)	21.007	10.717	31.296	**0.000**
clav freecurv prox	*H. sapiens (41) - G. gorilla (15)*	0.001	-0.001	0.003	0.434
	H. lar (10) - G. gorilla (15)	0.005	0.002	0.008	**0.000**
	M. fascicularis (9)- G. gorilla (15)	0.004	0.001	0.007	**0.000**
	P. paniscus (11) - G. gorilla (15)	0.007	0.004	0.010	**0.000**
	P. troglogytes (15) - G. gorilla (15)	0.004	0.001	0.007	**0.000**
	P. pygmaeus (14) - G. gorilla (15)	-0.005	-0.008	-0.001	**0.001**
	H. lar (10) - H. sapiens (41)	0.004	0.001	0.006	**0.002**
	M. fascicularis (9) - H. sapiens (41)	0.003	0.000	0.005	**0.017**
	P. paniscus (11) - H. sapiens (41)	0.006	0.003	0.009	**0.000**
	P. troglogytes (15) - H. sapiens (41)	0.003	0.000	0.005	**0.014**
	P. pygmaeus - H. sapiens (41)	-0.006	-0.009	-0.003	**0.000**
	M. fascicularis (9) - H. lar (10)	-0.001	-0.004	0.003	0.998
	P. paniscus (11) - H. lar (10)	0.002	-0.001	0.006	0.453
	P. troglogytes (15) - H. lar (10)	-0.001	-0.004	0.002	0.991
	P. pygmaeus - H. lar (10)	-0.009	-0.013	-0.006	**0.000**
	P. paniscus (11) - M. fascicularis (9)	0.003	-0.001	0.006	0.182
	P. troglogytes (15) - M. fascicularis (9)	0.000	-0.003	0.003	1.000
	P. pygmaeus - M. fascicularis (9)	-0.009	-0.013	-0.005	**0.000**
	P. troglogytes (15) - P. paniscus (11)	-0.003	-0.006	0.000	0.109
	P. pygmaeus - P. paniscus (11)	-0.012	-0.016	-0.008	**0.000**
	P. pygmaeus - P. troglogytes (15)	-0.009	-0.012	-0.005	**0.000**
clav freecurv dist	*H. sapiens (41) - G. gorilla (15)*	0.001	-0.007	0.010	0.999
	H. lar (10) - G. gorilla (15)	-0.022	-0.034	-0.009	**0.000**
	M. fascicularis (9)- G. gorilla (15)	0.045	0.032	0.058	**0.000**
	P. paniscus (11) - G. gorilla (15)	0.013	-0.001	0.027	0.070
	P. troglogytes (15) - G. gorilla (15)	0.010	-0.002	0.021	0.206
	P. pygmaeus (14) - G. gorilla (15)	-0.010	-0.025	0.005	0.455
	H. lar (10) - H. sapiens (41)	-0.023	-0.035	-0.011	**0.000**
	M. fascicularis (9) - H. sapiens (41)	0.044	0.032	0.056	**0.000**
	P. paniscus (11) - H. sapiens (41)	0.012	-0.001	0.025	0.095
	P. troglogytes (15) - H. sapiens (41)	0.008	-0.003	0.019	0.276
	P. pygmaeus - H. sapiens (41)	-0.011	-0.026	0.004	0.261
	M. fascicularis (9) - H. lar (10)	0.067	0.052	0.082	**0.000**

Table 30 cont'd – Table of ANOVA TukeyHSD post-hoc results of between species differences in angles (2D) and curvatures (3D), with adjusted p-values (p-adj) upper and lower bounds of the 95% confidence interval (lwr, upr), and difference between means (diff).

Measurement	*Species*	diff	lwr	upr	p-adj
clav freecurv dist	*P. paniscus (11) - H. lar (10)*	0.035	0.019	0.051	**0.000**
	P. troglogytes (15) - H. lar (10)	0.031	0.017	0.046	**0.000**
	P. pygmaeus - H. lar (10)	0.012	-0.006	0.029	0.399
	P. paniscus (11) - M. fascicularis (9)	-0.032	-0.048	-0.016	**0.000**
	P. troglogytes (15) - M. fascicularis (9)	-0.036	-0.050	-0.021	**0.000**
	P. pygmaeus - M. fascicularis (9)	-0.055	-0.072	-0.038	**0.000**
	P. troglogytes (15) - P. paniscus (11)	-0.004	-0.019	0.012	0.992
	P. pygmaeus - P. paniscus (11)	-0.023	-0.041	-0.005	**0.004**
	P. pygmaeus - P. troglogytes (15)	-0.019	-0.036	-0.003	**0.013**

First of all, the 'freecurve' methodology is better suited than the 2D measurements for fitting the Gompertz distributions (figures 53-54). This protocol also produces a clearer distinction between the ontogenetic development of the distal and proximal curvatures, as opposed to the 2D protocol, which shows a greater amount of overlap between curvatures (figures 53-54). This is also the case when the sample is split into age categories: the 'freecurves' show the clearest pattern and the most differences between age categories within species for both proximal and distal curvatures, whereas the pattern is unclear for the 2D measurements, with only very few significant differences between age categories within species ($p>0.05$; figures 56-61). This is an important observation, since the overall lack of a clear ontogenetic pattern in the traditional 2D measurements alone would suggest that clavicle curvatures are generally not developmentally plastic, but rather genetically conserved in hominoids and macaques (which is in fact the traditionally accepted view, based on angle measurements of the human neonate clavicle [Corrigan 1960]). The observation that this is not the case when using the 'freecurve' protocol leads to the opposite conclusion: that the curvatures of the clavicle do seem to develop throughout growth, in tandem with clavicular length (figure 62). It is likely that dissecting the curvatures into 2D planes fails to capture ontogenetic changes, which isn't the case with the 'freecurve' protocol that combines information from both planes of view.

Secondly, and perhaps more relevantly, the ‘freecurve’ protocol yields more conservative results with regards to the phylogenetic regressions, with both curvatures being correlated with only two shoulder variables each (table 28). In contrast, the 2D angles correlate with more shoulder variables across all four angles allowing for a wider variety, and thus more complex, functional interpretations. This is also an important observation since the differences in these PGLS correlations will not only lead to important differences in the functional interpretations of clavicle morphology in extant hominoids, but will also significantly impact the predictive models that can be built using these phylogenetic correlations. For example, according to the ‘freecurve’ PGLS results, clavicular length and cranio-caudal thickness are good predictors of proximal curvature in hominoids, while only one variable can adequately predict the distal curvature. This is not the case with the 2D curvatures, where a number of shoulder variables, including size, are estimated to be good predictors for both curvatures in both cranial and ventral views.

Differences in the PGLS regressions between protocols may also result from differences in the nature of the measurements collected (angles versus curvatures). This may explain why we do not see differences in the range of variation between proximal and distal curvatures in the 2D angles, but we do see them with the ‘freecurve’ measurements (figure 68). When the results of the PGLS regressions for the 3D ‘freecurve’ measurements are compared to those obtained with the 2D angle measurements, we notice that the distal ‘freecurve’ correlates with the orientation of the glenoid fossa relative to the scapula spine, which is also true for the proximal and distal 2D angles in cranial view. The proximal ‘freecurve’ correlates with clavicle thickness (cranio-caudal) and length, which is also true for the proximal ventral 2D angle (table 28). However, all other PGLS correlations obtained with the 2D angles disappear with the ‘freecurve’ measurements, suggesting that this protocol is more conservative than the traditional method.

Lastly, with regards to between-species differences in adult individuals, the ‘freecurve’ distal measurements produce less extreme distinctions between hominoid

species. Indeed, in 2D there is a rather substantial distinction between the suspensory gibbons (and orangutans to a lesser extent) and the rest of the primates in the distal angle, and a more subtle distinction between *Macaca* and the hominoids – with the gibbons possessing significantly flatter distal clavicles ($p<0.05$) and *Macaca* possessing more curved distal clavicles compared to the rest of the primates albeit not significantly different in all cases (figure 68 & table 29). When using the 'freecurve' method, on the other hand, the differences between *Macaca* and hominoids are exacerbated relative to the differences between the suspensory Asian apes and the terrestrial African apes and humans, which are instead attenuated, with significant differences between *Macaca fascicularis* and the rest of the primates ($p<0.05$) (figure 68 & table 29). However, there are also significant differences in proximal and distal angles (2D)/curvatures (3D) between species within the great apes. These results suggest that there is a clade-specific pattern in hominoid distal curvature that is distinct from that of monkeys, with further between-species differences within hominoids that seem to distinguish broadly between locomotor types. Additionally, the proximal 'freecurves' indicate less range of variation in curvature across species compared to the distal 'freecurves', which is not observable when looking at the 2D measurements (figure 68). This is also a significant observation since based on the 'freecurves' we can conclude that the proximal curvature is more genetically conserved than the distal curvature, which is information that is lost when considering the 2D measurements. These differences in results between protocols likely emanate from the fact that the 'freecurve' methodology captures information on curvature from both planes combined, thus the boxplot of between-species differences in distal 'freecurves' essentially summarizes the information obtained from the two 2D distal curvatures (figure 68). As a result, this boxplot shows more pronounced differences between clades (*Macaca* and hominoids) and less pronounced differences between hominoid species (suspensory apes and quadrupedal apes).

It is important to note, however, that whether one protocol should be favoured over the other should depend on 1) how well the protocol reflects the biological significance of the clavicle's curvatures, and 2) whether it can be applied across

different (primate) species. I suggest that because the 'freecurve' protocol combines information on clavicular curvatures from both planes, rather than deconstructing the anatomy of the clavicle and forcing it to adhere to two-dimensional planes of view, it allows for a more biologically relevant and holistic framework for the analysis of clavicular curvatures. Additionally, while the flatter cranio-caudal anatomical configuration of the human clavicle permits it to be placed into two perpendicular planes fairly easily, this is not the case for the other hominoid species whose clavicles have a more 'twisted' appearance (see for example the gorilla, gibbon or macaque clavicle, figure 69). Thus, while it may not be an issue for humans, forcing the non-human hominoid clavicles to adhere to two perpendicular 2D planes may fail to reflect the three-dimensionality of these curves, which are likely functionally relevant. In fact, these results indicate that the only significant correlation between clavicle 'freecurves' and 2D angles across hominoid species occurs between the distal 'freecurve' and the distal cranial angle (2D) (table 2), suggesting that most of the curvature in the distal clavicle in hominoids occurs in cranial view. Conversely, the lack of relationship between the proximal 'freecurve' and the proximal 2D angles of the hominoid clavicle, suggests that the proximal curvature is more complex and doesn't necessarily adhere to one particular 2D plane, even though it can essentially be forced into both a cranial and a ventral plane. Moreover, because, unlike the 'freecurve' protocol, the traditional 2D planes do not reflect homologous anatomical landmarks/structures across hominoid and primate species, I therefore suggest that this approach should be favoured, at least in some cross-comparative contexts, over the traditional 2D quantification of clavicular curvatures.

On the other hand, the more traditional 2D method allows isolating specific aspects of clavicular curvature thus facilitating functional interpretations, as shown by the PGLS regressions and boxplots (tables 28). The 2D angle measurements correlate with more variables than the 'freecurve' measurements (table 28) and different planes of view highlight different between species differences in proximal and distal curvature thus allowing to pint-point which aspects of clavicle morphology best distinguish between species. Thus, there are both advantages and disadvantages to using either method,

and these should be chosen in function of the question being addressed. Overall it appears that the 'freecurve' methodology is better suited to capture ontogenetic changes, while the 2D method is better suited for analysing more detailed aspects of function.

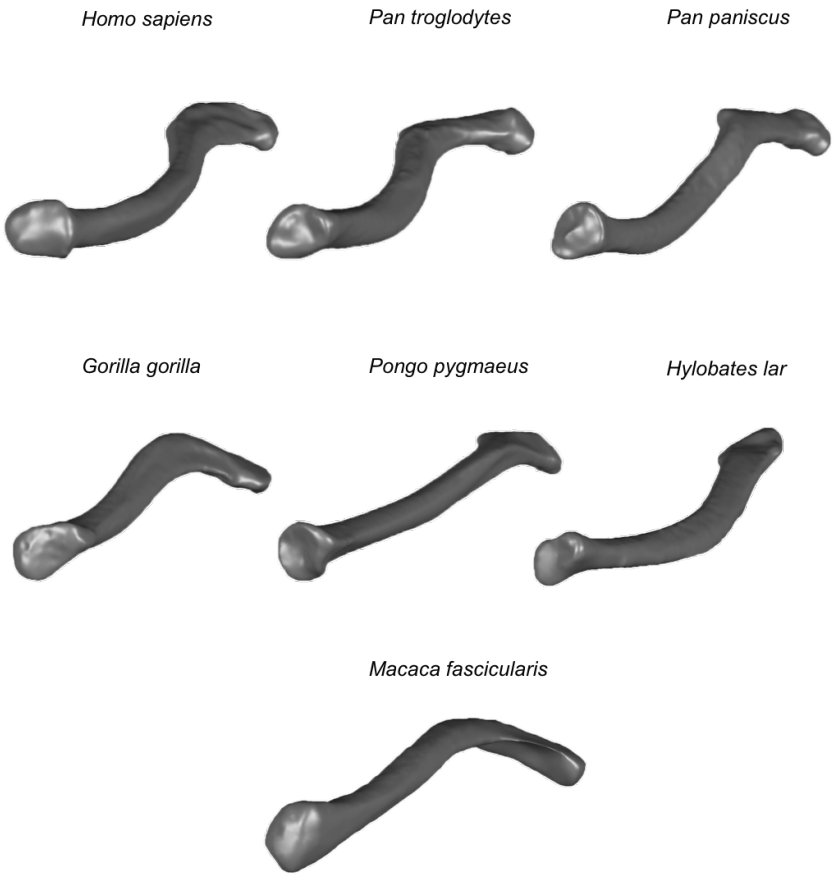

Figure 69 – Adult left clavicles in hominoids and *Macaca fascicularis* (sternal view), showing the twisted S-shape appearance of the clavicle in the various species..

4.2. Ontogeny of the clavicle's curvatures

The application of Gompertz growth curves to the 'freecurve' measurements reveals that clavicular curvatures in hominoids develop throughout ontogeny, with both proximal and distal curvatures becoming increasingly flatter with growth (figure 55). This finding contradicts the traditional view that the clavicle is 'ontogenetically stable', changing little from the neonate stage into its adult form (Corrigan 1960). These results are likely due to differences in how curvature is measured since the lack

of a clear ontogenetic pattern in the traditional 2D measurements in the present study would also suggest that clavicle curvatures are not developmentally plastic, but rather genetically conserved in hominoids and macaques (figure 52 & 53). The 'freecurve' results indicate that the curvatures of the clavicle are more curved at birth and gradually flatten out with growth, reaching adult values after M3 eruption (figure 55). These results also show that infants are significantly different from the juveniles and the adults specimens across species (figures 56-61), suggesting that overall, the clavicle in hominoids undergoes changes in curvature after infancy (7 years for humans, 3.5 years for great apes, and 1.75 for macaques and gibbons), becoming flatter during juvenility, at which point it attains near-adult values form. This suggests that the clavicle is developmentally plastic, with the majority of change occurring before the juvenile stage. These changes in clavicular curvature during ontogeny are likely to reflect differences in the infant thoracic shape; Corrigan (1959), for example, found that in humans, the neonate clavicle is positioned slightly higher and more anteriorly due to the elevated position of the shoulder and the rotundity of the thorax in neonates. Indeed, the relatively large sagittal diameter of the thorax in newborn humans results in a more ventrally directed glenoid cavity compared to that in the adult – which may be why, functionally, it is more appropriate to crawl before walking (Ljunggren 1979). On the other hand, clavicular curvatures remain proportionally stable relative to each other throughout growth (figure 55), implying that these curvatures are ontogenetically stable all the while the clavicle is still developing. This stability in clavicular curvatures is in fact quite remarkable since the clavicle is the first bone to ossify and the last bone to fuse, with the lateral epiphyses appearing and uniting around 17-19 years and the medial epiphyses fusing during the mid to late 20's in humans (Todd and D'Errico 1928; Scheuer and Black 2000; Langley-Shirley and Jantz 2010). This is consistent with the observation that the 'sagittal diameter-length index' in human clavicles is maintained throughout life (Terry 1932; Corrigan 1960), suggesting that there are elements of the clavicle that are structurally conserved throughout ontogeny.

The idea that the clavicle is ontogenetically conserved is therefore not entirely falsified here; it is likely that because of its role in both 1) protecting the thoracic inlet and the important soft-tissue structures passing through it, and in 2) stabilizing the shoulder joint during pulling and weight-bearing, it is important for the clavicle's curvatures to be partially conserved in shape and proportion relative to the thorax and the other shoulder elements. Interestingly, among the hominoids, gibbons appear to be derived in their development of clavicular curvature, having similar degrees of curvature on both the proximal and distal ends of the clavicle throughout growth, unlike the rest of the hominoids whose distal curvature is substantially more curved from birth (figure 55). This is also evident when considering the boxplots of adult distal curvature, particularly in 2D, which show that the distal angles of the clavicle are visibly flatter in the more suspensory gibbons (and to a lesser extent in orangutans), and more acute in the more terrestrial hominoids and particularly in the macaques (figure 68). This may be due to the fact that gibbons are unique among apes in having a rather flat distal clavicle, which is thought to be associated with the demands of brachiation and the need for increased rigidity of the shoulder girdle (Voisin 2006). This flat distal joint allows for the formation of a coracoclavicular joint, which is unique to this species, and which limits shoulder movement outside the vertical plane (Voisin 2006). Conversely, the more curved distal clavicles in more terrestrial primates are thought to provide increased mobility at the shoulder joint by allowing a greater range of scapular rotation (Voisin 2006).

4.3. Phylogenetic and functional significance of the clavicle's curvatures:

These results indicate that the two protocols used in this study produce significant differences in the PGLS regressions, with the 'freecurve' methodology yielding more conservative results (i.e. correlating with less variables), likely because this method incorporates information on clavicular curvature from both planes. The more traditional 2D curvature measurements, on the other hand, because they deconstruct clavicular curvature into two distinct planes, produce more complex results with both the distal and proximal 2D angles correlating with a greater variety of shoulder

variables (table 28). Interestingly, the 2D angles and the 3D 'freecurves' correlate largely with different and non-overlapping variables suggesting that the two methods impact functional interpretations of clavicular curvature (table 28).

Indeed, using the 'freecurve' protocol, the significant correlations are between the proximal curvature, clavicular length and midshaft clavicular thickness (cranio-caudal) (table 28); the distal curvature significantly correlates with the angulation of the scapular spine relative to the glenoid fossa, as well as the distal cranial 2D angle, (table 28). These results show that across hominoids, the flatter the proximal curvature is, the thicker and longer the clavicle, and conversely, the more curved the proximal curvature is, the thinner and shorter the clavicle (table 28 & figure 66). This is in line with previous observations that the length and thickness of the clavicle are genetically (and ontogenetically) conserved (Terry 1932; Corrigan 1959), and the present results seem to suggest that this may also be the case for the proximal curvature. According to these results, orangutans have the longest, thickest and flattest clavicles among hominoids, while it is shorter, thinner and more curved in gibbons, chimpanzees and humans, with gorillas being intermediate between the two (figure 66). The inverse relationship between the degree of curvature and clavicular thickness supports the observation that increased sinuosity of the clavicle increases its flexibility and mobility, but also its weakness and likelihood of breakage (Harrington Jr et al. 1993; Mays et al. 1999; Voisin 2006). Voisin (2006) suggests that a marked proximal curvature of the clavicle is advantageous for powerful and rapid arm elevation such as seen in gibbons, chimpanzees and humans because it increases the action of the pectoralis major muscle (an important arm flexor) by acting as a crankshaft which in turn allows the glenoid fossa of the scapula to rotate cranially (the greater the curvature, the more pronounced the crankshaft effect) (Stern et al. 1980; Jungers and Stern 1981; Gagey 1985; Voisin 2006). On the other hand, primates like the gorilla and other terrestrial primates who are less frequently tree-dwelling than chimpanzees, have a less pronounced proximal curvature, and in fact, a pronounced proximal curvature is not advantageous for terrestrial quadrupeds because it increases the risk of clavicle fracture (Olivier 1953; Hill 1966, 1970, 1974; Voisin 2006). The

pronounced curvature of the human clavicle, for example, increases the crankshaft effect but also increases the weakness of this bone in flexion and torsion (Harrington Jr et al. 1993; Mays et al. 1999; Voisin 2006). It is therefore not surprising that the clavicle is one of the most commonly fractured bones in humans (Andermahr et al. 2007), with 70-80% of fractures occurring on the middle third of the shaft (Harrington Jr et al. 1993; Andermahr et al. 2007; Haque et al. 2011). Chimpanzees, on the other hand, who also frequently walk on the ground, have a less pronounced proximal curvature and thus a stronger clavicle than humans (Voisin 2006). Interestingly, *Pongo* shows a pattern that is very derived relative to the rest of the hominoids (very long, thin and flat). In particular, the orangutan clavicle is long when compared to that of African apes and humans, and according to other studies this is still the case when the clavicle is scaled to trunk length (e.g., Schultz 1968). Schultz (1930) suggests that the lengthened clavicle in this species results from the unusually high position of the shoulders, which are situated high above the suprasternal notch of the neck, and the need to bridge the long gap between the sternum and acromial process of the scapula as a result of dorsally placed scapular on a particularly dorsoventrally flattened upper thoracic cage (Kagaya et al. 2008; Kagaya et al. 2010).

Because of its role in protecting the thoracic inlet as well as its role as a crankshaft for shoulder elevation, it is possible that selective pressures acting on the hominoid shoulder joint stabilize the architecture of the proximal curvature of the clavicle relative to its length and thickness in hominoids and perhaps primates in general. This idea is supported by the more constrained ranges of variation found in adult proximal curvature compared to the distal curvature (‘freecurve’), which suggest that the proximal curvature is more genetically conserved than the distal curvature in hominoids and *Macaca* (figure 68). Indeed, the present results suggest that the distal curvature (’freecurve’) is not associated to length and thickness, but rather to a more functional trait: the angle of the scapular spine relative to the glenoid fossa – with flatter curvatures being associated with more cranially oriented spines relative to the glenoid fossa (such as in *Hylobates*), and more curved clavicles associated to more laterally oriented spines (African apes and humans) (table 28; figure 67) – suggesting

that this curvature is more functionally significant (more cranially directed spines being associated to more suspensory lifestyles and more laterally oriented spines associated to more quadrupedal postures). These results are also largely in line with previous observations that the distal angle of the clavicle is more variable between primate species because it is associated with range of motion and mode of locomotion: according to Voisin (2006), the distal curvature in apes is essential in allowing a greater range of movements of the shoulder compared to other primates, and is particularly important for the pendulum movement in gibbons. Indeed, gibbons are unique among hominoids in having a virtually absent distal curvature, and therefore the presence of a coracoclavicular joint (Voisin 2006). With this joint, the scapula-clavicle complex becomes more rigid and thus more efficient for brachiation because it increases force diffusion and limits movement outside the vertical plane of the supporting hand (Voisin 2006). In quadrupedal primates and great apes on the other hand, a pronounced distal curvature is necessary because it allows a greater range of movements of the shoulder as the scapula-clavicle complex does not need to be very rigid (Voisin 2006).

These results thus seem to suggest that, on the one hand, the proximal curvature is phylogenetically conserved – perhaps because of its role in shoulder joint stability and in protecting the thoracic inlet –, while on the other hand, the distal curvature is more functionally driven – because of its association with locomotion and arm elevation. This in turn suggests the existence of a relative independence between distal and proximal clavicle curvatures in primates. This idea is further supported by the PGLS results, which indicate that the proximal and distal curvatures of the clavicle do not significantly correlate with each other (both in 2D and in 3D) and that they correlate with non-overlapping shoulder variables (table 28). This implies that different forces act on either end of the clavicle to shape its morphology – likely due to the different functions of these curvatures. The combination of these two morphologies (distal and proximal) thus influences force diffusion at the shoulder joint and by consequence, locomotion, in each primate species (Voisin 2006). The present results further show a lack of integration between clavicle curvatures and the other shoulder elements, thus

suggesting a relative independence between the evolution of clavicle morphology and the rest of the shoulder complex. This is in line with Larson's (2007) observations on the evolution of the hominin shoulder girdle, where she describes the mosaic patterns of shoulder morphologies in various hominin species. In particular, the elongation of the clavicle seems to take place relatively late in the hominin lineage (after *Homo erectus*), well after the scapula has taken its more modern configuration (being positioned low on the thorax and with laterally facing glenoid fossae).

The more traditional 2D curvature measurements, on the other hand, produce slightly more complex results, with both the distal and proximal 2D angles correlating with a greater variety of shoulder variables, particularly with relation to the glenoid fossa, the orientation of the scapular spine, and the overall size of the shoulder girdle (geometric mean) (table 28). Specifically, the results of the PGLS regressions show that in cranial view, the proximal curvature is associated with increased size of the shoulder (geometric mean), with flatter curvatures associated with larger shoulder sizes, and more curved clavicles to smaller shoulder sizes (table 28 & figure 63). On the other hand, the distal curvature is associated with the distal 'freecurve', humeral torsion, and the angle of the scapular spine relative to the glenoid fossa (figure 64). The present results show that flatter distal clavicles in this plane are associated with decreased humeral torsion, and more cranially oriented scapular spines relative to the glenoid fossa and larger shoulder size. These results suggest that in this plane, the proximal curvature mainly shows a relationship with shoulder size – with the exception of humans who share exceptional similarities with gibbons in the degree of proximal curvature despite their differences in size –, while the distal curvature mainly shows a relationship with humeral torsion and the orientation of the scapular spine. The latter is likely associated with the angle of pull of the deltoid muscle relative to the position of the glenoid fossa – more terrestrial African apes tend to have more lateral facing glenoid fossae and scapular spines, while the more suspensory gibbons, and to a lesser degree orangutans, possess more cranially facing glenoid fossae and spines (Alemseged et al. 2006). The orientation of both structures in Asian apes produces smaller glenoid-to-scapular spine angles than those of African

apes and humans. These results thus indicate that in this plane of view, a curved distal end, which has been associated to shoulder mobility, is found in African apes and humans, while a flatter distal curvature, which is thought to be associated with shoulder rigidity, is typical of gibbons and to a lesser extent, orangutans (Voisin 2006). The observation that the increased distal curvature in African apes and humans is associated with increased humeral torsion, is also in line with the presence of increased shoulder mobility in these species likely leading to greater rotational stresses on the head of the humerus. Additionally, the exceptional similarities between humans and gibbons in the degree of proximal curvature may relate to the demands for powerful and rapid arm elevation in these species: the greater the curvature, the more pronounced the crankshaft effect (Voisin 2006), as well as the absence of weight-bearing under compression postures.

In ventral view, the PGLS results show that the distal curvature is associated with clavicle thickness (cranio-caudal and antero-posterior), glenoid version, the angle of the scapular spine relative to the glenoid fossa and size of the shoulder (geometric mean) (table 28 & figure 65). The present results indicate that the more curved the distal clavicle is in this plane, the thicker it is (both cranio-caudally and antero-posteriorly), the more ventrally the glenoid fossa is rotated (version), the more cranially oriented the spine is relative to the glenoid fossa, and the smaller the overall size of the shoulder. The proximal curvature, on the other hand, is associated with the angulation of the scapular spine relative to the lateral and medial borders of the scapula – the more curved the proximal curvature, the more cranially oriented the spine is relative to the lateral border of the scapula (figures 62). This is the case in *Pan* and gibbons whose scapular spine and lateral border are largely parallel to each other and with a cranially facing glenoid fossa, which is a condition found in suspensory species (Churchill et al. 2013). Conversely, *Pongo, Gorilla* and humans have larger spine-to-lateral border angles and therefore more laterally facing scapular spines, typical of more terrestrial species (Churchill et al. 2013).

In combination, these results on the 2D angles suggest that the proximal ventral angle is more functionally informative than the proximal cranial angle which only correlates with overall shoulder size, while the distal angle (in both planes) relays more functionally relevant information, being correlated to many aspects of glenoid and scapular spine orientation that match with aspects of shoulder mobility/rigidity and locomotor patterns among hominoids. In particular, the orientation of the scapular spine relative to the glenoid fossa seems to be especially important since 3 of the 4 angles show a relationship with this variable. Interestingly, none of the measurements (including the 'freecurve' measurements) show a relationship with clavicular torsion, which is slightly unexpected given the twisted appearance of the clavicle, or the orientation of the glenoid fossa relative to the scapular borders, which is also slightly unexpected given the emphasis on the importance of the 'bar-glenoid' angle in the literature (e.g., Inouye and Shea 1997; Haile-Selassie et al. 2010).

These 2D results also suggest that while in cranial view, it is the increased flatness of the curvature that is associated with increased shoulder size (geometric mean), in ventral view it is rather its increased curvature that is associated with this variable. This indicates that this curvature follows opposite patterns between planes: the more sinuous it is in ventral view, the flatter it is in cranial view, and vice versa – the former being more typical in gibbons, and the latter more typical of African apes. This would also explain the lack of correlation between the proximal 'freecurve' and the proximal 2D angles (table 28). The present results further show that in either plane, the proximal and distal curvatures do not significantly correlate with each other, and both the distal and the proximal curvatures are associated with different and non-overlapping shoulder variables, supporting the idea of relative independence between both ends of the clavicle. Additionally the clavicle's curvatures show phylogenetic correlations with other elements of the shoulder, particularly the scapular spine and glenoid fossa, which suggest a degree of integration with these shoulder structures, particularly when the clavicle's curvatures are dissected into two planes of view. These results are in line with Voisin's (2006) observations about clavicle curvature and scapular position. Namely, the author suggests that clavicular curvatures in

ventral view provide information about the position of the scapula relative to the thorax in primates, and that is cranial view these relate information regarding the parameters of arm elevation.

Overall, these results suggest that even though some of this information is captured by the 'freecurve' methodology, dissecting the clavicle into two perpendicular 2D planes provides slightly more detailed functional information about clavicle morphology in a phylogenetic context. Thus, while the 'freecurve' method may be better suited for capturing ontogenetic development, the more traditional 2D method appears to be better suited for capturing functional information.

5. Conclusion

The aim of this study was to propose a new and more streamlined 3D protocol ('freecurve') for analysing clavicle curvatures across primate species, as an alternative to forcing the clavicle into 2D planes. Overall, the 'freecurve' methodology yields a clearer ontogenetic signal with clearer distinctions between proximal and distal curvatures and between age groups, but the traditional 2D method allows for clearer functional interpretations. These differences in results between protocols likely emanate from the fact that the 'freecurve' methodology captures information on curvature from both planes combined, therefore exacerbating some of the differences between species/curves/variables while attenuating others.

With regards to the ontogenetic development of the clavicle's curvatures, the present findings suggest that the clavicle is both partially developmentally plastic and partially ontogenetically conserved, contradicting the traditional view that the clavicle is ontogenetically stable (Corrigan 1959). While on the one hand there are visible changes in clavicular curvature prior to M1 eruption across hominoids, on the other hand, clavicular curvatures remain proportionally stable relative to each other and to clavicular length throughout growth, with adult curvatures being established around the time the clavicle ceases growing in length. This suggests that the clavicle's

curvatures are genetically constrained to a certain extent, and suggests that there are elements of the clavicle that are structurally conserved throughout ontogeny.

With regards to the phylogenetic analyses, the present findings suggest that the clavicle's curvatures do significantly correlate with aspects of scapular morphology, in particular the orientation of the scapular spine relative to the glenoid fossa, as well as to the size of the clavicle (namely cranio-caudal thickness) and overall shoulder girdle size. Moreover, results indicate that the proximal curvature is more often associated with elements of size (clavicle thickness, length and shoulder size), and that the distal curvature is more often associated to functionally relevant variables. These results seem to indicate that, on the one hand, the proximal curvature is phylogenetically conserved – perhaps because of its role in shoulder joint stability and in protecting the thoracic inlet –, while on the other hand, the distal curvature is more variable and plastic – perhaps because of its association with locomotion and arm elevation. This idea is supported by the more constrained ranges of variation found in adult proximal curvature compared to the distal curvature. The lack of correlation between proximal and distal curvatures further suggests the existence of a relative independence between distal and proximal clavicle curvatures in primates.

Because of its role in protecting the thoracic inlet as well as its role as a crankshaft for shoulder elevation, it is possible that selective pressures acting on the hominoid shoulder joint stabilize the architecture of the proximal curvature of the clavicle relative to its length and thickness (both ontogenetically and phylogenetically) in hominoids and perhaps primates in general. Conversely, the distal curvature shows first and foremost, a clade-specific pattern in hominoid distal curvature that is distinct from that of monkeys, with further between-species differences within hominoids distinguishing between locomotor types (suspensory Asian apes versus terrestrial African apes and humans). These results are also largely in line with previous observations that the distal angle of the clavicle is more variable because it is associated with range of motion and mode of locomotion: with flatter curvatures (as seen in Asian apes) increasing shoulder rigidity and stability for suspension and

brachiation, while increased curvatures (as seen in the more terrestrial African apes and humans) allow for a greater range of movement at the shoulder joint compared to other primates.

Overall, these results advance our understanding of clavicle morphology in extant hominoids and provide a simple and reproducible 3D protocol for analysing 3D curvatures that can be applied to clavicles across species, which should be particularly useful when tracking ontogenetic development of the clavicle, even though the more traditional 2D methods capture more detailed functional information. This method should additionally be useful for quantifying curvatures in fossil specimens, whose incomplete clavicles may be difficult, if not impossible, to place in 2D planes.

– Chapter 7 –

Developmental changes in the hominoid scapular angles: does the human pattern really diverge from the apes'?

1. Introduction

Of the three shoulder elements, the primate scapula is by far the most variable in shape and, because it is suspended almost entirely by muscles, much of this variation corresponds closely with locomotor habits, often irrespective of phylogeny (Schultz 1930; Inman and Abbot 1944; Ashton and Oxnard 1964; Oxnard 1967, 1969; Roberts 1974; Larson 1993; Young 2008; Green and Alemseged 2012), with many studies linking variation in primate scapular form to musculoskeletal, behavioural, locomotor, and/or ecological variables (Ashton and Oxnard 1963; Oxnard 1967, 1969, 1977; Roberts 1974; Ashton et al. 1976; Larson and Stern 1986, 1989, 1987, 1992; Shea 1986; Larson et al. 1991; Larson 1993, 1995; Taylor 1995, 1997; Young 2008). Within hominoids, even though there are remarkable similarities in scapular morphology (cranio-caudally elongated scapular blades, with large scapular fossae, and cranial oriented glenoid fossae that are wide, round and flat [Schultz 1930; Miller 1933; Ashton and Oxnard 1963, 1964; Ashton et al. 1965, 1971, 1976; Oxnard 1963, 1967]), mostly as a result of scapular repositioning onto the dorsum (Miller 1933; Erikson 1963; Le Gros 1959; Roberts and Davidson 1975; Schultz 1969; Cartmill and Milton 1977; Cartmill 1985; Aiello and Dean 1990; Gebo 1996), there are also important differences between species that directly reflect the type and frequency of locomotor behaviours, with the more suspensory species exhibiting more cranio-caudally elongated scapular bodies and more cranially directed glenoid cavities and spines, while the more terrestrial species exhibit mesio-laterally broader scapulae and more laterally facing glenoid cavities and spines (a configuration which is particularly evident in humans) (e.g., Schultz 1930; Larson and Stern 1986; Aiello and Dean 1990; Larson 1995).

Although a variety of metrics have been used in cross comparative studies of scapular morphology (e.g., Roberts 1974; Young 2006, 2008; Shea 1986; Larson 1995; Green and Alemseged 2012), some authors have suggested that it is potentially more informative to explore geometric relationships within the bone's primary infrastructure – i.e., the relative spatial orientations of its glenoid plane (glenohumeral joint), axillary border (rotator cuff), spine (trapezius, infraspinatus, and supraspinatus), and vertebral border (rhomboids and serratus anterior) (e.g., Hailie-Selassie 2010) – and in fact, one of the most diagnostic features in hominoid scapular morphology is the orientation of the glenoid fossa and the scapular spine relative to the scapular body, which are associated with frequent use of overhead movements in suspensory species (e.g., Stern Jr and Susman 1983; Inouye and Shea 1997). Indeed, the orientation of the glenoid cavity of the scapula which may be an adaptation to more effectively distribute strain over the joint capsule during climbing and reaching when the upper limb is loaded (Hunt 1991), has been granted great importance in assessing locomotor behaviour in hominoid primates (Ashton and Oxnard 1964; Roberts 1974; Jenkins et al. 1978), and studies have utilised this measurement to make inferences about fossil hominid locomotion (Inouye and Shea 1997; Morwood et al. 2005; Larson et al. 2007b; Haile-Selassie et al. 2010; Green and Alemseged 2012; Churchill et al. 2013). The orientation of the scapular spine is also thought to be associated with the degree of arm elevation in apes because functionally, the obliquity of the spine is of aid to the trapezius and deltoid in initiating abduction movements of the shoulder and arm (Miller 1933; Schultz 1969). Additionally, the orientation of the spine is thought to be the principal determinant of dorsal scapular fossa shape, which influences the size and direction of pull of the infraspinatus and supraspinatus muscles and consequently, the proportion of the supraspinous-to-infraspinous muscle sizes (Larson et al. 1991). In particular, a narrow infraspinous region with an obliquely oriented scapular spine is thought to be a more effective configuration for the infraspinatus' role in stabilizing the shoulder joint during suspensory activities (Larson and Stern 1986; Larson 1995). In contrast, an enlarged infraspinous fossa allows the muscle to pass broadly behind the humeral head, which facilitates joint

stability when the arm is loaded from below as individuals engage more regularly in knuckle-walking activities (Larson 1995; Green and Alemseged 2012).

Because of this rather clear association between form and function in scapular morphology, it is assumed that forelimb function and ontogenetic shifts in locomotor behaviour have a significant influence in the development of scapular shape (Schultz 1930, 1956; Oxnard 1967; Shea 1986; Taylor 1995; Inouye and Shea 1997; Green and Alemseged 2012; but see Young 2006, 2008; Green 2013). Such ontogenetic studies are important because they provide context for interpreting the locomotor habits of extinct hominids, which is of particular interest in the case of australopithecines, where some debate still exists over the importance of climbing and arboreality in their locomotor repertoire (e.g., Ward 2002; Larson 2007, 2013; Green and Alemseged 2012; Venkataraman et al. 2013). Namely, a recent study conducted by Green and Alemseged (2012) on the ontogeny of the hominoid scapula indicates that humans deviate from the ape pattern in showing ontogenetic changes in the angle of the glenoid cavity and scapular spine relative to the scapular body, while in apes this angle is stable throughout ontogeny. Green and Alemseged (2012) conclude that this indicates the presence of arboreal/suspensory behaviours from infancy in apes, and since the authors also find a lack of significant differences between the juvenile and adult A. afarensis scapulae (with cranially directed glenoid fossae and scapular spines), they conclude that this distinctly apelike shoulder joint configuration in A. afarensis throughout ontogeny, indicates that this species was actively engaging in arboreal/climbing behaviours from infancy too (Green and Alemseged 2012).

However, Green and Alemseged's (2012) conclusions seem contradictory since behavioural data suggests the presence of substantial shifts in locomotion throughout ontogeny in great apes but not in humans (e.g., Rose and Gamble 1994; Payne and Isaacs 2005; Doran 1992, 1997; Doran et al. 1996; Taylor 1997; van Adrichem et al. 2006). Indeed, Green and Alemseged's (2012) results suggest that there are ontogenetic changes in scapular shape in humans, who effectively are obligate bipeds from the first year of life (Burnett and Johnson 1971a, 1971b; Hensinger 1986;

Stanitski et al. 2000; Ruff 2003), and conversely suggest that there are no ontogenetic shifts in the scapulae of apes, whose locomotor habits do change rather substantially throughout growth (Doran 1992, 1997; Doran et al. 1996 Taylor 1997; van Adrichem et al. 2006). The authors then use these results to support that the lack of significant differences between infant and adult scapulae in A. afarensis is evidence of arboreal/ climbing behaviours from infancy in this species. However, it could also be argued that the lack of ontogenetic changes in the scapula of A. afarensis is evidence of a phylogenetic retention, and not necessarily reflective of actual locomotion during life – especially when considering the rest of the postcranial morphology in this species, particularly the lower limbs (e.g., DeSilva et al. 2013). If this is the case, then the association between ontogenetic changes in scapular morphology and its link to activity needs to be clarified.

Part of the issue is that the degree of developmental plasticity in these scapular traits (scapular spine and glenoid fossa orientation) is unknown, and dividing the data into age categories does not allow to observe the amount of relative change occurring throughout growth in the various species; nor does it allow to compare these changes with changes in other, more developmentally plastic measurements – namely lengths and widths. It is possible that there are indeed slight changes in glenoid fossa and scapular spine orientation in the great apes, which are not necessarily observable when dividing the data into categories. For this reason, this chapter attempts to address this issue by tracking the ontogenetic development of the geometric relationships within the hominoid scapula's primary structures – i.e., the relative spatial orientations of the glenoid fossa (glenohumeral joint function), lateral/axillary border (rotator cuff), scapular spine (trapezius, infraspinatus, and supraspinatus), and medial/vertebral border (rhomboids and serratus anterior) – using growth curves rather than age categories. The aim is to see whether ontogenetic change (and how much of it) exits in the orientation of these structures in the hominoid species, and whether humans differ from the apes in the ontogenetic development of these structures as observed by Green and Alemseged (2012) when using growth curves. I also compare the ontogenies of these structures with the ontogenies of other scapular

metrics that are expected to have a more straightforward relationship to age and growth, such as lengths and widths of the scapula. These analyses should inform on the amount of developmental plasticity occurring in these geometric properties of the scapula within the hominoid clade, as well as inform on between-species differences in scapular development, within the hominoid clade.

2. Materials and Methods

2.1. Sample and analysis

For the purpose of this chapter, I used 6 measurements of the scapula relating to the angles of the glenoid fossa and scapular spine relative to the scapular borders, as well as 9 measurements (including 4 ratios) relating to the size of the scapula (table 31). These measurements were collected on left scapulae of 6 hominoid species: Hylobates lar (n=24), Pongo pygmaeus (n=25), Pan paniscus (n=23), Pan troglodytes (n=45), Gorilla gorilla (n=42) and Homo sapiens (n=97) of all ages (0 to 70 years in humans; 0 to 13+ years in great apes; 0 to 7+ years in Macaca and Hylobates). A standard three-parameter Gompertz model was fitted to the distributions using the self-starting function SSgompertz in R version 2.12.2 (2011). The Gompertz function estimates three parameters: the asymptotic value (Asym), the value at x = 0 (b2), and a numeric parameter relating to the rate of growth (b3), for each distribution. Additionally, boxplots and ANOVAs were performed by dividing the data into age categories according to M1 and M3 eruption – with infants being represented by individuals prior to M1 eruption (7 years for humans, 3.5 years for great apes, and 1.75 for macaques and gibbons), juveniles represented by individuals prior to M3 eruption (18 years for humans, 11 for great apes, 7 years for macaques and 8 years for gibbons), and adults represented by individuals with erupted M3s (Smith 1989). Further details on how the measurements were collected, on how individual specimens were aged, and on the Gompertz function, can be found in the Materials and Methods Chapter 2.

2.2. Measurements

Because of their functional implications for glenohumeral mobility and locomotion, the present study quantifies the angulation of the glenoid fossa and scapular spine relative to the scapular borders, as well as the orientation of the glenoid fossa relative to a plane perpendicular to the scapular body (glenoid version) (see table 31 and Materials and Methods Chapter). Apart from the latter, these angles have all been reported in the most recent literature concerning scapular morphology in extant hominoids and fossil hominins (Haile-Selassie et al. 2010; Green and Alemseged 2012; Churchill et al. 2013; Green 2013).

2.2.1. Glenoid fossa orientation

Of all measurements, the relationship of the glenoid fossa relative to the lateral border of the scapula has perhaps received the most attention in the primate literature. Indeed, the 'bar-glenoid' angle is thought to indicate arboreal propensities in both extant and extinct hominoid primates (Inouye and Shea 1997). This measurement is first described by Stern and Susman (1983) and measures the angle between the line of the 'ventral bar' – a stress-bearing beam medial of the lateral or axillary border of the scapula – and a line connecting the superior and inferior limits of the glenoid fossa. The authors quantified the orientation of the glenoid fossa in this way (i.e., through the ventral bar rather than the lateral or axillary border of the scapula) because they describe greater amounts of variability in the lateral/axillary border. According to the authors, low 'bar-glenoid' angles are indicative of a more cranially directed glenoid fossa, an adaptation to use of the upper limb in elevated positions advantageous for climbing, while high angles indicate a more lateral facing glenoid fossa typical of more terrestrial primates (Stern and Susman 1983). A subsequent study by Inouye and Shea (1997) however suggests that this measurement is allometrically scaled in humans – with smaller angles (more cranially directed glenoids) present in smaller individuals and larger angles (more laterally facing glenoids) in larger individuals – thus casting doubt on the validity of this

measurement for functional/locomotor interpretations. More recently though, Green and Alemseged's (2012) study dispels these concerns by showing that the a small bodied Homo floresiensis has a very high bar-glenoid angle, more so than the average human, and that larger australopithecine specimens Sts 7 and Stw 162 have lower bar-glenoid angles than the smaller bodied Lucy (AL 211-1). Furthermore, Haile-Selassie et al's (2010) study shows that the bar–glenoid and lateral/axillary border–glenoid angles are highly correlated, suggesting that either measurement adequately describes the relationship of the glenoid angle relative to the border of the scapula.

In the present study, I describe the angulation of the glenoid fossa relative to the lateral/axillary border of the scapula because the 'ventral bar' is not present or easily distinguishable in very young individuals.

2.2.2. Scapular spine orientation

The orientation of the scapular spine is thought to be a principal determinant of dorsal scapular fossa shape (Larson et al. 1991) and by consequence a determinant of the size and orientation of the supraspinatus and infraspinatus muscles and their relative sizes to each other (Larson 1995; Green and Alemseged 2012; Larson and Stern Jr 2013; Bello-Hellegouarch et al. 2013). Indeed, Larson and Stern (1986) note that the orientation of the scapular spine in apes has a significant impact on the line of action of infraspinatus in its role of resisting transarticular tensile stress at the shoulder during suspension; chimpanzees are thus able to recruit all parts of infraspinatus to stabilize the shoulder during suspension due to their very oblique scapular spine (Larson and Stern 1986, 2013). Its orientation is also thought to be crucial for arm-raising movements because scapular rotation during arm-raising movements is achieved via the combined action of the cranial trapezius (which attaches to the scapular spine) and caudal serratus anterior (which attaches to the medial/vertebral border of the scapula) (Inman and Abbott 1944; Ashton and Oxnard 1964). However, subsequent EMG analyses (Tuttle and Basmajian 1977; Larson et al. 1991) show that the cranial trapezius is relatively unimportant in arm-raising in large-bodied

hominoids and its recruitment is more directly linked to head-turning motions (Larson et al. 1991), indicating that the orientation of the scapular spine cannot be directly related to the importance of arm-raising. Larson and Stern (1986) instead use the orientation of the base of the scapular spine as they suggest it might be related to suspensory behaviours because it has a significant impact on the line of action of the infraspinatus (Larson 1995). Anapol and Fleagle (1988) measure the 'spino-axillary border angle' (scapular spine to lateral/axillary border) in primates and find no strong functional signal in this variable and propose that the spino-axillary border angle is mainly useful as a taxonomic indicator (see also Ashton et al. 1965 and Larson 1995). In recent literature, the angle of scapular spine to the borders of the scapula has been measured in both ways: either from the base of the spine (Green and Alemseged 2012) or from the spine itself (Churchill et al. 2013). Churchill et al (2013) measure this angle relative to both the lateral/axillary border of the scapula and the medial/vertebral border of the scapula and suggest that angles based on the latter axis are better indicators of glenoid fossa and spinal orientation than are angles based on the more commonly used lateral/axillary border because the long axis of the scapula is defined by the superior and inferior angles of the body which lies parallel to the vertebral column in humans, thus providing an indication of the anatomical orientation of the bone (Churchill et al. 2013). In both Haile-Selassie et al's (2010) and Churchill et al's (2013) papers, the glenoid fossa's orientation is measured relative to the lateral/axillary border and the medial/vertebral border of the scapula; additionally, both structures' orientation relative to each other are also reported.

The present study also quantifies these angles (spine to lateral/axillary border, spine to medial/vertebral border, and spine to glenoid fossa). The orientation of the scapular spine is measured from the spine itself rather than from its base (see table 31 and Materials and Methods Chapter). I also report results for the ratio between supraspinous and infraspinous scapular dimensions (lengths, breadths, surface areas) since changes in scapular spine orientation are thought to affect this relationship.

2.2.3. Glenoid version

Glenoid version is defined by the orientation of the glenoid cavity in relation to a plane perpendicular to the scapular body and is thought to play an important role in the stability and loading of the glenohumeral joint, with abnormalities in this angle in humans being related to glenohumeral instability and shoulder joint pathologies (Nyffeler et al. 2003). In humans, an increase in anterior version has been found to result in anterior translation of the humeral head and in excessive loading of the anterior part of the glenoid, while posterior version is associated with posterior displacement and posterior loading of the glenoid (Nyffeler et al. 2003). Both are associated to greater incidence of rotator cuff injuries in humans (Tètreault et al. 2004).

Table 31 – Table of the measurements used in this chapter.

Measurement name	Measurement description
glen_angle_medborder	Angle of the glenoid fossa relative to the medial border of the scapula
spine_angle_medborder	Angle of the scapular spine relative to the medial border of the scapula
glen_angle_latborder	Angle of the glenoid fossa relative to the lateral border of the scapula
glen_angle_spine	Angle of the glenoid fossa relative to the spine of the scapula
latborder_spine_angle	Angle of the scapular spine relative to the lateral border of the scapula
glen_version	Angle of the glenoid fossa relative to the body of the scapula, in cranial view
scap_height	Maximum height of the scapular body
scap_breadth_spine_glen	Maximum breadth of the scapula from the glenoid fossa to where the long axis of the scapular spine and the vertebral border meet
scap_spine_length	Maximum length of the scapular spine from the medial border to the tip of the acromion
ratio_scap_infra_supra_length	Ratio of the maximum length of the infraspinous fossa to the supraspinous fossa of the scapula
ratio_scap_infra_supra_length_90	Ratio of the maximum length of the infraspinous fossa to the supraspinous fossa of the scapula (at 90 degree angle from spine)
ratio_scap_infra_supra_breadth	Ratio of the maximum breadth of the scapula's infraspinous fossa (below the spine) to the scapula's supraspinous fossa (above the spine)
ratio_scap_infra_supra_surf	Ratio of the surface area of the infraspinous fossa to the infraspinous fossa of the Scapula

Although this angle has been quantified in the human literature and its relationship to shoulder instability both anterior (Cyprien et al. 1983; Randelli and Gambrioli 1986; Saha 1971) and posterior (Brewer et al. 1986) extensively studied in human samples (see Bokor et al. 1999), this angle has to date not been reported for non-human

primates. In this study I also report the glenoid version angle as described by Bokor et al (1999) and Nyffeler et al (2003) (see table 31 & Materials and Methods Chapter).

3. Results

3.1. Gompertz growth curves

Standard three-parameter Gompertz growth models were fitted to the species' distributions of angle measurements (log values) (figure 70). Overall, the model provided a good fit for the spine_angle_medborder, glen_angle_medborder, glen_angle_spine and glen_version measurements across species, but was a less adequate fit for the glen_angle_latborder and larborder_spine_angle measurements (figure 70). These results suggest that the model can be fitted to most distributions, even though the variation across time in these angle measurements is very small. In fact, the results show that there are very low degrees of within-species variation across species across measurements, with the exception of the glen_angle_medborder measurement and the latborder_spine_angle measurement as can be observed from the graphs (figure 70).

Overall, my results indicate that the Gompertz models do not fit the human distributions better than the ape distributions; in fact the model could not be fitted at all to the glen_angle_latborder and latborder_spine_angle distributions in humans but fit some of the ape distributions.

In contrast, when the Gompertz model is fitted to measurements that have a more straightforward relationship to size (such a lengths, heights, widths, breadths), the Gompertz models fit all distributions across all samples, with the exception of Pongo, whose single neonate value prevents the model from adequately predicting the Gompertz parameters across all analyses (figure 77, table 34). These results show that these measurements change significantly throughout ontogeny, as the scapula grows into its adult dimensions. These results therefore indicate that sample size is unlikely

to be an issue for scapular angle measurements, since the model adequately fits all of the size measurements.

The Gompertz distributions did not fit the scapular ratio data for any measurement, for any species (figure 83).

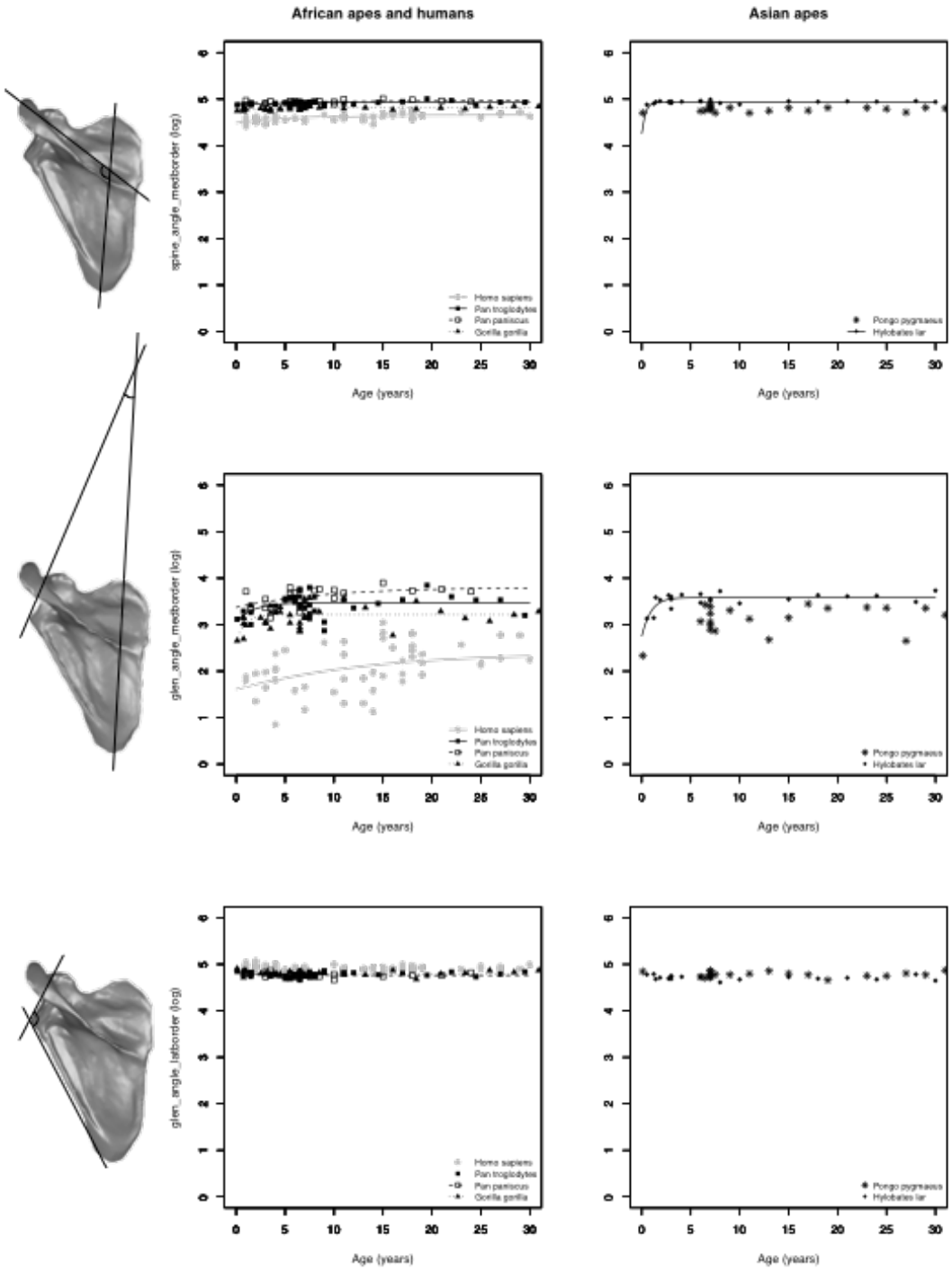

Figure 70 – Gompertz growth curves fitted to the sample distributions for all hominoid species (angle measurements).

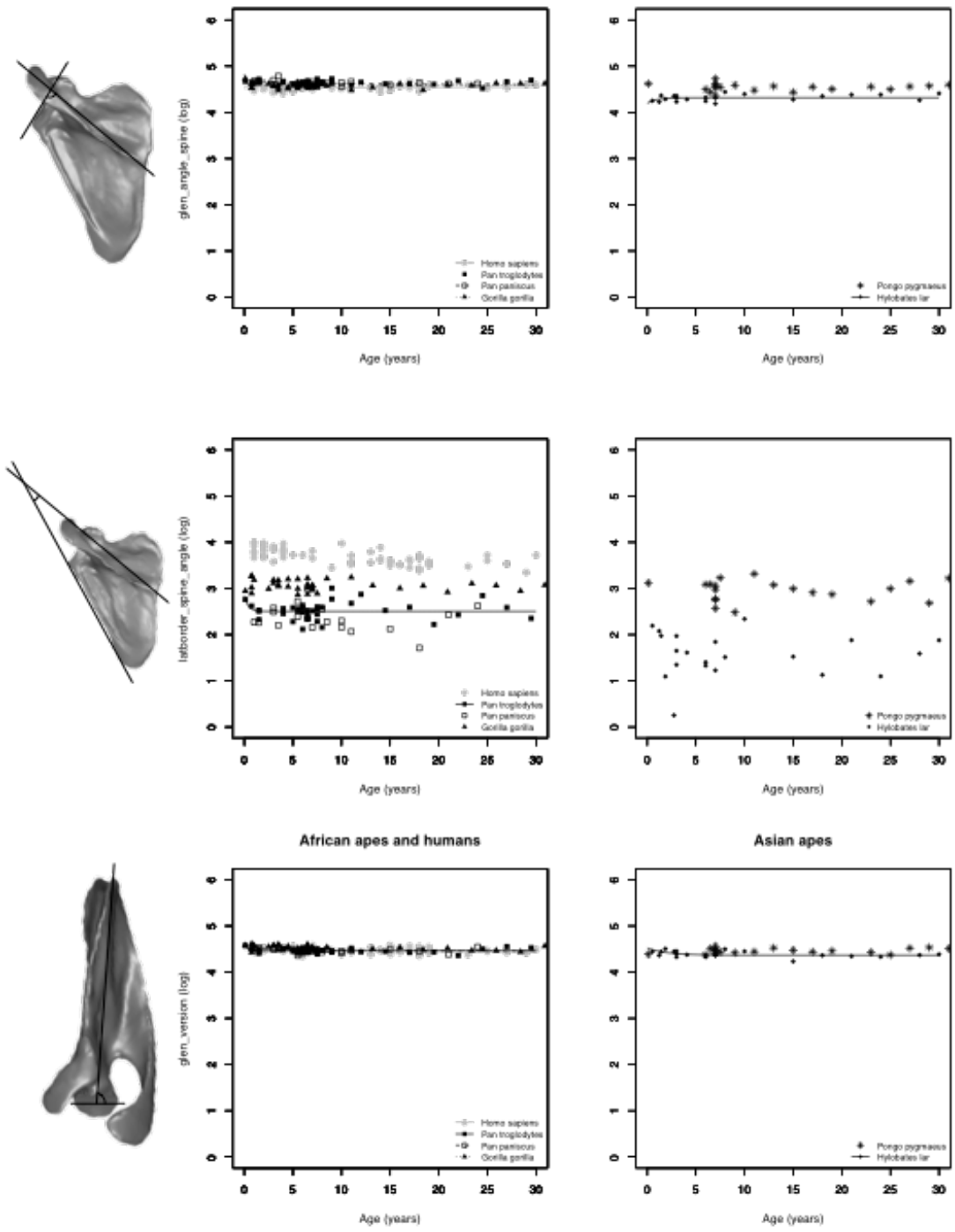

Figure 70 cont'd – Gompertz growth curves fitted to the sample distributions for all hominoid species (angle measurements).

Table 32 – Gompertz parameter for the 6 scapular angle measurements showing estimated value at growth completion (log) Asymptote estimated value at x=0 (b2), estimated rate of growth (b3), and the Residual Standard Error.

Measurement	Species	Asymptote	Gompertz b2	Gompertz b3	RSE	D
spine_angle_medborder	*H. sapiens*	4.652 (± 0.011)	0.036 (± 0.007)	0.843 (± 0.072)	0.050	37
	P. troglodytes	4.936 (± 0.011)	0.011 (± 0.003)	0.863 (± 0.070)	0.026	39
	G. gorilla	4.813 (± 0.008)	0.012 (± 0.003)	0.771 (± 0.108)	0.025	36
	P. paniscus	4.971 (± 0.030)	0.012 (± 0.006)	0.919 (± 0.115)	0.037	19
	H. lar	4.940 (± 0.009)	0.148 (± 0.151)	0.063 (± 0.121)	0.040	20
	P.pygmaeus	-	-	-	-	-
glen_angle_medborder	*H. sapiens*	2.390 (± 0.095)	0.395 (± 0.113)	0.915 (± 0.041)	0.443	77
	P. troglodytes	3.470 (± 0.045)	0.121 (± 0.064)	0.554 (± 0.317)	0.204	37
	G. gorilla	3.216 (± 0.040)	0.193 (± 0.097)	0.313 (± 0.267)	0.215	36
	P. paniscus	3.800 (± 0.101)	0.120 (± 0.039)	0.891 (± 0.081)	0.169	19
	H. lar	3.581 (± 0.030)	0.260 (± 0.113)	0.308 (± 0.157)	0.114	19
	P.pygmaeus	-	-	-	-	-
glen_angle_latborder	*H. sapiens*	-	-	-	-	-
	P. troglodytes	-	-	-	-	-
	G. gorilla	4.797 (± 0.009)	-0.028 (± 0.017)	0.058 (± 0.140)	0.050	36
	P. paniscus	4.759 (± 0.018)	-0.012 (± 0.010)	0.801 (± 0.243)	0.045	19
	H. lar	-	-	-	-	-
	P.pygmaeus	-	-	-	-	-
glen_angle_spine	*H. sapiens*	4.569 (± 0.017)	0.007 (± 0.004)	0.950 (± 0.069)	0.052	89
	P. troglodytes	-	-	-	-	-
	G. gorilla	4.574 (± 0.008)	-0.052 (± 0.029)	0.010 (± 0.052)	0.047	36
	P. paniscus	4.594 (± 0.027)	-0.020 (± 0.008)	0.892 (± 0.095)	0.045	19
	H. lar	4.315 (± 0.018)	0.027 (± 0.049)	0.334 (± 0.681)	0.072	20
	P.pygmaeus	-	-	-	-	-
latborder_spine_angle	*H. sapiens*	-	-	-	-	-
	P. troglodytes	2.503 (± 0.030)	-0.127 (± 0.108)	0.093 (± 0.423)	0.180	37
	G. gorilla	-	-	-	-	-
	P. paniscus	-	-	-	-	-
	H. lar	-	-	-	-	-
	P.pygmaeus	-	-	-	-	-
glen_version	*H. sapiens*	4.414 (± 0.041)	-0.019 (± 0.008)	0.970 (± 0.031)	0.053	88
	P. troglodytes	4.461 (± 0.007)	-0.033 (± 0.020)	0.050 (± 0.209)	0.045	37
	G. gorilla	4.442 (± 0.422)	-0.024 (± 0.092)	0.946 (± 0.293)	0.050	36
	P. paniscus	4.457 (± 0.022)	-0.023 (± 0.017)	0.705 (± 0.327)	0.047	19
	H. lar	4.366 (± 0.025)	-0.035 (± 0.015)	0.615 (± 0.273)	0.062	20
	P.pygmaeus	-	-	-	-	-

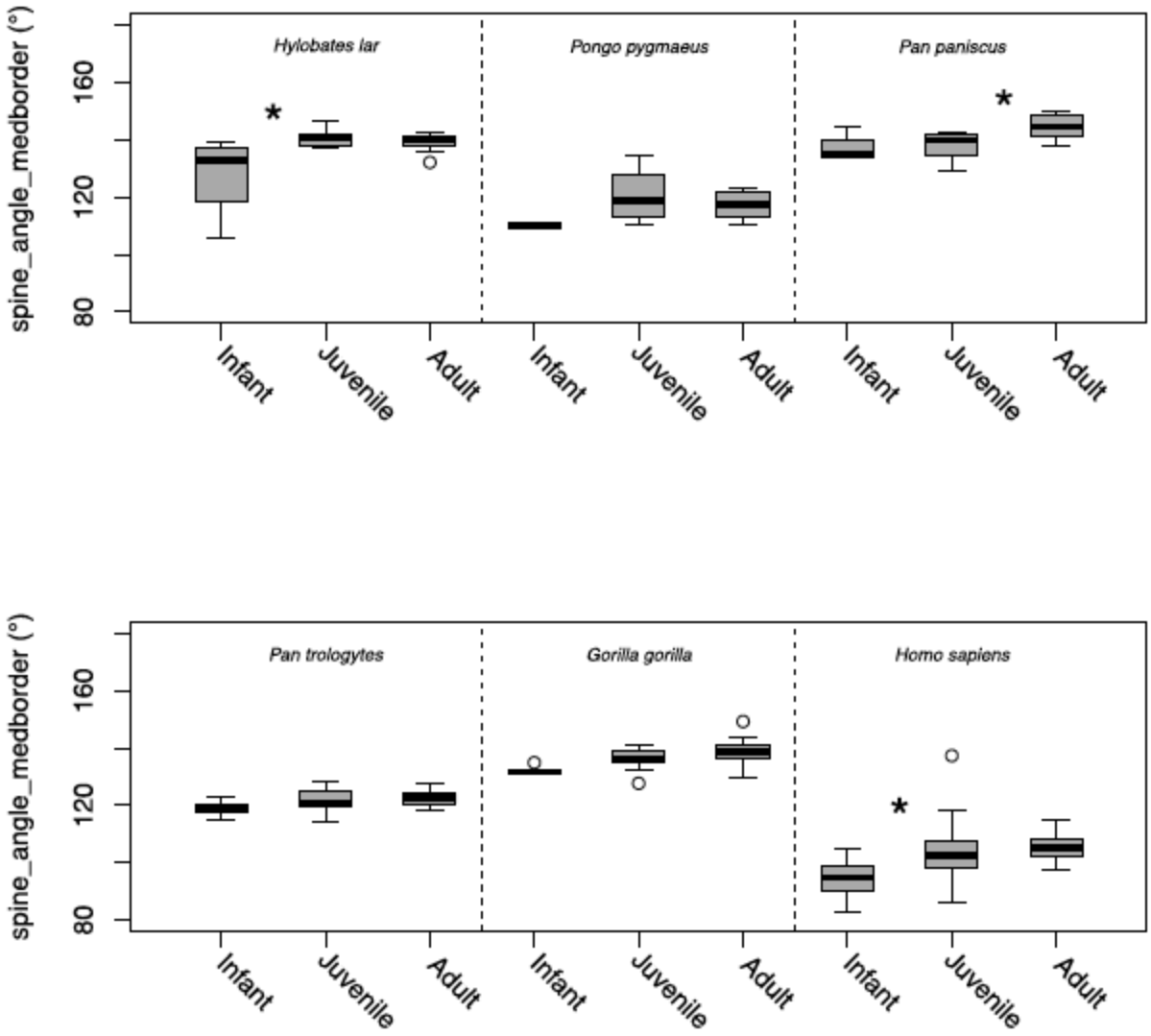

Figure 71 – Boxplots of infant, juvenile and adult hominoid specimens. Significant difference (95% CI) between adjacent categories marked with asterisk ($p<0.05$). Boxes represent the upper and lower quartile ranges, the black lines, the means, and the whiskers, the highest and lowest values within 1.5 times the interquartile range of the upper and lower quartiles. The circles represent outliers within 3 times the i nterquartile range of the upper and lower quartiles. ANOVAs indicate a lack of significant differences between age categories for most species (H. lar: p-value=0.007, F=6.067, df=2; P. pygmaeus: p-values=0.414, F=0.963, df=2; P. paniscus: p-value=0.012, F=5.636, df=2; P. troglodytes: p-value=0.006, F=5.899, df=2; G. gorilla: p-value=0.022, F=4.238, df=2; H. sapiens: p-value=0.000, F=28.273, df=2).

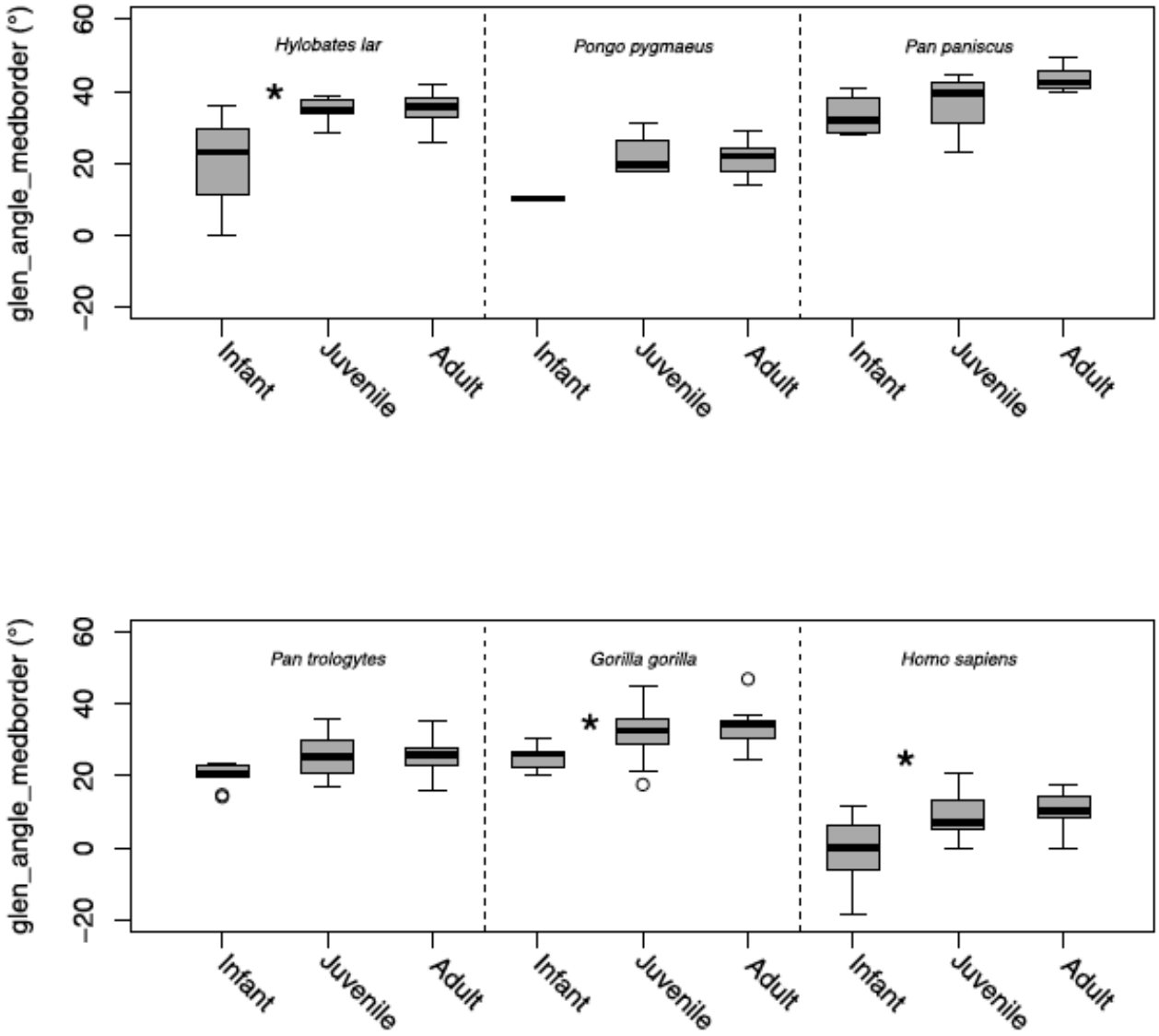

Figure 72 – Boxplots of infant, juvenile and adult hominoid specimens. Significant difference (95% CI) between adjacent categories marked with asterisk ($p<0.05$). Boxes represent the upper and lower quartile ranges, the black lines, the means, and the whiskers, the highest and lowest values within 1.5 times the interquartile range of the upper and lower quartiles. The circles represent outliers within 3 times the interquartile range of the upper and lower quartiles. ANOVAs indicate a lack of significant differences between age categories for most species (H. lar: p-value=0.003, F=7.648, df=2; P. pygmaeus: p-values=0.183, F=2.014, df=2; P. paniscus: p-value=0.024, F=4.533, df=2; P. troglodytes: p-value=0.043, F=3.424, df=2; G. gorilla: p-value=0.033, F=3.763, df=2; H. sapiens: p-value=0.000, F=29.775, df=2).

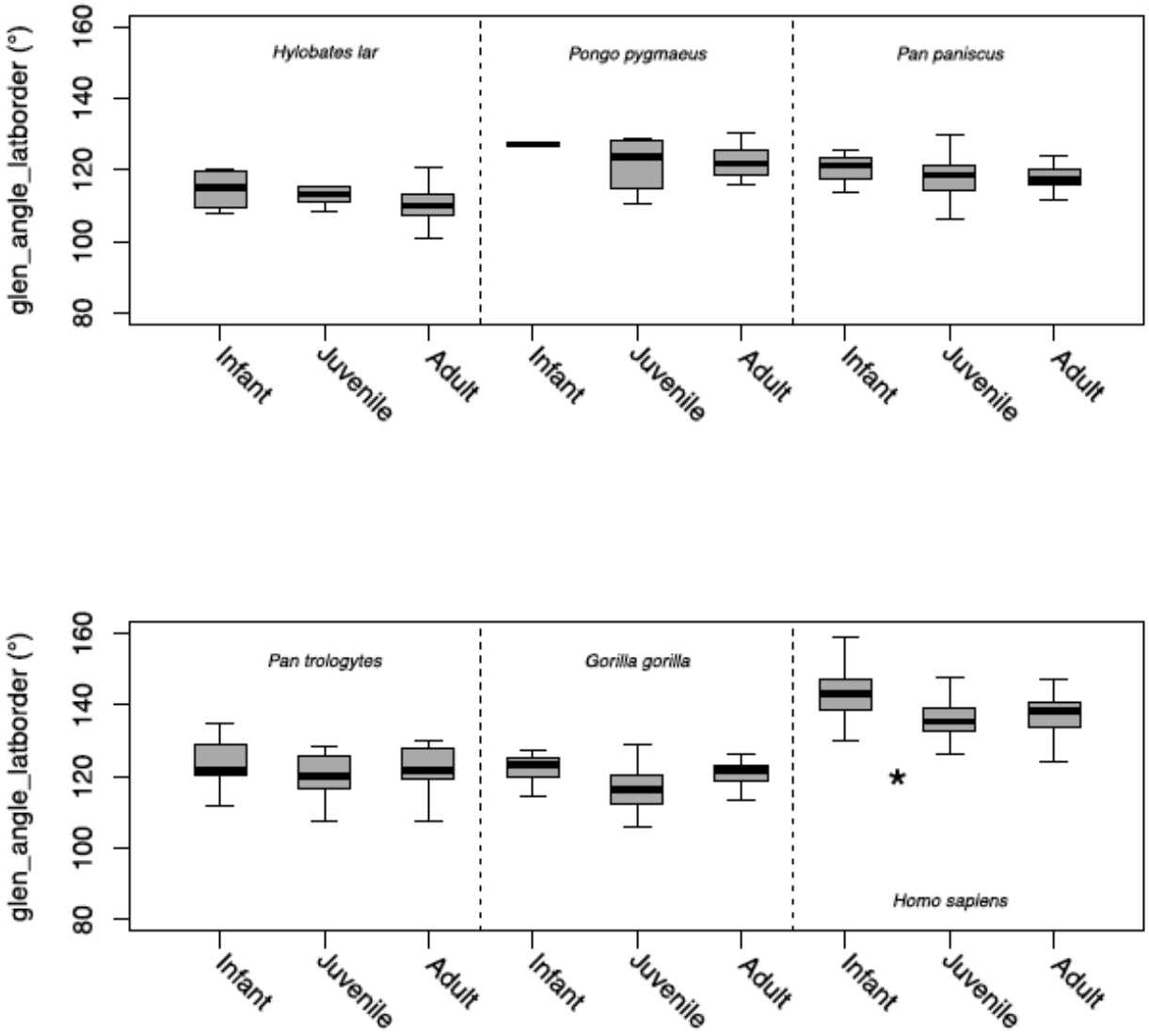

Figure 73 – Boxplots of infant, juvenile and adult hominoid specimens. Significant difference (95% CI) between adjacent categories marked with asterisk ($p<0.05$). Boxes represent the upper and lower quartile ranges, the black lines, the means, and the whiskers, the highest and lowest values within 1.5 times the interquartile range of the upper and lower quartiles. The circles represent outliers within 3 times the interquartile range of the upper and lower quartiles. ANOVAs indicate a lack of significant differences between age categories for most species (H. lar: p-value=0.350, F=1.102, df=2; P. pygmaeus: p-values=0.751, F=0.294, df=2; P. paniscus: p-value=0.744, F=0.305, df=2; P. troglodytes: p-value=0.019, F=4.357, df=2; G. gorilla: p-value=0.320, F=1.175, df=2; H. sapiens: p-value=0.000, F=10.817, df=2).

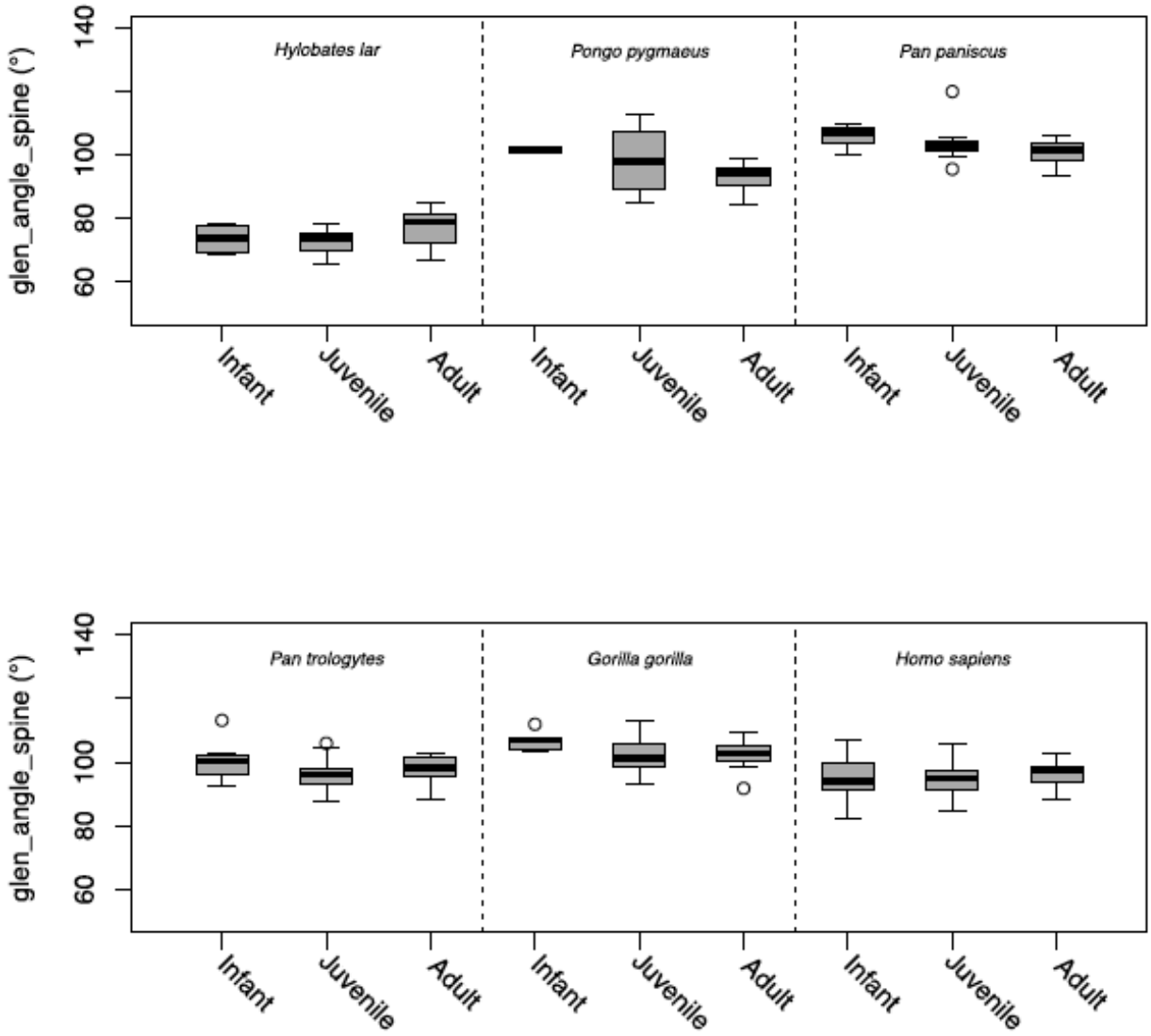

Figure 74 – Boxplots of infant, juvenile and adult hominoid specimens. Significant difference (95% CI) between adjacent categories marked with asterisk ($p<0.05$). Boxes represent the upper and lower quartile ranges, the black lines, the means, and the whiskers, the highest and lowest values within 1.5 times the interquartile range of the upper and lower quartiles. The circles represent outliers within 3 times the interquartile range of the upper and lower quartiles. ANOVAs indicate a lack of significant differences between age categories for all species (H. lar: p-value=0.227, F=1.594, df=2; P. pygmaeus: p-values=0.402, F=0.995, df=2; P. paniscus: p-value=0.290, F=1.316, df=2; P. troglodytes: p-value=0.151, F=1.976, df=2; G. gorilla: p-value=0.227, F=1.539, df=2; H. sapiens: p-value=0.204, F=1.611, df=2).

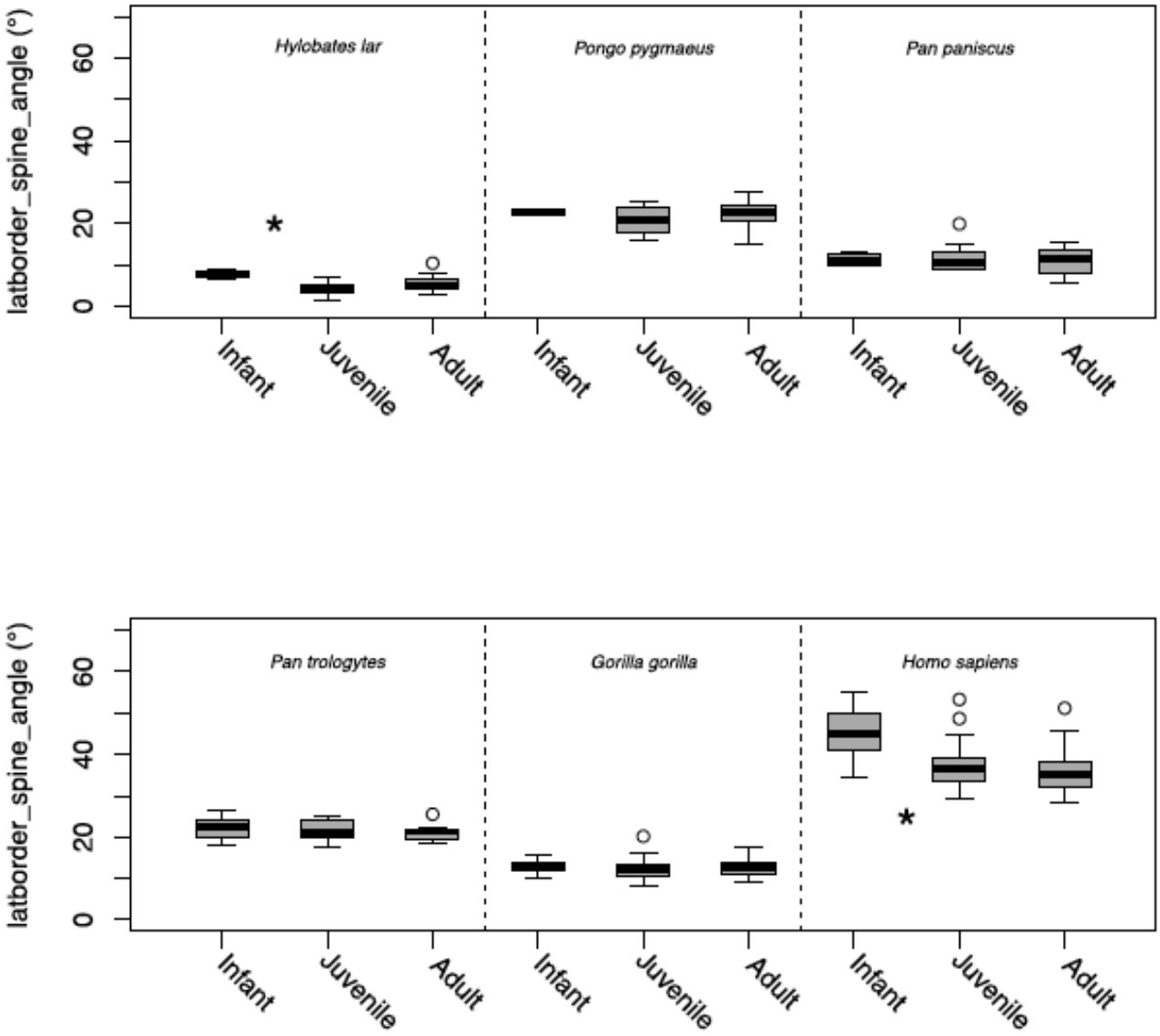

Figure 75 – Boxplots of infant, juvenile and adult hominoid specimens. Significant difference (95% CI) between adjacent categories marked with asterisk ($p<0.05$). Boxes represent the upper and lower quartile ranges, the black lines, the means, and the whiskers, the highest and lowest values within 1.5 times the interquartile range of the upper and lower quartiles. The circles represent outliers within 3 times the interquartile range of the upper and lower quartiles. ANOVAs indicate a lack of significant differences between age categories for most species (H. lar: p-value=0.027, F=4.484, df=2; P. pygmaeus: p-values=0.793, F=0.238, df=2; P. paniscus: p-value=0.856, F=0.157, df=2; P. troglodytes: p-value=0.658, F=0.421, df=2; G. gorilla: p-value=0.548, F=0.611, df=2; H. sapiens: p-value=0.000, F=28.265, df=2).

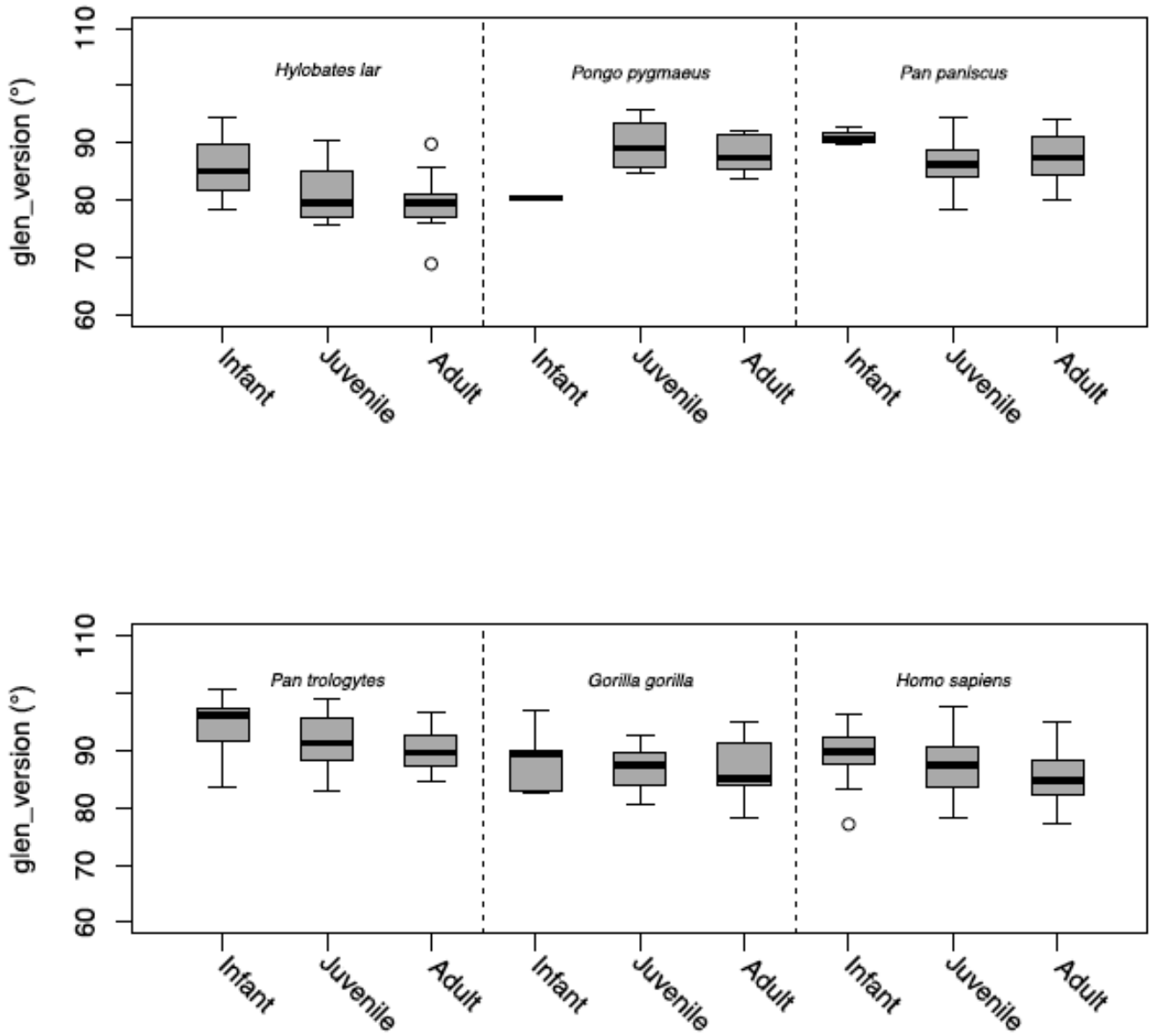

Figure 76 – Boxplots of infant, juvenile and adult hominoid specimens. Significant difference (95% CI) between adjacent categories marked with asterisk ($p<0.05$). Boxes represent the upper and lower quartile ranges, the black lines, the means, and the whiskers, the highest and lowest values within 1.5 times the interquartile range of the upper and lower quartiles. The circles represent outliers within 3 times the interquartile range of the upper and lower quartiles. ANOVAs indicate a lack of significant differences between age categories for most species (H. lar: p-value=0.182, F=1.823, df=2; P. pygmaeus: p-values=0.144, F=2.353, df=2; P. paniscus: p-value=0.209, F=1.699, df=2; P. troglodytes: p-value=0.748, F=0.291, df=2; G. gorilla: p-value=0.127, F=2.187, df=2; H. sapiens: p-value=0.000, F=7.482, df=2).

Table 33 – Table of ANOVA TukeyHSD post-hoc results of differences between age categories within species (angle measurements), with adjusted p-values (p-adj) upper and lower bounds of the 95% confidence interval (lwr, upr), and difference between means (diff).

Measurement	Species	Age Categories		diff	lwr	upr	p-adj
spine_angle_medborder	*H. lar*	Infant	Juvenile	12.661	3.234	22.087	**0.008**
		Juvenile	Adult	-1.471	-8.597	5.655	0.862
	P. pygmaeus	Infant	Juvenile	10.550	-10.815	31.915	0.400
		Juvenile	Adult	-3.325	-15.027	8.377	0.724
	P. paniscus	Infant	Juvenile	0.839	-6.022	7.700	0.948
		Juvenile	Adult	6.524	1.023	12.024	**0.019**
	P. troglodytes	Infant	Juvenile	4.105	-0.247	8.457	0.068
		Juvenile	Adult	2.495	-0.624	5.615	0.139
	G. gorilla	Infant	Juvenile	3.201	-0.103	6.505	0.059
		Juvenile	Adult	0.879	-2.138	3.895	0.758
	H. sapiens	Infant	Juvenile	9.713	5.570	13.856	**0.000**
		Juvenile	Adult	1.765	-1.990	5.520	0.504
glen_angle_medborder	*H. lar*	Infant	Juvenile	14.411	4.246	24.575	**0.005**
		Juvenile	Adult	0.370	-7.313	8.053	0.992
	P. pygmaeus	Infant	Juvenile	11.618	-4.943	28.178	0.183
		Juvenile	Adult	-0.556	-9.627	8.515	0.985
	P. paniscus	Infant	Juvenile	3.540	-5.484	12.563	0.588
		Juvenile	Adult	6.549	-0.686	13.784	0.080
	P. troglodytes	Infant	Juvenile	6.784	-0.482	14.051	0.071
		Juvenile	Adult	1.562	-3.647	6.771	0.747
	G. gorilla	Infant	Juvenile	5.572	0.230	10.915	**0.039**
		Juvenile	Adult	0.024	-4.853	4.901	1.000
	H. sapiens	Infant	Juvenile	9.169	5.363	12.975	**0.000**
		Juvenile	Adult	1.648	-1.801	5.098	0.493
glen_angle_latborder	*H. lar*	Infant	Juvenile	-1.809	-9.232	5.615	0.814
		Juvenile	Adult	-2.271	-7.882	3.340	0.573
	P. pygmaeus	Infant	Juvenile	-5.363	-24.931	14.206	0.740
		Juvenile	Adult	0.513	-10.205	11.230	0.991
	P. paniscus	Infant	Juvenile	-2.067	-10.308	6.174	0.802
		Juvenile	Adult	-0.483	-7.090	6.124	0.981
		Juvenile	Adult	4.431	0.055	8.807	**0.047**
	G. gorilla	Infant	Juvenile	-3.741	-9.920	2.439	0.313
		Juvenile	Adult	2.115	-3.526	7.757	0.634
	H. sapiens	Infant	Juvenile	-7.130	-11.140	-3.120	**0.000**
		Juvenile	Adult	1.117	-2.517	4.751	0.745

Table 33 cont'd– Table of ANOVA TukeyHSD post-hoc results of differences between age categories within species (angle measurements), with adjusted p-values (p-adj) upper and lower bounds of the 95% confidence interval (lwr, upr), and difference between means (diff).

Measurement	Species	Age Categories		diff	lwr	upr	p-adj
glen_angle_spine	*H. lar*	Infant	Juvenile	-0.581	-8.066	6.905	0.979
		Juvenile	Adult	3.854	-1.804	9.512	0.222
	P. pygmaeus	Infant	Juvenile	-3.000	-26.290	20.290	0.934
		Juvenile	Adult	-5.320	-18.076	7.436	0.511
	P. paniscus	Infant	Juvenile	-2.237	-10.158	5.685	0.756
		Juvenile	Adult	-2.762	-9.114	3.589	0.523
	P. troglodytes	Infant	Juvenile	-4.685	-10.440	1.071	0.130
		Juvenile	Adult	0.536	-3.590	4.662	0.946
	G. gorilla	Infant	Juvenile	-3.618	-8.662	1.426	0.200
		Juvenile	Adult	1.095	-3.510	5.699	0.831
	H. sapiens	Infant	Juvenile	-0.559	-3.871	2.753	0.915
		Juvenile	Adult	2.118	-0.884	5.120	0.218
glen_version	*H. lar*	Infant	Juvenile	-4.736	-12.798	3.326	0.320
		Juvenile	Adult	-1.345	-7.438	4.749	0.844
	P. pygmaeus	Infant	Juvenile	9.295	-2.461	21.051	0.126
		Juvenile	Adult	-1.635	-8.074	4.804	0.771
	P. paniscus	Infant	Juvenile	-4.503	-10.721	1.716	0.184
		Juvenile	Adult	1.073	-3.913	6.058	0.849
	P. troglodytes	Infant	Juvenile	-1.513	-6.441	3.415	0.737
		Juvenile	Adult	0.045	-3.488	3.578	0.999
	G. gorilla	Infant	Juvenile	-2.661	-7.217	1.894	0.338
		Juvenile	Adult	-1.536	-5.694	2.623	0.642
	H. sapiens	Infant	Juvenile	-1.925	-4.941	1.090	0.286
		Juvenile	Adult	-2.441	-5.174	0.292	0.090
atborder_spine_angle	*H. lar*	Infant	Juvenile	-3.318	-6.143	-0.492	0.020
		Juvenile	Adult	1.307	-0.829	3.443	0.292
	P. pygmaeus	Infant	Juvenile	-1.885	-13.518	9.748	0.898
		Juvenile	Adult	1.518	-4.854	7.889	0.795
	P. paniscus	Infant	Juvenile	0.595	-4.294	5.484	0.949
		Juvenile	Adult	-0.844	-4.764	3.076	0.849
	P. troglodytes	Infant	Juvenile	-0.746	-3.655	2.163	0.807
		Juvenile	Adult	0.685	-1.400	2.770	0.705
	G. gorilla	Infant	Juvenile	-0.921	-3.371	1.530	0.632
		Juvenile	Adult	-0.219	-2.455	2.018	0.969
	H. sapiens	Infant	Juvenile	-7.803	-11.217	-4.388	0.000
		Juvenile	Adult	-1.720	-4.815	1.374	0.386

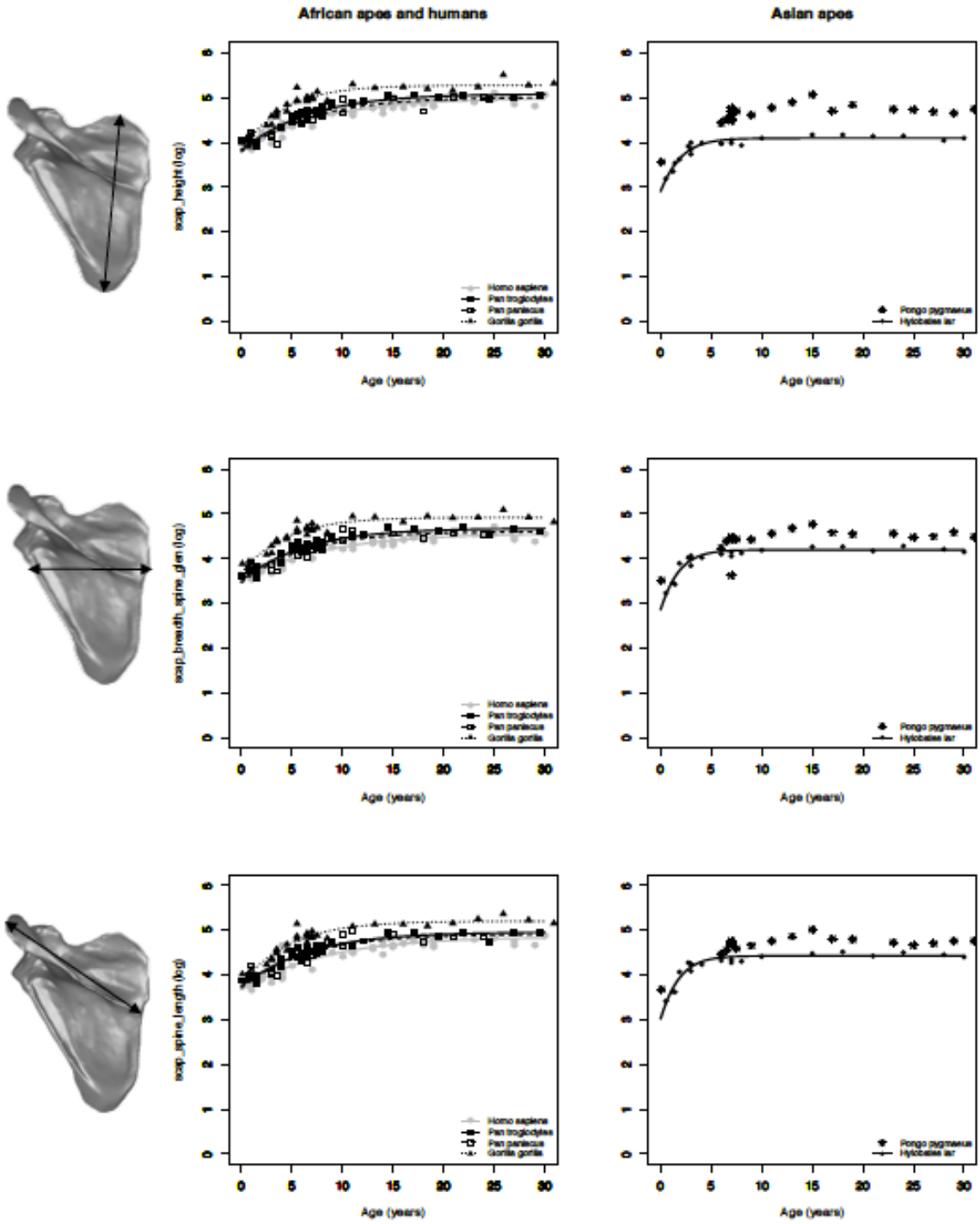

Figure 77 – Gompertz growth curves fitted to the sample distributions for all hominoid species (size measurements).

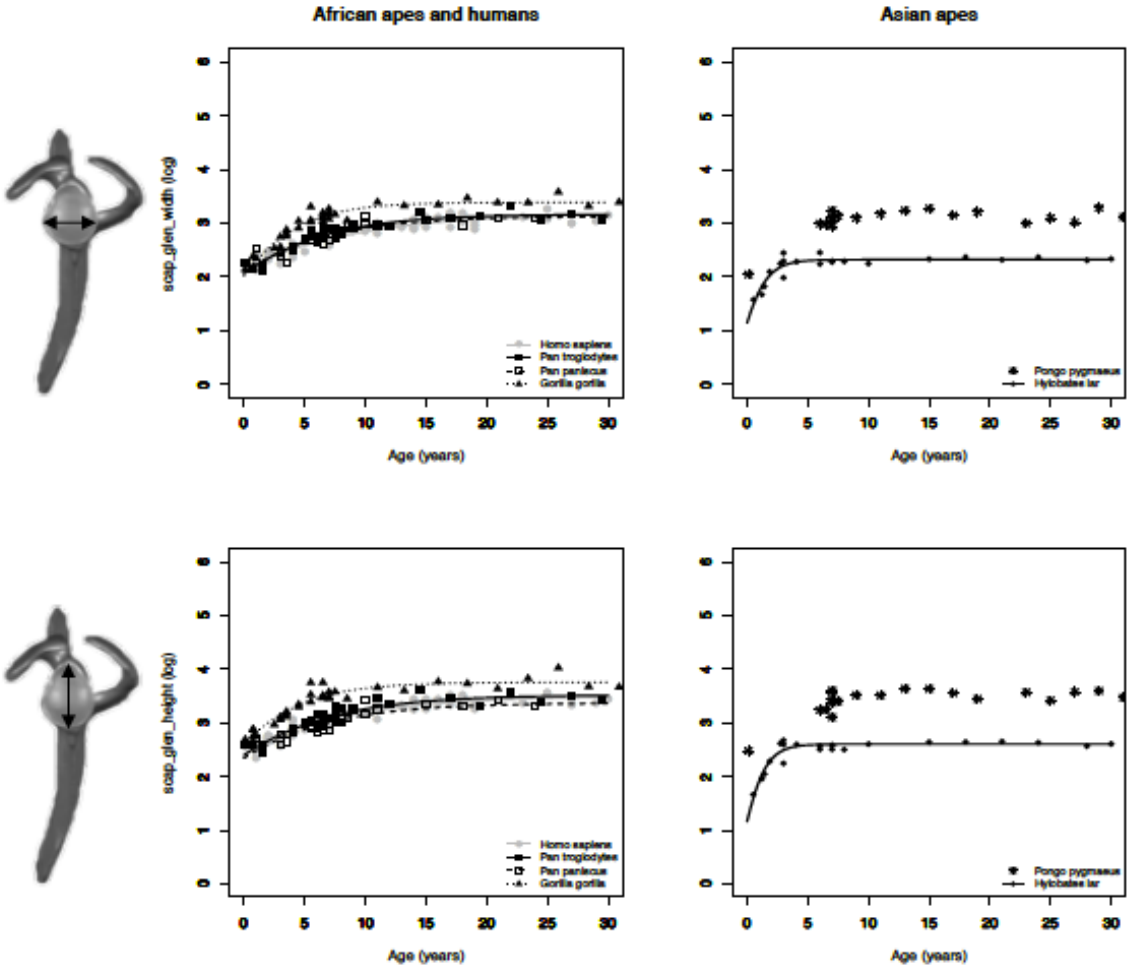

Figure 77 cont'd – Gompertz growth curves fitted to the sample distributions for all hominoid species (size measurements).

Table 34 - Gompertz parameter for the 5 scapular size measurements showing estimated value at growth completion (mm) (Asymptote), estimated value at x=0 (b2), estimated rate of growth (b3), and the Residual Standard Error.

Measurement	Species	Asymptote	Gompertz b2	Gompertz b3	RSE	df
scap_height	*H. sapiens*	4.995 (±0.015)	0.262 (±0.008)	0.872 (±0.008)	0.091	88
	P. troglodytes	5.084 (±0.034)	0.284 (±0.014)	0.847 (±0.012)	0.091	39
	G. gorilla	5.276 (±0.032)	0.315 (±0.014)	0.770 (±0.016)	0.103	36
	P. paniscus	5.011 (±0.066)	0.278 (±0.030)	0.852 (±0.027)	0.138	19
	H. lar	4.094 (±0.022)	0.343 (±0.036)	0.568 (±0.042)	0.078	20
	P. pygmaeus	-	-	-	-	-
scap_breadth_spine_gl	*H. sapiens*	4.565 (±0.013)	0.259 (±0.008)	0.875 (±0.007)	0.079	89
	P. troglodytes	4.680 (±0.031)	0.285 (±0.014)	0.840 (±0.012)	0.084	39
	G. gorilla	4.923 (±0.029)	0.288 (±0.013)	0.779 (±0.016)	0.093	36
	P. paniscus	4.609 (±0.063)	0.284 (±0.035)	0.838 (±0.032)	0.140	19
	H. lar	4.200 (±0.024)	0.383 (±0.043)	0.531 (±0.045)	0.086	20
	P. pygmaeus	-	-	-	-	-
scap_spine_length	*H. sapiens*	4.855 (±0.018)	0.280 (±0.010)	0.874 (±0.009)	0.108	88
	P. troglodytes	4.960 (±0.034)	0.280 (±0.014)	0.847 (±0.012)	0.089	39
	G. gorilla	5.205 (±0.033)	0.310 (±0.013)	0.796 (±0.014)	0.103	36
	P. paniscus	4.917 (±0.071)	0.279 (±0.034)	0.846 (±0.032)	0.151	19
	H. lar	4.430 (±0.025)	0.382 (±0.042)	0.535 (±0.044)	0.089	20
	P. pygmaeus	-	-	-	-	-
scap_glen_width	*H. sapiens*	3.194 (±0.017)	0.384 (±0.015)	0.886 (±0.008)	0.100	89
	P. troglodytes	3.168 (±0.031)	0.429 (±0.023)	0.837 (±0.013)	0.085	39
	G. gorilla	3.387 (±0.029)	0.514 (±0.024)	0.751 (±0.016)	0.097	36
	P. paniscus	3.127 (±0.058)	0.400 (±0.049)	0.842 (±0.030)	0.124	19
	H. lar	2.321 (±0.028)	0.707 (±0.148)	0.412 (±0.075)	0.105	20
	P. pygmaeus	-	-	-	-	-
scap_glen_height	*H. sapiens*	3.502 (±0.016)	0.339 (±0.013)	0.873 (±0.009)	0.097	89
	P. troglodytes	3.523 (±0.038)	0.382 (±0.023)	0.852 (±0.014)	0.098	39
	G. gorilla	3.759 (±0.034)	0.368 (±0.021)	0.780 (±0.020)	0.109	36
	P. paniscus	3.373 (±0.056)	0.362 (±0.041)	0.847 (±0.028)	0.118	19
	H. lar	2.605 (±0.026)	0.801 (±0.142)	0.379 (±0.061)	0.099	20
	P. pygmaeus	-	-	-	-	-

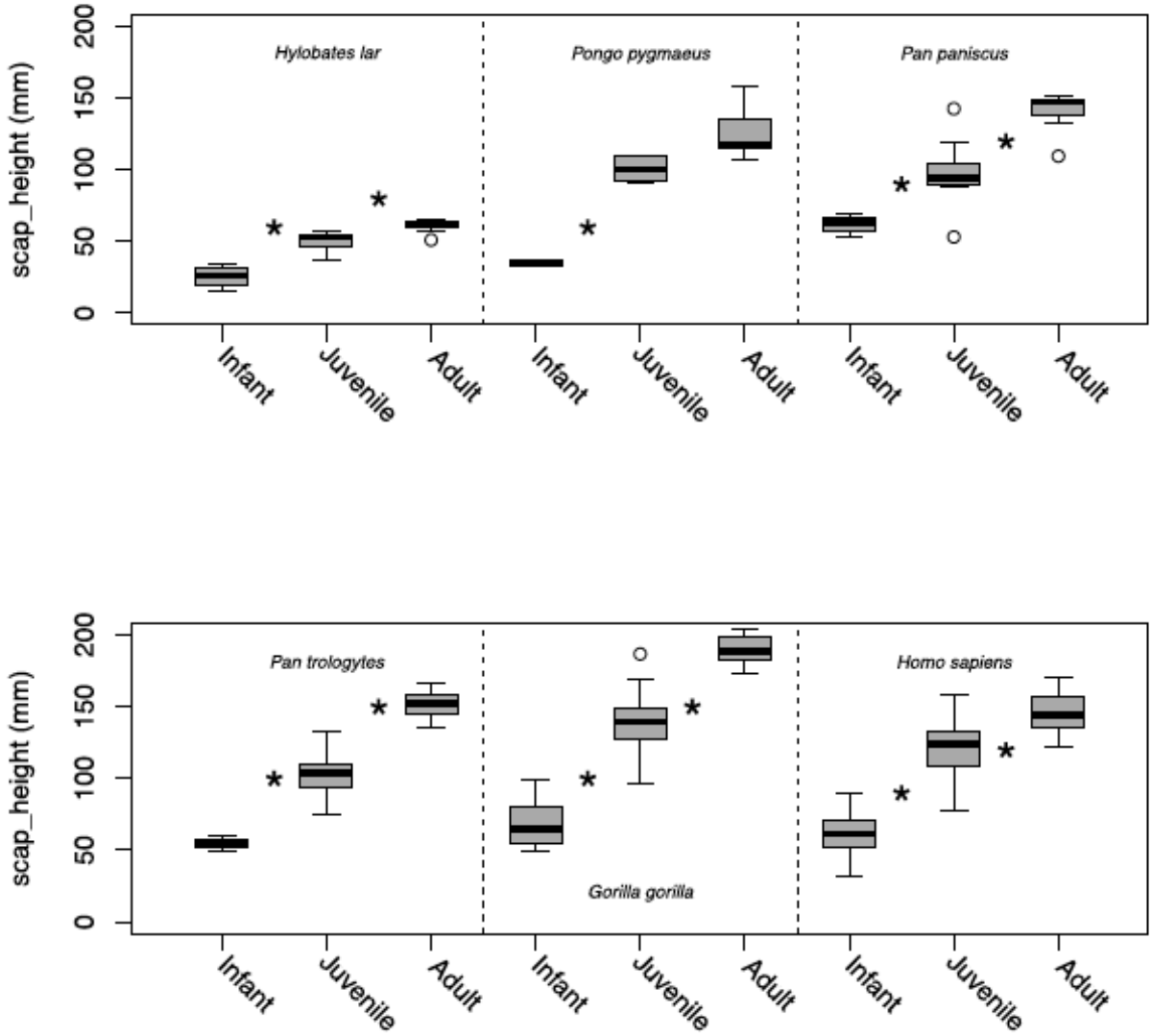

Figure 78 – Boxplots of infant, juvenile and adult hominoid specimens. Significant difference (95% CI) between adjacent categories marked with asterisk ($p<0.05$). Boxes represent the upper and lower quartile ranges, the black lines, the means, and the whiskers, the highest and lowest values within 1.5 times the interquartile range of the upper and lower quartiles. The circles represent outliers within 3 times the interquartile range of the upper and lower quartiles. ANOVAs indicate significant differences between age categories for most species (H. lar: p-value=0.000, F=53.31, df=2; P. pygmaeus: p-values=0.000, F=17.084, df=2; P. paniscus: p-value=0.000, F=27.443, df=2; P. troglodytes: p-value=0.000, F=119.26, df=2; G. gorilla: p-value=0.000, F=100.47, df=2; H. sapiens: p-value=0.000, F=248.59, df=2).

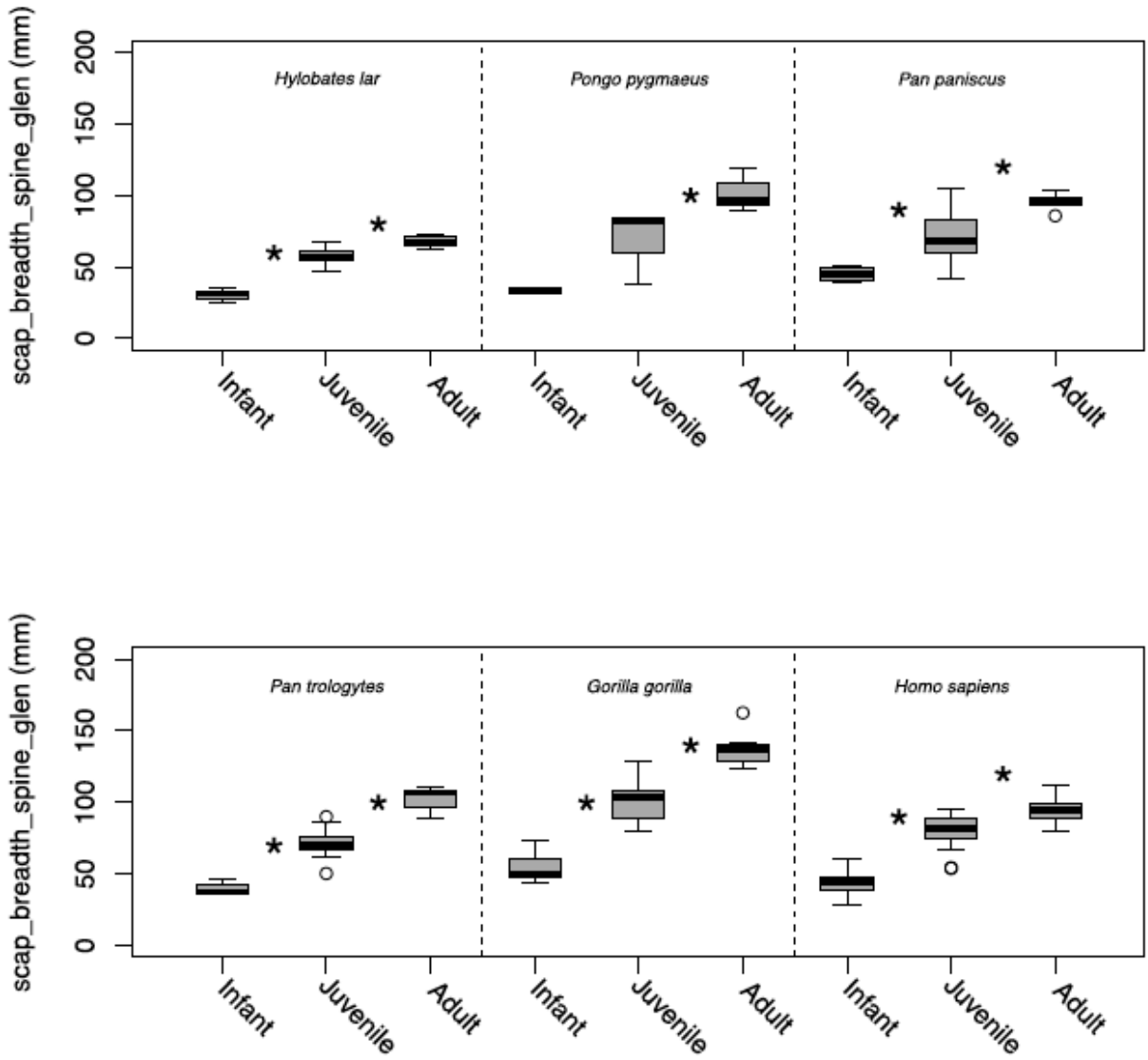

Figure 79 – Boxplots of infant, juvenile and adult hominoid specimens. Significant difference (95% CI) between adjacent categories marked with asterisk ($p<0.05$). Boxes represent the upper and lower quartile ranges, the black lines, the means, and the whiskers, the highest and lowest values within 1.5 times the interquartile range of the upper and lower quartiles. The circles represent outliers within 3 times the interquartile range of the upper and lower quartiles. ANOVAs indicate significant differences between age categories for most species (H. lar: p-value=0.000, F=80.135, df=2; P. pygmaeus: p-values=0.003, F=11.163, df=2; P. paniscus: p-value=0.000, F=22.591, df=2; P. troglodytes: p-value=0.000, F=131.32, df=2; G. gorilla: p-value=0.000, F=125.26, df=2; H. sapiens: p-value=0.000, F=282.4, df=2).

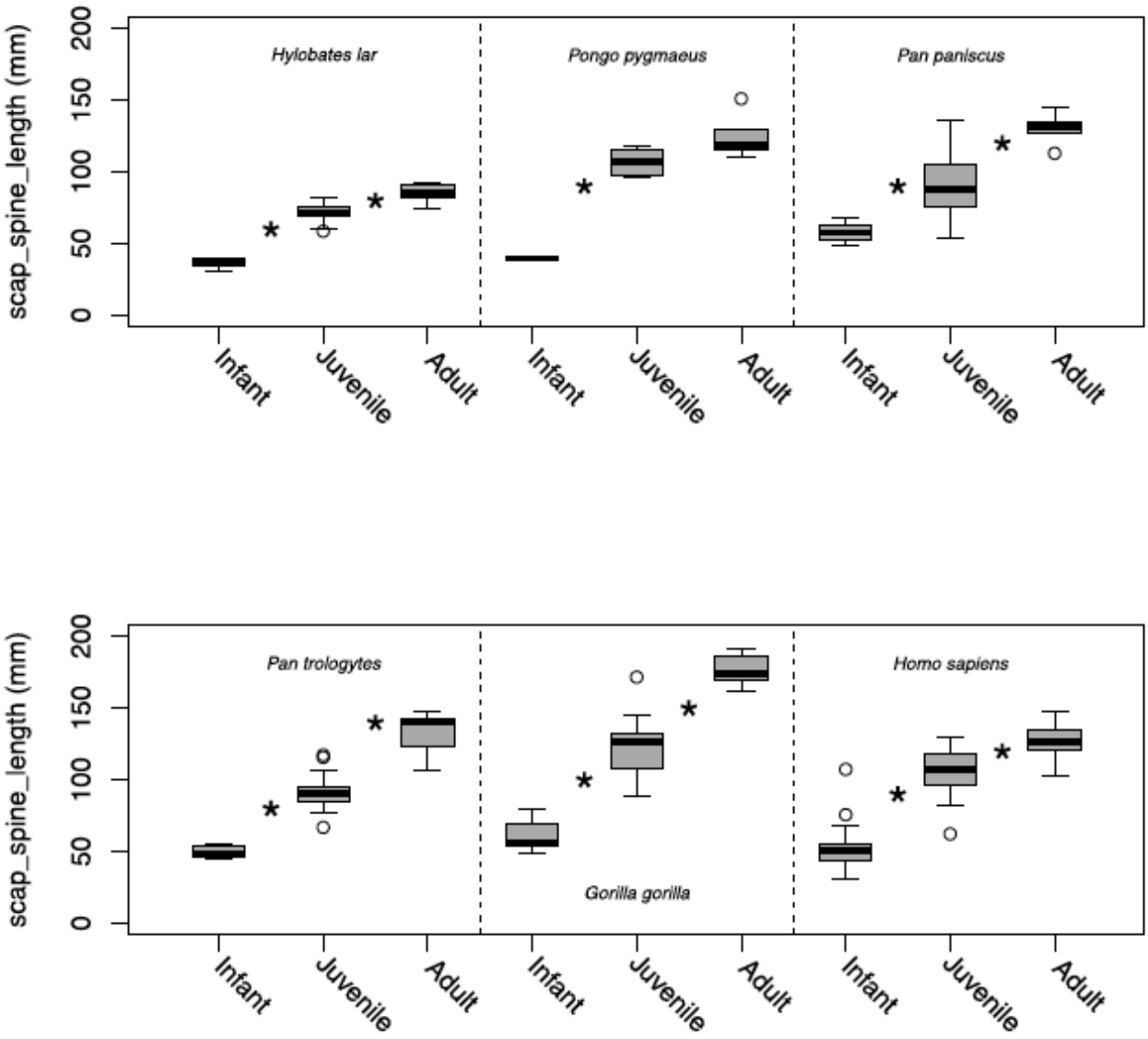

Figure 80 – Boxplots of infant, juvenile and adult hominoid specimens. Significant difference (95% CI) between adjacent categories marked with asterisk ($p<0.05$). Boxes represent the upper and lower quartile ranges, the black lines, the means, and the whiskers, the highest and lowest values within 1.5 times the interquartile range of the upper and lower quartiles. The circles represent outliers within 3 times the interquartile range of the upper and lower quartiles. ANOVAs indicate significant differences between age categories for most species (H. lar: p-value=0.000, F=88.901, df=2; P. pygmaeus: p-values=0.000, F=20.637, df=2; P. paniscus: p-value=0.000, F=25.861, df=2; P. troglodytes: p-value=0.000, F=105.26, df=2; G. gorilla: p-value=0.000, F=119.77, df=2; H. sapiens: p-value=0.000, F=232.51, df=2).

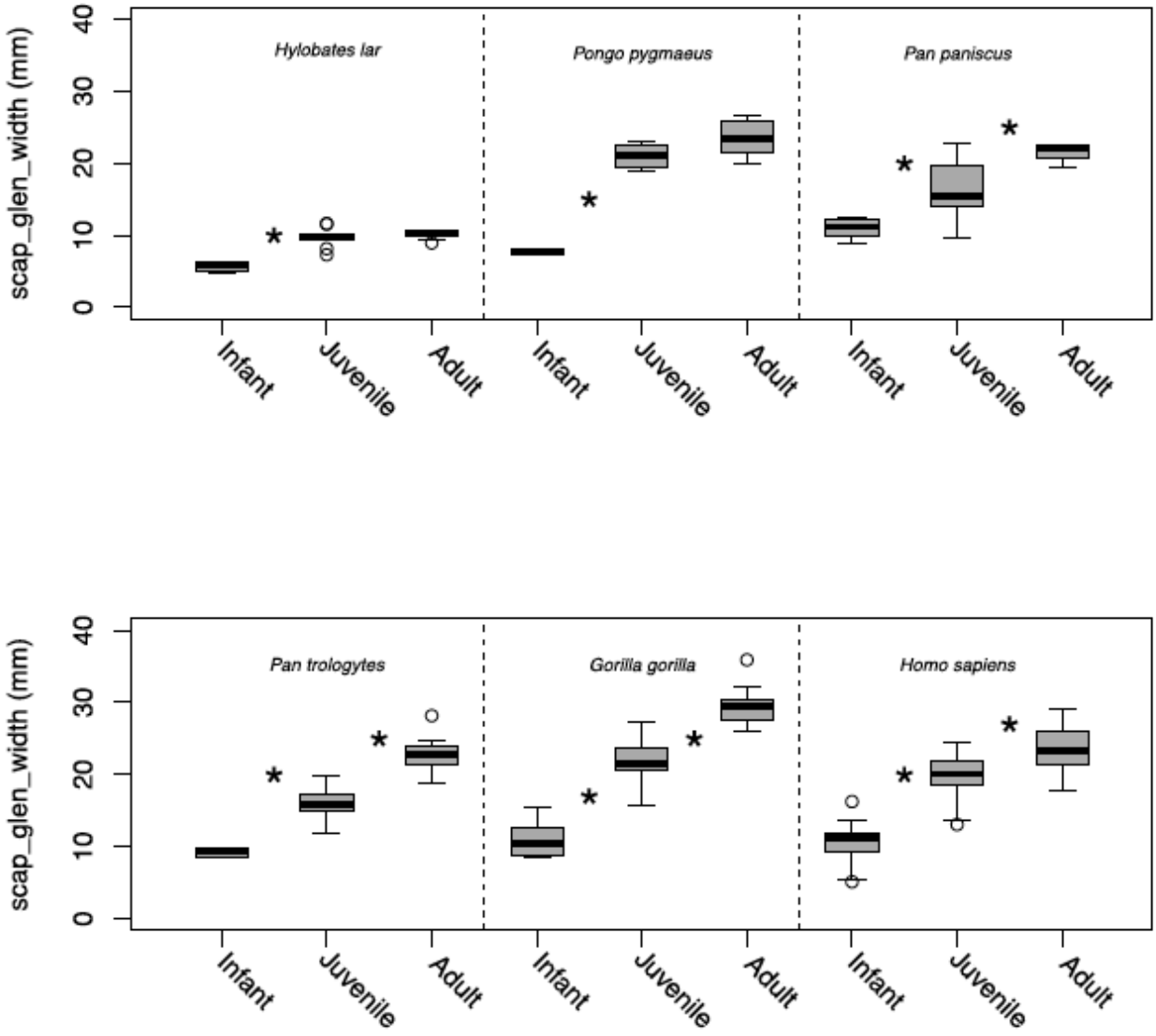

Figure 81 – Boxplots of infant, juvenile and adult hominoid specimens. Significant difference (95% CI) between adjacent categories marked with asterisk ($p<0.05$). Boxes represent the upper and lower quartile ranges, the black lines, the means, and the whiskers, the highest and lowest values within 1.5 times the interquartile range of the upper and lower quartiles. The circles represent outliers within 3 times the interquartile range of the upper and lower quartiles. ANOVAs indicate significant differences between age categories for most species (H. lar: p-value=0.000, F=32.668, df=2; P. pygmaeus: p-values=0.000, F=20.085, df=2; P. paniscus: p-value=0.000, F=20.294, df=2; P. troglodytes: p-value=0.000, F=10.294, df=2; G. gorilla: p-value=0.000, F=109.05, df=2; H. sapiens: p-value=0.000, F=109.05, df=2).

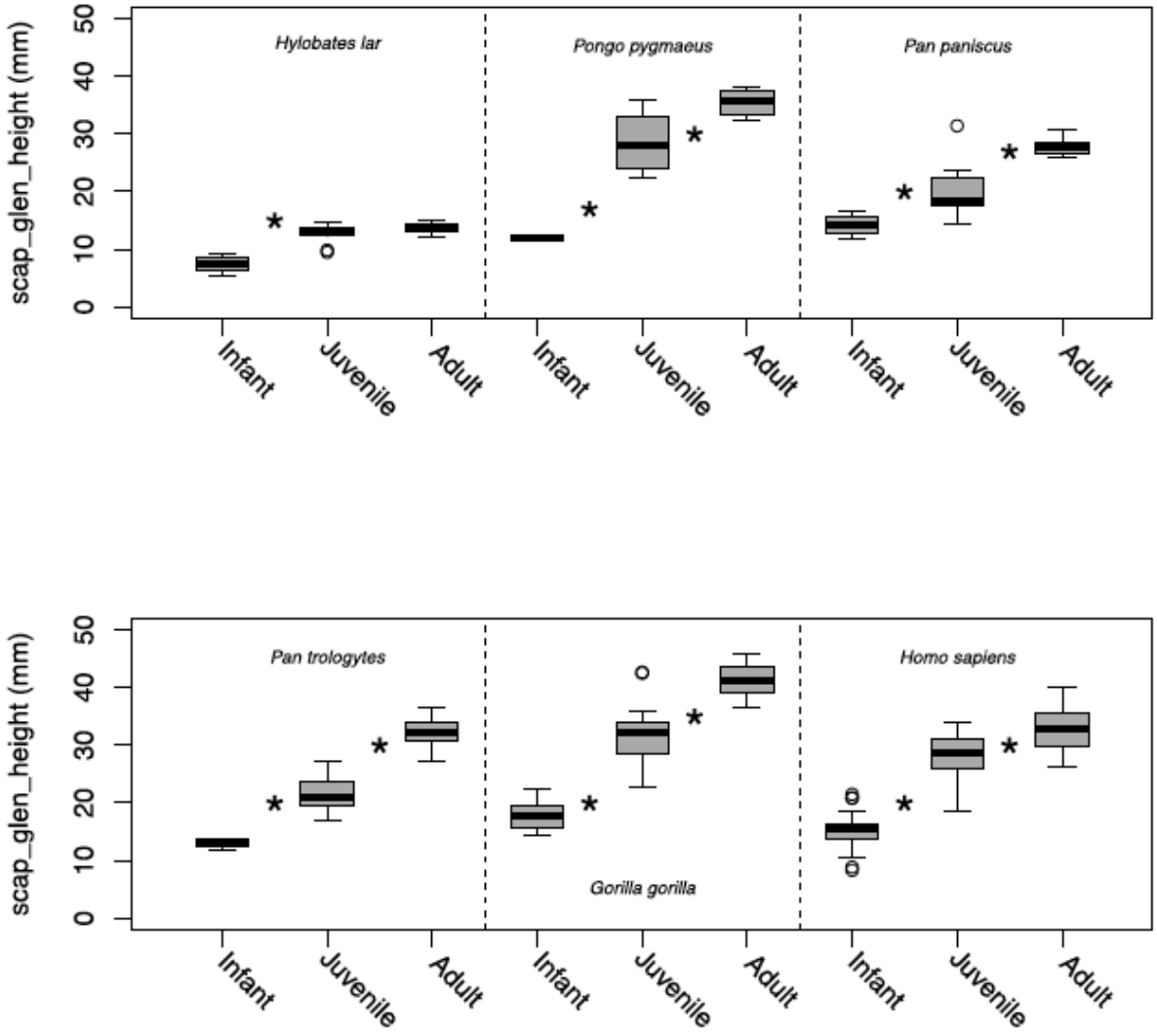

Figure 82 – Boxplots of infant, juvenile and adult hominoid specimens. Significant difference (95% CI) between adjacent categories marked with asterisk ($p<0.05$). Boxes represent the upper and lower quartile ranges, the black lines, the means, and the whiskers, the highest and lowest values within 1.5 times the interquartile range of the upper and lower quartiles. The circles represent outliers within 3 times the interquartile range of the upper and lower quartiles. ANOVAs indicate significant differences between age categories for most species (H. lar: p-value=0.000, F=31.387, df=2; P. pygmaeus: p-values=0.000, F=20.146, df=2; P. paniscus: p-value=0.000, F=21.606, df=2; P. troglodytes: p-value=0.000, F=106.1, df=2; G. gorilla: p-value=0.000, F=63.971, df=2; H. sapiens: p-value=0.000, F=214.34, df=2).

Table 35 – Table of ANOVA TukeyHSD post-hoc results of differences between age categories within species (size measurements), with adjusted p-values (p-adj) upper and lower bounds of the 95% confidence interval (lwr, upr), and difference between means (diff).

Measurement	Species	Age Categories		diff	lwr	upr	p-adj
scap_height	*H. lar*	Infant	Juvenile	24.442	15.857	33.026	**0.000**
		Juvenile	Adult	10.713	4.224	17.203	**0.001**
	P. pygmaeus	Infant	Juvenile	65.070	18.680	111.460	**0.008**
		Juvenile	Adult	24.975	-0.434	50.383	0.054
	P. paniscus	Infant	Juvenile	36.098	8.785	63.410	**0.009**
		Juvenile	Adult	42.875	20.976	64.774	**0.000**
	P. trog.	Infant	Juvenile	46.887	31.742	62.032	**0.000**
		Juvenile	Adult	50.596	39.739	61.453	**0.000**
	G. gorilla	Infant	Juvenile	70.406	50.316	90.497	**0.000**
		Juvenile	Adult	55.423	37.084	73.763	**0.000**
	H. sapiens	Infant	Juvenile	62.436	52.338	72.535	**0.000**
		Juvenile	Adult	21.547	12.375	30.718	**0.000**
scap_breadth_spine_glen	*H. lar*	Infant	Juvenile	26.319	18.979	33.659	**0.000**
		Juvenile	Adult	10.545	4.997	16.093	**0.000**
	P. pygmaeus	Infant	Juvenile	38.003	-8.988	84.993	0.116
		Juvenile	Adult	28.872	3.134	54.610	**0.029**
	P. paniscus	Infant	Juvenile	25.262	6.123	44.401	**0.009**
		Juvenile	Adult	25.661	10.316	41.007	**0.001**
	P. trog.	Infant	Juvenile	31.625	22.385	40.864	**0.000**
		Juvenile	Adult	31.473	24.850	38.097	**0.000**
	G. gorilla	Infant	Juvenile	46.577	34.775	58.380	**0.000**
		Juvenile	Adult	35.969	25.195	46.743	**0.000**
	H. sapiens	Infant	Juvenile	37.716	31.970	43.461	**0.000**
		Juvenile	Adult	13.778	8.571	18.986	**0.000**
scap_spine_length	*H. lar*	Infant	Juvenile	34.219	24.957	43.480	**0.000**
		Juvenile	Adult	14.763	7.762	21.764	**0.000**
	P. pygmaeus	Infant	Juvenile	66.841	28.700	104.981	**0.002**
		Juvenile	Adult	16.894	-3.997	37.784	0.116
	P. paniscus	Infant	Juvenile	32.880	7.001	58.758	**0.012**
		Juvenile	Adult	39.650	18.901	60.399	**0.000**
	P. trog.	Infant	Juvenile	41.848	27.964	55.732	**0.000**
		Juvenile	Adult	42.746	32.793	52.699	**0.000**
	G. gorilla	Infant	Juvenile	61.070	44.014	78.127	**0.000**
		Juvenile	Adult	55.345	39.774	70.915	**0.000**
	H. sapiens	Infant	Juvenile	54.130	44.993	63.267	**0.000**
		Juvenile	Adult	19.447	11.149	27.745	**0.000**

Table 35 cont'd – Table of ANOVA TukeyHSD post-hoc results of differences between age categories within species (size measurements), with adjusted p-values (p-adj) upper and lower bounds of the 95% confidence interval (lwr, upr), and difference between means (diff).

Measurement	Species	Age Categories		diff	lwr	upr	p-adj
scap_glen_width	*H. lar*	Infant	Juvenile	4.062	2.614	5.510	**0.000**
		Juvenile	Adult	0.414	-0.681	1.509	0.614
	P. pygmaeus	Infant	Juvenile	13.249	6.048	20.449	**0.001**
		Juvenile	Adult	2.491	-1.453	6.434	0.242
	P. paniscus	Infant	Juvenile	5.269	1.097	9.441	**0.012**
		Juvenile	Adult	5.266	1.921	8.610	**0.002**
	P. trog.	Infant	Juvenile	6.911	4.591	9.230	**0.000**
		Juvenile	Adult	6.670	5.007	8.333	**0.000**
	G. gorilla	Infant	Juvenile	10.854	7.991	13.717	**0.000**
		Juvenile	Adult	7.827	5.214	10.440	**0.000**
	H. sapiens	Infant	Juvenile	9.365	7.597	11.134	**0.000**
		Juvenile	Adult	3.812	2.209	5.415	**0.000**
scap_glen_height	*H. lar*	Infant	Juvenile	5.192	3.161	7.224	**0.000**
		Juvenile	Adult	1.118	-0.417	2.654	0.183
	P. pygmaeus	Infant	Juvenile	16.546	5.309	27.782	**0.006**
		Juvenile	Adult	6.930	0.775	13.084	**0.028**
	P. paniscus	Infant	Juvenile	6.120	0.775	11.465	**0.023**
		Juvenile	Adult	7.543	3.257	11.828	**0.001**
	P. trog.	Infant	Juvenile	8.802	5.558	12.047	**0.000**
		Juvenile	Adult	10.586	8.260	12.911	**0.000**
	G. gorilla	Infant	Juvenile	14.131	9.236	19.025	**0.000**
scap_glen_height	*G. gorilla*	Juvenile	Adult	10.334	5.866	14.802	**0.000**
	H. sapiens	Infant	Juvenile	13.009	10.765	15.253	**0.000**
		Juvenile	Adult	4.486	2.452	6.520	**0.000**

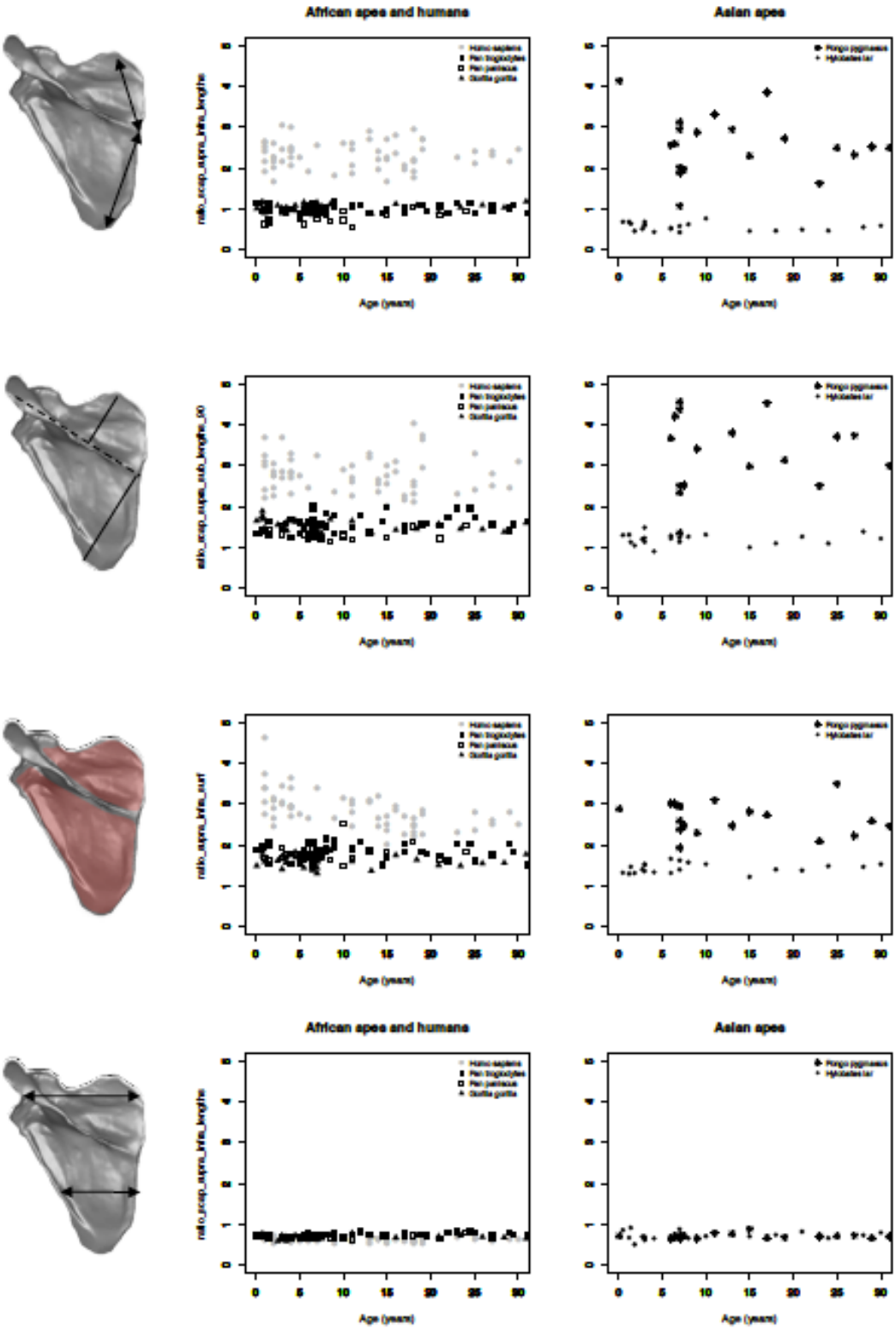

Figure 83 – Gompertz growth curves fitted to the sample distributions for all hominoid species (ratios). The ratios are obtained by dividing the infraspinous measurement by the supraspinous measurement in all instances. High ratios indicate relatively smaller supraspinous measurements relative to the infraspinous measurements, while small ratios indicate larger supraspinous measurments relative to the infraspinous measurements.

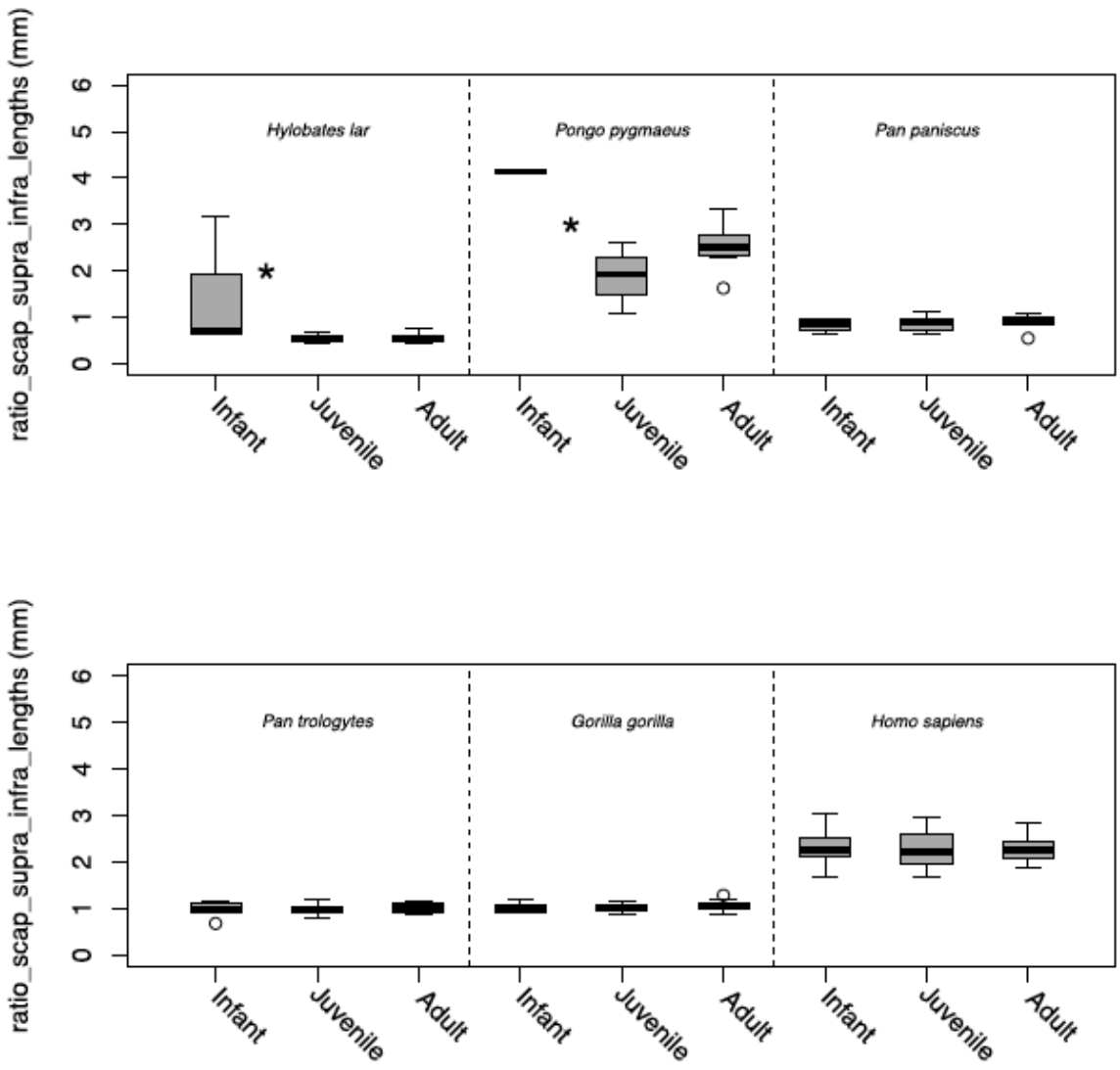

Figure 84 – Boxplots of infant, juvenile and adult hominoid specimens. Significant difference (95% CI) between adjacent categories marked with asterisk ($p<0.05$). Boxes represent the upper and lower quartile ranges, the black lines, the means, and the whiskers, the highest and lowest values within 1.5 times the interquartile range of the upper and lower quartiles. The circles represent outliers within 3 times the interquartile range of the upper and lower quartiles. ANOVAs indicate a lack of significant differences between age categories for most species (H. lar: p-value=0.031, F=4.127, df=2; P. pygmaeus: p-values=0.011, F=7.281, df=2; P. paniscus: p-value=0.748, F=0.294, df=2; P. troglodytes: p-value=0.729, F=0.318, df=2; G. gorilla: p-value=0.318, F=1.183, df=2; H. sapiens: p-value=0.719, F=0.330, df=2).

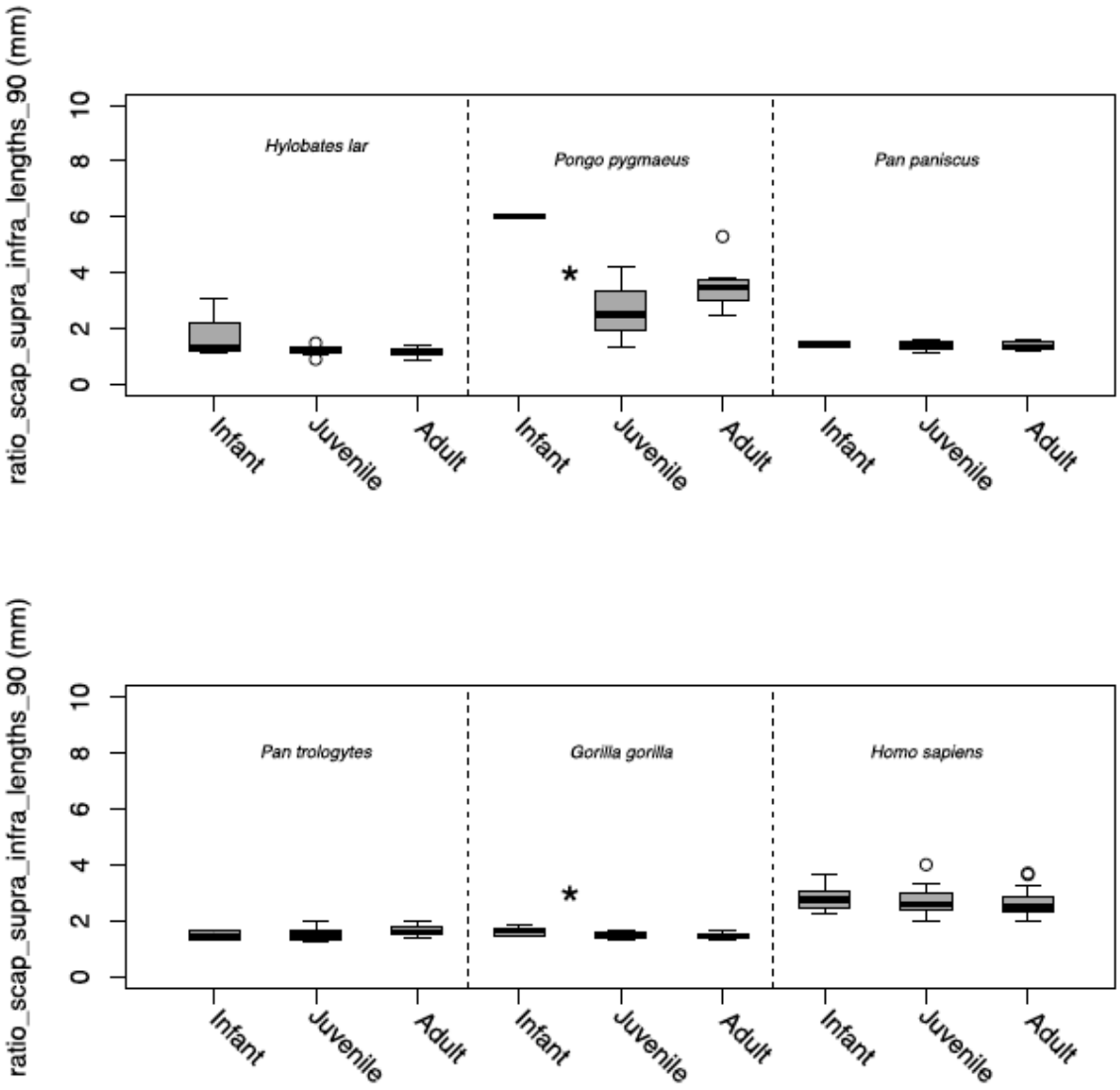

Figure 85 – Boxplots of infant, juvenile and adult hominoid specimens. Significant difference (95% CI) between adjacent categories marked with asterisk ($p<0.05$). Boxes represent the upper and lower quartile ranges, the black lines, the means, and the whiskers, the highest and lowest values within 1.5 times the interquartile range of the upper and lower quartiles. The circles represent outliers within 3 times the interquartile range of the upper and lower quartiles. ANOVAs indicate a lack of significant differences between age categories for most species (H. lar: p-value=0.055, F=3.317, df=2; P. pygmaeus: p-values=0.028, F=5.141, df=2; P. paniscus: p-value=0.849, F=0.164, df=2; P. troglodytes: p-value=0.206, F=1.639, df=2; G. gorilla: p-value=0.005, F=6.193, df=2; H. sapiens: p-value=0.093, F=2.438, df=2).

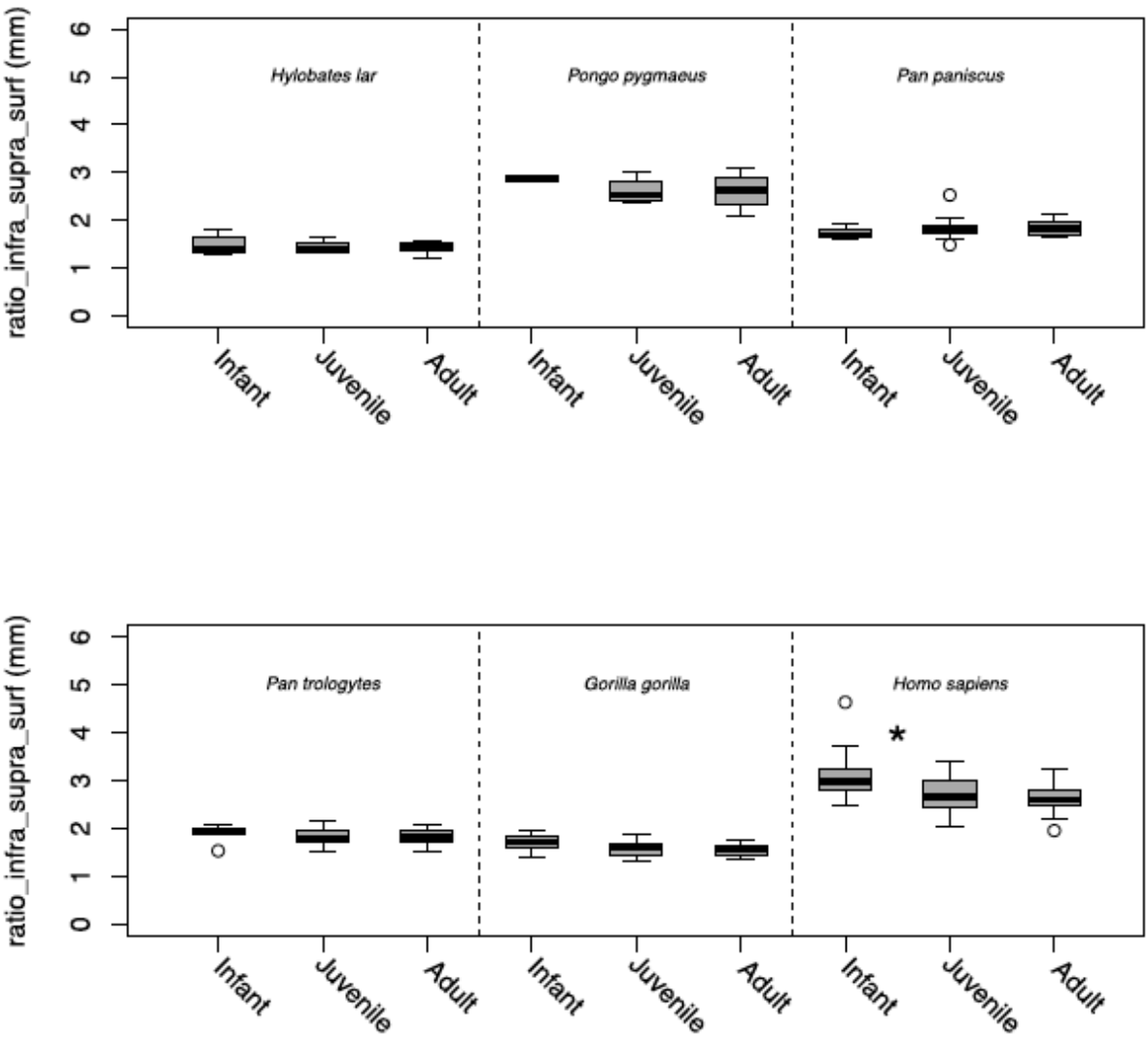

Figure 86 – Boxplots of infant, juvenile and adult hominoid specimens. Significant difference (95% CI) between adjacent categories marked with asterisk ($p<0.05$). Boxes represent the upper and lower quartile ranges, the black lines, the means, and the whiskers, the highest and lowest values within 1.5 times the interquartile range of the upper and lower quartiles. The circles represent outliers within 3 times the interquartile range of the upper and lower quartiles. ANOVAs indicate a lack of significant differences between age categories for most species (H. lar: p-value=0843, F=0.171, df=2; P. pygmaeus: p-values=0.753, F=0.291, df=2; P. paniscus: p-value=0.623, F=0.485, df=2; P. troglodytes: p-value=0.758, F=0.278, df=2; G. gorilla: p-value=0.111, F=2.345, df=2; H. sapiens: p-value=0.000, F=15.869, df=2).

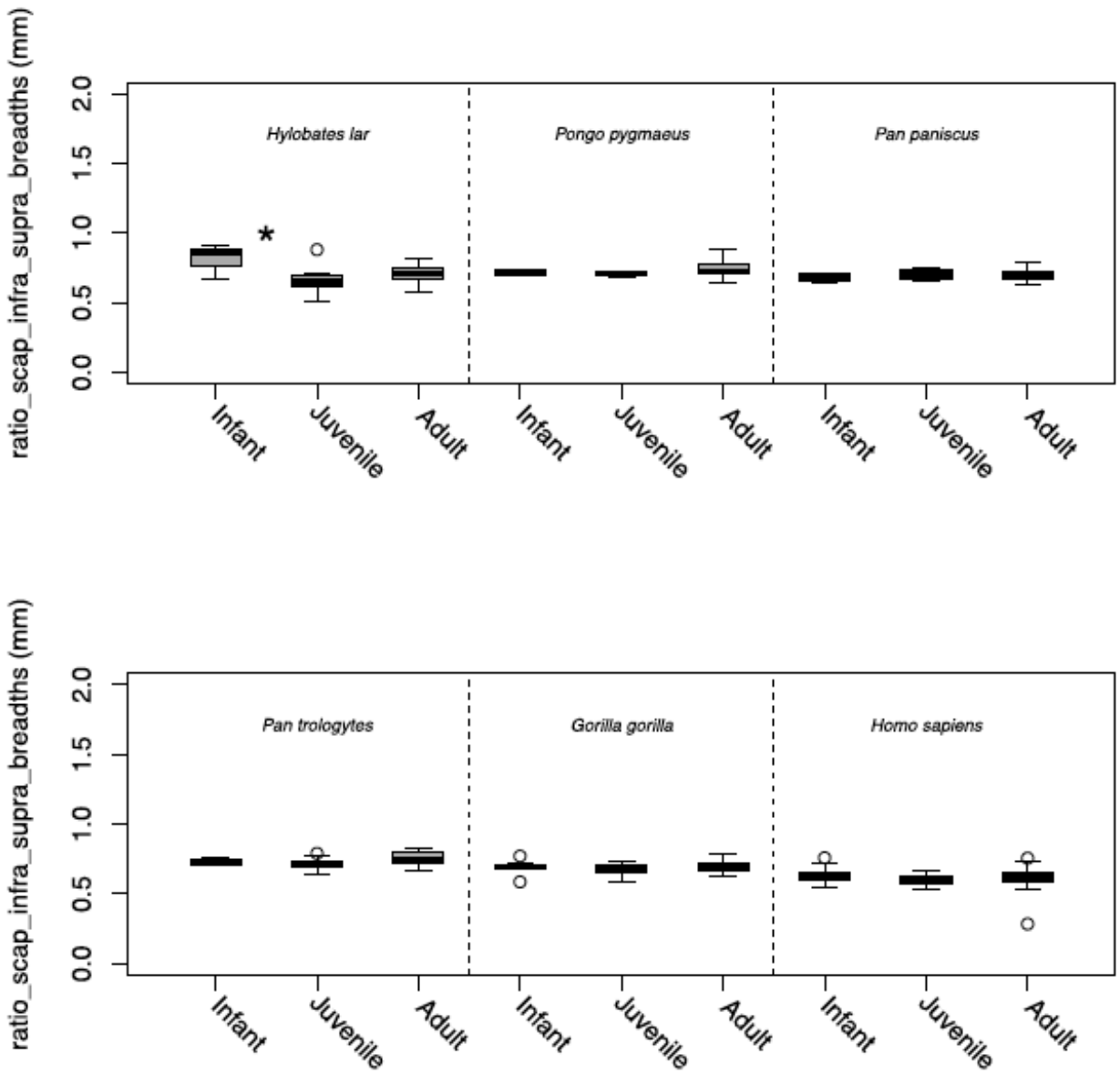

Figure 87 – Boxplots of infant, juvenile and adult hominoid specimens. Significant difference (95% CI) between adjacent categories marked with asterisk ($p<0.05$). Boxes represent the upper and lower quartile ranges, the black lines, the means, and the whiskers, the highest and lowest values within 1.5 times the interquartile range of the upper and lower quartiles. The circles represent outliers within 3 times the interquartile range of the upper and lower quartiles. ANOVAs indicate a lack of significant differences between age categories for most species (H. lar: p-value=0.05, F=3.65, df=2; P. pygmaeus: p-values=0.631, F=0.482, df=2; P. paniscus: p-value=0.522, F=0.671, df=2; P. troglodytes: p-value=0.0286, F=3.899, df=2; G. gorilla: p-value=0.203, F=1.669, df=2; H. sapiens: p-value=0.136, F=2.038, df=2).

Table 36 – Table of ANOVA TukeyHSD post-hoc results of differences between age categories within species (ratios), with adjusted p-values (p-adj) upper and lower bounds of the 95% confidence interval (lwr, upr), and difference between means (diff).

Measurement	Species	Age Categories		diff	lwr	upr	p-adj
ratio_scap_supra_infra_lengths	*H. lar*	Infant	Juvenile	-0.75	-1.46	-0.04	**0.037**
		Juvenile	Adult	0.004	-0.53	0.541	1.000
	P. pygmaeus	Infant	Juvenile	-2.25	-3.89	-0.61	**0.009**
		Juvenile	Adult	0.632	-0.26	1.529	0.181
	P. paniscus	Infant	Juvenile	0.018	-0.21	0.249	0.978
		Juvenile	Adult	0.045	-0.14	0.231	0.810
	P.trog.	Infant	Juvenile	0.005	-0.12	0.135	0.996
		Juvenile	Adult	0.029	-0.06	0.122	0.735
	G. gorilla	Infant	Juvenile	0.016	-0.07	0.110	0.911
		Juvenile	Adult	0.043	-0.04	0.129	0.444
	H. sapiens	Infant	Juvenile	-0.05	-0.26	0.148	0.790
		Juvenile	Adult	-0.00	-0.18	0.183	0.999
ratio_scap_supra_infra_lengths	*H. lar*	Infant	Juvenile	-0.51	-1.08	0.044	0.074
		Juvenile	Adult	-0.02	-0.45	0.401	0.988
	P. pygmaeus	Infant	Juvenile	-3.38	-6.29	-0.46	**0.024**
		Juvenile	Adult	0.888	-0.70	2.483	0.321
	P. paniscus	Infant	Juvenile	-0.04	-0.26	0.174	0.872
		Juvenile	Adult	-0.00	-0.18	0.168	0.996
	P.trog.	Infant	Juvenile	0.036	-0.22	0.296	0.938
		Juvenile	Adult	0.126	-0.06	0.312	0.237
	G. gorilla	Infant	Juvenile	-0.14	-0.26	-0.02	**0.018**
		Juvenile	Adult	-0.03	-0.15	0.073	0.676
	H. sapiens	Infant	Juvenile	-0.13	-0.40	0.135	0.459
		Juvenile	Adult	-0.08	-0.33	0.156	0.662
ratio_infra_supra_surf	*H. lar*	Infant	Juvenile	-0.03	-0.24	0.182	
		Juvenile	Adult	-0.01	-0.17	0.145	
	P. pygmaeus	Infant	Juvenile	-0.26	-1.30	0.765	
		Juvenile	Adult	0.000	-0.56	0.565	
	P. paniscus	Infant	Juvenile	0.129	-0.21	0.471	
		Juvenile	Adult	-0.01	-0.28	0.261	
	P.	Infant	Juvenile	-0.06	-0.28	0.154	
		Juvenile	Adult	-0.00	-0.16	0.153	
	G. gorilla	Infant	Juvenile	-0.11	-0.26	0.041	
		Juvenile	Adult	-0.02	-0.16	0.114	
	H. sapiens	Infant	Juvenile	-0.39	-0.61	-0.16	
		Juvenile	Adult	-0.07	-0.27	0.134	

Table 36 cont'd– Table of ANOVA TukeyHSD post-hoc results of differences between age categories within species (ratios), with adjusted p-values (p-adj) upper and lower bounds of the 95% confidence interval (lwr, upr), and difference between means (diff).

Measurement	Species	Age Categories	diff	lwr	upr	p-adj
ratio_scap_infra_supra_breadths	*H. lar*	Infant	Juvenile	-0.157	-0.305	-0.008
		Juvenile	Adult	0.050	-0.050	0.151
	P. pygmaeus	Infant	Juvenile	-0.010	-0.195	0.175
		Juvenile	Adult	0.035	-0.066	0.137
	P. paniscus	Infant	Juvenile	0.020	-0.039	0.078
		Juvenile	Adult	0.008	-0.039	0.055
	P. troglodytes	Infant	Juvenile	-0.028	-0.076	0.020
		Juvenile	Adult	0.038	0.003	0.072
	G. gorilla	Infant	Juvenile	-0.021	-0.061	0.019
		Juvenile	Adult	0.025	-0.011	0.062
	H. sapiens	Infant	Juvenile	-0.031	-0.068	0.006
		Juvenile	Adult	0.012	-0.022	0.045
		Juvenile	Adult	0.012	-0.022	0.045
ratio_infra_supra_surf	*H. lar*	Infant	Juvenile	-0.032	-0.247	0.182
		Juvenile	Adult	-0.017	-0.179	0.145
	P. pygmaeus	Infant	Juvenile	-0.268	-1.301	0.765
		Juvenile	Adult	0.000	-0.566	0.565
	P. paniscus	Infant	Juvenile	0.129	-0.213	0.471
		Juvenile	Adult	-0.014	-0.288	0.261
	P. troglodytes	Infant	Juvenile	-0.064	-0.282	0.154
		Juvenile	Adult	-0.003	-0.160	0.153
	G. gorilla	Infant	Juvenile	-0.113	-0.268	0.041
		Juvenile	Adult	-0.027	-0.168	0.114
	H. sapiens	Infant	Juvenile	-0.393	-0.618	-0.168
		Juvenile	Adult	-0.070	-0.275	0.134
ratio_scap_infra_supra_breadths	*H. lar*	Infant	Juvenile	-0.157	-0.305	-0.008
		Juvenile	Adult	0.050	-0.050	0.151
	P. pygmaeus	Infant	Juvenile	-0.010	-0.195	0.175
		Juvenile	Adult	0.035	-0.066	0.137
	P. paniscus	Infant	Juvenile	0.020	-0.039	0.078
		Juvenile	Adult	0.008	-0.039	0.055
	P. troglodytes	Infant	Juvenile	-0.028	-0.076	0.020
		Juvenile	Adult	0.038	0.003	0.072
	G. gorilla	Infant	Juvenile	-0.021	-0.061	0.019
		Juvenile	Adult	0.025	-0.011	0.062
	H. sapiens	Infant	Juvenile	-0.031	-0.068	0.006
		Juvenile	Adult	0.012	-0.022	0.045

3.2. Boxplots

When the scapular angle data is split into age categories, ANOVA results show that there are significant differences between age categories ($p<0.05$) across species for the spine_angle_medborder and for the glen_angle_medborder measurements (with the exception of Pongo, likely because of very small sample size) (figures 71-76). However, post-hoc tests indicate that only humans show significant differences ($p<0.05$) between age categories for 4 out of the 6 measurements: spine_angle_medborder, spine_angle_medborder, glen_angle_latborder and latborder_spine_angle tests (figures 71-76; table 33). There are also significant differences between infant and juvenile gibbons for 3 of these 6 measurements: spine_angle_medborder, spine_angle_medborder, and latborder_spine_angle. The bonobos show significant differences between infant and juvenile specimens in the spine_angle_medborder measurement (figures 71; table 33) and gorillas show differences between infants and juveniles for the glen_angle_medborder measurement (figure 72; table 33). There are no significant differences between age categories for any species in the glen_angle_spine and glen_version measurements (figures 74 & 76; table 33).

Overall these results suggest that humans do deviate from the ape pattern in that infants are consistently significantly different from the juveniles and adults for most measurements (all but the glen_angle_spine according to the ANOVA results), with the possible exception of gibbons, unlike the apes whose juvenile and adult values remain largely unchanged across measurements. These results also suggest that the more developmentally plastic angle measurements of the scapula across hominoids are the spine_angle_medborder and the glen_angle_medborder (figures 71 & 72).

For the size measurements, results show the presence of significant differences ($p<0.05$) between all age categories across species (figures 78-82; table 35). For the ratio measurements, results show the presence of significant differences in only a few cases (figures 84-87; table 36). In humans, there are only significant differences

($p<0.05$) between infant and juvenile specimens for the surface areas measurements (figure 86; table 36) but not lengths or breath (figure 84, 85, 87; table 36).

4. Discussion

4.1. Scapular angles: growth curves versus age categories

The results of this study show that there are discrepancies in results between both types of analyses for the angle measurements. Indeed while the Gompertz growth curves suggest the presence of ontogenetic changes in 4 out of the 6 angle measurements (spine_angle_medborder, glen_angle_medborder, glen_angle_spine and glen_version) across species (except for Pongo whose single neonate value prevents the curve from being fitted), dividing the data into age categories suggests, on the contrary, that there is little to no evidence of ontogenetic change in these measurements across species – except for the spine_angle_medborder and the glen_angle_medborder). Humans appear to be unique in showing significant changes between age caterogies for 4 of the 6 measurements (spine_angle_medborder, glen_angle_medborder, glen_angle_latborder, and latborder_spine_angle), as well as gibbons who show significant changes between age caterogies for 3 of the 6 measurements (spine_angle_medborder, glen_angle_medborder, and latborder_spine_angle) (figures 71-76; table 33).

This has important implications for functional interpretations, since depending on the type of analysis that is utilised, results lead to opposite conclusions about the presence or absence of ontogenetic changes in functionally relevant aspects of scapular morphology. For example, the present results indicate that the angle of the glenoid fossa's orientation relative to the lateral border (glen_angle_latborder) does not change throughout ontogeny in apes but does change in humans when the data is divided into age categories (figure 73), as is also shown by Green and Alemseged (2012) (but see Green 2013). However, according to the present growth curves, changes in ontogeny in humans seem to be negligible (unable to fit a Gompertz curve)

while there seem to be changes in the bonobo and gorilla samples (figure 70). While the former analysis would lead to the conclusion that this trait is ontogenetically conserved in apes and that humans are unique in deviating from this pattern, the growth curves indicate otherwise – i.e., that humans do not show marked ontogenetic changes in this trait and are not unique relative to the apes. Similarly, dividing the data into age categories suggests that there are no changes in the angulation of the glenoid fossa relative to the scapular spine (glen_angle_spine) in any of the species (figure 74), but the Gompertz growth curves do indicate the presence of ontogenetic changes in most species apart from P. troglodytes, and Pongo (figure 70) in this measurement. The same is true for the glenoid version measurement (glen_version) where there are no significant differences between age categories in any species (figure 76), while the Gompertz curves suggest that changes exist across all species (except Pongo) (figure 77).

Overall, these results suggest that dividing the data into age categories highlights differences between specific age sets (namely the infants from the juveniles and adults), and distinguishes the humans from the apes in showing substantial ontogenetic changes between infancy and juvenility for most measurements. However, these differences are no longer observable for some of these measurements when growth curves are fitted to the distributions. Conversely, the Gompertz model does in many instances fit the ape distributions, but when the data is split into age categories, results indicate a lack of significant differences between age categories in apes in most instances. Overall, this suggests that dividing the data into age categories obscures some of the ontogenetic patterns that seem to be present in the apes, but enhances differences between developmental stages in humans, and leads to contrasting conclusion – namely that humans are unique in relation to the apes (when considering age categories) or that they follow the ape pattern in the development of these scapular traits (when considering the growth curves). It is possible that because of the longer life histories in humans, infant humans are skeletally more immature comparatively to the apes – human infants have downward-facing glenoid fossae in infants for example (figure 88) –, and thus produce more noticeable ontogenetic

differences when the data is divided into age categories, and in fact there are no instances where there are significant differences between juveniles and adults in the human sample (figures 71-76). This does not however, affect the plotting of the growth curves since these merely track the growth trajectories in these measurements and not the amount of change between ages. In this sense, both analyses can actually be considered complimentary to each other, since the lack of significant differences between age categories in apes species does not necessarily equate a complete lack of ontogenetic change in these scapular traits, but merely that these changes might not be substantial, or at least not as substantial as those seen for some measurements in humans.

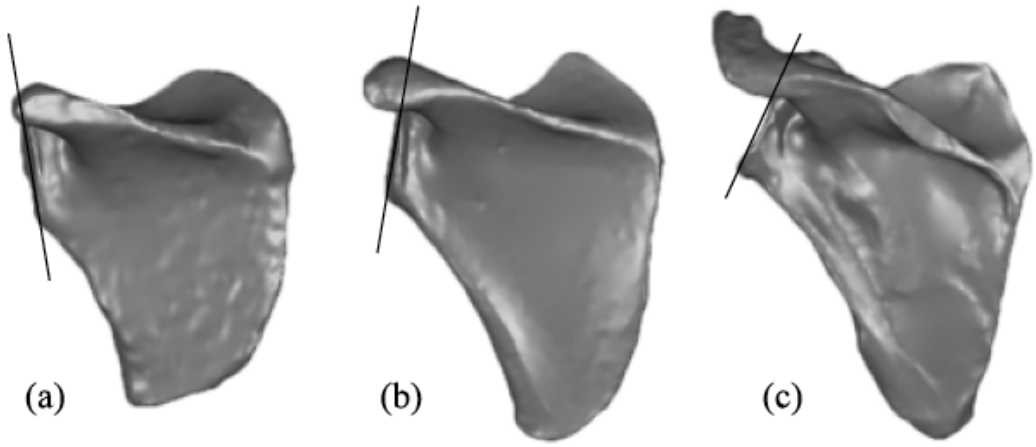

Figure 88 – 3D surface scan of left human infant (a), juvenile (b) and adult (c) scapulae, showing the downward rotation of the glenoid fossa in the infant human scapula. The glenoid fossa then becomes more cranially oriented with growth.

Interestingly, both analyses do however seem to agree that the angulation of the glenoid fossa and scapular spine relative to the medial border shows a clearer ontogentic signal than when the same structures are measured relative to the lateral border, with the Gompertz curves showing a clearer fit across species for the glen_angle_medborder and spine_angle_medborder (figures 70-72) than the glen_angle_latborder and latborder_spine_angle (figures 70, 73, 75). This is an

important observation especially since Green and Alemseged's (2012) conclusions about A. afarensis' locomotor repertoire rest on the observation that the glenoid fossa's angle in this species, just like in apes, remains unchanged throughout ontogeny. Based on their results, the authors thus conclude that the apelike shoulder joint configuration in A. afarensis throughout ontogeny indicates the presence of arboreal/climbing behaviours from infancy (Green and Alemseged 2012). Similarly, Green's (2013) study also finds a lack of ontogenetic change in scapular spine orientation in apes, with the exception of humans whose spines become more obliquely oriented throughout growth. However the current results show that this is only true when these angles are measured relative to the lateral border, because when they are measured from the medial border, my results suggest that in most cases the glenoid fossa and the scapular spine become more cranially oriented throughout ontogeny in apes as well as in humans. These results thus cast some doubt on Green and Alemseged's (2012) interpretations based on glenoid fossa orientation and rather indicate that just as in humans, apes also develop more cranially oriented glenoid fossae with age, perhaps as a result of increased size and arm use in humans and changing locomotor strategies throughout life in apes (Doran 1997; Doran 1992; Doran 1993a; Doran 1993b; Doran and Hunt 1996). Churchill et al (2013) suggest that angles based on the medial border are better indicators of glenoid fossa and spinal orientation than are angles based on the more commonly used lateral border because the long axis of the scapula is defined by the superior and inferior angles of the body which lies parallel to the vertebral column in humans, thus providing an indication of the anatomical orientation of the bone. If this is true, then glenoid fossa and scapular spine orientation are more adequately described relative to the medial border rather than the lateral border, and therefore the changes in ontogeny observed when using these angles are a more adequate measure of ontogenetic change in these variables. Consequently, interpretations about A. afarensis locomotor repertoire based on cranial orientation of the glenoid fossa could lead to different/opposite conclusions if measured instead from the medial border.

Differences between the types of analyses are also observed with regards to the ratio measurements. The inability to fit a Gompertz curve to these distributions suggests the proportion of the relationship of the supraspinous to the infraspinous size remains stable throughout ontogeny (figures 83), but ANOVAs suggest there are some instances where differences between age categories can be observed, but that this depends on the measurement used to quantify this ratio (figure 84-87; table 35).

Fitting Gompertz curves to measurements of the scapula that have a more straightforward relationship to size, such as lengths, widths and breadths (figures 77; table 34), further indicate that sample size is unlikely to be an issue for fitting the scapular angle measurements, since the model adequately fits all of the size measurements (except Pongo) (figures 77; table 34). Furthermore the size measurements of the scapula exhibit, as expected, a clearer ontogenetic signal with comparatively (to the angle measurements) more variation throughout growth (figures 77; table 34). Results also indicate the presence of significant differences between age categories across species across measurements (figures 78-82), in agreement with the growth curve data. These results show just how comparatively developmentally constrained the angle measurements are – which would partially explain the lack of significant differences when the samples are split into age categories. Interestingly, this is not the case for the latborder_spine_angle and the glen_angle_medborder measurements, which show substantial amounts of instraspecific variation (figure 70).

In sum, the Gompertz growth curves highlight the fact that these geometric properties of the scapula (glenoid fossa and scapular spine orientation) are generally developmentally plastic across species, even if the changes are very subtle, and that therefore dividing the data into age categories might not capture these subtle changes in most instances (except in humans where changes between infants and juveniles/ adults appear more substantial).

4.2. Scapular angles: ontogeny and implications for locomotion

The present results based on growth curves indicate that there are clearer ontogenetic changes in the orientation of the glenoid fossa and scapular spine relative to the medial border of the scapula across species compared to the lateral border (figure 70). These results suggest that the angles of both these structures relative to the lateral border may be more developmentally constrained, while their orientation relative to the medial border more developmentally plastic. This evidence suggests that measuring these angles this way may be more functionally relevant because the orientation of the medial border, unlike the lateral border, actually provides an indication of the anatomical orientation of the bone (Churchill et al. 2013). If this is the case the present study shows evidence of developmental changes in most species throughout ontogeny with the orientation of both the glenoid and spine becoming more obliquely oriented with age (although this is less clear when dividing the sample into age categories; figures 70-72). Evidence that there are ontogenetic changes in these two traits across hominoid species supports the existence of developmental plasticity in these structures in response to locomotor changes during an organism's lifetime (Ward 2002; Green 2013). Indeed, more cranially oriented glenoid fossae are thought to be more advantageous for orthograde suspensory locomotion because in this configuration the joint distributes strain more evenly (Hunt 1991; Green 2013). Similarly, a more oblique scapular spine is linked to the mechanical advantage of the trapezius and deltoid muscles and is thus more developed in taxa exhibiting greater amounts of orthograde suspensory activity (Taylor 1997; Green 2013). Although this is in line with evidence for changing locomotor strategies in apes (Doran 1997; Doran 1992; Doran 1993a; Doran 1993b; Doran and Hunt 1996), particularly in the more suspensory Pan and gibbons (Oxnard 1963, 1967; and Ashton and Oxnard 1964; Green 2013), the relationship between these specific morphological changes in these structures and locomotor changes across hominoid species is not entirely straightforward. For example, African apes become increasingly more quadrupedal and terrestrial with age (Doran 1997), in which case it would be expected that their glenoid fossae and scapular spines became less obliquely oriented with more laterally

oriented glenoid fossa with increasing age. The same is true of humans, who are essentially committed bipeds from the first year of life (Burnett and Johnson 1971a, 1971b; Hensinger 1986; Stanitski et al. 2000; Ruff 2003), in which case changes in these structures are not expected, at least not with relation to behaviour and locomotion in this species. It is possible on the other hand that the changing orientation of these structures relative to the medial border of the scapula are a product of changing body sizes and consequently increased muscle sizes independently of specific behaviours and locomotor types. If this is the case, then the relationship between ontogenetic changes in scapular morphology – at least with regards to the present geometric properties – are more complex than previously thought. Indeed, EMG analyses (Tuttle and Basmajian 1977; Larson et al. 1991) have shown that the cranial trapezius (attaching to the scapular spine) is relatively unimportant in arm-raising movements in large-bodied hominoids and its recruitment is more directly linked to head-turning motions (Larson et al. 1991). Because of the trapezius' role in head turning and head stabilisation movements, it is possible that the increasingly more oblique orientation of the scapular spine is instead a response to the greater need for head stabilisation movements in the face of increased body size, in both apes and humans. On the other hand, although African apes do become increasingly terrestrial with age, it is possible that the need to maintain suspensory adaptations in the shoulder is the principal selective pressure shaping these aspects of scapular morphology. In order words, it may be more important for African apes to have scapulae well adapted to suspensory locomotion even though they may engage in this type of locomotion less frequently, because it is a more physically demanding locomotor strategy. If this is the case, then it would be advantageous for these species to possess increasingly more cranially oriented spines and glenoid fossae with age for dealing with the demands of suspensory locomotion. Indeed, according to Doran's (1997) observations, adult chimpanzees spend less that 20% of their time engaging in arboreal activities, yet they possess a narrow scapula remarkably adapted to suspensory behaviour, which maximize the range of rotation so that during arm-hanging the glenoid fossa approaches a point more directly over the centre of gravity (Hunt 1991).

In addition, it is also possible that other aspects of shoulder morphology may influence changes in the orientation of the glenoid fossa and scapular spine (i.e., thorax shape and clavicle length/position). For example, Corrigan (1959) finds that in humans, the neonate clavicle is positioned slightly higher and more anteriorly due to the elevated position of the shoulder and the rotundity of the thorax in neonates. The author finds that the relatively large sagittal diameter of the thorax in newborn humans results in a more ventrally directed glenoid cavity compared to that in adults – which may be why, functionally, it is more appropriate to crawl before walking (Ljunggren 1979). Similarly, the same may be true of apes – i.e., that the cranial rotation of the glenoid fossa is a by-product of changes in scapular position on the thorax with age. Unfortunately the issue of scapular position and mobility is not entirely well understood as is the complex relationship between clavicle, thorax and scapula and its variation among primates of diverse locomotor behaviours (Chan 2007a,b). The boxplots and ANOVAs however, only show the presence of significant changes between age categories in humans, gibbons and bonobos (for scapular spine orientation) (figure 71) and humans, gibbons and gorillas (for glenoid fossa orientaion) (figure 72). In these instances where significant changes can be observed, the differences are between the infant and the juvenile stages suggesting that changes in spine and glenoid fossa orientation, where they exist, undergo the greatest amount of change during the transition between infancy to juvenility, consistent with the idea that thoracic shape changes may have an effect on the orientation of these structures. However, the boxplots do not show any differences between age categories in P. troglodytes for either measurement, which is curious given their size and locomotor repertoire (figures 71-72).

Interestingly, these measurements exhibit varying degrees of intraspecific variation: the angle of the spine relative to the lateral border shows more variation than when the spine is measured relative to the medial border, which seems to be more constrained (figure 70). Conversely, the angle of the glenoid fossa relative to the lateral border shows less intraspecific variation than when this angle is measured

relative to the medial border (figures 70). Overall, this seems to indicate that although both the scapular spine and the glenoid fossa show a clearer ontogenetic signal when measured relative to the medial border, the spine's orientation in relation to this axis is less variable across individuals than is the orientation of the glenoid fossa in relation to this same axis. Conversely, there doesn't appear to be much developmental plasticity in the orientation of the glenoid and spine relative to the lateral border, which suggests that these angles are rather developmentally constrained, possibly for biomechanical reasons; however, results suggest a tighter constraint on the glenoid fossa's orientation. These results suggest that these angles may not be as useful for functional interpretations.

The Gompertz curves also indicate the presence of ontogenetic changes in glenoid version (glen_version) and in the angle of the glenoid fossa relative to the scapular spine (glen_angle_spine) (figure 70) across species, although the boxplots do not indicate that these differences are substantial between age stages in any sample, not even in humans (figure 76-77). In fact, these are the only two measurements that do not show differences between infant and juvenile humans. These results suggest that although there are slight ontogenetic changes in these angles across species, they are overall quite developmentally conserved, which is all the more evident when considering the amount of intraspecific variation across samples for both measurements – as can be seen in the Gompertz graphs (figure 70). Perhaps because the relationship of the glenoid fossa to the scapular spine is biomechanically important (because it determines the angle of pull of the trapezius and deltoid), there is a need for this angle to remain relatively stable throughout growth across hominoids. Similarly, because glenoid version, which relates to the anterior (ventral) or posterior (dorsal) displacement of the glenoid fossa relative to the scapular body, is important for glenohumeral stability, it also appears to be rather conserved throughout ontogeny. In humans marked anteversion and retroversion of the glenoid fossa in the plane has been associated to anterior/posterior translation of he humerus and rotator cuff injuries (Nyffeler et al 2006). Given the physical demands of suspensory/arboreal

behaviours, it is not surprising that this angle should be more developmentally constrained.

Lastly, infraspinous-to-supraspinous scapular ratios show that these proportions remain rather constant throughout ontogeny in all species, regardless of how the dimensions are measured (figure 83). Although I was unable to fit a Gompertz growth curve to the distributions, results seem to show a possible decrease in infra- to supraspinous surface area in humans, which is evident when the data is split into age categories (figure 86) with the supraspinous fossa becoming relatively larger in relation to the infraspinous fossa. However this does not appear to be true of apes. Additionally, these results show that humans deviate from the apes, except for Pongo, in having comparatively smaller supraspinous fossa relative to their infraspinous fossae. This is line with recent evidence, which also describe similarities between Homo and Pongo in these proportions (Young 2008; Larson and Stern 2013; Bello-Hellegouarch et al. 2013). Namely, Bello-Hellebouarch et al (2013) suggest that the resemblance between Pongo and Homo offers evidence that the last common ancestor of the human–chimpanzee clade likely showed an overall suspensory shoulder girdle pattern (see also: Crompton et al. 2008; 2010; Kivell and Schmitt 2009; McHenry 1986; Oxnard 1984; Thorpe et al. 2007) instead of a knuckle-walker structure, as has been suggested (Begun 1992; Corruccini and McHenry 2001; Orr 2005; Richmond and Strait 2000; Richmond et al. 2001; Williams 2010). Larson and Stern (2013) however, caution that even though there are osteological similarities in these ratios between these two species, soft tissue data (EMG data and data on muscle mass and physiological cross sectional area [PCSA]), shows that orangutans do not have particularly small supraspinatus muscles or particularly large infraspinatus muscles, contrary to what would be expected given the high scapular infra- to supraspinous fossa ratios.

The present results also indicate that breadth measurements are substantially more conserved than surface areas and height dimensions in all instances, suggesting that the scapula's morphology in this dimension is more constrained (figure 83). These

results are interesting, especially in light of the suggestion that scapular spine orientation determines the shape and size of the infra- and supraspinous fossae, in which case changes in these ratios would be expected to follow changes in spine orientation. It is possible that differences in how the orientation of the scapula is measured may be responsible: in the present study the orientation of the spine was measured from the spine itself, whereas Larson and Stern (1986) and Larson (1995) instead measure the position of the base of the spine, which forms the boundary between the supra- and infraspinous fossae. It is possible that while the spine itself progressively moves more cranially, the base of the spine remains stable, which would be congruent with the general lack of ontogenetic change in scapular infra- and supraspinous fossa proportions. Future work should investigate whether this is indeed the case. Notwithstanding, these results seem to indicate that the relative sizes of scapular fossae in hominoids are overall developmentally stable and do not seem to accompany changes in locomotor strategies (i.e., shifts between more suspensory infants to more terrestrial adults in P. troglodytes and G. gorilla). It is important to note however, that recent analyses have demonstrated that a substantial amount of information about soft tissues is lost in osteological analyses (Bello-Hellegouarch et al. 2013) and that relative scapular fossa size is not in fact a good predictor of either the relative masses or cross-sectional areas of the rotator cuff muscles in apes, and relative fossa size gives a false impression of the importance of individual rotator cuff muscles to locomotor differences among apes (Larson and Stern 2013).

5. Conclusions

This study investigated the ontogeny of scapular angle measurements in hominoids and whether humans deviate from the ape pattern, as has been recently suggested (Green and Alemseged 2012). This study also explored whether differences between methods influence such functional interpretations. This topic was chosen because it bears important implications for the interpretation of functional and locomotor interpretations in fossil hominins (Green and Alemseged 2012).

My results show that the angulation of the glenoid fossa and scapular spine seem to show some developmental plasticity – becoming progressively more cranially oriented with growth – when these angles are measured relative to the medial border. This has important implication for the interpretation of fossil specimens, for which the orientation of the glenoid fossa is typically measured relative to the lateral border of the scapula. My own results suggest that this angle may be more developmentally constrained, and thus less functionally informative, at least in ontogenetic contexts; functional interpretation based on this latter measurement may thus mislead us to conclude that the orientation of the glenoid and spine are not developmentally plastic in apes.

This study also highlights how differences in analyses lead to different and even contradictory functional interpretations about the ontogenetic development of these scapular traits. Differences between the Gompertz growth curves and boxplots/ ANOVAs may however be useful in combination, since the lack of significant differences between age categories does not necessarily mean a complete lack of developmental plasticity, but rather that the changes are not substantial enough that they are captured when dividing the data into blocks. This is especially relevant in the case of traits that may be more constrained/less plastic due to their biomechanical/ functional properties, such as might be the case with regards to the geometric properties of the scapula's angles.

These results also do not support that humans are derived relatively to the apes, but rather support the relatively immaturity of the infant human scapula compared to that of apes – namely humans seem to possess a downward facing glenoid fossa at birth, which may simply reflect a lack of ossification of the glenoid fossa in these very young individuals, thus giving the false impression that glenoid orientation changes more substantially in this species compared to apes.

Overall, this study highlights the importance of ontogeny for making interpretations about locomotion and function in extant and extinct fossils. Namely, some of my

results contradict Green and Alemseged's (2012) observation of a lack of ontogenetic changes in glenoid fossa and scapular spine orientation in apes. Green's (2013) more recent study also somewhat contradicts his earlier finding, by showing the presence of ontogenetic differences in glenoid fossa orientation in Gorilla, Pongo and Macaca (as well as humans) when using a different age categorisation, which highlights the importance of analytical and methodological choices in the study of ontogeny, namely in how age is quantified.

However, Green and Alemseged's (2012) highlight a more important question about what the relationship between ontogeny and locomotion is, since in essence, they associate the presence of ontogenetic changes in morphology to a lack of ontogenetic changes in locomotion (Homo sapiens), while associating the absence of ontogenetic changes in morphology to the presence of locomotor shifts throughout growth (great apes and A. afarensis); they then take the lack of ontogenetic changes in the australopithecine scapula as evidence of this species' active engagement in arboreal locomotion. This seems contradictory and highlights how much we still need to understand about the link between ontogeny and function. My own results also suggest that ontogenetic changes (or lack thereof) in scapular properties does not fall in line with ontogenetic shifts in locomotion in hominoids – for example, an increasingly more cranial scapular spine is not in line with increased terrestrial quadrupedalism in apes – which also suggests that the link between ontogeny and locomotion is complex and needs further understanding.

– Chapter 8 –

Conclusions: what can the shoulder tell us about the mode of locomotion of the LCA of all hominoids?

The present study looked at the ontogeny, phylogeny and functional anatomy of the hominoid shoulder girdle. The main focus of the project dealt with aspects of ontogenetic change in the shoulder elements for the purpose of determining whether shared similarities in the shoulder joint of hominoids are more likely to be a product of homology (shared ancestry) or homoplasy (parallel evolution). Phylogenetic analyses were also conducted in the case of humeral torsion and clavicular curvatures – in the former, because humeral torsion is often discussed in the context of locomotor ancestry, and in the latter because clavicular curvatures have rarely been studied in a cross comparative context. I also included a chapter on the bilateral asymmetry of the humerus in order to address questions about the link between bone morphology/plasticity and individual behaviour.

1. Summary of results

1.1. Ontogeny: what can it tell us about morphology and function?

First and foremost, this study investigates whether the anatomical similarities in extant hominoid shoulder structures arise through similar developmental processes in order to assess whether they have arisen through shared ancestry or through parallel evolution. The project is particularly innovative in that it utilises Approximate Relative Dental Ages (ARDAs) based on X-ray images and histological sections of mandibular dentition (as per Dean and Wood's [1981] atlas method) to obtain an ontogenetic series for all non-human hominoid samples, as well as in the application of Gompertz growth curves to these samples in order to compare growth between elements within species, and within elements between species.

Overall my results provide a more detailed understanding of ontogenetic change in shoulder morphology across hominoid species, and demonstrate (1) high levels of plasticity in key diagnostic traits of hominoid shoulder morphology (such as humeral torsion and the distal curvature of the clavicle), and (2) a relative lack of phenotypic plasticity in other key traits (such as the proximal curvature of the clavicle and glenoid-axillary angle of the scapula). Specifically, my results show that humeral torsion in non-human hominoid primates develops throughout ontogeny and ceases around adulthood, and is the first study to establish this. This study shows that differences in the timing and expression of torsion between species appear with growth and match remarkably well with on the one hand (a) species locomotor repertoire, phylogenetic relationships, size and life history, and on the other hand, (b) changing locomotor patterns through life in the different species. The study also finds that macaques develop torsion in an entirely opposite way to that of hominoids: by reducing torsion throughout growth rather than increasing it, in order to achieve similar forearm positioning due to differences in scapular positioning. Most crucially, these divergent patterns between *Macaca* and hominoids indicate opposite relationships between torsion and locomotion in these clades, with relatively high torsion in hominoids relating to pronogrady/quadrupedalism, and relatively low torsion relating to orthograde suspensory behaviours, while in New World and Old World monkeys it is relatively low torsion that relates to pronogrady/quadrupedalism and relatively high torsion that relates to orthograde suspensory behaviours. This has important implications for the interpretation of locomotion from fossil postcranial remains, and particularly so for stem hominoid fossils who are expected to present a mosaic of shoulder characteristics that are both ape-like and monkey-like. However, because I propose that it is low torsion, rather than high torsion, that is the functionally significant condition in hominoids, and that this trait is related to suspension/climbing behaviours, my results can neither support or reject the independent or shared derivation of knuckle-walking in hominoids, and instead suggest that high torsion in African apes and humans arises as a by-product of decreased frequencies of orthograde suspensory/climbing activities and by

consequence, the greater importance of pronograde/quadrupedal locomotion – but not knuckle-walking specifically.

With regards to the clavicle's curvatures, the present findings suggest that the clavicle is both partially developmentally plastic and partially ontogenetically conserved, contradicting the traditional view that the clavicle is ontogenetically stable. While on the one hand there are visible changes in clavicular curvature across hominoids, on the other hand, clavicular curvatures remain proportionally stable relative to each other and to clavicular length throughout growth, with adult curvatures being established around the time the clavicle ceases growing in length. This suggests that the clavicle's curvatures are genetically constrained to a certain extent, and suggests that there are elements of the clavicle that are structurally conserved throughout ontogeny.

Finally, with regards the scapula, my results show that the angulation of the glenoid fossa and scapular spine are developmentally plastic to a certain extent – becoming slightly more cranially oriented with growth – when these angles are measured relative to the medial border, which contradicts recent suggestions that the orientation of these structures is completely developmentally stable in apes but not humans. This has important implication for the interpretation of fossil specimens, for which the orientation of the glenoid fossa is typically measured relative to the lateral border of the scapula. My own results suggest that the glenoid fossa and scapular spine's orientation relative to the lateral border may be more developmentally constrained, and thus less functionally informative, at least in ontogenetic contexts. Functional interpretation based on this latter measurement may thus mislead us to conclude that the orientation of the glenoid and spine are not developmentally plastic at all in apes. However, relative to other traits such as the distal curvature of the clavicle and humeral torsion, the glenoid-axillary angle of the scapula is much less developmentally plastic with less intra-specific variation.

1.2. Phylogeny: the application of Phylogenetic Comparative Methods for assessing postcranial evolution

I used Phylogenetic Comparative Methods (PCMs) to discern clade-specific patterns in the evolution of hominoid clavicle morphology and humeral torsion. In particular, I used the new method of 'Independent Evolution' (IE; Smaers and Vinicius, 2009; Smaers et al, 2012, 2013), to map phenotypic change in humeral torsion across individual branches of a phylogeny with the aim of identifying processes such as convergence and mosaic evolution within the skeleton. I also used Phylogenetic Generalized Least Squares (PGLS) regressions in the analysis of clavicular anatomy.

Results of these phylogenetic analyses suggest that despite the large amounts of intra-specific variation, levels of humeral torsion in early hominins are sufficiently distinct from that of extant great apes and humans, and therefore this trait can be explained as a symplesiomorphic character in early hominin species – retained from the LCA of hominoids –, and a parallelism between the great apes and humans – thus supporting the notion of parallel evolution of terrestrial quadrupedalism in the great apes, and specifically, the parallel evolution of knuckle-walking in the *Gorilla* and *Pan* stem lineages. However, because high levels of torsion are also found in *Pongo*, who are not knuckle-walkers, my results also support that torsion should not be discussed in the context of knuckle-walking specifically (Kivell and Schmitt 2009). My results also support that the high levels of torsion seen in modern humans are recently derived, possibly as a result of a reconfiguration of the shoulder girdle anatomy in this lineage (Larson 2007). Overall these result show that phenotypic plasticity and phylogenetic significance are not necessarily mutually exclusive concepts, since the incorporation of phylogenetic trait plasticity largely corroborates our understanding of the evolution of humeral torsion based on single fossil values.

With regards to the clavicle, my results suggest that the clavicle's curvatures significantly correlate with aspects of scapular morphology, in particular the orientation of the scapular spine relative to the glenoid fossa, as well as to the size of

the clavicle and shoulder. Moreover, results indicate that the proximal curvature is more often associated with elements of size, and that the distal curvature is more often associated to functional aspects of shoulder morphology related to mobility and stability. These results seem to indicate that, on the one hand, the proximal curvature is phylogenetically conserved – perhaps because of its role in shoulder joint stability and in protecting the thoracic inlet –, while on the other hand, the distal curvature is more variable and plastic – perhaps because of its association with locomotion and arm elevation. The lack of correlation between proximal and distal curvatures further suggests the existence of a relative independence between distal and proximal clavicle curvatures in primates.

1.3. Functional Morphology of the hominoid shoulder: insights from ontogeny and phylogenetic analyses

In combination, my methodological approaches contribute significantly to our understanding of the functional morphology of the hominoid shoulder as a whole, and provide information that can be used to interpret extinct hominoid and hominid morphologies. Methodologically, the project is innovative in its quantification of shoulder traits by using 3D surface scans and 3D imaging software to measure surface areas, torsion, angles and curvatures. For example, I propose a new protocol for quantifying clavicular curvatures in 3D in my thesis – this is an important development since the clavicle has traditionally been a poorly studied bone in cross-comparative studies. Specifically, this study also sheds light on the functional and evolutionary significance of humeral torsion by proposing that it is low torsion, rather than high torsion, that is the functionally significant condition in hominoids, and that this trait is related to orthograde suspension/climbing behaviours, or more generally, to any locomotor behaviours involving frequent use of the arms in overhead movements/postures. The study also sheds light on the function of clavicular curvature, by showing the more plastic nature of the distal curvature, which matches hominoid species' locomotor repertoires. Importantly, the study also highlights how differences in the quantification of glenoid fossa and scapular spine orientation impact

functional and evolutionary interpretations by showing that the relationship of these structures to the lateral border is more developmentally constrained than their relationship to the medial border, which is more mechanically informative.

Additionally, information on bilateral asymmetry patterns in torsion and length of the humerus in humans and African apes shows that humans are unique in presenting a population-level right bias for both humeral length and torsion, consistent with population-level right-handedness, while the African apes show no significant directionality in either measurement. However, my results do show that absolute torsion asymmetries in apes occur in the same magnitude as in humans, suggesting the existence of functional lateralization at the individual level. These results thus suggest a link exists between behaviour and morphology discernible both at the individual and population levels, in both humans and African apes.

2. The locomotion of the LCA: what does the ontogeny of the hominoid shoulder tell us?

Overall, by distinguishing between those traits that are relatively more static in their development (like the orientation of the glenoid fossa) and those that are developmentally much more plastic (such as humeral torsion and possibly the distal curvature of the clavicle), this study is able to offer insight into those shoulder traits that are potentially more phylogenetically informative and thus more useful in distinguishing between homologies and homoplasies. For example, as above-mentioned, this study indicates that key functional aspects of scapular and clavicular morphology tend to be developmentally more stable (or more constrained on terms of their developmental plasticity); this is the case for the orientation of the glenoid fossa, which is associated with use of overhead arm movements (e.g., Stern Jr and Susman 1983; Inouye and Shea 1997), and the proximal clavicular curvature, which allows for the scapula to be dorsally positioned (Jenkins et al. 1978; Chan 2008). The fact that all hominoids apart from humans exhibit dorsally placed scapulae with long curved clavicles and cranially directed genoid fossae, coupled with the fact that these traits

are more developmentally conserved across hominoid species, suggests that these are likely to be inherited through common descent and thus homologous to all hominoids. The fact that australopithecines also exhibit cranially oriented fossae from infancy (Alemseged et al 2006; Green and Alemseged 2012) supports this suggestion. Consequently, these observations are in line with the behavioural observation that generalised orthograde clambering is the locomotor behaviour that characterises the positional behaviour of all hominoids (e.g., Hunt 1991; Thorpe and Crompton 2006; but see Begun et al 2007). This is in line with Crompton et al's (2008) suggestion that the mode of locomotion of the LCA of hominoids was likely primarily orthograde clambering, with hand-assisted bipedality and quadrupedalism on large branches, but not specifically suspensory locomotion (Crompton et al 2008).

However, these results highlight homologies in those structures necessary for those locomotor/postural behaviours that are more costly – i.e., those that place high stresses on the bone – and not necessarily the ones that are the most frequently used. For example, African apes spend 50-99% of their locomotor time on the ground (Tuttle and Watts 1985; Hunt, 1991, 1992; Doran, 1993,1996; Begun and Kivell 2011), but this is not reflected in their shoulder morphology. In fact, chimpanzees exhibit very clear adaptations for orthograde suspension, such as long narrow scapulae, robust clavicular anchors, anteroposteriorly flattened, and cranially oriented glenoid fossae, despite it being the less frequent activity (Hunt 1991). The fact that hominoids show relative developmental stability in shoulder features related to facilitating overhead movements and maintaining a dorsally placed scapula, suggests that these are selectively and behaviourally important traits (otherwise they would not have been conserved through phylogenetic history), but not necessarily the ones needed the most frequently. This is an important observation, especially when attempting to make sense of extinct morphologies. For example, it is possible that australopithecines were more frequently bipedal but that being efficient in the trees was selectively more important. In this sense, the retention of traits associated to arboreality in this genus is neither evidence of 'phylogenetic baggage' nor evidence of a life mainly spent in the trees, but they simply reflect selection for maintaining those

structures associated to the more costly behaviours. In fact, studies have suggested that anatomical adaptations in apes are directed towards avoidance of falls (Pontzer and Wrangham 2004; Thorpe and Crompton 2006) since large animals are less likely to survive if they fall from any great height (Cartmill and Milton 1977). However, natural selection tends to shape anatomy to reduce muscular activity and structural stress in relation to the frequency of the behaviour (Basmajian, 1965; Cartmill et al., 1987; Hunt, 1991b, 1992) such that "positional behaviours for which an animal is well-adapted to are expected to require less muscle activity, and induce less stress in the skeleton and ligaments, than behaviours for which the animal is poorly adapted" (Thorpe and Crompton 2006:394). Given that being efficient in the trees is selectively more important than being efficient on the ground – because suspensory postures are more energetically expensive than terrestrial pronograde postures due to the effects of gravity and the discontinuous 3D environments – it is therefore likely that adaptations to the former will be more evident in the ape skeleton (Thorpe and Crompton 2006). In this sense, the fact that shoulder traits adapted to orthograde suspensory postures are developmentally and structurally homologous in hominoids indicates that this behaviour is the most selectively important for this clade, but this is not necessarily a reflection of the postural/locomotor behaviours that are most frequently used among hominoid species. In any case, this certainly suggests a common inheritance of these features from a LCA who must have been, at least partially, engaging in orthograde suspensory behaviours.

In contrast, my results demonstrate that humeral torsion is very much developmentally plastic with large degrees of intraspecific variation in hominoids, thus making it a good variable for inferring actual frequency of locomotion but not for distinguishing between behavioural homologies and homoplasies. Even though humeral torsion has often been used in the context of discussing the evolution of knuckle-walking as either a homology or homoplasy (Washburn 1967; Richmond and Strait 2000; Richmond et al. 2001; Begun 2004), my results show that torsion levels differentiate among hominoid species throughout growth due to the relative action of the medial and lateral rotators and according to differences in scapular positioning,

and thus reflect locomotor differences between species that develop during life. This indicates that mechanistically, this trait is homologous to all hominoid species, even though structurally this appears not to be the case. In fact, it is precisely this shared developmental mechanism that allows us to use this trait to look at differences in levels of activity between individuals of the same species (as in the case of *Pongo*; see Sarmiento 1985) and to look at differences in activity between limbs within individuals (Pieper 1998; Crockett et al. 2002; Osbahr et al. 2002; Whiteley et al. 2008, 2010; Taylor et al. 2009; Myers et al. 2009; Schwab and Blanch 2009). This suggests that on its own, humeral torsion is a poor indicator of shared behavioural ancestry and should not be used to make inferences about the locomotion of the LCA of hominoids – at least not on its own and in the absence of fossil evidence to provide a wider context. Indeed, when phylogenetic and fossil information is incorporated, my results suggest that despite the large amounts of intraspecific variation, levels of humeral torsion in early hominins are sufficiently distinct from that of extant great apes and humans that it supports the notion of parallel evolution of terrestrial quadrupedalism in the great apes, and specifically, the parallel evolution of knuckle-walking in the *Gorilla* and *Pan* stem lineages. However, because high levels of torsion are also found in *Pongo*, who are not knuckle-walkers, my results also support that torsion should not be discussed in the context of knuckle-walking specifically (Kivell and Schmitt 2009).

In sum, results of this study suggest that whereas on the one hand developmentally stable traits are useful in distinguishing homologies from homoplasies but not in determining frequency of behaviour during life, on the other hand, developmentally plastic traits are more likely to reflect actual frequency of behaviours during life and because of this are less useful in distinguishing homologies from homoplasies. In combination, both types of traits can help make sense of the morphological variations in shoulder anatomy between hominoid species: all hominoids are adapted to a life in the trees but depending on their greater or lesser frequencies of terrestrial pronograde locomotion, species' morphologies will be either more specialised for those arboreal behaviours (i.e., gibbons), or more 'compromised' in their anatomy (i.e. African apes)

to allow for successfully exploiting a variety of niches. Indeed, Pontzer and Wrangham (2004) suggest that chimpanzees and gorillas acquired their terrestrial knuckle-walking behaviours as a response to canopy fragmentation to access their typically ground-based fallback foods (Thorpe et al 2009). Recent evidence also suggests the same may be the case for *Pongo* who travel terrestrially more often than has been previously thought (Loken et al 2013; Ancrenaz et a; 2014). Loken et al (2013) suggest that this may be related to energy-efficiency since travelling on the ground is a more cost-efficient choice for the large bodied orangutan given the distribution of support structures and food resources. Moreover, the fossil relative taxa of *Pongo* are also thought to have used more ground locomotion than the extant *Pongo* (Begun and Kivell 2011; Harrison and Chivers 2006) which has in turn led to the suggestion that ancestral orangutans may have been able to cover larger distances on the ground (Von Koenigswald; 1982; Wich et al 2009). Overall, this suggests that knuckle-walking in African apes and fist-walking in orangutans may be a energetically-efficient and common locomotion choice for large bodied suspensory animals to move around terrestrially – this locomotor flexibility allows the large bodied hominoids to exploit a variety of niches and adapt to habitat changes and food availability.

3. Homology versus homoplasy: is plasticity an issue?

This study operated on the premise that (a) homologies reflect evolutionary changes arising from similar developmental processes, (b) parallelisms reflect developmental processes that may have diverged, and (c) convergences reflect divergent developmental processes (Hall 2003). However, because this study looked at development within the hominoid clade, convergences were not observed, and therefore results showed either the effect of homology or parallelism.

My results suggest that while developmentally stable traits are likely to be useful in distinguishing homologies from homoplasies (parallelism), developmentally plastic traits and those traits with large degrees of intra-specific variation are less useful in

this context because they are more likely to reflect actual frequency of locomotion and activity during life rather that reflect shared ancestry. Indeed, there is a fair amount of plasticity in the postcranial skeleton in general since bones change in size and shape throughout life in response to a variety of stimuli (multiple genes with multiple effects [pleiotropism], and a large number of non-genetic influences [Cheverud 1982; Atchley and Hall 1991; Herring 1993; Lieberman 1992]) which means that the ontogeny of morphological features can be highly mosaic and dissociated from phylogeny (Lieberman 1999). For example, Lieberman (1996) suggests that it is unlikely that measurements of bone thickness are ever good characters for phylogenetic analyses because phylogenetically irrelevant stimuli can elicit similar morphological responses. This may explain why reconstructing phylogenies from skeletal elements tends to be problematic (Zelditch et al. 1995; Monteiro 2000; Brehm et al. 2001; Naylor and Adams 2001; MacLeod and Forey 2002; Rohlf 2002; Hoekstra et al. 2004; Lockwood et al. 2004; Lycett and Collard 2005; Michaux et al. 2007; Cardini and Elton 2008; González-José et al. 2008; Polly 2001), especially in the case of the postcranial skeleton (e.g., Young 2003).

This suggests that developmental plasticity in traits may be a problem for assessing homologies because these traits are less likely to carry a phylogenetic signal. Harvati and Weaver (2006), for example, tested the reliability of morphological evidence from three regions of the cranium – face, temporal bone and vault – in tracking population history by comparing morphological distances among recent human groups and found that both the vault and the temporal bone shape preserved a stronger phylogenetic signal while facial shape seemed to be affected both by climatic factors and population history. However, studies based on the analysis of multiple primate species (e.g., Wood and Lieberman 200) and on human populations (e.g., Cramon-Taubadel 2009, 2014) found that even those regions of the cranium that are more plastic like, for example, those subject to masticatory-induced stress, were indeed significantly more variable than non-masticatory regions but were no less reliable for reconstructing primate phylogenetic relationships when subjected to parsimony analysis or inferring human population history. The same may be true of the

postcrania, which has typically been assumed to reflect postural and locomotor adaptations rather than phylogenetic relationships (Arias-Martorell et al., 2012; Lockwood, 1999; Pilbeam, 1996; Young, 2005) and it is now clear that many aspects of postcranial anatomy may reflect phylogenetic information to the same extent as the cranium (e.g. Betti et al., 2012, 2013; Lycett & von Cramon-Taubadel, 2013; Young, 2005). Our own results based on torsion suggest that despite the large amounts of intra-specific variation, levels of humeral torsion in early hominins are sufficiently distinct from that of extant great apes and humans that this trait can be explained as a symplesiomorphic character in hominins and a parallelism between the great apes and humans. This suggests that phenotypic plasticity and phylogenetic significance are not necessarily mutually exclusive, since the incorporation of phylogenetic trait plasticity largely corroborates our understanding of the evolution of humeral torsion based on single fossil values.

In this sense, trait plasticity and developmental plasticity are only problematic when trying to reconstruct phylogenies from morphological traits in the absence of *a priori* phylogenetic information. This illustrates the strength and advantage of using the current method – 'Independent Evolution' (IE) (Smaers and Vinicius 2009; Smaers et al. 2012, 2013) – because rather than 'removing', 'controlling' or 'accounting' for a phylogenetic signal, morphological traits are 'mapped' onto the existing phylogeny itself, thereby highlighting processes of adaption (including homoplasies) occurring across the branches of a phylogeny. Furthermore, it is possible to account for intra-specific variation and single fossil values by using a re-sampling technique and by reporting Standard Deviations associated with the estimated rates and ancestral values. This means that homologies, as well as homoplasies, can be identified regardless of trait plasticity. In fact, I would argue that this type of analysis is particularly interesting for analysing highly plastic traits, as highly conserved traits are expected to simply follow the known phylogenetic relationships. But how much plasticity is too much plasticity? As demonstrated in the humeral torsion analyses, there are varying degrees of uncertainty on different branches of the phylogeny (for example, *Pongo* is such a case), meaning that the reliability of the estimates varies

according to the degree of trait plasticity and levels of intra-specific variation. Although this may be problematic when attempting to reconstruct ancestral traits at specific nodes (depending on the degree of uncertainty associated with these estimates), this method allows for identifying clade-wide patterns in the evolution of developmentally plastic traits. The extent to which these traits are informative will largely depend on the amount of plasticity exhibited in particular traits, but results of this study show that even highly plastic postcranial traits like humeral torsion can be analysed in this context.

But how do we reconcile developmental plasticity and ontogeny in the context of identifying homologies versus homoplasies? This study shows that once phylogenetic relationships are known, developmental plasticity is useful to assess whether traits develop via homologous developmental processes or via divergent developmental processes because it sheds light on the developmental mechanisms and not just the developmental sequences by which morphologies grow – which is generally considered to be a better measure of homology (Lieberman, 1999). However, because homoplasies are often the result of compromises between intrinsic factors, such as genetic constraints, and extrinsic factors, imposed by the environment (Lockwood and Fleagle 1999), closely related taxa will tend to find similar morphological solutions to similar ecological challenges. This is particularly relevant when considering parallelisms, as is the case with hominoid morphologies, and for this reason, Lieberman (1999:147) describes parallelisms as "a particularly pernicious form of homoplasy because the similarities are, by definition, developmentally homologous". This is precisely the case with our own results: although in adults, humeral torsion levels appear to be structurally homoplastic, when looking at its development, this trait appears to be developmentally homologous (since the levels of torsion are largely similar at birth in all species and differentiate throughout life). It therefore appears unlikely that there truly exist developmentally homoplastic traits within closely related taxa as is the case with hominoids, but rather traits essentially exhibit varying degrees of homology. For this reason it may be more productive to think about 'homology versus homoplasy' processes as part of a continuum rather than a

dichotomy, as suggested by Hall (2007; 2012), because the more phylogenetically recent the last common ancestor, the greater the likelihood of phenotypic similarity. Given this, it is unlikely that any one morphological trait will be useful in addressing questions about homology/homoplasy and locomotor ancestry in the hominoid clade. The strength and originality of the current project is that it used a variety of shoulder metrics that have all been analysed 1) from an ontogenetic perspective, 2) within a phylogenetic context, and 3) in a cross comparative framework, thus demonstrating that while the more developmentally stable traits provide evidence for selection for costly behaviours (which can be shared or not), the more developmentally plastic traits are informative of actual frequency of behaviour and underlying developmental mechanisms (which can be shared or not) – a distinction which had not previously been established. In combination, both types of traits can help make sense of the morphological variations in shoulder anatomy between hominoid species.

4. Conclusions and future directions

Overall, studying the underlying ontogenetic patterns in key functional aspects of shoulder morphology in hominoids reveals essential information about the evolution of orthograde suspensory versus pronograde terrestrial locomotion in this clade, and makes sense of the majority of intra and inter-specific variation seen in these traits in hominoids by revealing the mechanisms behind such variation. This corroborates the notion that ontogeny is an important component in studies of comparative anatomy and should continue to be further incorporated into the study of functional morphology. Overall, this study highlights the importance of ontogeny for making interpretations about locomotion and function in extant and extinct fossils, because it gives insight into how these functional structures develop. With the use of growth curves it is possible therefore to discern, in greater detail, varying degrees of (1) developmental plasticity, (2) instraspecific variation across time, and (3) inter-specific variation in growth and development in these traits. Using this method versus dividing the data into age categories can however lead to divergent and even contradictory functional (and evolutionary) interpretations. These differences in results highlight the

importance of analytical and methodological choices in the study of ontogeny, namely in how age is quantified. Importantly, this study suggests that the lack of significant differences between age categories does not necessarily equate a complete lack of ontogenetic changes in these traits, but merely that these changes might not be very substantial. This may be particularly relevant for traits that are more developmentally conserved (such as scapular spine and glenoid orientation) than other more plastic traits (such as humeral torsion). Future work could compare the present results with those derived from alternative schemes of age categorisation, such as dental maturity scores (e.g., Kuykendall, 1996), and should continue to integrate as much data of specimens of known age into dental aging techniques as possible in order to maximise the information that can be drawn from ontogenetic analyses.

In sum, this study contributes to existing discussions regarding the extent to which similarities in hominoid upper limb morphology have evolved independently or reflect an ancestral morphotype, as well as discussions regarding the mode of locomotion of the last common ancestor (LCA) of apes and humans. The functional implications resulting from the ontogenetic, phylogenetic and asymmetry analyses should therefore have important implications for the interpretation of fossil specimens. Future work should continue to explore the use of growth curves in the study of ontogeny, and the incorporation of Phylogenetic Comparative Methods in the study of hominoid postcranial evolution.

Moreover, it is likely that no one morphological trait is sufficient to address the issue of homology versus homoplasy or questions about locomotor ancestry in the hominoid clade, and this study highlights the importance of placing structures in the context of whole anatomical areas. Future studies considering the whole shoulder/or whole joints will be instrumental in better understanding form-function relationships in complex joints such as the shoulder. Particularly, if these can incorporate *in vivo* behavioural data on how joints move as a unit.

This study also highlights the importance of analytical and methodological choices in the study of ontogeny. Further studies should focus on determining how age categorisations affect conclusions about ontogeny and development. Namely, future studies should explore how much ontogenetic change constitutes ‘significant’ change, and when these ontogenetic changes between species are sufficient for us to determine whether traits are developmentally homologous or not. Finally, the acquisition and integration of more and more detailed behavioural data from the field will be instrumental in reliably testing hypothesis of form-function relationships in the context of evolutionary adaptation.

– Appendix 1 –

Table of specimens.

Species	Specimen	Collection	RDA	Sex	Side
Macaca fascicularis	AS 1678	Zurich	2.50	M	L
Macaca fascicularis	PAL 41	Zurich	2.50	M	L
Macaca fascicularis	PAL 36	Zurich	3.50	M	L
Macaca fascicularis	PAL 38	Zurich	3.50	F	L
Macaca fascicularis	PAL 40	Zurich	3.50	M	L
Macaca fascicularis	PAL 33	Zurich	4.00	M	L
Macaca fascicularis	PAL 18	Zurich	5.00	M	L
Macaca fascicularis	PAL 31	Zurich	5.00	M	L
Macaca fascicularis	PAL 30	Zurich	6.50	F	L
Macaca fascicularis	PAL 32	Zurich	6.50	M	L
Macaca fascicularis	PAL 39	Zurich	6.50	M	L
Macaca fascicularis	8851	Zurich	7.00	F	L
Macaca fascicularis	9308	Zurich	7.00	F	L
Macaca fascicularis	9325	Zurich	7.00	F	L
Macaca fascicularis	9553	Zurich	7.00	F	L
Macaca fascicularis	10125	Zurich	7.00	M	L
Macaca fascicularis	10136	Zurich	7.00	M	L
Macaca fascicularis	10139	Zurich	7.00	M	L
Macaca fascicularis	10140	Zurich	7.00	M	L
Macaca fascicularis	10574	Zurich	7.00	M	L
Macaca fascicularis	13483	Zurich	7.00	F	L
Hylobates lar	1575	Zurich	0.52	F	L
Hylobates lar	1634	Zurich	0.52	F	R
Hylobates lar	1633	Zurich	1.22	F	L
Hylobates lar	1655	Zurich	1.42	M	L
Hylobates lar	1628	Zurich	1.86	F	L
Hylobates lar	1629	Zurich	2.74	F	L
Hylobates lar	1631	Zurich	3.00	M	L
Hylobates lar	1639	Zurich	3.00	F	L
Hylobates lar	10220	Zurich	3.00	M	L
Hylobates lar	1630	Zurich	4.08	M	L
Hylobates lar	1619	Zurich	6.00	M	L
Hylobates lar	1627	Zurich	6.00	M	R
Hylobates lar	1632	Zurich	7.00	F	L
Hylobates lar	7566	Zurich	7.00	-	L
Hylobates lar	1580	Zurich	8.00	F	L
Hylobates lar	1581	Zurich	8.00	F	L
Hylobates lar	1582	Zurich	8.00	F	L
Hylobates lar	1583	Zurich	8.00	F	L

Table of specimens cont'd.

Species	Specimen	Collection	RDA	Sex	Side
Hylobates lar	1608	Zurich	8.00	M	L
Hylobates lar	1609	Zurich	8.00	M	L
Hylobates lar	1610	Zurich	8.00	M	L
Hylobates lar	1611	Zurich	8.00	F	L
Hylobates lar	1612	Zurich	8.00	M	L
Hylobates lar	1616	Zurich	8.00	M	L
Pongo pygmaeus	2004.953	NHM	0.10	-	L
Pongo pygmaeus	1901/1	Munich	7.00	-	L
Pongo pygmaeus	1907/379	Munich	7.50	M	R
Pongo pygmaeus	1907/483	Munich	11.00	F	R
Pongo pygmaeus	1907/486	Munich	11.00	M	R
Pongo pygmaeus	1907/607	Munich	-	-	L
Pongo pygmaeus	1907/614	Munich	11.00	M	R
Pongo pygmaeus	1907/621	Munich	-	-	L
Pongo pygmaeus	1907/625	Munich	-	F	L
Pongo pygmaeus	1907/626	Munich	-	F	L
Pongo pygmaeus	1907/628	Munich	-	-	L
Pongo pygmaeus	1907/629a	Munich	-	F	L
Pongo pygmaeus	1907/633b	Munich	11.00	F	L
Pongo pygmaeus	1907/634	Munich	-	M	L
Pongo pygmaeus	1907/636	Munich	11.00	F	R
Pongo pygmaeus	1907/643	Munich	-	-	L
Pongo pygmaeus	1907/644	Munich	-	-	L
Pongo pygmaeus	1907/646	Munich	7.00	F	R
Pongo pygmaeus	1907/648	Munich	-	-	L
Pongo pygmaeus	1907/649	Munich	11.00	-	R
Pongo pygmaeus	1907/652a	Munich	-	-	R
Pongo pygmaeus	1907/660	Munich	11.00	F	L
Pongo pygmaeus	1909/841	Munich	11.00	M	R
Pongo pygmaeus	1914/1551	Munich	6.50	M	R
Pongo pygmaeus	No Number	Munich	-	F	L
Pan paniscus	29003	Tervuren	1.00	-	R
Pan paniscus	11293	Tervuren	1.50	M	L
Pan paniscus	12087	Tervuren	3.00	M	L
Pan paniscus	23464	Tervuren	3.00	-	R
Pan paniscus	22336	Tervuren	3.50	-	R
Pan paniscus	29028	Tervuren	5.50	M	L
Pan paniscus	29058	Tervuren	5.50	M	R
Pan paniscus	29056	Tervuren	6.00	M	R
Pan paniscus	11528	Tervuren	6.50	F	L
Pan paniscus	22908	Tervuren	7.00	-	L

Table of specimens cont'd.

Species	Specimen	Collection	RDA	Sex	Side
Pan paniscus	5374	Tervuren	8.00	-	R
Pan paniscus	29053	Tervuren	8.50	M	R
Pan paniscus	23509	Tervuren	10.00	M	L
Pan paniscus	29047	Tervuren	10.00	M	R
Pan paniscus	29060	Tervuren	11.00	F	L
Pan paniscus	13201	Tervuren	11.00	F	R
Pan paniscus	15295	Tervuren	11.00	F	R
Pan paniscus	27696	Tervuren	11.00	M	R
Pan paniscus	27699	Tervuren	11.00	M	L
Pan paniscus	29052	Tervuren	11.00	M	R
Pan paniscus	15293	Tervuren	11.00	F	L
Pan paniscus	15296	Tervuren	11.00	F	L
Pan paniscus	15294	Tervuren	-	M	R
Pan troglodytes	CAM202	PCM	0.10	-	L
Pan troglodytes	M475 (2ND SERIES)	PCM	0.75	F	L
Pan troglodytes	1948.438	NHM	1.50	M	L
Pan troglodytes	M152	PCM	1.50	M	L
Pan troglodytes	M465	PCM	1.50	F	L
Pan troglodytes	29076	Tervuren	4.00	M	R
Pan troglodytes	1846.10.23.11	NHM	4.00	-	L
Pan troglodytes	M358	PCM	5.00	M	L
Pan troglodytes	M507	PCM	5.00	F	L
Pan troglodytes	559	Tervuren	5.50	F	L
Pan troglodytes	M675	PCM	5.50	M	L
Pan troglodytes	29072	Tervuren	6.00	M	L
Pan troglodytes	CAM118	PCM	6.00	M	L
Pan troglodytes	M881	PCM	6.00	F	L
Pan troglodytes	M94	PCM	6.00	M	L
Pan troglodytes	M145	PCM	6.50	F	L
Pan troglodytes	M363	PCM	6.50	M	L
Pan troglodytes	M454	PCM	6.50	F	L
Pan troglodytes	M746	PCM	6.50	M	L
Pan troglodytes	M801	PCM	6.50	M	L
Pan troglodytes	M805	PCM	6.50	F	R
Pan troglodytes	M636	PCM	7.00	M	L
Pan troglodytes	M170	PCM	7.50	M	L
Pan troglodytes	M274	PCM	7.50	F	L
Pan troglodytes	M382	PCM	7.50	F	L
Pan troglodytes	M455	PCM	7.50	M	L
Pan troglodytes	M371	PCM	8.00	F	L
Pan troglodytes	M52	PCM	8.00	M	L

Table of specimens cont'd.

Species	Specimen	Collection	RDA	Sex	Side
Pan troglodytes	458	Tervuren	9.00	F	L
Pan troglodytes	29077	Tervuren	9.00	M	L
Pan troglodytes	M506 (3RD SERIES)	PCM	11.00	F	L
Pan troglodytes	M676	PCM	11.00	F	L
Pan troglodytes	M677	PCM	11.00	F	L
Pan troglodytes	M706	PCM	11.00	F	L
Pan troglodytes	M720	PCM	11.00	F	L
Pan troglodytes	M724	PCM	11.00	M	L
Pan troglodytes	M707	PCM	11.00	M	L
Pan troglodytes	M712	PCM	11.00	M	R
Pan troglodytes	M440	PCM	11.00	M	L
Pan troglodytes	M272	PCM	11.00	M	L
Pan troglodytes	CAM II 62	PCM	11.00	M	R
Pan troglodytes	M506 (2ND SERIES)	PCM	11.00	F	R
Pan troglodytes	1976.436	NHM	-	F	L
Pan troglodytes	1976.437	NHM	-	F	L
Pan troglodytes	1981.749	NHM	-	F	L
Gorilla gorilla	M476	PCM	0.10	M	L
Gorilla gorilla	1948.437	NHM	0.75	F	L
Gorilla gorilla	22.12.19.3	NHM	0.75	-	L
Gorilla gorilla	FC129	PCM	0.75	M	R
Gorilla gorilla	M887	PCM	0.75	F	L
Gorilla gorilla	M756	PCM	1.00	M	L
Gorilla gorilla	M117	PCM	2.50	F	L
Gorilla gorilla	M409	PCM	3.00	F	L
Gorilla gorilla	M99	PCM	3.00	M	L
Gorilla gorilla	M333	PCM	3.50	F	L
Gorilla gorilla	M471	PCM	3.50	M	L
Gorilla gorilla	M880	PCM	3.50	F	L
Gorilla gorilla	M463	PCM	4.50	M	R
Gorilla gorilla	M855	PCM	4.50	F	L
Gorilla gorilla	1861.7.29.27	NHM	5.50	F	L
Gorilla gorilla	M160	PCM	5.50	F	L
Gorilla gorilla	M847 (series 1)	PCM	5.50	F	L
Gorilla gorilla	M667	PCM	6.50	F	L
Gorilla gorilla	M691	PCM	6.50	F	L
Gorilla gorilla	M841	PCM	6.50	F	L
Gorilla gorilla	MER.II.1	PCM	6.50	F	L
Gorilla gorilla	M180	PCM	7.00	F	L
Gorilla gorilla	M674	PCM	7.00	M	L
Gorilla gorilla	M689	PCM	7.00	M	L

Table of specimens cont'd.

Species	Specimen	Collection	RDA	Sex	Side
Gorilla gorilla	M875	PCM	7.00	F	L
Gorilla gorilla	M387	PCM	7.50	F	L
Gorilla gorilla	FC114	PCM	8.50	F	L
Gorilla gorilla	M342	PCM	11.00	M	L
Gorilla gorilla	M505	PCM	11.00	M	L
Gorilla gorilla	M89	PCM	11.00	M	L
Gorilla gorilla	M464	PCM	11.00	M	L
Gorilla gorilla	M717	PCM	11.00	M	L
Gorilla gorilla	M696	PCM	11.00	F	R
Gorilla gorilla	M340	PCM	11.00	M	L
Gorilla gorilla	M799	PCM	11.00	F	R
Gorilla gorilla	M138	PCM	11.00	F	R
Gorilla gorilla	M150	PCM	11.00	F	L
Gorilla gorilla	M136	PCM	11.00	F	R
Gorilla gorilla	M174	PCM	11.00	F	L
Gorilla gorilla	1864.12.1.3	NHM	-	-	L
Gorilla gorilla	1916.11.1.1	NHM	-	F	L
Gorilla gorilla	1962.6.25.1	NHM	-	M	L
Homo sapiens	2147	NHM	0.00	M	L
Homo sapiens	2242	NHM	0.00	M	R
Homo sapiens	2277	NHM	0.00	M	R
Homo sapiens	2834	NHM	0.00	M	L
Homo sapiens	81	Lisbon	1.00	M	L
Homo sapiens	2282	NHM	1.00	F	L
Homo sapiens	2582	NHM	1.00	M	R
Homo sapiens	2724	NHM	1.00	F	L
Homo sapiens	2737	NHM	1.00	F	L
Homo sapiens	2792	NHM	1.00	M	L
Homo sapiens	466	Lisbon	2.00	M	R
Homo sapiens	2206	NHM	2.00	M	R
Homo sapiens	2420	NHM	2.00	M	L
Homo sapiens	2431	NHM	2.00	M	R
Homo sapiens	2455	NHM	2.00	F	L
Homo sapiens	2735	NHM	2.00	M	L
Homo sapiens	2365	NHM	3.00	M	R
Homo sapiens	2456	NHM	3.00	F	L
Homo sapiens	2815	NHM	3.00	F	L
Homo sapiens	371	Lisbon	4.00	M	L
Homo sapiens	522	Lisbon	4.00	M	R
Homo sapiens	1399	Lisbon	4.00	M	L
Homo sapiens	2621	NHM	4.00	M	L

Table of specimens cont'd.

Species	Specimen	Collection	RDA	Sex	Side
Homo sapiens	2625	NHM	4.00	M	R
Homo sapiens	2845	NHM	4.00	M	R
Homo sapiens	338	Lisbon	5.00	F	L
Homo sapiens	389	Lisbon	6.00	M	L
Homo sapiens	385	Lisbon	7.00	M	R
Homo sapiens	2264	NHM	7.00	M	L
Homo sapiens	1200	Lisbon	9.00	F	R
Homo sapiens	2139	NHM	10.00	M	R
Homo sapiens	365	Lisbon	11.00	F	R
Homo sapiens	516	Lisbon	11.00	F	L
Homo sapiens	1579	Lisbon	11.00	M	L
Homo sapiens	1582	Lisbon	11.00	F	L
Homo sapiens	1584	Lisbon	11.00	M	L
Homo sapiens	291	Lisbon	13.00	M	L
Homo sapiens	2721	NHM	13.00	F	L
Homo sapiens	83	Lisbon	14.00	F	L
Homo sapiens	1564	Lisbon	14.00	M	L
Homo sapiens	1577	Lisbon	14.00	M	R
Homo sapiens	204	Lisbon	15.00	F	L
Homo sapiens	336	Lisbon	15.00	M	L
Homo sapiens	380	Lisbon	15.00	M	L
Homo sapiens	452	Lisbon	15.00	F	L
Homo sapiens	258	Lisbon	16.00	M	L
Homo sapiens	1566	Lisbon	16.00	F	R
Homo sapiens	1568	Lisbon	17.00	M	L
Homo sapiens	1570	Lisbon	17.00	M	L
Homo sapiens	2752	NHM	17.00	F	L
Homo sapiens	8	Lisbon	18.00	F	L
Homo sapiens	1403	Lisbon	18.00	F	L
Homo sapiens	1418	Lisbon	18.00	F	L
Homo sapiens	1587	Lisbon	18.00	M	L
Homo sapiens	1588	Lisbon	18.00	F	L
Homo sapiens	39	Lisbon	19.00	F	L
Homo sapiens	1565	Lisbon	19.00	F	L
Homo sapiens	2605	NHM	19.00	F	L
Homo sapiens	177	Lisbon	23.00	F	L
Homo sapiens	495	Lisbon	25.00	M	L
Homo sapiens	2720	NHM	25.00	M	L
Homo sapiens	276	Lisbon	27.00	F	L
Homo sapiens	2872	NHM	27.00	F	L
Homo sapiens	2459	NHM	29.00	F	L

Table of specimens cont'd.

Species	Specimen	Collection	RDA	Sex	Side
Homo sapiens	305	Lisbon	30.00	M	L
Homo sapiens	505	Lisbon	32.00	F	L
Homo sapiens	1423	Lisbon	32.00	F	L
Homo sapiens	154	Lisbon	35.00	M	L
Homo sapiens	238	Lisbon	35.00	M	L
Homo sapiens	2728	NHM	37.00	M	R
Homo sapiens	2173	NHM	40.00	M	L
Homo sapiens	308	Lisbon	43.00	M	L
Homo sapiens	404	Lisbon	43.00	F	L
Homo sapiens	181	Lisbon	44.00	F	L
Homo sapiens	1547	Lisbon	44.00	M	L
Homo sapiens	2368	NHM	45.00	F	L
Homo sapiens	334	Lisbon	51.00	F	L
Homo sapiens	317	Lisbon	52.00	M	L
Homo sapiens	2544	NHM	52.00	F	L
Homo sapiens	343	Lisbon	53.00	F	L
Homo sapiens	2240	NHM	53.00	F	R
Homo sapiens	2541	NHM	53.00	M	L
Homo sapiens	2750	NHM	53.00	F	L
Homo sapiens	477	Lisbon	54.00	M	L
Homo sapiens	2189	NHM	55.00	F	L
Homo sapiens	2369	NHM	55.00	F	L
Homo sapiens	2622	NHM	55.00	M	L
Homo sapiens	2424	NHM	56.00	M	L
Homo sapiens	2162	NHM	58.00	M	L
Homo sapiens	2748	NHM	60.00	F	R
Homo sapiens	2808	NHM	60.00	M	L
Homo sapiens	138	Lisbon	61.00	F	L
Homo sapiens	455	Lisbon	62.00	F	L
Homo sapiens	201	Lisbon	63.00	M	R
Homo sapiens	310	Lisbon	63.00	M	L
Homo sapiens	2632	NHM	63.00	M	L
Homo sapiens	2753	NHM	66.00	M	L

– Appendix 2 –

Node labels, with associated estimated humeral torsion node values (estimated using IE). See Chapter 4 for details.

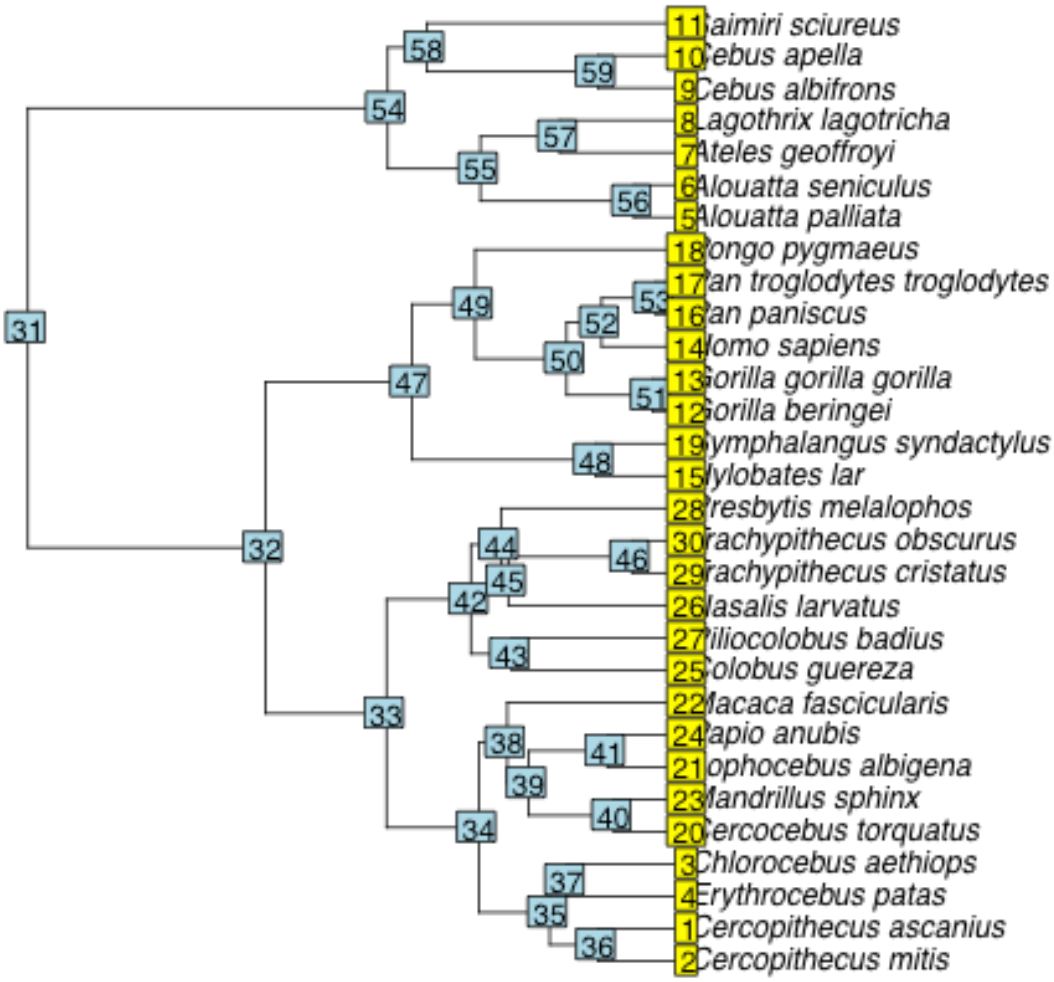

Figure 1 – Phylogenetic tree with extant primate species only.

Table 1 – Table of mean estimated ancestral node values and standard deviation (SD) for humeral torsion for extant primates. Node labels correspond to node numbers in Figure 1 (node_anc: ancestral node number; node_desc: descendant node number; value_anc: estimated ancestral value; values_desc: estimated descendant value).

node_anc	node_desc	value_anc	SD	value_desc	SD
31	32	110.220	1.696	111.500	1.721
32	33	111.500	1.721	109.280	2.75
33	34	109.280	2.75	107.470	4.873
34	35	107.470	4.873	97.870	6.599
35	36	97.870	6.599	96.390	7.843
36	2	96.390	7.843	90.310	9.442
36	1	96.390	7.843	91.640	10.94
35	37	97.870	6.599	89.780	6.117
37	4	89.780	6.117	83.990	4.545
37	3	89.780	6.117	87.530	8.348
34	38	107.470	4.873	106.980	5.561
38	39	106.980	5.561	105.190	6.909
39	40	105.190	6.909	99.570	8.423
40	20	99.570	8.423	89.370	14.52
40	23	99.570	8.423	95.940	7.733
39	41	105.190	6.909	101.580	8.426
41	21	101.580	8.426	93.280	8.509
41	24	101.580	8.426	98.220	11.666
38	22	106.980	5.561	101.180	5.331
33	42	109.280	2.75	107.420	3.495
42	43	107.420	3.495	101.160	6.749
43	25	101.160	6.749	96.310	12.068
43	27	101.160	6.749	96.450	7.144
42	44	107.420	3.495	106.350	4.077
44	45	106.350	4.077	105.840	4.589
45	26	105.840	4.589	103.110	10.427
45	46	105.840	4.589	102.550	5.811
46	29	102.550	5.811	91.940	6.683
46	30	102.550	5.811	103.140	8.686
44	28	106.350	4.077	96.890	7.62
32	47	111.500	1.721	116.430	3.266
47	48	116.430	3.266	111.930	4.692
48	15	111.930	4.692	111.840	6.632
48	19	111.930	4.692	103.310	7.602
47	49	116.430	3.266	134.260	7.611

Table 1 – cont'd.

node_anc	node_desc	value_anc	SD	value_desc	SD
49	50	134.260	7.611	143.830	7.656
50	51	143.830	7.656	152.310	9.839
51	12	152.310	9.839	157.400	12.771
51	13	152.310	9.839	159.990	10.495
50	52	143.830	7.656	146.450	8.313
52	14	146.450	8.313	168.340	8.833
52	53	146.450	8.313	146.390	8.535
53	16	146.390	8.535	151.490	10.435
53	17	146.390	8.535	152.740	10.432
49	18	134.260	7.611	135.920	8.81
31	54	110.220	1.696	104.460	2.141
54	55	104.460	2.141	104.460	2.65
55	56	104.460	2.65	99.010	4.821
56	5	99.010	4.821	98.530	6.854
56	6	99.010	4.821	98.900	11.787
55	57	104.460	2.65	107.600	5.109
57	7	107.600	5.109	116.740	6.28
57	8	107.600	5.109	106.160	8.771
54	58	104.460	2.141	103.980	2.656
58	59	103.980	2.656	102.610	3.962
59	9	102.610	3.962	103.150	8.199
59	10	102.610	3.962	100.330	7.551
58	11	103.980	2.656	106.510	8.566

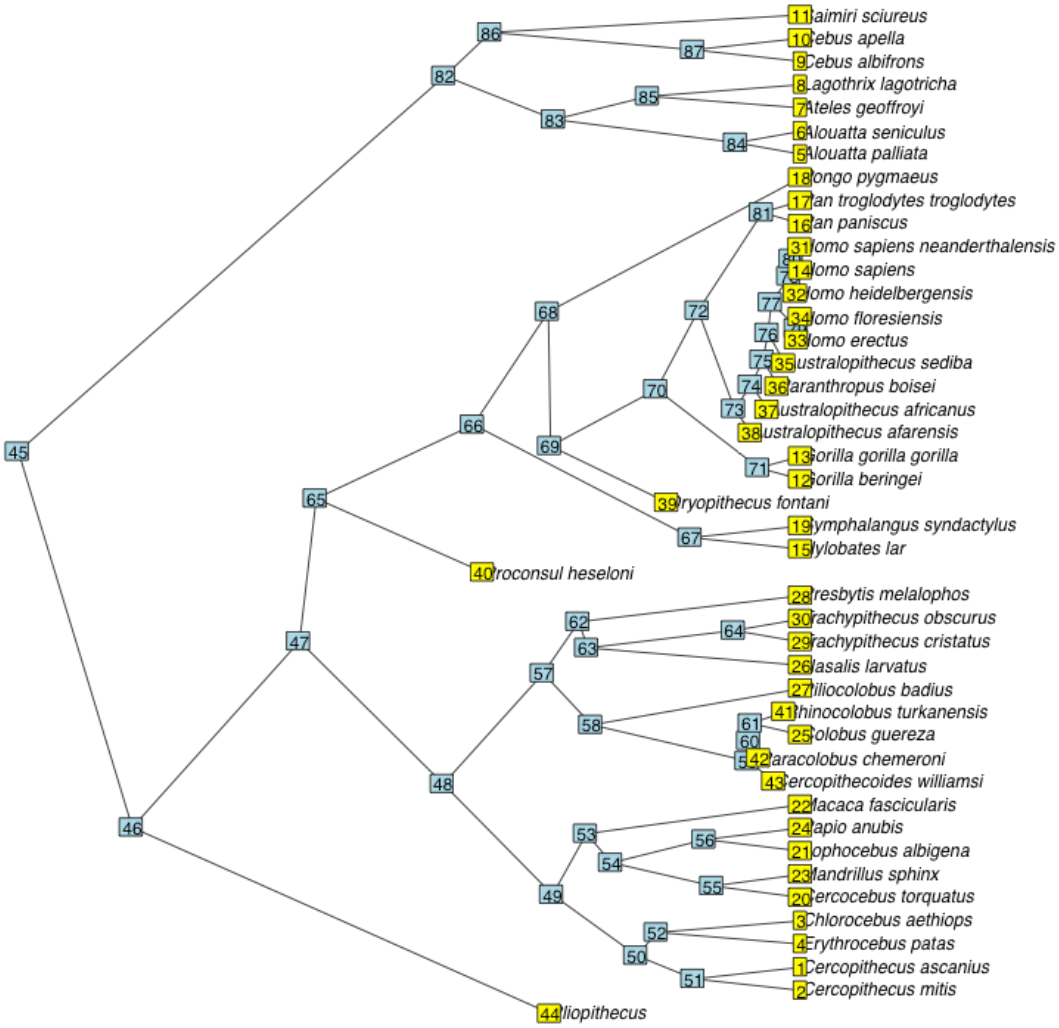

Figure 2 – Phylogenetic tree with primate fossils included.

Table 2 – Table of mean estimated ancestral node values and standard deviation (SD) for humeral torsion for extant primates. Node labels correspond to node numbers in Figure 2 (node_anc: ancestral node number; node_desc: descendant node number; value_anc: estimated ancestral value; values_desc: estimated descendant value).

node_anc	node_desc	value_anc	SD	value_desc	SD
45	46	112.230	1.557	112.740	1.618
46	47	112.740	1.618	113.150	1.646
46	44	112.740	1.618	108.990	9.805
47	48	113.150	1.646	109.960	2.765
48	49	109.960	2.765	106.040	4.294
49	50	106.040	4.294	98.280	6.681
50	51	98.280	6.681	95.700	7.309
51	2	95.700	7.309	90.260	6.247
51	1	95.700	7.309	91.160	12.037
50	52	98.280	6.681	91.590	8.27
52	4	91.590	8.27	83.780	12.837
52	3	91.590	8.27	87.390	8.047
49	53	106.040	4.294	105.060	4.847
53	54	105.060	4.847	102.770	5.863
54	55	102.770	5.863	96.610	6.622
55	20	96.610	6.622	89.770	4.049
55	23	96.610	6.622	95.160	9.587
54	56	102.770	5.863	100.810	7.203
56	21	100.810	7.203	93.430	8.188
56	24	100.810	7.203	98.140	9.025
53	22	105.060	4.847	101.270	9.52
48	57	109.960	2.765	109.250	3.515
57	58	109.250	3.515	106.640	4.863
58	59	106.640	4.863	106.310	5.4
59	60	106.310	5.4	105.930	5.701
59	43	106.310	5.4	94.440	10.717
60	61	105.930	5.701	104.420	6.702
60	42	105.930	5.701	102.490	13.182
61	25	104.420	6.702	95.850	7.439
61	41	104.420	6.702	104.380	10.468
58	27	106.640	4.863	96.200	6.377
57	62	109.250	3.515	106.980	4.185
62	63	106.980	4.185	106.200	4.326
63	26	106.200	4.326	102.850	8.162
63	64	106.200	4.326	103.320	3.936

Table 2 – cont'd.

node_anc	node_desc	value_anc	SD	value_desc	SD
64	29	103.320	3.936	91.940	6.624
64	30	103.320	3.936	103.130	4.066
62	28	106.980	4.185	96.210	11.485
47	65	113.150	1.646	113.220	1.655
65	66	113.220	1.655	114.960	1.889
65	40	113.220	1.655	92.510	9.748
66	67	114.960	1.889	108.770	4.242
67	15	108.770	4.242	111.990	11.073
67	19	108.770	4.242	103.650	7.518
66	68	114.960	1.889	115.950	2.177
68	69	115.950	2.177	115.960	2.183
69	70	115.960	2.183	125.900	4.29
69	39	115.960	2.183	102.300	7.716
70	71	125.900	4.29	154.480	6.941
71	12	154.480	6.941	158.310	7.619
71	13	154.480	6.941	160.160	9.549
70	72	125.900	4.29	125.880	4.287
72	73	125.880	4.287	125.890	4.304
73	74	125.890	4.304	130.630	3.262
73	38	125.890	4.304	123.950	11.534
74	75	130.630	3.262	132.150	3.881
74	37	130.630	3.262	127.910	7.671
75	76	132.150	3.881	132.380	4.081
75	36	132.150	3.881	111.040	9.626
76	77	132.380	4.081	132.470	4.384
76	35	132.380	4.081	116.290	11.44
77	78	132.470	4.384	134.770	7.718
77	79	132.470	4.384	126.990	8.261
79	33	126.990	8.261	126.310	8.748
79	34	126.990	8.261	109.510	11.419
78	80	134.770	7.718	138.900	10.375
78	32	134.770	7.718	141.590	9.459
80	14	138.900	10.375	168.820	9.234
80	31	138.900	10.375	138.220	11.654
72	81	125.880	4.287	146.580	8.804
81	16	146.580	8.804	151.990	11.114
81	17	146.580	8.804	153.020	10.235
68	18	115.950	2.177	136.450	11.65
45	82	112.230	1.557	106.100	1.816
82	83	106.100	1.816	105.750	2.419
83	84	105.750	2.419	99.280	4.946

Table 2 – cont'd.

node_anc	node_desc	value_anc	SD	value_desc	SD
84	5	99.280	4.946	98.680	10.579
84	6	99.280	4.946	98.570	11.435
83	85	105.750	2.419	108.060	5.44
85	7	108.060	5.44	116.190	10.348
85	8	108.060	5.44	106.280	11.224
82	86	106.100	1.816	105.400	2.857
86	87	105.400	2.857	103.470	5.188
87	9	103.470	5.188	102.770	12.264
87	10	103.470	5.188	100.330	9.02
86	11	105.400	2.857	106.420	8.221

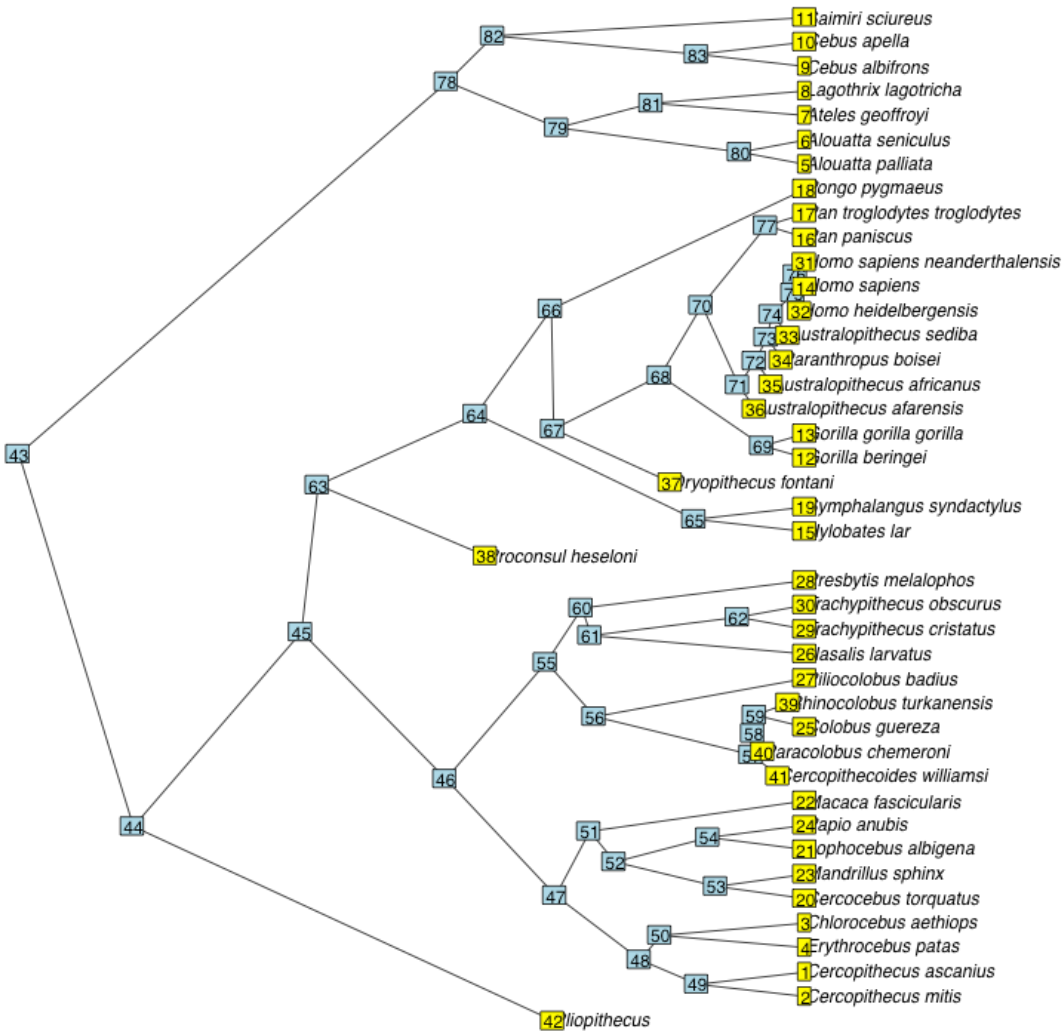

Figure 3 – Phylogenetic tree with primate fossils included, except *Homo erectus* and *Homo floresiensis*.

Table 3 – Table of mean estimated ancestral node values and standard deviation (SD) for humeral torsion for extant primates. Node labels correspond to node numbers in Figure 3 (node_anc: ancestral node number; node_desc: descendant node number; value_anc: estimated ancestral value; values_desc: estimated descendant value).

node_anc	node_desc	value_anc	SD	value_desc	SD
43	44	111.930	1.451	112.430	1.504
44	45	112.430	1.504	112.800	1.506
44	42	112.430	1.504	108.760	10.988
45	46	112.800	1.506	110.260	2.743
46	47	110.260	2.743	105.650	3.887
47	48	105.650	3.887	97.660	6.264
48	49	97.660	6.264	95.680	7.51
49	2	95.680	7.51	89.800	8.902
49	1	95.680	7.51	91.550	9.579
48	50	97.660	6.264	90.630	6.908
50	4	90.630	6.908	84.000	8.76
50	3	90.630	6.908	87.490	8.14
47	51	105.650	3.887	104.980	4.268
51	52	104.980	4.268	102.810	5.021
52	53	102.810	5.021	97.700	6.168
53	20	97.700	6.168	90.320	8.846
53	23	97.700	6.168	95.530	6.996
52	54	102.810	5.021	100.820	6.282
54	21	100.820	6.282	93.810	10.993
54	24	100.820	6.282	97.730	5.549
51	22	104.980	4.268	101.660	8.667
46	55	110.260	2.743	110.110	3.708
55	56	110.110	3.708	106.630	3.904
56	57	106.630	3.904	106.540	4.089
57	58	106.540	4.089	106.260	4.354
57	41	106.540	4.089	94.310	10.372
58	59	106.260	4.354	104.910	5.503
58	40	106.260	4.354	102.460	8.373
59	25	104.910	5.503	96.390	7.954
59	39	104.910	5.503	104.270	7.595
56	27	106.630	3.904	96.260	4.367
55	60	110.110	3.708	108.210	5.714
60	61	108.210	5.714	107.540	6.35

Table 3 – cont'd.

node_anc	node_desc	value_anc	SD	value_desc	SD
61	26	107.540	6.35	103.000	8.17
61	62	107.540	6.35	103.700	9.042
62	29	103.700	9.042	92.340	5.988
62	30	103.700	9.042	102.570	12.085
60	28	108.210	5.714	96.710	8.114
45	63	112.800	1.506	112.870	1.509
63	64	112.870	1.509	114.370	1.669
63	38	112.870	1.509	92.050	7.774
64	65	114.370	1.669	108.930	4.152
65	15	108.930	4.152	112.160	9.623
65	19	108.930	4.152	103.340	10.026
64	66	114.370	1.669	115.390	2.124
66	67	115.390	2.124	115.410	2.139
67	68	115.410	2.139	125.690	4.493
67	37	115.410	2.139	102.180	8.922
68	69	125.690	4.493	154.490	7.232
69	12	154.490	7.232	157.880	10.344
69	13	154.490	7.232	160.440	5.788
68	70	125.690	4.493	125.680	4.488
70	71	125.680	4.488	125.670	4.494
71	72	125.670	4.494	131.690	3.152
71	36	125.670	4.494	123.510	9.825
72	73	131.690	3.152	133.600	3.054
72	35	131.690	3.152	127.820	11.99
73	74	133.600	3.054	133.750	3.172
73	34	133.600	3.054	111.120	7.382
74	75	133.750	3.172	137.920	4.982
74	33	133.750	3.172	117.240	13.178
75	76	137.920	4.982	139.460	6.148
75	32	137.920	4.982	142.210	10.014
76	14	139.460	6.148	168.400	9.824
76	31	139.460	6.148	138.410	7.379
70	77	125.680	4.488	147.310	7.236
77	16	147.310	7.236	151.540	7.698
77	17	147.310	7.236	153.290	10.429
66	18	115.390	2.124	136.140	10.132
43	78	111.930	1.451	105.660	1.675
78	79	105.660	1.675	105.480	2.428
79	80	105.480	2.428	98.950	3.969
80	5	98.950	3.969	98.410	10.095
80	6	98.950	3.969	98.430	6.627

Table 3 – cont'd.

node_anc	node_desc	value_anc	SD	value_desc	SD
79	81	105.480	2.428	107.920	5.418
81	7	107.920	5.418	116.170	10.41
81	8	107.920	5.418	106.420	10.319
78	82	105.660	1.675	104.770	2.341
82	83	104.770	2.341	103.020	3.13
83	9	103.020	3.13	102.830	6.342
83	10	103.020	3.13	100.140	3.997
82	11	104.770	2.341	106.160	8.805

References

Aiello L, and Dean C. 1990. An introduction to human evolutionary anatomy: Access Online via Elsevier.

Alba DM, Moyà-Solà S, and Almécija S. 2011. A partial hominoid humerus from the middle miocene of Castell de Barberà (Vallès-Penedès Basin, Catalonia, Spain). American Journal of Physical Anthropology 144(3):365-381.

Alemseged Z, Spoor F, Kimbel WH, Bobe R, Geraads D, Reed D, and Wynn JG. 2006. A juvenile early hominin skeleton from Dikika, Ethiopia. Nature 443(7109):296-301.

Almécija S, Alba D, Moyà-Solà S, and Köhler M. 2007. Orang-like manual adaptations in the fossil hominoid *Hispanopithecus laietanus*: first steps towards great ape suspensory behaviours. Proceedings of the Royal Society B: Biological Sciences 274(1624):2375-2384.

Almécija S, Alba DM, and Moyà-Solà S. 2009. *Pierolapithecus* and the functional morphology of Miocene ape hand phalanges: paleobiological and evolutionary implications. Journal of human evolution 57(3):284.

Anapol F, and Fleagle JG. 1988. Fossil platyrrhine forelimb bones from the early Miocene of Argentina. American Journal of Physical Anthropology 76(4): 417-428.

Andermahr J, Jubel A, Elsner A, Johann J, Prokop A, Rehm KE, and Koebke J. 2007. Anatomy of the clavicle and the intramedullary nailing of midclavicular fractures. Clinical Anatomy 20(1):48-56.

Andrews P, and Groves C. P. 1976. Gibbons and brachiation. Gibbon Siamang 4:167-218.

Arcadi A, Wallauer W. 2011. Individual-level lateralization in the asymmetrical gaits of wild chimpanzees (*Pan troglodytes*): implications for hand preference and skeletal asymmetry? Behaviour 148:1419–1441.

Argue D, Donlon D, Groves C, and Wright R. 2006. *Homo floresiensis*: Microcephalic, pygmoid *Australopithecus*, or *Homo*? Journal of human evolution 51(4):360-374.

Argue D, Morwood M, Sutikna T, and Saptomo E. 2009. *Homo floresiensis*: a cladistic analysis. Journal of human evolution 57(5):623-639.

Arnold C, and Nunn CL. 2010. Phylogenetic targeting of(Morwood et al. 2005) research effort in evolutionary biology. The American Naturalist 176(5): 601-612.

Ashton E, Flinn R, Oxnard C, and Spence T. 1971. The functional and classifieatory significance of combined metrical features of the primate shoulder girdle. Journal of Zoology 163(3):319-350.

Ashton E, Flinn R, Oxnard C, and Spence T. 1976. The adaptive and classificatory significance of certain quantitative features of the forelimb in primates. Journal of Zoology 179(4):515-556.

Ashton EH, and Oxnard CE. 1963. The musculature of the primate shoulder. The Transactions of the Zoological Society of London 29(7):553-650.

Ashton E, and Oxnard C. 1964. Functional adaptations in the primate shoulder girdle. Proceedings of the Zoological Society of London: Wiley Online Library pp 49-66.

Ashton E, Oxnard C, and Spence T. 1965. Scapular shape and primate classification. Proceedings of the Zoological Society of London: Wiley Online Library. p 125-142.

Attene M, Katz S, Mortara M, Patané G, Spagnuolo M, and Tal A. 2006. Mesh segmentation-a comparative study. Shape Modeling and Applications, 2006 SMI 2006 IEEE International Conference on: IEEE. p 7-7.

Auerbach BM, Raxter MH. 2008. Patterns of clavicular bilateral asymmetry in relation to the humerus: variation among humans. Journal of Human Evolution 54:663–674

Auerbach BM, Ruff CB. 2006. Limb bone bilateral asymmetry: variability and commonality among modern humans. Journal of Human Evolution 50:203–218.

Avis V. 1962. Brachiation: the crucial issue for man's ancestry. Southwestern Journal of Anthropology:119-148.

Baab KL, McNulty KP, and Harvati K. 2013. Homo floresiensis Contextualized: A Geometric Morphometric Comparative Analysis of Fossil and Pathological Human Samples. PLoS One 8(7):e69119.

Bachoura A, Deane AS, Wise JN, and Kamineni S. 2013. Clavicle morphometry revisited: a 3-dimensional study with relevance to operative fixation. Journal of Shoulder and Elbow Surgery 22(1):e15-e21.

Balolia KL, Soligo C, and Lockwood CA. 2013. Sexual Dimorphism and Facial Growth Beyond Dental Maturity in Great Apes and Gibbons. International Journal of Primatology:1-27.

Bareggi R, Grill V, Zweyer M, Sandrucci MA, Narducci P, Forabosco A. 1994. The growth of long bones in human embryological and fetal upper limbs and its relationship to other developmental patterns. Anatomy and Embryology 189:19–24.

Begun DR. 1992a. *Dryopithecus crusafonti* sp. nov., a new Miocene hominoid species from Can Ponsic (Northeastern Spain). American Journal of Physical Anthropology 87(3):291-309.

Begun DR. 1992b. Phyletic diversity and locomotion in primitive European hominids. American Journal of Physical Anthropology 87(3):311-340.

Begun DR. 1992c. Miocene fossil hominids and the chimp-human clade. Science 257(5078):1929-1933.

Begun DR. 1994. Relations among the great apes and humans: new interpretations based on the fossil great ape *Dryopithecus*. American Journal of Physical Anthropology 37(S19):11-63.

Begun DR. 2004. Knuckle-walking and the origin of human bipedalism. From Biped to Strider: The Emergence of Modern Human Walking Kluwer, New York: 9-33.

Begun DR. 2005. *Sivapithecus* is east and *Dryopithecus* is west, and never the twain shall meet. Anthropological Science 113(1):53-64.

Begun DR. 2007. How to identify (as opposed to define) a homoplasy: Examples from fossil and living great apes. Journal of human evolution 52(5):559-572.

Begun DR. 2010. Miocene hominids and the origins of the African apes and humans. Annual review of Anthropology 39:67-84.

Begun DR, and Kivell TL. 2011. Knuckle-walking in *Sivapithecus*? The combined effects of homology and homoplasy with possible implications for pongine dispersals. Journal of Human Evolution 60(2):158-170.

Begun DR, Teaford MF, and Walker A. 1994. Comparative and functional anatomy of Proconsul phalanges from the Kaswanga primate site, Rusinga Island, Kenya. Journal of human evolution 26:89-165.

Behrensmeyer AK, Todd NE, Potts R, and McBrinn GE. 1997. Late Pliocene faunal turnover in the Turkana basin, Kenya and Ethiopia. Science 278(5343): 1589-1594.

Bello-Hellegouarch G, Potau JM, Arias-Martorell J, Pastor JF, and Pérez-Pérez A. 2013. A Comparison of Qualitative and Quantitative Methodological Approaches to Characterizing the Dorsal Side of the Scapula in Hominoidea and Its Relationship to Locomotion. International journal of primatology:1-22.

Blackburn A. 2011. Bilateral asymmetry of the humerus during growth and development. American Journal of Physical Anthropology 145:639–646.

Blomberg SP, and Garland T. 2002. Tempo and mode in evolution: phylogenetic inertia, adaptation and comparative methods. Journal of Evolutionary Biology 15(6):899-910.

Blomberg SP, Garland Jr T, and Ives AR. 2003. Testing for phylogenetic signal in comparative data: behavioral traits are more labile. Evolution 57(4):717-745.

Bobe R, Behrensmeyer AK, and Chapman RE. 2002. Faunal change, environmental variability and late Pliocene hominin evolution. Journal of human evolution 42(4):475-497.

Bogin B. 2003. The human pattern of growth and development in paleontological perspective. Cambridge Studies In Biological And Evolutionary Anthropology:15-44.

Bokor DJ, O'Sullivan MD, and Hazan GJ. 1999. Variability of measurement of glenoid version on computed tomography scan. Journal of shoulder and elbow surgery 8(6):595-598.

Botsch M, Pauly M, Kobbelt L, Alliez P, Lévy B, Bischoff S, and Röossl C. 2007. Geometric modeling based on polygonal meshes. Int'l Conf on Computer Graphics and Interactive Techniques, ACM SIGGRAPH courses.

Boughner JC, and Dean MC. 2008. Mandibular shape, ontogeny and dental development in bonobos (Pan paniscus) and chimpanzees (Pan troglodytes). Evolutionary Biology 35(4):296-308.

Boughner JC, Dean MC, and Wilgenbusch CS. 2012. Permanent tooth mineralization in bonobos (*Pan paniscus*) and chimpanzees (*P. troglodytes*). American Journal of Physical Anthropology 149(4):560-571.

Brehm A, Khadem M, Jesus J, Andrade P, and Vicente L. 2001. Lack of congruence between morphometric evolution and genetic differentiation suggests a recent dispersal and local habitat adaptation of the Madeiran lizard Lacerta dugesii. Genetics Selection Evolution 33(6):671-686.

Brown P, Sutikna T, Morwood MJ, and Soejono RP. 2004. A new small-bodied hominin from the Late Pleistocene of Flores, Indonesia. Nature 431(7012): 1055-1061.

Brewer BJ, Wubben R, and Carrera G. 1986. Excessive retroversion of the glenoid cavity. J Bone Joint Surg Am 68:724-731.

Burnett CN, and Johnson EW. 1971a. Development of gait in childhood. Part I: Method. Developmental Medicine & Child Neurology 13(2):196-206.

Burnett CN, and Johnson EW. 1971b. Development of gait in childhood: Part II. Developmental Medicine & Child Neurology 13(2):207-215.

Byrne R, Byrne J. 1991. Hand preferences in the skilled gathering tasks of mountain gorillas (*Gorilla g. beringei*). Cortex 27:521–546.

Byrne RW. 2004. Sex difference in chimpanzee handedness. American Journal of Physical Anthropology 123:62–68.

Calzada N, Aguilar A, Grau E, and Lockyer C. 1997. Patterns of growth and physical maturity in the western Mediterranean striped dolphin, *Stenella coeruleoalba* (Cetacea: *Odontoceti*). Canadian Journal of Zoology 75(4):632-637.

Campbell CJ, Fuentes A, MacKinnon KC, and Panger M. 2006. Primates in perspective.

Cant JG. 1987a. Effects of sexual dimorphism in body size on feeding postural behavior of Sumatran orangutans (*Pongo pygmaeus*). American Journal of Physical Anthropology 74(2):143-148.

Cant JG. 1987b. Positional behavior of female Bornean orangutans (*Pongo pygmaeus*). American Journal of Primatology 12(1):71-90.

Cant J. 1986. Locomotion and feeding postures of spider and howling monkeys: field study and evolutionary interpretation. Folia Primatologica 46(1):1-14.

Cannon CH, and Manos PS. 2001. Combining and comparing morphometric shape descriptors with a molecular phylogeny: the case of fruit type evolution in Bornean Lithocarpus (Fagaceae). Systematic biology 50(6):860-880.

Cardini A, and Elton S. 2008. Does the skull carry a phylogenetic signal? Evolution and modularity in the guenons. Biological Journal of the Linnean Society 93(4):813-834.

Cardoso HF. 2005. Brief communication: the collection of identified human skeletons housed at the Bocage Museum (National Museum of Natural History), Lisbon, Portugal. American Journal of Physical Anthropology 129(2):173-176.

Carlson KJ. 2006. Muscle architecture of the common chimpanzee (*Pan troglodytes*): perspectives for investigating chimpanzee behavior. Primates 47: 218–229.

Carpenter CR. Suspensory behavior of gibbons (*H. lar*) – a photo essay. In: Rumbaugh DM, editor. Gibbon and Siamang: A Series of Volumes on the Lesser Apes, Suspensory Behavior, Locomotion and other Behaviors of Captive Gibbons: Cognition. Basel: Karger; 1976. pp. 1–20. Vol. 4.

Cartmill M. 1985. Climbing. In Functional Vertebrate Morphology (ed. M. Hildebrand, D.M. Bramble, K. F. Liem & D. B. Wake), pp. 73-88. Cambridge, MA: Belknap Press

Cartmill M, and Milton K. 1977. The lorisiform wrist joint and the evolution of "brachiating" adaptations in the Hominoidea. American Journal of Physical Anthropology 47(2):249-272.

Cashmore L. 2009. Can hominin 'handedness' be accurately assessed? Annals of Human Biology 36:624–641.

Cashmore L, Zakrzewski SR. 2011. Assessment of musculoskeletal stress marker development in thehand. International Journal of Osteoarchaeology 47:218–229.

Cashmore L, Uomini N, Chapelain A. 2008. The evolution of handedness in humans and great apes: a review and current issues. Journal of Anthropological Sciences Rivista di Antropologia JASS Instituto Italiano di Antropologia 86:7–35.

Caswell JL, Mallick S, Richter DJ, Neubauer J, Schirmer C, Gnerre S, and Reich D. 2008. Analysis of chimpanzee history based on genome sequence alignments. PLoS genetics 4(4):e1000057.

Caumul R, and Polly PD. 2005. Phylogenetic and environmental components of morphological variation: skull, mandible, and molar shape in marmots (Marmota, Rodentia). Evolution 59(11):2460-2472.

Cerling TE, Wynn JG, Andanje SA, Bird MI, Korir DK, Levin NE, Mace W, Macharia AN, Quade J, and Remien CH. 2011. Woody cover and hominin environments in the past 6 million years. Nature 476(7358):51-56.

Chan LK. 2007a. Glenohumeral mobility in primates. Folia Primatologica 78(1):1-18.

Chan LK. 2007b. Scapular position in primates. Folia Primatologica 78(1):19-35.

Chan LK. 2008. The range of passive arm circumduction in primates: Do hominoids really have more mobile shoulders? American Journal of Physical Anthropology 136(3):265-277.

Churchill SE, Formicola V. 1997. A case of marked bilateral asymmetry in the upper limbs of an Upper Palaeolithic male from Barma Grande (Liguria), Italy. International Journal of Osteoarchaeology 7:18–38.

Churchill SE, Holliday TW, Carlson KJ, Jashashvili T, Macias ME, Mathews S, Sparling TL, Schmid P, de Ruiter DJ, and Berger LR. 2013. The upper limb of *Australopithecus sediba*. Science 340(6129).

Churchill SE, Holliday TW, Carlson KJ, Jashashvili T, Macias ME, Mathews S, Sparling TL, Schmid P, de Ruiter DJ, and Berger LR. 2013. The upper limb of *Australopithecus sediba*. Science 340(6129).

Codine P, Bernard PL, Pocholle M, Benaim C, and Brun V. 1997. Influence of sports discipline on shoulder rotator cuff balance. Medicine and science in sports and exercise 29(11):1400.

Collard M, and O'Higgins P. 2001. Ontogeny and homoplasy in the papionin monkey face. Evolution & development 3(5):322-331.

Collard M, and Wood B. 2000. How reliable are human phylogenetic hypotheses? Proceedings of the National Academy of Sciences 97(9):5003-5006.

Collard M, and Wood B. 2001. How reliable are current estimates of fossil catarrhine phylogeny? An assessment using extant great apes and Old World monkeys. Hominoid Evolution and Climatic Change in Europe: Volume 2: Phylogeny of the Neogene Hominoid Primates of Eurasia 2.

Collard M, and Wood B. 2007. Hominin homoiology: an assessment of the impact of phenotypic plasticity on phylogenetic analyses of humans and their fossil relatives. Journal of human evolution 52(5):573.

Corballis MC. 2003. From mouth to hand: gesture, speech, and the evolution of right-handedness. Behavioral and Brain Sciences 26:199–208.

Corrigan G. 1960. The neonatal clavicle. Neonatology 2(2):79-92.

Corruccini RS. 1978. Comparative osteometrics of the hominoid wrist joint, with special reference to knuckle-walking. Journal of human evolution 7(4): 307-321.

Corruccini RS, and Ciochon RL. 1976. Morphometric affinities of the human shoulder. American Journal of Physical Anthropology 45(1):19-37.

Corruccini RS, and McHenry HM. 2001. Knuckle-walking hominid ancestors. Journal of human evolution 40(6):507-511.

Corruccini RS, Ciochon RL, and McHenry HM. 1976. The postcranium of Miocene hominoids: Were dryopithecines merely “dental apes”? Primates 17(2): 205-223.

Cowgill LW. 2007. Humeral torsion revisited: A functional and ontogenetic model for populational variation. American Journal of Physical Anthropology 134(4): 472-480.

Crockett HC, Gross LB, Wilk KE, Schwartz ML, Reed J, O'Mara J, Reilly MT, Dugas JR, Meister K, and Lyman S. 2002. Osseous adaptation and range of motion at the glenohumeral joint in professional baseball pitchers. The American journal of sports medicine 30(1):20.

Crompton R, and Thorpe S. 2007. Response to Comment on "Origin of Human Bipedalism As an Adaptation for Locomotion on Flexible Branches". Science 318(5853):1066-1066.

Crompton R, Vereecke E, and Thorpe S. 2008. Locomotion and posture from the common hominoid ancestor to fully modern hominins, with special reference to the last common panin/hominin ancestor. Journal of Anatomy 212(4): 501-543.

Crompton RH, Sellers WI, and Thorpe SK. 2010. Arboreality, terrestriality and bipedalism. Philosophical Transactions of the Royal Society B: Biological Sciences 365(1556):3301-3314.

Cyprien J, Vasey H, Burdet A, Bonvin J, Kritsikis N, and Vuagnat P. 1983. Humeral retrotorsion and glenohumeral relationship in the normal shoulder and in recurrent anterior dislocation (scapulometry). Clinical orthopaedics and related research 175:8-17.

Dainton M, and Macho GA. 1999. Did knuckle walking evolve twice? Journal of human evolution 36(2):171.

Dainton M, Lovejoy C, Heiple K, and Meindl R. 2001. Palaeoanthropology: Did our ancestors knuckle-walk? Nature:324-326.

Daruwalla ZJ, Courtis P, Fitzpatrick C, Fitzpatrick D, and Mullett H. 2010. Anatomic variation of the clavicle: A novel three−dimensional study. Clinical Anatomy 23(2):199-209.

David B, and Laurin B. 1996. Morphometrics and cladistics: measuring phylogeny in the sea urchin Echinocardium. Evolution:348-359.

Day MH. 1978. Functional interpretations of the morphology of postcranial remains of early African hominids. Early hominids of Africa London: Duckworth: 311-345.

Dean M, and Wood B. 1981. Developing pongid dentition and its use for ageing individual crania in comparative cross-sectional growth studies. Folia Primatologica 36:111-127.

Deane AS, and Begun DR. 2008. Broken fingers: retesting locomotor hypotheses for fossil hominoids using fragmentary proximal phalanges and high-resolution polynomial curve fitting (HR-PCF). Journal of Human Evolution 55(4): 691-701.

Delgado Jr RA, and Van Schaik CP. 2000. The behavioral ecology and conservation of the orangutan (*Pongo pygmaeus*): a tale of two islands. Evolutionary Anthropology: Issues, News, and Reviews 9(5):201-218.

Demenocal PB. 2004. African climate change and faunal evolution during the Pliocene–Pleistocene. Earth and Planetary Science Letters 220(1):3-24.

DeSilva JM, Holt KG, Churchill SE, Carlson KJ, Walker CS, Zipfel B, and Berger LR. 2013. The lower limb and mechanics of walking in *Australopithecus sediba*. Science 340(6129).

Dirks W. 1998. Histological reconstruction of dental development and age at death in a juvenile gibbon (*Hylobates lar*). Journal of Human Evolution 35(4):411-425.

Dirks W. 2003. Effect of diet on dental development in four species of catarrhine primates. American journal of primatology 61(1):29-40.

Dirks W, and Bowman JE. 2007. Life history theory and dental development in four species of catarrhine primates. Journal of Human Evolution 53(3):309-320.

Doran DM. 1992. The ontogeny of chimpanzee and pygmy chimpanzee locomotor behavior: a case study of paedomorphism and its behavioral correlates. Journal of Human Evolution 23(2):139-157.

Doran DM. 1993a. Comparative locomotor behavior of chimpanzees and bonobos: the influence of morphology on locomotion. American Journal of Physical Anthropology 91(1):83-98.

Doran DM. 1993b. Sex differences in adult chimpanzee positional behavior: the influence of body size on locomotion and posture. American Journal of Physical Anthropology 91(1):99-115.

Doran DM. 1997. Ontogeny of locomotion in mountain gorillas and chimpanzees. Journal of Human Evolution 32(4):323.

Doran DM, and Hunt KD. 1996. Comparative locomotor behavior of chimpanzees and bonobos. Chimpanzee Cultures: With a Foreword by Jane Goodall:93.

Drapeau MSM. 2008. Enthesis bilateral asymmetry in humans and African apes. Journal of Comparative Human Biology 59:93–109.

Dunsworth HM. 2006. *Proconsul heseloni* feet from Rusinga Island, Kenya: ProQuest.

Edelson G. 1999. Variations in the retroversion of the humeral head. Journal of Shoulder and Elbow Surgery 8(2):142-145.

Edelson G. 2000. The development of humeral head torsion Journal of Shoulder and Elbow Surgery 9:316–318.

Erikson G. 1963. Brachiation in New World monkeys and in anthropoid apes. Symp Zool Soc Lond. p 135-164.

Evans FG, and Krahl VE. 1945. The torsion of the humerus: a phylogenetic survey from fish to man. American Journal of Anatomy 76(3):303-337.

Falk D, Hildebolt C, Smith K, Morwood MJ, Sutikna T, Saptomo EW, Imhof H, Seidler H, and Prior F. 2007. Brain shape in human microcephalics and *Homo floresiensis*. Proceedings of the National Academy of Sciences 104(7): 2513-2518.

Farmer MA, and German RZ. 2004. Sexual dimorphism in the craniofacial growth of the guinea pig (*Cavia porcellus*). Journal of Morphology 259(2):172-181.

Fatah A, El Hak E, Shirley NR, Mahfouz MR, Auerbach BM. 2012. A three-dimensional analysis of bilateral directional asymmetry in the human clavicle. American Journal of Physical Anthropology 149:547–559.

Fiorello CV, and German R. 1997. Heterochrony within species: craniofacial growth in giant, standard, and dwarf rabbits. Evolution:250-261.

Fleagle J. 1974. Dynamics of a brachiating siamang [*Hylobates* (*Symphalangus*) *syndactylus*]. Nature 248:259–260.

Fleagle JG. 1976. Locomotion and posture of the Malayan siamang and implications for hominoid evolution. Folia primatologica 26(4):245-269.

Fleagle J, Stern Jr J, Jungers W, Susman R, Vangor A, and Wells J. 1981. Climbing: a biomechanical link with brachiation and with bipedalism. Vertebrate Locomotion:359-375.

Fleagle JG. 1976. Locomotion and posture of the Malayan siamang and implications for hominoid evolution. Folia Primatologica 26(4):245-269.

Fleagle JG. 1985. Size and adaptation in primates. Size and scaling in primate biology:1-19.

Frost SR, Marcus LF, Bookstein FL, Reddy DP, and Delson E. 2003. Cranial allometry, phylogeography, and systematics of large-bodied papionins (primates: Cercopithecinae) inferred from geometric morphometric analysis of landmark data. The Anatomical Record Part A: Discoveries in Molecular, Cellular, and Evolutionary Biology 275(2):1048-1072.

Gagey O. 1985. Étude de l'élévation du membre supérieur: rôle des ligaments articulaires et des muscles fléchisseurs de l'articulation scapulo-humérale: Laboratoire d'anatomie de la Faculté de médecine.

Galatius A. 2005. Sexually dimorphic proportions of the harbour porpoise (*Phocoena phocoena*) skeleton. Journal of Anatomy 206(2):141-154.

Galatius A. 2010. Paedomorphosis in two small species of toothed whales (*Odontoceti*): how and why? Biological Journal of the Linnean Society 99(2): 278-295.

Galatius A, Berta A, Frandsen MS, and Goodall RNP. 2011. Interspecific variation of ontogeny and skull shape among porpoises (*Phocoenidae*). Journal of Morphology 272(2):136-148.

Galatius A, and Goldin P. 2011. Geographic variation of skeletal ontogeny and skull shape in the harbour porpoise (*Phocoena phocoena*). Canadian Journal of Zoology 89(9):869-879.

Galatius A, Jansen OE, and Kinze CC. 2012. Parameters of growth and reproduction of white-beaked dolphins (*Lagenorhynchus albirostris*) from the North Sea. Marine Mammal Science 29(2):348–355.

Garland Jr T, Bennett AF, and Rezende EL. 2005. Phylogenetic approaches in comparative physiology. Journal of experimental Biology 208(16):3015-3035.

Gebo DL. 1996. Climbing, brachiation, and terrestrial quadrupedalism: historical precursors of hominid bipedalism. American Journal of Physical Anthropology 101(1):55-92.

Gebo DL. 1998. Climbing, brachiation, and terrestrial quadrupedalism: historical precursors of hominid bipedalism. American Journal of Physical Anthropology 101(1):55-92.

German R, and Meyers L. 1989. The role of time and size in ontogenetic allometry: II. An empirical study of human growth. Growth, Development, and Aging: GDA 53(3):107.

Gjerdrum T, Walker P, Andrushko V. 2003. Humeral retroversion: an activity pattern index in prehistoric southern California. American Journal of Physical Anthropology 34(suppl): 100–101.

González PN, Perez SI, and Bernal V. 2010. Ontogeny of robusticity of craniofacial traits in modern humans: a study of South American populations. American Journal of Physical Anthropology 142(3):367-379.

González-José R, Escapa I, Neves WA, Cúneo R, and Pucciarelli HM. 2008. Cladistic analysis of continuous modularized traits provides phylogenetic signals in Homo evolution. Nature 453(7196):775-778.

Gould SJ. 1977. Ontogeny and phylogeny: Belknap press.

Green DJ, and Alemseged Z. 2012. *Australopithecus afarensis* Scapular Ontogeny, Function, and the Role of Climbing in Human Evolution. Science 338(6106): 514-517.

Groves CP. 1972. Systematics and phylogeny of gibbons. Gibbon and siamang 1:1-89.

Haile-Selassie Y, Latimer BM, Alene M, Deino AL, Gibert L, Melillo SM, Saylor BZ, Scott GR, and Lovejoy CO. 2010. An early *Australopithecus afarensis* postcranium from Woranso-Mille, Ethiopia. Proceedings of the National Academy of Sciences 107(27):12121-12126.

Hall BK. 1999. Evolutionary developmental biology: Springer.

Hall BK. 2007. Homoplasy and homology: Dichotomy or continuum? Journal of Human Evolution 52(5):473-479.

Haque M, Mansur D, Krishnamurthy A, Karki R, Sharma K, and Shakya R. 2011. Morphometric analysis of clavicle in Nepalese population. Kathmandu Univ Med J 35(3):193-197.

Hanna JB, and Schmitt D. 2011. Interpreting the role of climbing in primate locomotor evolution: are the biomechanics of climbing influenced by habitual substrate use and anatomy? International journal of primatology 32(2): 430-444.

Harmon LJ, Weir JT, Brock CD, Glor RE, and Challenger W. 2008. GEIGER: investigating evolutionary radiations. Bioinformatics 24(1):129-131.

Harrington Jr M, Keller T, Seiler III J, Weikert D, Moeljanto E, and Schwartz H. 1993. Geometric properties and the predicted mechanical behavior of adult human clavicles. Journal of biomechanics 26(4):417-426.

Heizmann EP, and Begun DR. 2001. The oldest Eurasian hominoid. Journal of human evolution 41(5):463-481.

Hensinger RN. 1986. Standards in pediatric orthopedics: tables, charts, and graphs illustrating growth.

Hepper PG, McCartney GR, Shannon EA. 1998. Lateralised behaviour in first trimester human foetuses. Neuropsychologia 36:531–534.

Hershkovitz I, Kornreich L, and Laron Z. 2007. Comparative skeletal features between *Homo floresiensis* and patients with primary growth hormone insensitivity (Laron Syndrome). American Journal of Physical Anthropology 134(2):198-208.

Hildebrand M. 1967. Symmetrical gaits of primates. American Journal of Physical Anthropology 26:119–130.

Hill A. 1995. In: Paleoclimate and Evolution with Emphasis on Human Origins. (eds Vrba, E. S., Denton, G. H., Partridge, T. C. & Burckle, L. H.) pp. 178–193. Yale Univ. Press, New Haven.

Hill DWCO. 1966. Primates, Comparative Anatomy and Taxonomy VI: Catarrhini, Cercopithecoidea, Cercopithecines. Monograph: University Press.

Hill WCO. 1970. Primates Comparative Anatomy and Taxonomy VIII Cynopithecinae: Edinburgh University Press.

Hill WCO. 1974. Primates: comparative anatomy and taxonomy: Halsted Press.

Hoekstra H, Krenz J, and Nachman M. 2004. Local adaptation in the rock pocket mouse (*Chaetodipus intermedius*): natural selection and phylogenetic history of populations. Heredity 94(2):217-228.

Hollihn U. 1984. Bimanual suspensory behavior: morphology, selective advantages and phylogeny. The lesser apes: Evolutionary and behavioral biology:85-95.

Hopkins WD, Cantalupo C. 2004. Handedness in chimpanzees (*Pan troglodytes*) is associated with asymmetries of the primary motor cortex but not with homologous language areas. Behavioral Neuroscience(118):1176.

Hopkins WD, Cantalupo C. 2005. Individual and setting differences in the hand preferences of chimpanzees (*Pan troglodytes*): a critical analysis and some alternative explanations. Laterality: Asymmetries of Body, Brain, and Cognition 10:65–80.

Hopkins WD, Nir TM. 2010. Planum temporale surface area and grey matter asymmetries in chimpanzees (*Pan troglodytes*): the effect of handedness and comparison with findings in humans. Behavioural Brain Research 208:436–443.

Hopkins WD, Bard KA, Griner KM. 1997. Locomotor adaptation and leading limb asymmetries in neonatal chimpanzees (*Pan troglodytes*). International Journal of Primatology 18:105–114.

Hopkins WD, Russell JL, Cantalupo C. 2007. Neuroanatomical correlates of handedness for tool use in chimpanzees (*Pan troglodytes*) implication for theories on the evolution of language. Psychological Science, 18(11):971-977.

Hopkins WD, Phillips KA, Bania A, Calcutt SE, Gardner M, Russell J, Schaeffer J, Lonsdorf EV, Ross SR, Schapiro SJ. 2011. Hand preferences for coordinated bimanual actions in 777 great apes: implications for the evolution of handedness in Hominins. Journal of Human Evolution 60: 605–611.

Horton JA, Bariteau JT, Loomis RM, Strauss JA, and Damron TA. 2008. Ontogeny of skeletal maturation in the juvenile rat. The Anatomical Record: Advances in Integrative Anatomy and Evolutionary Biology 291(3):283-292.

Humle T, Matsuzawa T. 2009. Laterality in hand use across four tool-use behaviors among the wild chimpanzees of Bossou, Guinea, West Africa. American Journal of Primatology 71:40–48.

Humphrey LT. 1998. Growth patterns in the modern human skeleton. American Journal of Physical Anthropology 105(1):57-72.

Humphrey LT. 1999. Relative mandibular growth in humans, gorillas and chimpanzees. Cambridge Studies In Biological And Evolutionary Anthropology:65-87.

Hunt KD. 1991. Positional behavior in the Hominoidea. International Journal of Primatology 12(2):95-118.

Hunt KD. 1994. The evolution of human bipedality: ecology and functional morphology. Journal of Human Evolution 26:183–202.

Inman VT, and Abbott LC. 1944. Observations on the function of the shoulder joint. The Journal of Bone and Joint Surgery (American) 26(1):1-30.

Inman VT, and Saunders JDM. 1946. Observations on the function of the clavicle. California medicine 65(4):158.

Inouye SE. 1994. Ontogeny of knuckle-walking hand postures in African apes. Journal of human evolution 26(5-6):459-485.

Inouye SE, and Shea BT. 1997. What's Your Angle? Size Correction and Bar–Glenoid Orientation in “Lucy”(AL 288-1). International journal of primatology 18(4): 629-650.

Inouye SE. 2003. Intraspecific and ontogenetic variation in the forelimb morphology of Gorilla. Cambridge Studies In Biological And Evolutionary Anthropology: 194-236.

Ishida H, Kunimatsu Y, Takano T, Nakano Y, and Nakatsukasa M. 2004. *Nacholapithecus* skeleton from the Middle Miocene of Kenya. Journal of Human Evolution 46(1):69-103.

Ivanović A, Sotiropoulos K, Üzüm N, Džukić G, Olgun K, Cogălniceanu D, and Kalezić ML. 2012. A phylogenetic view on skull size and shape variation in the smooth newt (*Lissotriton vulgaris, Caudata, Salamandridae*). Journal of Zoological Systematics and Evolutionary Research, 50(2), 116-124.

Jenkins FA. 1974. Primate locomotion: Academic Press.

Jenkins F, and Fleagle JG. 1975. Knuckle-walking and the functional anatomy of the wrists in living apes. Primate functional morphology and evolution:213-227.

Jenkins FA, Dombrowski PJ, and Gordon E. 1978. Analysis of the shoulder in brachiating spider monkeys. American Journal of Physical Anthropology 48(1):65-76.

Jolicoeur P. 1963. Bilateral symmetry and asymmetry in limb bones of *Martes americana* and man. Revue Canadienne de Biologie/Editée par l'Université de Montréal 22:409.

Jolicoeur P. 1985. A flexible 3-parameter curve for limited or unlimited somatic growth. Growth 49(4):271-281.

Jolicoeur P, Pontier J, Pernin M-O, and Sempé M. 1988. A lifetime asymptotic growth curve for human height. Biometrics:995-1003.

Jombart T, Balloux F, and Dray S. 2010. adephylo: new tools for investigating the phylogenetic signal in biological traits. Bioinformatics 26(15):1907-1909.

Jungers WL, and Stern JT. 1981. Preliminary electromyographical analysis of brachiation in gibbon and spider monkey. International journal of primatology 2(1):19-33.

Jungers WL, and Susman RL. 1984. Body size and skeletal allometry in African apes. The pygmy chimpanzee: Springer. p 131-177.

Kagaya M, Ogihara N, and Nakatsukasa M. 2008. Morphological study of the anthropoid thoracic cage: scaling of thoracic width and an analysis of rib curvature. Primates 49(2):89-99.

Kagaya M, Ogihara N, and Nakatsukasa M. 2010. Is the Clavicle of Apes Long? An Investigation of Clavicular Length in Relation to Body Mass and Upper Thoracic Width. International Journal of Primatology 31(2):209-217.

Kagaya M, Ogihara N, and Nakatsukasa M. 2008. Morphological study of the anthropoid thoracic cage: scaling of thoracic width and an analysis of rib curvature. Primates 49(2):89-99.

Kate B. 1968. The torsion of the humerus in central India. J Indian Anthropol Soc 3:17-30.

Kelley J, and Schwartz GT. 2010. Dental development and life history in living African and Asian apes. Proceedings of the National Academy of Sciences 107(3):1035-1040.

Kimes KR, Siegel MI, and Sadler DL. 2005. Musculoskeletal scapular correlates of plantigrade and acrobatic positional activities in *Papio cynocephalus anubis* and *Macaca fascicularis*. American Journal of Physical Anthropology 55(4): 463-472.

Kivell TL, and Begun DR. 2007. Frequency and timing of scaphoid-centrale fusion in hominoids. Journal of Human Evolution 52(3):321-340.

Kivell TL, and Schmitt D. 2009. Independent evolution of knuckle-walking in African apes shows that humans did not evolve from a knuckle-walking ancestor. Proceedings of the National Academy of Sciences 106(34):14241-14246.

Klingenberg CP, and Gidaszewski NA. 2010. Testing and quantifying phylogenetic signals and homoplasy in morphometric data. Systematic biology 59(3): 245-261.

Kontulainen S, Sievnen H, Kannus P, Pasanen M, Vuori I. 2002. Effect of long-term impact of loading on mass, size, and estimated strength of humerus and radius of female racquet sports players: a peripheral quantitative computed tomography study between young and old starters and controls. Journal of Bone and Mineral Research 17:2281–2289.

Koppe T, Klauke T, Lee S, and Schumacher G-H. 2000. Growth Pattern of the Maxillary Sinus in the Miniature Pig (*Sus scrofa*). Cells Tissues Organs 167(1):58-67.

Krahl VE. 1947. The torsion of the humerus: its localization, cause and duration in man. American Journal of Anatomy 80(3):275-319.

Krahl VE. 1976. The phylogeny and ontogeny of humeral torsion. American Journal of Physical Anthropology 45(3):595-599.

Krahl VE, and Evans FG. 1945. Humeral torsion in man. American Journal of Physical Anthropology 3(3):229-253.

Kunimatsu Y, Nakatsukasa M, Sawada Y, Sakai T, Hyodo M, Hyodo H, Itaya T, Nakaya H, Saegusa H, and Mazurier A. 2007. A new Late Miocene great ape

from Kenya and its implications for the origins of African great apes and humans. Proceedings of the National Academy of Sciences 104(49): 19220-19225.

Laird AK. 1967. Evolution of the human growth curve. Growth 31: 345–355.

Langley−Shirley N, and Jantz RL. 2010. A Bayesian Approach to Age Estimation in Modern Americans from the Clavicle. Journal of forensic sciences 55(3): 571-583.

Larson SG. 1988. Subscapularis function in gibbons and chimpanzees: implications for interpretation of humeral head torsion in hominoids. American Journal of Physical Anthropology 76(4):449-462.

Larson SG. 1993. Functional morphology of the shoulder in primates. Postcranial adaptation in nonhuman primates:45-69.

Larson SG. 1995. New characters for the functional interpretation of primate scapulae and proximal humeri. American Journal of Physical Anthropology 98(1): 13-35.

Larson SG. 1996. Estimating humeral torsion on incomplete fossil anthropoid humeri. Journal of Human Evolution 31(3):239-257.

Larson SG. 1998. Parallel evolution in the hominoid trunk and forelimb. Evolutionary Anthropology: Issues, News, and Reviews 6(3):87-99.

Larson SG. 2007a. The definition of humeral torsion: a comment on Rhodes (2006). American Journal of Physical Anthropology 133(2):819-820.

Larson SG. 2007b. Evolutionary transformation of the hominin shoulder. Evolutionary Anthropology: Issues, News, and Reviews 16(5):172-187.

Larson SG. 2009. Evolution of the hominin shoulder: early *Homo*. The First Humans–Origin and Early Evolution of the Genus *Homo*:65-75.

Larson SG. 2013. Shoulder morphology in early hominin evolution. The paleobiology of *Australopithecus*: Springer pp 247-261.

Larson SG, Stern JT. 1986. EMG of chimpanzee shoulder muscles during knuckle walking: problems of terrestrial locomotion in a suspensory adapted primate. Journal of Zoology 212:629–655.

Larson SG, and Stern JT. 1987. EMG of chimpanzee shoulder muscles during knuckle−walking: problems of terrestrial locomotion in a suspensory adapted primate. Journal of Zoology 212(4):629-655.

Larson S, and Stern Jr J. 1989. The role of propulsive muscles of the shoulder during quadrupedalism in vervet monkeys (*Cercopithecus aethiops*): implications for neural control of locomotion in primates. Journal of motor behavior 21(4):457.

Larson SG, and Stern JT. 1992. Further evidence for the role of supraspinatus in quadrupedal monkeys. American Journal of Physical Anthropology 87(3): 359-363.

Larson SG, and Stern JT. 2006. Maintenance of above-branch balance during primate arboreal quadrupedalism: Coordinated use of forearm rotators and tail motion. American Journal of Physical Anthropology 129(1):71-81.

Larson SG, and Stern Jr JT. 2013. Rotator cuff muscle function and its relation to scapular morphology in apes. Journal of human evolution.

Larson SG, Stern JT, and Jungers WL. 1991. EMG of serratus anterior and trapezius in the chimpanzee: scapular rotators revisited. American Journal of Physical Anthropology 85(1):71-84.

Larson SG, Jungers WL, Morwood MJ, Sutikna T, Saptomo EW, Due RA, and Djubiantono T. 2007. *Homo floresiensis* and the evolution of the hominin shoulder. Journal of Human Evolution 53(6):718-731.

Latimer B. 1991. Locomotor adaptations in *Australopithecus afarensis*: the issue of arboreality. Origine(s) de la Bipédie chez les Hominidés:169-176.

Latimer B, and Lovejoy CO. 1989. The calcaneus of *Australopithecus afarensis* and its implications for the evolution of bipedality. American Journal of Physical Anthropology 78(3):369-386.

Latimer HB, Lowrance E. 1965. Bilateral asymmetry in weight and in length of human bones. The Anatomical Record 152:217–224.

Lazenby RA. 2002. Skeletal biology, functional asymmetry and the origins of ‘handedness’. Journal of Theoretical Biology 218:129–138.

Lazenby RA, Cooper DM, Angus S, Hallgrímsson B. 2008. Articular constraint, handedness, and directional asymmetry in the human second metacarpal. Journal of Human Evolution 54: 875–885.

Le Gros CW. 1959. The antecedents of man. Edinburgh, Univ Pr, in-8.

Leal HP, and Checchia SL. 2006. A retroversão da cabeça do úmero: revisão de literatura e mensuração em 113 úmeros de cadáveres. Rev Bras Ortop 41(4): 122-127.

Leakey R, and Walker A. 1989. Early *Homo erectus* from West Lake Turkana, Kenya. Hominidae Jaca, Milan:209-215.

Leigh SR, and Shea BT. 1996. Ontogeny of body size variation in African apes. American Journal of Physical Anthropology 99(1):43-65.

Leinonen T, Cano J, Mäkinen H, and Merilä J. 2006. Contrasting patterns of body shape and neutral genetic divergence in marine and lake populations of threespine sticklebacks. Journal of Evolutionary Biology 19(6):1803-1812.

Lewis OJ. 1969. The hominoid wrist joint. American journal of physical anthropology 30(2):251-267.

Lewis OJ. 1974. The wrist articulations of the Anthropoidea. Primate locomotion: 143-169.

Lewis OJ. 1971. Biological Sciences: Brachiation and the Early Evolution of the Hominoidea. Nature 230:577-579.

Lewis OJ. 1985. Derived morphology of the wrist articulations and theories of hominoid evolution. Part I. The lorisine joints. Journal of anatomy 140(Pt 3): 447.

Lewis OJ. 1989. Functional morphology of the evolving hand and foot: Clarendon Press Oxford.

Lewis OJ, and Towers B. 1972. Naked ape or *Homo sapiens*?: Garnstone Press.

Lewis OJ, Hamshere R, and Bucknill T. 1970. The anatomy of the wrist joint. Journal of Anatomy 106(Pt 3):539.

Lieberman DE. 1997. Making behavioral and phylogenetic inferences from hominid fossils: considering the developmental influence of mechanical forces. Annual review of Anthropology:185-210.

Lieberman DE. 1999. Homology and hominid phylogeny: Problems and potential solutions. Evol Anthropol 7:142–151.

Lieberman DE. 2000. Ontogeny, homology and phylogeny in the hominid craniofacial skeleton: the problem of the browridge. Linnean Society Synposium Series. pp 85-122.

Lieberman DE, Polk JD, Demes B. 2003. Predicting long bone loading from cross sectional geometry. American Journal of Physical Anthropology 123:156–171.

Lieberman DE, Wood BA, and Pilbeam DR. 1996. Homoplasy and early *Homo*: an analysis of the evolutionary relationships of *H. habilis* sensu stricto and *H. rudolfensis*. Journal of Human Evolution 30(2):97-120.

Liversidge H, and Molleson T. 1999. Deciduous tooth size and morphogenetic fields in children from Christ Church, Spitalfields. Archives of oral biology 44(1): 7-26.

Liversidge HM. 2005. Accuracy of age estimation from developing teeth of a population of known age (0–5.4 years). International Journal of Osteoarchaeology 4(1):37-45.

Ljunggren AE. 1979. Clavicular function. Acta Orthopaedica 50(3):261-268.

Llorente M, Riba D, Palou L, Carrasco L, Mosquera M, Colell M, Feliu O. 2011. Population level right-handedness for a coordinated bimanual task in naturalistic housed chimpanzees: replication and extension in 114 animals from Zambia and Spain. American Journal of Primatology 73:281–290.

Lockwood CA. 1999. Homoplasy and adaptation in the atelid postcranium. American Journal of Physical Anthropology 108(4):459-482.

Lockwood CA, and Fleagle JG. 1999. The recognition and evaluation of homoplasy in primate and human evolution. American Journal of Physical Anthropology 110(S29):189-232.

Lockwood CA, Kimbel WH, and Lynch JM. 2004. Morphometrics and hominoid phylogeny: support for a chimpanzee–human clade and differentiation among great ape subspecies. Proceedings of the National Academy of Sciences of the United States of America 101(13):4356-4360.

Lonsdorf EV, Hopkins WD. 2005. Wild chimpanzees show population-level handedness for tool use. Proceedings of the National Academy of Sciences of the United States of America 102:12634–12638.

Lordkipanidze D, Jashashvili T, Vekua A, de León MSP, Zollikofer CP, Rightmire GP, Pontzer H, Ferring R, Oms O, and Tappen M. 2007. Postcranial evidence from early Homo from Dmanisi, Georgia. Nature 449(7160):305-310.

Lovejoy CO. 1978. A biomechanical review of the locomotor diversity of early hominids. Early hominids of Africa 403:429.

Lovejoy CO. 1988. Evolution of human walking. Scientific American 259(5):82-89.

Lovejoy CO, Cohn MJ, and White TD. 1999. Morphological analysis of the mammalian postcranium: a developmental perspective. Proceedings of the National Academy of Sciences 96(23):13247-13252.

Lovejoy CO, Suwa G, Simpson SW, Matternes JH, and White TD. 2009. The great divides: *Ardipithecus ramidus* reveals the postcrania of our last common ancestors with African apes. Science 326(5949):73-106.

Lycett SJ, and Collard M. 2005. Do homoiologies impede phylogenetic analyses of the fossil hominids? An assessment based on extant papionin craniodental morphology. Journal of human evolution 49(5):618-642.

MacKinnon J. 1974. The behaviour and ecology of wild orang-utans (*Pongo pygmaeus*). Animal Behaviour 22(1):3-74.

Maclatchy L. 2004. The oldest ape. Evolutionary Anthropology: Issues, News, and Reviews 13(3):90-103.

MaClatchy L, Gebo D, Kityo R, and Pilbeam D. 2000. Postcranial functional morphology of *Morotopithecus bishopi*, with implications for the evolution of modern ape locomotion. Journal of Human Evolution 39(2):159-183.

MacLeod N, and Forey PL. 2002. Morphology, shape and phylogeny: CRC.

Madar SI, Rose MD, Kelley J, MacLatchy L, and Pilbeam D. 2002. New *Sivapithecus* postcranial specimens from the Siwaliks of Pakistan. Journal of human evolution 42(6):705-752.

Mair SD, Uhl TL, Robbe RG, and Brindle KA. 2004. Physeal changes and range-of-motion differences in the dominant shoulders of skeletally immature baseball players. Journal of Shoulder and Elbow Surgery 13(5):487-491.

Manning J, Chamberlain A. 1991. Left-side cradling and brain lateralization. Ethology and Sociobiology 12:237–244.

Manning J, Heaton R, Chamberlain A. 1994. Left-side cradling: similarities and differences between apes and humans. Journal of Human Evolution 26:77–83.

Martin C. 1933. The cause of torsion of the humerus and of the notch on the anterior edge of the glenoid cavity of the scapula. Journal of Anatomy 67(Pt 4):573.

Marchant L, McGrew W. 1991. Laterality of function in apes: a meta-analysis of methods. Journal of Human Evolution 21:425–438.

Marchant L, McGrew W. 1996. Laterality of limb function in wild chimpanzees of Gombe National Park: comprehensive study of spontaneous activities. Journal of Human Evolution 30:427–443.

Marchant L, McGrew W. 2007. Ant fishing by wild chimpanzees is not lateralised. Primates 48:22–26.

Marchi D. 2007. Relative strength of the tibia and fibula and locomotor behavior in hominoids. Journal of Human Evolution 53:647–655.

Marchi D. 2008. Relationships between lower limb cross sectional geometry and mobility: the case of a Neolithic sample from Italy. American Journal of Physical Anthropology 137:188–200.

Martin CP. 1933. The cause of torsion of the humerus and of the notch on the anterior edge of the glenoid cavity of the scapula. Journal of Anatomy 67:572–582.

Mathieu P-A, Marcheix P-S, Hummel V, Valleix D, and Mabit C. 2013. Anatomical study of the clavicle: endomedullary morphology. Surgical and Radiologic Anatomy:1-5.

Matsudaira K, and Ishida T. 2010. Phylogenetic relationships and divergence dates of the whole mitochondrial genome sequences among three gibbon genera. Molecular phylogenetics and evolution 55(2):454-459.

Matsui A, Rakotondraparany F, Munechika I, Hasegawa M, and Horai S. 2009. Molecular phylogeny and evolution of prosimians based on complete sequences of mitochondrial DNAs. Gene 441(1):53-66.

Matsumura A, Gunji H, Takahashi Y, Nishida T, Okada M. 2010. Cross-sectional morphology of the femoral neck of wild chimpanzees. International Journal of Primatology 31:219–238.

Matsumura A, Takahashi Y, Okada M. 2002. Cross-sectional geometric properties along the diaphysis of femur and humerus in chimpanzees and humans. Zeitschrift für Morphologie und Anthropologie 83:373–382.

Mays S, Steele J, Ford M. 1999. Directional asymmetry in the human clavicle. International Journal of Osteoarchaeology 9:18–28.

McGrew WC, Marchant LF. 1996. On which side of the apes? Ethological study of laterality of hand use. In: Great Ape Societies (McGrew WC, Marchant L, Nichida T, eds), pp 255–272. Cambridge, Cambridge University Press.

McGrew WC, Marchant LF. 1997. On the other hand: current issues in and meta-analysis of the behavioural laterality of hand function in nonhuman primates. American Journal of Physical Anthropology 104:201–232.

McGrew WC, Marchant LF. 2001. Ethological study of manual laterality in the chimpanzees of the Mahale Mountains, Tanzania. Behaviour 138:329–358.

McHenry H, and Corruccini R. 1983. The wrist of *Proconsul africanus* and the origin of hominoid postcranial adaptations. New Interpretations of Ape and Human Ancestry Plenum Press, New York:353-367.

Meguerditchian A, Calcutt SE, Lonsdorf EV, Ross SR, Hopkins WD. 2010. Brief communication: captive gorillas are right handed for bimanual feeding. American Journal of Physical Anthropology 141:638–645.

Michaux J, Chevret P, and Renaud S. 2007. Morphological diversity of Old World rats and mice (*Rodentia, Muridae*) mandible in relation with phylogeny and adaptation. Journal of Zoological Systematics and Evolutionary Research 45(3):263-279.

Michilsens F, Vereecke EE, D'Août K, and Aerts P. 2009. Functional anatomy of the gibbon forelimb: adaptations to a brachiating lifestyle. Journal of Anatomy 215(3):335-354.

Miller RA. 1933. Evolution of the pectoral girdle and fore limb in the primates. American Journal of Physical Anthropology 17(1):1-56.

Molleson T, Cox M, Waldron A, and Whittaker D. 1993. The Spitalfields Project Volume 2 The Anthropology The Middling Sort. CBA research report 86:9-21.

Monteiro LR. 2000. Why morphometrics is special: the problem with using partial warps as characters for phylogenetic inference. Systematic biology 49(4): 796-800.

Morbeck ME, Galloway A, Zihlman AL, Mowbray KM. 1994. Skeletal asymmetry and hand preference during termite fishing by Gombe chimpanzees. Primates 35:99–103.

Morcillo A, Fernandez Carriba S, Loeches A. 2006. Asymmetries in postural control and locomotion in chimpanzees (*Pan troglodytes*). American Journal of Primatology 68:802–811.

Moyà-Solà S, Alba DM, Almécija S, Casanovas-Vilar I, Köhler M, De Esteban-Trivigno S, Robles JM, Galindo J, and Fortuny J. 2009. A unique Middle Miocene European hominoid and the origins of the great ape and human clade. Proceedings of the National Academy of Sciences 106(24):9601-9606.

Moyà-Solà S, and Köhler M. 1996. A *Dryopithecus* skeleton and the origins of great-ape locomotion. Nature 379(6561):156-159.

Moyà-Solà S, Köhler M, Alba DM, Casanovas-Vilar I, and Galindo J. 2004. *Pierolapithecus catalaunicus*, a new Middle Miocene great ape from Spain. Science 306(5700):1339-1344.

Murachovsky J, Ikemoto RY, Nascimento LGP, Bueno RS, Strose E, and Almeida LH. 2010. Does the presence of proximal humerus growth plate changes in young baseball pitchers happen only in symptomatic athletes? An x-ray evaluation of 21 young baseball pitchers. British Journal of Sports Medicine 44(2):90-94.

Myers JB, Oyama S, Goerger BM, Rucinski TJ, Blackburn JT, and Creighton RA. 2009. Influence of humeral torsion on interpretation of posterior shoulder tightness measures in overhead athletes. Clinical Journal of Sport Medicine 19(5):366.

Nakatsukasa M, Kunimatsu Y, Nakano Y, Takano T, and Ishida H. 2003. Comparative and functional anatomy of phalanges in *Nacholapithecus kerioi*, a Middle Miocene hominoid from northern Kenya. Primates 44(4):371-412.

Nakatsukasa M, Pickford M, Egi N, and Senut B. 2007. Femur length, body mass, and stature estimates of Orrorin tugenensis, a 6 Ma hominid from Kenya. Primates 48(3):171-178.

Napier JR, Davis PR, and Clark WELG. 1959. The Forelimb Skeleton and Association Remains of *Pronconsul Africanus*: British Museum (Natural History).

Naylor GJP, and Adams DC. 2001. Are the Fossil Data Really at Odds with the Molecular Data/Morphological Evidence for Cetartiodactyla Phylogeny Reexamined. Systematic biology 50(3):444-453.

Neustupa J, and Skaloud P. 2007. Geometric morphometrics and qualitative patterns in the morphological variation of five species of *Micrasterias* (*Zygnemophyceae, Viridiplantae*). Preslia 79(4):401.

Nelson G. 1978. Ontogeny, phylogeny, paleontology, and the biogenetic law. Systematic Biology 27(3):324-345.

Nyffeler RW, Jost B, Pfirrmann CW, and Gerber C. 2003. Measurement of glenoid version: conventional radiographs versus computed tomography scans. Journal of shoulder and elbow surgery 12(5):493-496.

O'Meara BC, Ané C, Sanderson MJ, and Wainwright PC. 2006. Testing for different rates of continuous trait evolution using likelihood. Evolution 60(5):922-933.

Ohman JC. 1986. The first rib of hominoids. American Journal of Physical Anthropology 70(2):209-229.

Oishi M, Ogihara N, Endo H, and Asari M. 2008. Muscle architecture of the upper limb in the orangutan. Primates 49(3):204-209.

Oishi M, Ogihara N, Endo H, Ichihara N, and Asari M. 2009. Dimensions of forelimb muscles in orangutans and chimpanzees. Journal of anatomy 215(4):373-382.

Olivier G. 1951. Technique de mesure des courbures de la clavicule. Comptes Rendus de l'Association des Anatomistes XXXIXe Réunion (Nancy) 69:753-764.

Olivier G. 1953. La clavicule du Semnopithèque. Mammalia 17(3):173-186.

Orr CM. 2005. Knuckle-walking anteater: A convergence test of adaptation for purported knuckle-walking features of african Hominidae. American Journal of Physical Anthropology 128(3):639-658.

Osbahr DC, Cannon DL, and Speer KP. 2002. Retroversion of the humerus in the throwing shoulder of college baseball pitchers. The American Journal of Sports Medicine 30(3):347-353.

Oxnard C. 1963. Locomotor adaptations in the primate forelimb. Symposia of the Zoological Society of London. p 165-182.

Oxnard CE. 1967. The functional morphology of the primate shoulder as revealed by comparative anatomical, osteometric and discriminant function techniques. American Journal of Physical Anthropology 26(2):219-240.

Oxnard CE. 1969. Evolution of the human shoulder: some possible pathways. American Journal of Physical Anthropology 30(3):319-331.

Oxnard CE. 1973. Functional inferences from morphometrics: problems posed by uniqueness and diversity among the primates. Systematic biology 22(4): 409-424.

Oxnard C. 1977. Morphometric affinities of the human shoulder. American Journal of Physical Anthropology 46(2):367-374.

Pande B, Singh I. 1971. One-sided dominance in the upper limbs of human fetuses as evidenced by asymmetry in muscle and bone weight. Journal of Anatomy 109:457–459.

Paradis E, Claude J, and Strimmer K. 2004. APE: analyses of phylogenetics and evolution in R language. Bioinformatics 20(2):289-290.

Parnell RJ. 2001. Hand preference for food processing in wild western lowland gorillas (*Gorilla gorilla gorilla*). Journal of Comparative Psychology 115:365–375.

Patterson C. 1982. Morphological characters and homology. Problems of phylogenetic reconstruction 21:21-74.

Payne, V. & Isaacs, L. D. 2005. Human motor development: A lifespan approach, 6th edn. Blacklick, OH: McGraw-Hill Compani.

Pearson O, Cordero R, Busby A. 2006. How different were Neanderthals' habitual activities? A comparative analysis with diverse groups of recent humans. In Neanderthals Revisited: New Approaches and Perspectives (Harvati K, Harrison T, eds), pp 135–156. Dordrecht, Springer.

Pieper HG. 1998. Humeral torsion in the throwing arm of handball players. The American Journal of Sports Medicine 26(2):247.

Pilbeam D, Rose MD, Barry JC, and Shah SI. 1990. New *Sivapithecus* humeri from Pakistan and the relationship of *Sivapithecus* and *Pongo*. Nature 348(6298): 237-239.

Pilbeam D, and Simons E. 1971. Biological Sciences: Humerus of *Dryopithecus* from Saint Gaudens, France.

Plavcan JM. 2000. Inferring social behavior from sexual dimorphism in the fossil record. Journal of Human Evolution 39(3):327-344.

Plavcan JM, and van Schaik CP. 1997. Intrasexual competition and body weight dimorphism in anthropoid primates. American journal of physical anthropology 103(1):37-68.

Polly PD. 2001. Paleontology and the comparative method: ancestral node reconstructions versus observed node values. The American Naturalist 157(6): 596-609.

Porac C, Coren S. 1981. Lateral Preferences and Human Behavior. New York, Springer.

Potts R. 1998. Environmental hypotheses of hominin evolution. American Journal of Physical Anthropology 107(27):93-136.

Pouydebat E, Reghem E, Gorce P, Bels V. 2010. Influence of the task on hand preference: individual differences among gorillas (*Gorilla gorilla gorilla*). Folia Primatologica 81:273–281.

Pöyhiä TH, Nietosvaara YA, Remes VM, Kirjavainen MO, Peltonen JI, Lamminen AE. 2005. MRI of rotator cuff muscle atrophy in relation to glenohumeral joint incongruence in brachial plexus birth injury. Pediatric Radiology 35:402–409.

Preuschoft H, and Demes B. 1984. Biomechanics of brachiation. The lesser apes: Evolutionary and behavioral biology:96-118.

Preuschoft H, Hohn B, Scherf H, Schmidt M, Krause C, and Witzel U. 2010. Functional analysis of the primate shoulder. International journal of primatology 31(2):301-320.

Pritchett JW. 1991. Growth plate activity in the upper extremity. Clinical orthopaedics and related research 268:235.

R Development Core Team (2010). R: A Language and Environment for Statistical Computing. Vienna, Austria.

Raaum RL, Sterner KN, Noviello CM, Stewart C-B, and Disotell TR. 2005. Catarrhine primate divergence dates estimated from complete mitochondrial genomes: concordance with fossil and nuclear DNA evidence. Journal of human evolution 48(3):237-257.

Ramos RMA, Di Beneditto APM, and Lima NRW. 2000. Growth parameters of *Pontoporia blainvillei* and *Sotalia fluviatilis* (Cetacea) in northern Rio de Janeiro, Brazil. Aquatic Mammals 26(1):65-75.

Randelli M, and Gambrioli P. 1986. Glenohumeral osteometry by computed tomography in normal and unstable shoulders. Clinical orthopaedics and related research 208:151-156.

Raymond M, Pontier D. 2004. Is there geographical variation in human handedness? Laterality: Asymmetries of Body, Brain and Cognition 9:35–51.

Read AJ, and Tolley KA. 1997. Postnatal growth and allometry of harbour porpoises from the Bay of Fundy. Canadian Journal of Zoology 75(1):122-130.

Reagan K, Meister K, Horodyski MB, Werner DW, Carruthers C, and Wilk K. 2002. Humeral retroversion and its relationship to glenohumeral rotation in the shoulder of college baseball players. The American Journal of Sports Medicine 30(3):354.

Reed KE. 1997. Early hominid evolution and ecological change through the African Plio-Pleistocene. Journal of human evolution 32(2):289-322.

Rein TR, Harrison T, and Zollikofer CP. 2011. Skeletal correlates of quadrupedalism and climbing in the anthropoid forelimb: implications for inferring locomotion in Miocene catarrhines. Journal of Human Evolution 61(5):564-574.

Remis M. 1995. Effects of body size and social context on the arboreal activities of lowland gorillas in the Central African Republic. American Journal of Physical Anthropology 97:413–433.

Revell LJ. 2012. phytools: an R package for phylogenetic comparative biology (and other things). Methods in Ecology and Evolution.

Revell LJ, Harmon LJ, and Collar DC. 2008. Phylogenetic signal, evolutionary process, and rate. Systematic biology 57(4):591-601.

Rhodes JA. 2006. Adaptations to humeral torsion in medieval Britain. American Journal of Physical Anthropology 130(2):160-166.

Rhodes JA. 2007. Humeral torsion and retroversion in the literature: a reply to Larson. American Journal of Physical Anthropology 133(2):820-821.

Rhodes JA, and Churchill SE. 2009. Throwing in the Middle and Upper Paleolithic: inferences from an analysis of humeral retroversion. Journal of human evolution 56(1):1-10.

Rhodes JA, and Knüsel CJ. 2005. Activity-related skeletal change in medieval humeri: Cross-sectional and architectural alterations. American Journal of Physical Anthropology 128(3):536-546.

Richmond BG, Begun DR, and Strait DS. 2001. Origin of human bipedalism: The knuckle-walking hypothesis revisited. American Journal of Physical Anthropology 116(S33):70-105.

Richmond BG, and Strait DS. 2000. Evidence that humans evolved from a knuckle-walking ancestor. Nature 404(6776):382-385.

Riedl R, and Jefferies RPS. 1978. Order in living organisms: a systems analysis of evolution: Wiley New York.

Roach NT, Lieberman DE, Gill IV TJ, Palmer WE, and Gill III TJ. 2012. The effect of humeral torsion on rotational range of motion in the shoulder and throwing performance. Journal of Anatomy.

Roberts D. 1974. Structure and function of the primate scapula. Primate locomotion: 171-200.

Roberts D, and Davidson I. 1975. The lemur scapula. Lemur Biology: Springer. p 125-147.

Rodman PS. 1979. Skeletal differentiation of *Macaca fascicularis* and *Macaca nemestrina* in relation to arboreal and terrestrial quadrupedalism. American Journal of Physical Anthropology 51(1):51-62.

Rohlf FJ. 2002. Geometric morphometrics and phylogeny. Systematics Association Special Volume 64:175-193.

Roos C, and Geissmann T. 2001. Molecular phylogeny of the major hylobatid divisions. Molecular Phylogenetics and Evolution 19(3):486-494.

Rose M. 1989. New postcranial specimens of catarrhines from the Middle Miocene Chinji Formation, Pakistan: descriptions and a discussion of proximal humeral functional morphology in anthropoids. Journal of Human Evolution 18(2): 131-162.

Rose M. 1993. Locomotor anatomy of Miocene hominoids. Postcranial Adaptation in Nonhuman Primates:252-272.

Rose M. 1994. Quadrupedalism in some Miocene catarrhines. Journal of Human Evolution 26(5):387-411.

Rose M. 1997. Functional and phylogenetic features of the forelimb in Miocene hominoids. Begun et al:79-100.

Rose J, Gamble JG. 1994. Human Walking.Baltimore, Maryland:Williams and Wilkins.

Roth VL. 1988. 1. The Biological Basis of Homology. Ontogeny and systematics:1.

Roy TA, Ruff CB, Plato CC. 1994. Hand dominance and bilateral asymmetry in the structure of the second metacarpal. American Journal of Physical Anthropology 94:203–211.

Ruff C. 1987. Sexual dimorphism in human lower limb bone structure: relationship to subsistence strategy and sexual division of labor. Journal of Human Evolution 16:391–416.

Ruff C. 1990. Body mass and hindlimb bone cross-sectional and articular dimensions in anthropoid primates. In: Body Size in Mammalian Paleobiology: Estimation and Biological Implications (Damuth J, McFadden BJ, eds), pp 119–149. Cambridge, Cambridge University Press.

(Larson and Stern Jr 2013) CB. 2003. Long bone articular and diaphyseal structure in Old World monkeys and apes. II. Estimation of body mass. American Journal of Physical Anthropology 120:16–37.

Ruff CB, Hayes WC. 1983. Cross-sectional geometry of Pecos Pueblo femora and tibiae – a biomechanical investigation. II. Sex, age, and side differences. American Journal of Physical Anthropology 60:383–400.

Ruff CB, Trinkaus E, Walker A, Larsen CS. 1993. Postcranial robusticity in *Homo*. I. Temporal trends and mechanical interpretation. American Journal of Physical Anthropology 91:21–53.

Ruvolo M. 1997. Molecular phylogeny of the hominoids: inferences from multiple independent DNA sequence data sets. Molecular Biology and Evolution 14(3): 248-265.

Sabick MB, Kim YK, Torry MR, Keirns MA, and Hawkins RJ. 2005. Biomechanics of the shoulder in youth baseball pitchers. The American journal of sports medicine 33(11):1716-1722.

Saha A. 1971. Dynamic stability of the glenohumeral joint. Acta Orthopaedica 42(6): 491-505.

Sakamoto M, and Ruta M. 2012. Convergence and divergence in the evolution of cat skulls: temporal and spatial patterns of morphological diversity. PLoS One 7(7):e39752.

Sarmiento EE. 1985. Functional differences in the skeleton of wild and captive orang-utans and their adaptive significance: New York University.

Sarringhaus L, Stock J, Marchant L, McGrew W. 2005. Bilateral asymmetry in the limb bones of the chimpanzee (*Pan troglodytes*). American Journal of Physical Anthropology 128:840–845.

Scheuer L, and Black S. 2000. Developmental juvenile osteology: Academic Press.

Schultz AH. 1930. The skeleton of the trunk and limbs of higher primates. Human Biology 2(3):303-438.

Schultz AH. 1937. Proportions, variability and asymmetries of the long bones of the limbs and the clavicles in man and apes. Human Biology 9:281–328.

Schultz AH. 1956. Postembryonic age changes. Primatologia 1:887-964.

Schultz AH. 1969. The life of primates: Weidenfeld & Nicolson London.

Schliep KP. 2011. phangorn: Phylogenetic analysis in R. Bioinformatics 27(4): 592-593.

Schmitt D, and Lemelin P. 2002. Origins of primate locomotion: gait mechanics of the woolly opossum. American Journal of Physical Anthropology 118(3):231-238.

Schmitt D. 2003. Insights into the evolution of human bipedalism from experimental studies of humans and other primates. J Exp Biol 206(9):1437-1448.

Schrago CG, and Russo CA. 2003. Timing the origin of New World monkeys. Molecular Biology and Evolution 20(10):1620-1625.

Schultz AH. 1968. The recent hominoid primates. Perspectives on human evolution 1:122-195.

Schwab LM, and Blanch P. 2009. Humeral torsion and passive shoulder range in elite volleyball players. Physical Therapy in Sport 10(2):51-56.

Shah R, Trivdei B, Patel J, Shah G, and Nirvan A. 2006. A Study of Angle of Humeral Torsion. Journal of Anatomical Society of India 55(2):43-47.

Shaw CN. 2011. Is hand preference ‘coded’ in the hominin skeleton? An *in-vivo* study of bilateral morphological variation. Journal of Human Evolution 61:480–487.

Shaw CN, Hofmann CL, Petraglia MD, Stock JT, Gottschall JS. 2012. Neandertal humeri may reflect adaptation to scraping tasks, but not spear thrusting. PLoS One 7:e40349.

Shaw CN, Stock JT. 2009a. Habitual throwing and swimming correspond with upper limb diaphyseal strength and shape in modern human athletes. American Journal of Physical Anthropology 140:160–172.

Shaw CN, Stock JT. 2009b. Intensity, repetitiveness, and directionality of habitual adolescent mobility patterns influence the tibial diaphysis morphology of athletes. American Journal of Physical Anthropology 140:149–159.

Shaw CN, Stock JT. 2011. The influence of body proportions on femoral and tibial midshaft shape in hunter-gatherers. American Journal of Physical Anthropology 144:22–29.

Shea BT. 1986. Scapula form and locomotion in chimpanzee evolution. American Journal of Physical Anthropology 70(4):475-488.

Sherwood CC, Wahl E, Erwin JM, Hof PR, Hopkins WD. 2007. Histological asymmetries of primary motor cortex predict handedness in chimpanzees (*Pan troglodytes*) . The Journal of Comparative Neurology 503:525–537.

Singleton M. 2002. Patterns of cranial shape variation in the Papionini (Primates: Cercopithecinae). Journal of human evolution 42(5):547-578.

Sladek V, Berner M, Sosna D, Sailer R. 2007. Human manipulative behavior in the central European late Neolithic and early bronze age: humeral bilateral asymmetry. American Journal of Physical Anthropology133:669–681.

Smaers J, and Vinicius L. 2009. Inferring macro-evolutionary patterns using an adaptive peak model of evolution. Evol Ecol Res 11(7):991-1015.

Smaers JB, Dechmann DKN, Goswami A, Soligo C, and Safi K. 2012. Comparative analyses of evolutionary rates reveal different pathways to encephalization in bats, carnivorans, and primates. Proceedings of the National Academy of Sciences 109(44):18006-18011.

Smaers JB, Steele J, Case CR, and Amunts K. 2013. Laterality and the evolution of the prefronto-cerebellar system in anthropoids. Annals of the New York Academy of Sciences.

Smaers JB, Steele J, and Zilles K. 2011. Modeling the evolution of cortico-cerebellar systems in primates. Annals of the New York Academy of Sciences 1225(1): 176-190.

Smith BH. 1989. Dental development as a measure of life history in primates. Evolution 43(3):683-688.

Smith BH, and Tompkins RL. 1995. Toward a life history of the Hominidae. Annual review of Anthropology:257-279.

Stanitski DF, Nietert PJ, Stanitski CL, Nadjarian RK, and Barfield W. 2000. Relationship of factors affecting age of onset of independent ambulation. Journal of Pediatric Orthopaedics 20(5):686-688.

Stern JT. 1971. Functional myology of the hip and thigh of cebid monkeys and its implications for the evolution of erect posture. Basel: S. Karger.

Stern Jr JT, and Susman RL. 1983. The locomotor anatomy of Australopithecus afarensis. American Journal of Physical Anthropology 60(3):279-317.

Taylor AB. 1995. Effects of ontogeny and sexual dimorphism on scapula

Stern JT, Wells JP, Jungers WL, Vangor AK, and Fleagle JG. 1980. An electromyographic study of the pectoralis major in atelines and *Hylobates*, with special reference to the evolution of a pars clavicularis. American Journal of Physical Anthropology 52(1):13-25.

Steele J. 2000a. Handedness in past human populations: skeletal markers. Laterality: Asymmetries of Body, Brain and Cognition 5:193–220.

Steele J. 2000b. Skeletal indicators of handedness. In Human Osteology (Cox M, Mays S, eds.), pp 307–323. London, Greenwich Medical Media.

Steele J, Mays S. 1995. Handedness and directional asymmetry in the long bones of the human upper limb. International Journal of Osteoarchaeology 5:39–49.

Stern JT. 2000. Climbing to the top: a personal memoir of *Australopithecus afarensis*. Evolutionary Anthropology Issues News and Reviews 9(3):113-133.

Stirland A. 1993. Asymmetry and activity, age-related change in the male humerus. International Journal of Osteoarchaeology 3:105–113.

Stock J, Pfeiffer S. 2001. Linking structural variability in long bone diaphyses to habitual behaviors: foragers from the southern African Later Stone Age and the Andaman Islands. American Journal of Physical Anthropology 115:337–348.

Stock JT, Pfeiffer SK. 2004. Long bone robusticity and subsistence behaviour among Later Stone Age foragers of the forest and fynbos biomes of South Africa. Journal of Archaeological Science 31: 999–1013.

Stout D, Chaminade T. 2012. Stone tools, language and the brain in human evolution. Philosophical Transactions of the Royal Society B: Biological Sciences 367:75–87.

Suwa G, Kono RT, Katoh S, Asfaw B, and Beyene Y. 2007. A new species of great ape from the late Miocene epoch in Ethiopia. Nature 448(7156):921-924.

Swindler D. 1985. Nonhuman primate dental development and its relationship to human dental development. Nonhuman primate models for human growth and development:67-94.

Takahashi LK. 1990. Morphological Basis of Arm-Swinging: Multivariate Analyses of the Forelimbs of *Hylobates* and *Ateles*. Folia Primatologica 54(1-2):70-85.

Taylor AB. 1995. Effects of ontogeny and sexual dimorphism on scapula morphology in the mountain gorilla (Gorilla gorilla beringel). American Journal of Physical Anthropology 98(4):431-445.

Taylor AB. 1997. Relative growth, ontogeny, and sexual dimorphism in Gorilla (*Gorilla gorilla gorilla* and *G. g. beringei*): Evolutionary and ecological considerations. American Journal of Primatology 43(1):1-31.

Taylor R, Zheng C, Jackson R, Doll J, Chen J, Holzbaur K, Besier T, and Kuhl E. 2009. The phenomenon of twisted growth: humeral torsion in dominant arms of high performance tennis players. Computer Methods in Biomechanics and Biomedical Engineering 12(1):83-93.

Temerin LA, and Cant JG. 1983. The evolutionary divergence of Old World monkeys and apes. American Naturalist:335-351.

Terry RJ. 1932. The clavicle of the American Negro. American Journal of Physical Anthropology 16(3):351-379.

Tètreault P, Krueger A, Zurakowski D, and Gerber C. 2004. Glenoid version and rotator cuff tears. Journal of orthopaedic research 22(1):202-207.

Thinh VN, Rawson B, Hallam C, Kenyon M, Nadler T, Walter L, and Roos C. 2010. Phylogeny and distribution of crested gibbons (genus *Nomascus*) based on

mitochondrial cytochrome b gene sequence data. American Journal of Primatology 72(12):1047-1054.

Thomas SJ, Swanik CB, Kaminski TW, Higginson JS, Swanik KA, Bartolozzi AR, and Nazarian LN. 2012. Humeral retroversion and its association with posterior capsule thickness in collegiate baseball players. Journal of Shoulder and Elbow Surgery 21(7):910-916.

Thorpe SK, and Crompton RH. 2005. Locomotor ecology of wild orangutans (*Pongo pygmaeus abelii*) in the Gunung Leuser Ecosystem, Sumatra, Indonesia: A multivariate analysis using log-linear modelling. American Journal of Physical Anthropology 127(1):58-78.

Thorpe SK, and Crompton RH. 2006. Orangutan positional behavior and the nature of arboreal locomotion in Hominoidea. American Journal of Physical Anthropology 131(3):384-401.

Thorpe SK, Holder R, and Crompton R. 2007. Origin of human bipedalism as an adaptation for locomotion on flexible branches. Science 316(5829): 1328-1331.

Trinkaus E, Churchill SE, Ruff CB. 1994. Postcranial robusticity in *Homo*. II. Humeral bilateral asymmetry and bone plasticity. American Journal of Physical Anthropology 93:1–34.

Todd TW, and D'Errico J. 1928. The clavicular epiphyses. American Journal of Anatomy 41(1):25-50.

Tuttle RH. 1967. Knuckle-walking and the evolution of hominoid hands. American Journal of Physical Anthropology 26(2):171-206.

Tuttle RH. 1975. Knuckle-walking and knuckle-walkers: a commentary on some recent perspectives on hominoid evolution. Primate functional morphology and evolution:203-212.

(Anapol and Fleagle 1988) RH. 1986. Apes of the world: Their social behavior, communication, mentality, and ecology: Noyes Publications.

Tuttle R, and Basmajian JV. 1974. Electromyography of brachial muscles in *Pan gorilla* and hominoid evolution. American Journal of Physical Anthropology 41(1):71-90.

Tuttle RH, Watts DP. 1985. The positional behavior and adaptive complexes of *Pan gorilla*. Primate morphophysiology, locomotor analyses and human bipedalism Tokyo University Press, Tokyo:261-288.

Usherwood JR, Larson SG, and Bertram JE. 2003. Mechanisms of force and power production in unsteady ricochetal brachiation. American Journal of Physical Anthropology 120(4):364-372.

Valverde E, Gálvez-López E, Alba-Fernández C, del Río L, and Casinos A. 2010. Lumbar ontogenetic growth and sexual dimorphism in modern humans. American Journal of Human Biology 22(5):596-603.

van Adrichem GG, Utami SS, Wich SA, van Hooff JA, and Sterck EH. 2006. The development of wild immature Sumatran orangutans (*Pongo abelii*) at Ketambe. Primates 47(4):300-309.

Van Der Sluijs J, Van Ouwerkerk W, De Gast A, Wuisman P, Nollet F, and Manoliu R. 2002. Retroversion of the humeral head in children with an obstetric brachial plexus lesion. Journal of Bone & Joint Surgery, British Volume 84(4):583-587.

Varady T. 2008. Automatic procedures to create CAD models from measured data. Computer-Aided Design and Applications 5(5):577-588.

Veeger H, and Van Der Helm F. 2007. Shoulder function: the perfect compromise between mobility and stability. Journal of biomechanics 40(10):2119-2129.

Venkataraman VV, Kraft TS, and Dominy NJ. 2013. Tree climbing and human evolution. Proceedings of the National Academy of Sciences 110(4): 1237-1242.

Voisin JL. 2006. Clavicle, a neglected bone: morphology and relation to arm movements and shoulder architecture in primates. The Anatomical Record Part A: Discoveries in Molecular, Cellular, and Evolutionary Biology 288(9): 944-953.

Vilensky JA, Larson SG. 1989. Primate locomotion: utilization and control of symmetrical gaits. Annual Review of Anthropology 18:17–35.

Wagner GP. 1989. The biological homology concept. Annual Review of Ecology and Systematics 20:51-69.

Ward, C. V. 1997. Functional anatomy and phyletic implications of the hominoid trunk and hindlimb. Function, Phylogeny, and Fossils: Miocene Hominoid Evolution and Adaptations. Plenum Press, New York, 101-130.

Walker A, Leakey RE. 1993. The Nariokotome *Homo erectus* skeleton: Harvard University Press.

Washburn SL. 1967. Behaviour and the origin of man. Proceedings of the Royal Anthropological Institute of Great Britain and Ireland:21-27.

Ward CV. 1998. *Afropithecus, Proconsul*, and the primitive hominoid skeleton. Primate locomotion: recent advances New York: Plenum p:337-352.

Ward CV. 2007. Postcranial and locomotor adaptations of hominoids. Handbook of paleoanthropology 2:1011-1030.

Ward S, Brown B, Hill A, Kelley J, and Downs W. 1999. *Equatorius*: a new hominoid genus from the middle Miocene of Kenya. Science 285(5432):1382-1386.

Warton D, Duursma R, Falster D, Taskinen S (2011). Smatr: (standardized) major axis estimation and testing routines. R package version 3.2.3. http://CRAN.R-project.org/package=smatr.

Waters PM, Smith GM, Jaramillo D. 1998. Glenohumeral deformity secondary to brachial birth palsy. Journal of Bone & Joint Surgery, American Volume 80:668–676.

Washburn SL. 1967. Behaviour and the origin of man. Proceedings of the Royal Anthropological Institute of Great Britain and Ireland:21-27.

Waters PM, Smith GR, and Jaramillo D. 1998. Glenohumeral deformity secondary to brachial plexus birth palsy. The Journal of Bone & Joint Surgery 80(5): 668-677.

Weiss E. 2009. Sex differences in humeral bilateral asymmetry in two hunter-gatherer populations: California Amerinds and British Columbian Amerinds. American Journal of Physical Anthropology 140:19–24.

White TD, Black MT, and Folkens PA. 2011. Human osteology: Academic Press.

Whiteley R, Adams R, Nicholson L, Ginn K. 2008. Shoulder proprioception is associated with humeral torsion in adolescent baseball players. Physical Therapy in Sport 9:177–184.

Whiteley R, Adams R, Ginn K, and Nicholson L. 2010. Playing level achieved, throwing history, and humeral torsion in Masters baseball players. Journal of Sports Sciences 28(11):1223-1232.

Whiteley R, Adams R, Nicholson L, and Ginn K. 2008. Shoulder proprioception is associated with humeral torsion in adolescent baseball players. Physical Therapy in Sport 9(4):177-184.

Whiteley R, Ginn K, Nicholson L, and Adams R. 2006. Indirect ultrasound measurement of humeral torsion in adolescent baseball players and non-athletic adults: reliability and significance. Journal of Science and Medicine in Sport 9(4):310-318.

Whiteley R, Oceguera MV, Valencia EB, and Mitchell T. 2012. Adaptations at the Shoulder of the Throwing Athlete and Implications for the Clinician. Techniques in Shoulder & Elbow Surgery 13(1):36.

Wich S, Utami-Atmoko S, Setia TM, Rijksen H, Schürmann C, Van Hooff J, and Van Schaik C. 2004. Life history of wild Sumatran orangutans (*Pongo abelii*). Journal of Human Evolution 47(6):385-398.

Wilkinson RD, Steiper ME, Soligo C, Martin RD, Yang Z, and Tavaré S. 2011. Dating primate divergences through an integrated analysis of palaeontological and molecular data. Systematic biology 60(1):16-31.

Williams SA. 2010. Moprhological Integration and the Evolutio of Knuckle-Walking. Journal of Human Evolution 58(5): 432-440.

Wood BA. 2007. Are" Robust" Australopithecines a Group? Evolutionary History of the" robust" Australopithecines:269.

Wray GA. 1994. Developmental evolution: new paradigms and paradoxes. Developmental Genetics 15(1):1-6.

Wunderlich R, Jungers W. 2009. Manual digital pressures during knuckle-walking in chimpanzees (*Pan troglodytes*). American Journal of Physical Anthropology 139(3):394-403.

Wyland DJ, Pill SG, Shanley E, Clark J, Hawkins RJ, Noonan TJ, Kissenberth MJ, and Thigpen CA. 2012. Bony Adaptation of the Proximal Humerus and

Glenoid Correlate Within the Throwing Shoulder of Professional Baseball Pitchers. The American Journal of Sports Medicine 40(8):1858-1862.

Wilcox RR. 2001. Fundamentals of Modern Statistical Methods: Substantially Improving Power and Accuracy. New York, Springer.

Young NM. 2003. A reassessment of living hominoid postcranial variability: implications for ape evolution. Journal of Human Evolution 45(6):441-464.

Young NM, and MacLatchy L. 2004. The phylogenetic position of *Morotopithecus*. Journal of Human Evolution 46(2):163-184.

Young NM. 2008. A comparison of the ontogeny of shape variation in the anthropoid scapula: functional and phylogenetic signal. American Journal of Physical Anthropology 136(3):247-264.

Zapfe H. 1958. The skeleton of *Pliopithecus* (*Epipliopithecus*) *vindobonensis*. American Journal of Physical Anthropology 16(4):441-457.

Zapfe H. 1960. A new fossil anthropoid from the Miocene of Austria. Current Anthropology 1(5/6):428-429.

Zelditch ML, Fink WL, and Swiderski DL. 1995. Morphometrics, homology, and phylogenetics: quantified characters as synapomorphies. Systematic biology 44(2):179-189.

Zihlman AL, Mcfarland RK, and Underwood CE. 2011. Functional Anatomy and Adaptation of Male Gorillas (*Gorilla gorilla gorilla*) With Comparison to Male Orangutans (*Pongo pygmaeus*). The Anatomical Record: Advances in Integrative Anatomy and Evolutionary Biology 294(11):1842-1855.